

Soil biogeochemistry, aridity and plant adaptation responses in southern Africa savannas

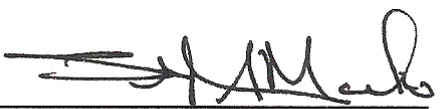




Lixin Wang
ChengDe, Hebei Province, China

Bachelor of Science, Hebei University, 2001
Master of Science, University of North Carolina at Greensboro, 2004

A Dissertation presented to the Graduate Faculty
of the University of Virginia in Candidacy for the Degree of
Doctor of Philosophy

Department of Environmental Sciences

University of Virginia
May, 2008

Abstract

Savannas cover about 20% of the Earth's land area and 50% of Africa, crossing a wide range of climatic conditions. It remains unclear how the relative importance of water and nutrient limitations varies with the mean climatic conditions in the savanna ecosystems. This dissertation used the Kalahari Transect (KT) in southern Africa as a representative savanna ecosystem and combined multiple tools to understand the variations in soil biogeochemistry and subsequent responses of plants on this immense rainfall gradient.

The large spatial scale field manipulation experiment shows that nitrogen (N) may not be a limiting factor in tropical savanna ecosystems. The fertilization experiment demonstrates that even at the wet end of the transect, water remains the principal factor limiting grass productivity. Natural abundance of foliar $\delta^{15}\text{N}$ and $\delta^{13}\text{C}$ reveals different water and N use for C_3 and C_4 plants. The consistently higher foliar $\delta^{15}\text{N}$ for C_3 plants suggests that C_4 plants may be superior competitors for N. The foliar $\delta^{13}\text{C}$ data may indicate that the C_3 plants have an advantage over C_4 plants when competing for water resources. The differences in water and nitrogen use between C_3 and C_4 plants likely collectively contribute to the tree-grass coexistence in savannas. The soils along the KT rainfall gradient show clear differences in belowground nutrient content and $\delta^{15}\text{N}$ distributions between wet and dry seasons. The results also show how the formation of "fertility islands" is not necessarily coupled with belowground processes in that the distribution of soil nutrients at the surface does not match belowground patterns. The modeling framework largely agrees with the field observations and shows that, at daily time scales, there are distinct dynamics for soil moisture, decomposition and nitrogen

mineralization between soil plots located under tree canopies and in open canopy areas. The modeling study shows that in savanna ecosystems, water availability determines the patterns and rates of nutrient cycling at large scales, while at the local scales, vegetation patchiness plays an important role in nutrient cycling. Lastly, this dissertation discusses the potential combination of isotopic and remote sensing techniques, which holds promise to allow spatially continuous estimates of isotopic compositions.

TABLE OF CONTENTS

Table of Contents.....	4
List of Figures.....	7
List of Tables.....	13
Acknowledgements.....	15
Preface.....	16
Chapter 1: INTRODUCTION.....	17
Chapter 2: BIOGEOCHEMISTRY OF KALAHARI SANDS	
Abstract.....	23
Introduction.....	24
Materials and Methods.....	27
Physical properties of Kalahari sands.....	30
Biogeochemical properties of Kalahari sands.....	38
Root distribution in the Kalahari.....	46
Soil crusts in Kalahari sand formations.....	48
Summary.....	50
Acknowledgements.....	50
Chapter 3: COMBINED EFFECTS OF SOIL MOISTURE AND NITROGEN AVAILABILITY VARIATIONS ON GRASS PRODUCTIVITY IN AFRICAN SAVANNAS	
Abstract.....	52
Introduction.....	54
Materials and Methods.....	56
Results.....	62
Discussion.....	67
Conclusions.....	71
Acknowledgements.....	71
Chapter 4: PATTERNS AND IMPLICATIONS OF PLANT-SOIL $\delta^{13}\text{C}$ AND $\delta^{15}\text{N}$ VALUES IN AFRICAN SAVANNA ECOSYSTEMS	
Abstract.....	73
Introduction.....	74
Materials and Methods.....	76
Results.....	79
Discussion.....	83
Acknowledgements.....	89
Chapter 5: ISOTOPE COMPOSITION AND ANION CHEMISTRY OF SOIL PROFILES ALONG THE KALAHARI TRANSECT	

Abstract.....	90
Introduction.....	91
Materials and Methods.....	93
Results and Discussion.....	96
Summary.....	106
Acknowledgements.....	107
Chapter 6: PREFERENCE AND ADAPTATION MAINTENANCE IN PLANT NITROGEN UPTAKE	
Abstract.....	108
Introduction.....	109
Materials and Methods.....	112
Results and Discussion.....	115
Acknowledgements.....	122
Chapter 7: CARBON AND NITROGEN DYNAMICS IN SOUTHERN AFRICAN SAVANNAS: THE EFFECT OF VEGETATION-INDUCED PATCH- SCALE HETEROGENEITIES AND LARGE SCALE RAINFALL GRADIENTS	
Abstract.....	123
Introduction.....	124
Materials and Methods.....	125
Results.....	131
Discussion.....	136
Acknowledgements.....	141
Chapter 8: CARBON AND NITROGEN PARASITISM BY XYLEM-TAPPING MISTLETOE ALONG THE KALAHARI TRANSECT: A STABLE ISOTOPE STUDY	
Abstract.....	142
Introduction.....	143
Materials and Methods.....	145
Results.....	148
Discussion.....	152
Acknowledgements.....	154
Chapter 9: SPATIAL HETEROGENEITY AND SOURCES OF SOIL CARBON IN SOUTHERN AFRICAN SAVANNAS	
Abstract.....	156
Introduction.....	158
Materials and Methods.....	160
Results and Discussion.....	165
Summary and Conclusions.....	170
Acknowledgements.....	172
Chapter 10: PREDICTING LEAF AND CANOPY ¹⁵N COMPOSITIONS FROM REFLECTANCE SPECTRA	
Abstract.....	173

Introduction.....	174
Materials and Methods.....	175
Results and Discussion.....	178
Conclusions.....	183
Acknowledgements.....	185
Chapter 11: SUMMARY.....	186
REFERENCE.....	190

LIST OF FIGURES

Figure 2.1. Locations of available data on soil physical and hydraulic as well as soil biogeochemistry properties along Kalahari transect. The column charts are the mean annual monthly precipitation data (1961-1990) of four sampling locations from Shugart et al. 2004.

Figure 2.2. Scanning electron microscope analysis of soil particles under canopy (A), inter-canopy (B) in Mongu and under canopy (C), inter-canopy (D) in Tshane.

Figure 2.3. Water retention curves for both beneath canopy (solid line) and intercanopy (dashed line) at four sampling locations (-7 – 0 MPa).

Figure 2.4. Depth profiles of carbon (left) and nitrogen (right) content of soils along Kalahari transect between and under canopies.

Figure 2.5. Depth profiles of soil $\delta^{15}\text{N}$ (left) and soil $\delta^{13}\text{C}$ (right) along Kalahari transect between and under canopies.

Figure 2.6. Soil surface CO_2 flux before and after the soil wetting in four locations along Kalahari transect.

Figure 2.7. Root density profiles for tree and grass functional types in different locations. A and B are from Hipondoka et al. 2003 and C is from Williams and Albertson 2004.

Figure 3.1. Study sites along the Kalahari Transect and the habitat characteristics. The values in each photo are the mean annual rainfall for each site (A). (B) The experimental layout and sampling scheme in 2005 (left) and 2006 (right).

Figure 3.2. Foliar $\delta^{15}\text{N}$ signatures in each treatment at each site for the wet season 2005 (A) and 2006 (B). Different capital letters indicate different means for the four treatments at each location.

Figure 3.3. Soil $\delta^{15}\text{N}$ signatures (0-5 cm) in each treatment at each site for the first year treatment (A) and second year treatment (B) in 2006. Different capital letters indicate different means for the four treatments at each location.

Figure 3.4. Foliar %N in each treatment at each site for the wet season 2005 (A) and 2006 (second year) (B). Different capital letters indicate different means for the four treatments in each location.

LIST OF FIGURES (CONTINUED)

Figure 3.5. Plant biomass in each treatment from each location in the wet season 2005 (A) and 2006 (B). Different capital letters indicate different means for the four treatments in each location. The insert in A shows the average soil moisture for the 2005 and 2006 growing seasons (D'Odorico et al. 2007) and the insert in B shows the wet season (October-April) rainfall data from satellite measurements from NASA's Tropical Rainfall Measuring Mission for 2005 and 2006.

Figure 3.6. Soil respirations in each treatment from each location in the wet season 2006.

Figure 4.1. Sampling locations along the Kalahari Transect precipitation gradient in southern Africa. Numbers in each photo are the mean annual precipitation.

Figure 4.2. The relationships between foliar $\delta^{15}\text{N}$ signatures and mean annual precipitation for C_3 and C_4 vegetation during dry and wet seasons along the Kalahari Transect. The liner equations for C_3 and C_4 vegetation: C_3 in wet season: $y = -0.0094x + 10.23$, $R^2 = 0.78$, $p < 0.0001$; C_3 in dry season: $y = -0.0106x + 10.86$, $R^2 = 0.62$, $p = 0.0003$; C_4 in wet season: $y = -0.0069x + 7.60$, $R^2 = 0.49$, $p < 0.0001$; C_4 in dry season: $y = -0.0069x + 7.96$, $R^2 = 0.28$, $p = 0.008$.

Figure 4.3. The relationships between foliar $\delta^{13}\text{C}$ signatures and mean annual precipitation for C_3 (A) and C_4 (B) vegetation during dry and wet seasons along the Kalahari Transect. The equations for C_3 and C_4 vegetation: C_3 in wet season: $y = -0.0042x - 24.37$, $R^2 = 0.96$, $p < 0.0001$; C_3 in dry season: $y = -0.0002x - 25.07$, $R^2 = 0.02$, $p > 0.05$; C_4 in wet season: $y = -0.000005x^2 + 0.0063x - 15.58$, $R^2 = 0.97$, $p < 0.0001$; C_4 in dry season: $y = -0.000004x^2 + 0.0042x - 14.93$, $R^2 = 0.61$, $p < 0.0001$.

Figure 4.4. The soil $\delta^{15}\text{N}$ (A) and $\delta^{13}\text{C}$ (B) signatures for C_3 and C_4 vegetation at wet and dry seasons along the Kalahari Transect. Different letters at each location indicate different means between four plant functional types and seasonality combinations within one site.

Figure 5.1. The Kalahari sands and sampling locations of the soil profiles. The Kalahari sand sheet distribution is adopted from Thomas and Shaw (1991).

Figure 5.2. The anion concentrations along the soil profiles in the dry season 2004: chloride, under tree/shrub canopy (A); chloride, between canopy (B); sulfate, under tree/shrub canopy (C); sulfate, between canopy (D); phosphate, under tree/shrub canopy (E); phosphate, between canopy (F); nitrate, under tree/shrub canopy (G); and nitrate, between canopy (H).

LIST OF FIGURES (CONTINUED)

Figure 5.3. The anion concentrations along the soil profiles in the wet season 2005: chloride, under tree/shrub canopy (A); chloride, between canopy (B); sulfate, under tree/shrub canopy (C); sulfate, between canopy (D); phosphate, under tree/shrub canopy (E); phosphate, between canopy (F); nitrate, under tree/shrub canopy (G); and nitrate, between canopy (H).

Figure 5.4. Soil moisture profiles from wet season 2005 (October-April) for under canopy (A) and between canopy (B) soils. The data are based on D'Odorico et al. (2007).

Figure 5.5. Soil $\delta^{15}\text{N}$ distributions for under tree/shrub canopy (A) and between canopy (B) soils in dry season 2004, and for under tree/shrub canopy (C) and between canopy (D) soils in wet season 2005.

Figure 6.1. Geographic location and vegetation structure of each study site along the Kalahari Transect. The grey area in the map is the Kalahari sand sheet.

Figure 6.2. Ammonium and nitrate abundance ($\mu\text{g cm}^{-3}$) of each study site along the Kalahari Transect based on nutrient data (Feral et al. 2003) and soil bulk density data (Wang et al. 2007a).

Figure 6.3. Greenhouse results for the $\delta^{15}\text{N}$ signature in plant roots and leaves for species from Tshane (A), Ghanzi (B), Pandamatenga (C) and Mongu (D) along the Kalahari Transect (KT). Dashed lines separate species at one site. The different capital letters indicate significantly different means between treatments (ammonium, nitrate and control) for either root or foliar samples for each species at each site using one-way ANOVA and Tukey *post hoc* test ($p < 0.05$). A significantly higher $\delta^{15}\text{N}$ signature in one of the labeled N forms (ammonium vs. nitrate) in any part of the plant sample (root, foliar or both) indicates the plant preference for that labeled N form. Panel E is the summary of changes in plant nitrogen uptake preference along the KT in greenhouse study. The x-axis identifies the different locations by mean annual precipitation (MAP). The y-axis is the $\delta^{15}\text{N}$ signature difference between $^{15}\text{NH}_4^+$ and $^{15}\text{NO}_3^-$ treatments for the species at each location. If the difference is a positive value, the plant prefers nitrate; if negative, the plant prefers ammonium. A value of 0 indicates no significant difference was detected. The larger difference was used to indicate the maximum preference if the ^{15}N signature in both the root and foliar samples were significantly different between $^{15}\text{NH}_4^+$ and $^{15}\text{NO}_3^-$ treatments.

Figure 6.4. Field results for the $\delta^{15}\text{N}$ signature in plant roots and leaves for species from Tshane (A), Ghanzi (B), Maun (C) and Pandamatenga (D) along the Kalahari Transect (KT). Dashed lines separate species at one site. The different capital letters indicate

LIST OF FIGURES (CONTINUED)

significantly different means between treatments (ammonium, nitrate and control) for either root or foliar samples for each species at each site using one-way ANOVA and Tukey *post hoc* test ($p < 0.05$). A significantly higher $\delta^{15}\text{N}$ signature in one of the labeled N forms (ammonium vs. nitrate) in any part of the plant sample (root, foliar or both) indicates the plant preference for that labeled N form. Panel E is the summary of changes in plant nitrogen uptake preference along the KT in field study with the same layout as Figure 3E.

Figure 6.5. Greenhouse results for the $\delta^{15}\text{N}$ signatures in plant roots and leaves for species from Pandamatenga. A doubled mineral N concentration with the same $\delta^{15}\text{N}$ enrichment was used for these two species. Dashed lines separate the two species. The different capital letters indicate significant differences in the means among treatments (ammonium, nitrate and control) for either root or foliar samples for each species using one-way ANOVA and Tukey *post hoc* test ($p < 0.05$). A significantly higher $\delta^{15}\text{N}$ signature in one of the labeled N forms (ammonium vs. nitrate) in any part of the plant sample (root, foliar or both) indicates the plant (at the sample base, not the population base) preference for that labeled N form.

Figure 7.1. Schematic representation of compartments and fluxes of the coupled C-N model. White compartments and dashed lines represent N pools and fluxes; shaded compartments and continuous lines refer to the corresponding C pools and fluxes (Eqs. (2) – (7)). The combination of the fluxes Φ (defined to keep $(\text{C} / \text{N})_b$ constant) and Φ_{MIT} (the fraction of decomposed N transferred to ammonium) define gross mineralization and immobilization, as described by Porporato et al. (2003) and Manzoni and Porporato (2007).

Figure 7.2. Soil moisture dynamics (s) and rainfall depth time series (h) in the under canopy (thick lines) and in the open canopy areas (light lines) in Tshane (A) and Pandamatenga (B). Right panels show the theoretical steady state soil moisture pdfs for the different locations and microsites (pdfs are computed following Laio et al., 2001).

Figure 7.3. Soil litter C dynamics (left panels) and pdfs (right panels) in the under canopy (thick lines) and in the open canopy soils (thin lines) in Tshane (A) and Pandamatenga (B). Note that, at a certain site, the same stochastic rainfall realization has been used for both open canopy and under canopy areas.

Figure 7.4. Soil nitrate pool dynamics in the under canopy soils and in the open canopy areas in Tshane and Pandamatenga. The solid line represents the mean of the observed values.

LIST OF FIGURES (CONTINUED)

Figure 7.5. Soil nitrate leaching dynamics in the under canopy soils and in the open canopy areas in Tshane and Pandamatenga.

Figure 8.1. Sampling locations for mistletoe-host pairs along the Kalahari transect.

Figure 8.2. *Tapinanthus oleifolius* (Wendl.) Danser grows on *Acacia mellifera* Benth. (A) and *Acacia leuderitzii* Engl. (B) in Tshane.

Figure 8.3. The correlation between foliar $\delta^{15}\text{N}$ of mistletoes and their host plants. Each point represents a mistletoe-host pair ($r = 0.64$, $p = 0.02$).

Figure 8.4. The correlation between foliar %N of mistletoes and their host plants. Each point represents a mistletoe-host pair ($r = 0.13$, $p = 0.68$).

Figure 8.5. The correlation between $\delta^{13}\text{C}$ and host %N for either mistletoes or host plants. Each point represents either an individual mistletoe or an individual host ($r = 0.66$, $p = 0.01$ for mistletoes and $r = -0.14$, $p = 0.64$ for hosts).

Figure 9.1. Sampling locations and rainfall characteristics along the Kalahari Transect. The column charts are the mean annual monthly precipitation data (1961-1990) of the two sampling locations from Shugart et al. (2004).

Figure 9.2. Semivariograms of $\delta^{13}\text{C}$ at Tshane (A), Mongu (B), and semivariograms of %C at Tshane (C) and Mongu (D) along the Kalahari Transect using spherical models, and semivariograms of $\delta^{13}\text{C}$ (E) and %C (F) at Tshane using hole-effect model. For (E) and (F), the open circles are actual data points and the filled circles are the modeled data points, and the $R^2 = 0.932$ and 0.928 for (E) and (F) respectively. Under the curve is the summary of semivariogram spherical model parameters. Proportion structural variation ($C/(C + C_0)$) is used as an index of the magnitude of spatial dependence.

Figure 9.3. The relative contributions to soil C from C_3 and C_4 vegetation for both under canopy (grey bar) and between canopy (white bar) areas at Tshane and Mongu. The contribution differences between under and between canopy areas for each vegetation type at one particular location (e.g., C_3 vegetation contributions to soil C at under and between canopy areas at Tshane) were tested using Kuiper two-sample nonparametric test (due to the spatial correlations between the data points) and the significant differences at 0.05 significance level were indicated by asterisk.

Figure 9.4. The percentage of tree contributions to soil carbon at Tshane (A) and Mongu (B) along the entire 300 m transect using $\delta^{13}\text{C}$ mixing ratio calculations. The solid lines are the means of the contribution at each site. SD stands for standard deviation.

LIST OF FIGURES (CONTINUED)

Figure 10.1 (A) Canopy level foliar $\delta^{15}\text{N}$ in four successional fields at the Blandy Experimental Farm, Virginia (Different capital letters indicate different mean values of foliar $\delta^{15}\text{N}$). (B) Species sampling list and leaf level foliar $\delta^{15}\text{N}$ in Ghanzi, Botswana. ALE (*Acacia leuderitzii*), AME (*Acacia mellifera*), GFL (*Grewia flava*), SPA (*Schmidtia pappophoroides*), TSE (*Terminalia sericea*).

Figure 10.2 (A) Coefficients of correlation between foliar $\delta^{15}\text{N}$ and leaf-level reflectance (R) (dash horizontal bars indicate the area of significance, $p < 0.05$; solid horizontal bars indicate the area of significance, $p < 0.01$, the regions marked with an asterisk indicate regions that may be useful for predicting foliar $\delta^{15}\text{N}$, the ranges of wavelength for

asterisk regions from left to right are $\lambda = 483\text{-}517$ and $\lambda = 617\text{-}703$ nm). (B) Coefficients of correlation between foliar $\delta^{15}\text{N}$ and canopy-level reflectance (R) (dash horizontal bars indicate the area of significance, $p < 0.05$; solid horizontal bars indicate the area of significance, $p < 0.01$, the regions marked with an asterisk indicate regions that may be useful for predicting foliar $\delta^{15}\text{N}$, the ranges of wavelength for asterisk regions from left to right are $\lambda = 670\text{-}694$, $\lambda = 1098\text{-}1319$ and $\lambda = 1480\text{-}1522$ nm).

Figure 10.3 (A) Coefficients of correlation between foliar $\delta^{15}\text{N}$ and leaf-level first difference of $\log 1/R$ ($\log 1/R$)' (dash horizontal bars indicate the area of significance, $p < 0.05$; solid horizontal bars indicate the area of significance, $p < 0.01$, the regions marked with an asterisk indicate regions that may be useful for predicting foliar $\delta^{15}\text{N}$, the ranges of wavelength for asterisk regions from left to right are $\lambda = 587\text{-}637$, $690\text{-}745$, $798\text{-}940$ and $1504\text{-}1573$ nm). (B) Coefficients of correlation between foliar $\delta^{15}\text{N}$ and canopy-level first difference of $\log 1/R$ ($\log 1/R$)' (dash horizontal bars indicate the area of significance, $p < 0.05$; solid horizontal bars indicate the area of significance, $p < 0.01$, the regions marked with an asterisk indicate regions that may be useful for predicting foliar $\delta^{15}\text{N}$, the ranges of wavelength for asterisk regions from left to right are $\lambda = 517\text{-}535$, $580\text{-}590$, $639\text{-}661$, $693\text{-}708$, $1249\text{-}1254$, $1345\text{-}1358$, $1509\text{-}1604$ and $1760\text{-}1778$ nm).

LIST OF TABLES

Table 2.1. Location and general characteristic of four sampling sites along Kalahari transect.

Table 2.2. Soil physical and hydraulic properties of Kalahari sands.

Table 2.3. Soil color and particle distribution with depth for under canopy and intercanopy soil samples for the four Kalahari-transect sites. Munsell color system has three components: hue (a specific color), value (lightness and darkness), and chroma (color intensity). Soil color is noted as: hue value/chroma and actual color.

Table 2.4. Surface soil (0-20cm) particle distribution for under canopy and inter-canopy sands at the Mongu and Tshane locations.

Table 2.5. Relative soil moisture at wilting point between inter-canopy and under canopy of the four locations along Kalahari Transect.

Table 2.6. Soil surface (0-5cm) C, N and their isotopic composition changes (mean \pm stderr, n = 5) along the transect measured for dry season (August) 2004.

Table 2.7. Soil ammonium and nitrate concentration and their isotopic compositions along the Kalahari transect.

Table 2.8. Soil crusts N fixing activities along the Kalahari transect estimated by *in situ* acetylene reduction assays.

Table 3.1. The two-way ANOVA results (F-values) on various response variables with site and treatment as two main effects.

Table 4.1. The %C, %N and isotope (^{13}C and ^{15}N) content (Mean \pm Standard error) for C_4 vegetation along the Kalahari Transect in wet season 2005.

Table 4.2. The % C, %N and isotope ($\delta^{13}\text{C}$ and $\delta^{15}\text{N}$) content (Mean \pm Standard error) for C_3 vegetation along Kalahari Transect in wet season 2005.

Table 5.1. Location, site general characteristic and soil physical properties of the four sampling sites along the Kalahari Transect.

Table 6.1. Field characteristics of five study sites along the Kalahari Transect and species list for greenhouse and field experiment.

Table 7.1. Soil, vegetation and rainfall parameters at Tshane and Pandamatenga along the Kalahari Transect.

LIST OF TABLES (CONTINUED)

Table 7.2. Observed soil moisture, nitrogen and carbon pool size and fluxes at Tshane and Pandamatenga along the Kalahari Transect.

Table 7.3. Model output of the current and predicted changes in soil moisture, nitrogen and carbon pool size and fluxes (mean \pm standard deviation) at Tshane and Pandamatenga along the Kalahari Transect.

Table 8.1. The foliar $\delta^{15}\text{N}$, $\delta^{13}\text{C}$, %C, %N and C/N of mistletoe samples (*Tapinanthus oleifolius*) and their host plant at different sampling times and locations, and the heterotropy (H) of mistletoes. For each specific index (e.g., %C), different numbers indicate different means between the mistletoes and its host (paired t -test, $\alpha = 0.05$); different lower-case letters indicate different means for the same species (*Acacia leuderitzii* and *Acacia mellifera*) at two sampling times in Tshane (ANOVA, $\alpha = 0.05$); different upper-case letters indicate different means for *Acacia mellifera* at different locations (ANOVA, $\alpha = 0.05$).

Table 9.1. Summary of statistical parameters of soil $\delta^{13}\text{C}$ and %C at Tshane (dry) and Mongu (wet).

Table 9.2. Range (m) and proportion of structured variance ($C/(C_0 + C)$) for spherical models of variograms from both sites. "M" denote the mean jackknife estimate. "L" and "U" denote the lower and upper bounds of the 95% confidence estimates, respectively.

Table 10.1. Regressions predicting foliar $\delta^{15}\text{N}$ at both leaf level and canopy level.

Acknowledgement

During the past four years of study at the University of Virginia as a PhD student, I greatly benefited from the consistent encouragement and great guidance provided by my co-advisors Dr. Stephen Macko and Dr. Paolo D'Odorico. Their attitude toward science and life also influenced me a lot. It has been a great pleasure and fortune for me to work with them. I would also like to thank the rest of my committee: Dr. Howie Epstein, Dr. Bob Swap and Dr. Fred Damon for their generous support in lending instruments and sharing ideas during the pursuit of my degree. The success of the field research in rural African countries largely depended on the generous collaborations with the Ministry of Agriculture of Botswana, the office of the Permanent Secretary for the Western Province of Zambia, the Zambian Department of Meteorology and the Harry Oppenheimer Okavango Research Centre of the University of Botswana. This project originated from collaboration among several institutions. I would like to thank many people who have been involved in this project over the past four years: Lydia Ries, Greg Okin, Kelly Caylor, Chris Feral, Kebonyethata Dintwe, Todd Scanlon, Billy Mogojwa, Thoralf Meyer, Natalie Mladenov, Barney Kgope, Matt Therrell and Sue Ringrose.

My research was mainly funded by NASA-IDS2 (NNG-04-GM71G); with additional support from the Blandy Experimental Farm, Exploratory Award and a Moore Research Award from the Department of Environmental Sciences of University of Virginia.

Ms. Wendy Crannage in the Department of Biology at University of Virginia provided tremendous help in the greenhouse maintenance and the greenhouse work is an indispensable part of my dissertation.

My research has greatly benefited from the interactions with the interdisciplinary faculty and students in the department of Environmental Sciences. I especially thank Hank Shugart, Dave Carr, Manuel Lerdaui and Deb Lawrence for their “ecological input” to my dissertation in various ways. I would also like to thank Lydia Ries, Sujith Ravi and Junran Li for their companionship and the sharing of ideas on arid land research. I thank my lab mates, especially Bill Gilhooly, Pei-Jen Lee and Steph Harbeson for their technical support and instrument sharing. Thanks to the efforts of the current and former graduate students in Environmental Sciences, the department offers a very social and interactive atmosphere, which has made my busy academic life much more enjoyable. I am indebted for all those efforts.

Last and, of course, not least, I thank my lovely wife Jin Wang and my family for their consistent moral support and sacrifice during my years at graduate school. Their steadfast support will be the strong base and source of my long-term life and career goals.

Preface

This dissertation is comprised of eleven chapters. Chapters two through ten of this dissertation are designed as stand-alone research papers. At the time of writing, I have submitted nine of these as first author manuscripts that are either published (Chapter two and Chapter ten), in press (Chapter seven and Chapter eight) or currently in peer review (Chapter three to Chapter six and Chapter nine).

As a consequence of the structure of this dissertation (stand-alone manuscripts for each chapter), some introductory materials and method descriptions (e.g., the uniqueness of the Kalahari Transect and the Kalahari map) are repetitive. I apologize for this inconvenience, but I have chosen to leave these manuscripts unmodified (with the exception of the references which have been removed from the chapters, concatenated and placed in an identical format for consistency) in order to preserve the integrity of the original research papers. The single compiled reference list has been placed after Chapter eleven (the Summary section). I have also substituted the use of first-person plural in the research manuscripts with first-person singular in each chapter.

Lixin Wang
Charlottesville, VA
March 18, 2008

Chapter 1 Introduction

Savanna Ecosystems: Global Relevance and Scientific Challenges

Savannas are ecosystems where trees and grasses co-exist. Typically found both in temperate and tropical regions (e.g., Scholes and Archer, 1997), savannas are a very important biome. First, savanna ecosystems cover about 20% of the land surface of the Earth and contribute to approximately 29% of global terrestrial net primary productivity (Grace et al., 2006). Second, although savanna ecosystems cover a wide range of climatic conditions, they are mostly located in arid or semi-arid areas, where they are susceptible to the land-degradation dynamics associated with overgrazing, erosion-induced losses of soil nutrients, and a consequential diminishing in many ecosystem functions (e.g., Thomas et al., 2005). This process, known also as “desertification” has important impacts on both the environment and societies, owing to detrimental effects on local economies and the ability to cause mass migration (Reynolds et al., 2007). Third, savannas are one of the major unknowns in the evaluation of the global carbon budget and the improvement of current climate change predictions, requiring a better understanding of their CO₂ sink/source relationships. Currently savannas are considered a carbon neutral system (Veenendaal et al., 2004; Williams et al., 2007), however, depending on the disturbance regime and land management practices, savannas have the potential to become either large sinks or sources of carbon. Fourth, the impact of savannas on climate is not limited to their role on the global carbon budget. Simulations with regional climate models have indicated that tropical savannas (particularly those in sub-Saharan Africa) have an important impact on the regional climatology and rainfall regime, owing to their modification of surface attributes such as albedo (Charney, 1975), roughness, and soil moisture (Xue and Shukla,

1993; Xue and Shukla, 1996; Wang and Eltahir, 1999; Zeng et al., 1999), and consequentially enhance precipitation.

The picture emerging from these points is that the loss or disturbance of savanna ecosystems, particularly in the palaeo-tropics, may have important detrimental effect on the regional and global environment, as it may result in enhanced erosion (Thomas et al., 2005), changes in hydroclimatic conditions (e.g., Zeng et al., 1999), and the consequent loss in many ecosystem functions and services (Millennium Ecosystem Assessment) (2005).

Human beings are an important component of savanna ecosystems, particularly in southern Africa, where humans have been present for the last several thousands years. The the effect of humans on the coupled biosphere-climate system has been mostly mediated by their effect on vegetation. Vegetation is the most active player in these climate-ecosystem feedbacks. In order to investigate the impact of a changing climate on the savannas, it is crucial to understand the controlling factors of vegetation structure and function. The role of water availability as a limiting factor on savanna dynamics has been comprehensively documented (e.g., Scanlon et al, 2003; Scholes et al., 2002; Caylor et al. 2003). The role of soil nutrients, however, is much less understood and the effect of interactions between water and soil nutrients on vegetation productivity and how such interactions change as mean climatic conditions change are even less understood. Previous modeling and physiological studies conjectured a switch between water and nitrogen limitations taking place as annual precipitation exceeded a critical value in savanna ecosystems (Scanlon and Albertson, 2003; Midgley et al., 2004). In addition, although surface soil chemical properties have been investigated and documented for a

number of savanna ecosystems (Scholes and Walker 1993; Feral et al., 2003), the belowground resource distribution and its relation to aboveground properties, is less known. Besides soil nutrients, other aspects of savanna ecosystems, including the overall carbon budget, the soil carbon pool and its heterogeneity, sources of soil organic carbon (i.e., the relative importance of trees or grass plant residues as contributors to the soil organic matter), and their potential response to climate change remain poorly understood and quantified. Because climate change will likely alter the relative balance of plant type (C_3/C_4) in savannas, such a gap in knowledge will not only limit the understanding of southern African carbon cycling but also the contribution of this region globally. Addressing all of these questions will shed light on the functioning of savanna ecosystems under current climatic condition as well as their response to changes in climate.

This dissertation will concentrate on savanna ecosystems in the palaeo-tropics (i.e., the tropics of “the old world”), where the co-existence of trees and grasses has lasted for at least millions of years. To investigate possible changes in the soil biogeochemistry and vegetation responses of savanna ecosystems, this dissertation will rely on a “space for time substitution” along a rainfall gradient. To this end, the study area was selected in the Kalahari region, where a rainfall gradient exists on consistent uniform sandy soils. Situated in southern Africa, the Kalahari sand sheet covers a 2.5 million km² area, and is probably the largest continuous surface of sand in the world (Leistner, 1967). Geologically the Kalahari has been an area of active sediment accumulation from the late-Cretaceous, and the Kalahari sands are the most recent phase of this deposition. The absence of permanent surface water over most of the Kalahari has kept human settlement

to a minimum. As a consequence, the Kalahari is probably the most pristine of the southern African biomes.

The Kalahari Transect (KT) within the Kalahari sand sheet was identified by the IGBP (International Geosphere-Biosphere Programme) as one of the “mega-transects” for global change studies. The KT traverses a dramatic aridity gradient (from ~ 200 mm to more than 1000 mm of mean annual precipitation, through the Republic of South Africa, Botswana, Namibia and Zambia), on relatively homogenous soils (deep Kalahari sands). Recently field observations along the KT also showed that while nitrate levels remain fairly constant along the transect, ammonium is more abundant at the wetter end of the transect (Feral et al., 2003), leading to an ammonium/nitrate ratio gradient along the KT. Thus, with a remarkable rainfall and nutrient gradient on a homogeneous soil substrate, the KT provides the ideal setting to study carbon cycling, as well as nutrient and vegetation dynamics, without confounding soil effects.

Research questions/goals:

This thesis focuses on the relationships between soil biogeochemistry/soil water content, and the uptake of water and nutrients by savanna vegetation. Particularly, this study concentrates on southern African savanna ecosystems. To assess the impact of changes in climate on savanna ecosystems the following major questions are addressed,

1. What are the factors limiting grass production in savanna ecosystems, and how do the factors differ across regional rainfall gradients?
2. How do trees and grasses differ in water and nutrient use in these savanna ecosystems?

3. What are the belowground resource distributions, and how do they link to aboveground resource distributions?
4. What is the effect of rainfall variation on soil biogeochemical processes in these systems?
5. What determines the nitrogen uptake preferences of plants and how does this preference change with the variations of climatic conditions?
6. What are the contributions to soil carbon from trees and grasses, and how do they change with variations of climatic conditions?

Structure of the thesis

The thesis is structured as follows: This first chapter provides the rationale, framework and research objectives of this study. The second chapter presents a review of the current understanding of the physical and biogeochemical properties of Kalahari sands. The third chapter concentrates on the results of a field fertilization experiment to assess water and nitrogen limitations on grass productivity under different rainfall regimes along the rainfall/aridity gradient of the Kalahari Transect. The fourth chapter addresses the differences in water and nitrogen use between C₃ and C₄ plant functional types in the Kalahari region through the analysis of the natural abundance of stable isotopes ($\delta^{13}\text{C}$ and $\delta^{15}\text{N}$). The fifth chapter discusses the belowground distribution of resources in these systems. The sixth chapter investigates nitrogen uptake through both field and greenhouse experiments, using the unique rainfall/nutrient gradient existing along the Kalahari Transect. The seventh chapter presents a model-based study of water and nitrogen dynamics in the Kalahari at a daily time scale. The eighth chapter discusses the effect of plant-parasite relationships on the savanna vegetation in the Kalahari. The

ninth chapter explores the southern Africa soil carbon pool, its heterogeneity and sources (from trees or grasses). The tenth chapter presents a new technique developed to monitor the nitrogen stable isotope compositions in these savanna ecosystems and possibly elsewhere. The final chapter is a summary of the findings from this dissertation and an outlook for future directions.

Chapter 2 Biogeochemistry of Kalahari sands

ABSTRACT

The Kalahari sand sheet, with a 2.5-million km² area, is probably the largest continuous surface of sand in the world. The Kalahari Transect (KT) is one of a set of IGBP “megatransects” identified for global change studies and provides an ideal setting to investigate changes in ecosystem dynamics, vegetation composition and structure, and carbon or nutrient cycles along a spatial precipitation gradient without confounding soil effects. Soil physical properties remain poorly characterized along the KT. The present work provides a review of previous studies on the Kalahari soils combined with new results from recent analyses of physical (mostly hydraulic) and biogeochemical properties of the soil. In summary, the Kalahari soil is acidic, dominated by sand and nutrient poor. Nutrient contents, soil textures and soil hydraulic properties differ under and between canopies. Roots are concentrated in the top 80 cm of the soil, with grass roots more abundant and dominant close to the surface. Moreover, the distribution of tree roots does not exhibit a clear dominance over grasses at deeper soil layers. This review provides important baseline information for this system, as well as insights as to how biochemical processes vary along a rainfall gradient.

Keywords: Kalahari Transect, Hydraulic Properties, Biogeochemistry, Stable Isotopes, Sand Deposits

Wang, L., P. D’Odorico, S. Ringrose, S. Coetzee and S. Macko. 2007. Biogeochemistry of Kalahari sands. *Journal of Arid Environments*, 71(3) 259-279

1. INTRODUCTION

The north-south transect of the Kalahari (known as the Kalahari Transect, KT) is one of a set of IGBP (International Geosphere-Biosphere Programme) “megatransects” (e.g., Koch et al., 1995; Scholes et al., 2002) identified for global change studies. This work focuses on an analysis of the biogeochemistry of the Kalahari sands in order to develop insights as to how biochemical processes vary along the north-south rainfall gradient. The KT provides an ideal setting to investigate changes in ecosystem dynamics, composition and structure of vegetation, and carbon (C) or nutrient cycles along a spatial gradient of precipitation while minimizing the confounding effects of soil heterogeneity.

The Kalahari is essentially a plateau area uplifted following the breakup of Gondwanaland, at least 65 million years ago (Thomas and Shaw, 1991). The plateau edges were uplifted as the continent moved northwards. Both fluvial and dune sediments are believed to have infilled the uplifted basin with mainly sands interbedded with calcrete and silcrete. Areas within the basin have also been shown to comprise weathered material (Haddon, 2000; McFarlane and Eckardt, 2004). Most of the sands have assumed diverse post Gondwana histories including up to 5.0 Ma of weathering, resorting and deposition on previously exposed African surface (Baillieul, 1975; Thomas and Shaw, 1991; Ringrose et al., 2002; Huntsman-Mapila et al., 2005). Most palaeo-environmental work has focused in the central Kalahari Makgadikgadi-Okavango-Zambezi (MOZ) basin area either on Kalahari dune sequences (e.g., Grove, 1969; Lancaster, 1986; Lancaster, 2000; Thomas and Shaw, 2002; Thomas et al., 2003) or on multiple palaeo-lake sequences as described in Cooke (1980) and Cooke and Verstappen (1984). Thomas and Shaw (1991; 1993; 2002) and Huntsman-Mapila et al. (2006) identify wetter (flooding) periods at ca. 40 000

BP or later partially based on ^{14}C ages. Multiple periods of aeolian activity have been age-dated as occurring in the late Pleistocene with Optical Stimulated Luminescence (OSL) ages indicating more arid episodes between 95-115, 41-46 and 20-26 Ka BP (Stokes et al., 1997).

The present day Kalahari climate ranges from arid to semi-arid/subhumid with relatively strong seasonal and interannual variations in precipitation. A major characteristic is that potential evapotranspiration (PET) is typically 3 times the annual rainfall; the rainfall variability ranges from less than 200 mm in southwest Botswana to over 1000 mm in the north (i.e., western Zambia). The rainy season (Fig. 2.1) is typically from October to April during the austral summer months when maximum growth is experienced while dormancy is characteristic of the dry winter months (Shugart et al., 2004).

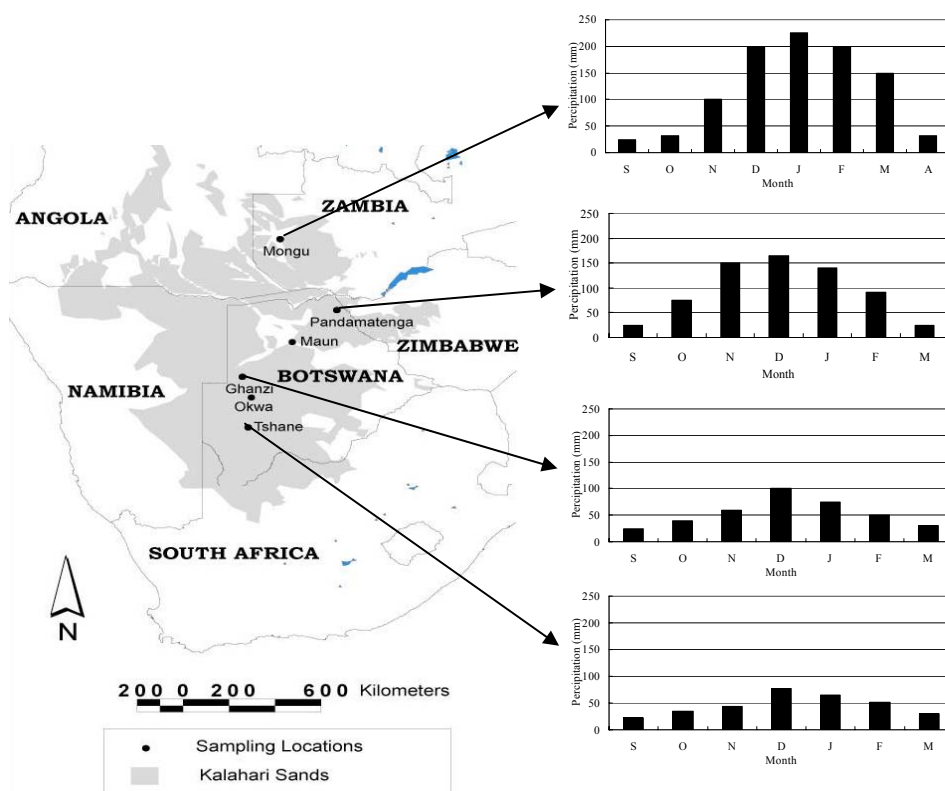


Figure 2.1. Locations of available data on soil physical and hydraulic as well as soil biogeochemistry properties along Kalahari transect. The column charts are the mean annual monthly precipitation data (1961-1990) of four sampling locations from Shugart et al. 2004.

Vegetation on the KT is dominated by different types of savannas ranging from fine-leaved plants in the south (nutrient-rich) to broad-leaved plants in the north (nutrient-poor). The distribution of Kalahari vegetation has been investigated through a number of field observations (e.g., Ringrose et al., 1998; Scholes et al., 2002; Caylor et al., 2003; Privette et al., 2004; Scholes et al., 2004) and modeling studies (Jeltsch et al., 1998; Jeltsch et al., 1999b; Caylor et al., 2004; Privette et al., 2004). Some key findings from these studies include the assessments that: 1) woody plant biomass increases from south to north. Above the minimum level of 200 mm MAP, the woody basal area increases at a rate of ca. $2.5 \text{ m}^2 \text{ ha}^{-1}$ per 100 mm MAP. The mean height of the 10% tallest trees also increases along the gradient, reaching 20 m at ca. 800 mm MAP (Scholes et al., 2002); 2) aggregation of plant individuals has been observed in the vegetation communities at most sites, with the exception of the arid southernmost sites. The spatial distribution for the largest 25% of individuals is predominantly random but juveniles tend to cluster around mature individuals (Caylor et al., 2003); 3) interactions among different life forms play a crucial role in vegetation productivity across the rainfall gradient (Caylor et al., 2004).

Despite the relevance of the KT to regional and global change studies, the soil physical properties remain poorly characterized (c.f., Joshua, 1981). This is a major limitation, as the response of arid and semiarid ecosystems to changes in rainfall regime is mediated by variations in the soil moisture dynamics, which, in turn, depend on the soil hydraulic properties. In contrast, a few studies have investigated the biogeochemical properties of the Kalahari sands (Skarpe and Bergstrom, 1986; Dougill et al., 1998; Feral et al., 2003; Hudak et al., 2003; Pardo et al., 2003; Aranibar et al., 2004; Bird et al., 2004) although a comprehensive synthesis of the main results remains to be accomplished. This

paper provides a brief review of previous studies on the sandy Kalahari soils (hereafter called the Kalahari sands) combined with previously unpublished results from recent analyses of the soil physical (mostly hydraulic) and biogeochemical properties.

2. MATERIALS AND METHODS

2.1 Field Sampling

The new results presented in this review were obtained from soil samples collected at four locations (Tshane, Ghanzi, Pandamatenga and Mongu) along the Kalahari transect during the dry season (August) of 2004 (Fig. 2.1). The climate and vegetation characteristics of these field sites are reported in Table 2.1. At each site, surface soil samples were collected (in five replicates) from both beneath tree canopies and in open areas. Two 1-meter-deep soil pits were dug from each of the four locations: one in an open area and the other under a tree canopy. The soil pits were used to establish the soil profile at different depths (at 10 cm intervals). All soil samples were air-dried in the field and stored in plastic bags. In the wet season of 2006, two to three soil pits were dug

Table 2.1. Location and general characteristic of four sampling sites along Kalahari transect.

	Location	Elevation (m)	Rainfall, mm/yr ^a	Vegetation type	Woody cover ^a
Tshane	24.17°S 21.89°E	1115	365	Open <i>Acacia</i> savanna	14
Ghanzi	21.65°S 21.81°E	1125	400	<i>Acacia-Terminalia</i> woodland	20
Pandamatenga	18.66°S 25.50°E	1082	698	Baikea woodland	40
Mongu	15.44°S 23.25°E	1076	879	Miombo woodland	65

^a Rainfall, woody cover data are from Caylor et al. (2006).

from each location, and soil samples from every 10 cm interval were collected for soil particle analysis, soil color and soil scanning electron microscope (SEM) analysis.

2.2 Measurement of physical/hydraulic properties

Soil physical properties were measured on composite samples obtained by mixing five soil samples collected at each site, either from intercanopy or from subcanopy soils. The size of soil grains was expressed using phi (ϕ) units defined as $[\phi = -\log_2(D_{\text{mm}}/1_{\text{mm}})]$, where D_{mm} is the grain diameter in mm. Soil samples were dry-sieved at 1 and 0.5 ϕ intervals (c.f., Lancaster, 1986) after passing through a sample splitter. Sieving took place using nested sieves (2.0-0.063 μm or -1 to 4 ϕ) on an automatic Retsch shaker, whereby 100 g of loose sand was sieved for 15 min. Size analysis followed procedures devised by Folk and Ward (1957) as updated in Tucker (2001). The saturated hydraulic conductivity (K_s) was measured using a falling-head permeameter on composite samples (~300g) from sub-canopy and inter-canopy soils at each site. Five or six measurements were made for each sample and averaged (Table 2.2). One-way ANOVA was used to compare the difference (at 0.05 significance level) in K_s between intercanopy and subcanopy soils at each sampling location.

The bulk density, ρ_b , was calculated at each site for both subcanopy and intercanopy soils by determining the weight of 40 ml of oven-dried samples (105°C for 48 hours). Soil porosity, n , was estimated as $n = 1 - \rho_b/\rho_s$, assuming a value of 2.65 g/cm³ for the density, ρ_s , of the grains of quartz sand (Brady and Weil, 1999).

Soil pH values were measured using a portable pH meter (Hanna Instruments-HI 9023, Woonsocket, RI, USA) on 5-gram samples of composite soil mixed with DI water.

The mixing consisted of 1 hour of shaking, followed by a half-hour-long settling before making measurements (Thomas, 1996). To quantify the soil surface CO₂ flux along the transect, soil respiration was measured in 24 random locations using EGM-4 CO₂ analyzer at each site in January 2006. To examine the effect of precipitation on the soil surface CO₂ flux, 600 mL water was poured into a soil collar (40 cm x 20 cm) before measurement, and CO₂ fluxes were measured immediately after the water had infiltrated.

The water retention curves for composite soil samples from both intercanopy and subcanopy soils were determined at each site by measuring the water potential values - using a water activity meter, DECAGON AquaLab Series 3T (DECAGON Devices, Pullman, WA, USA) and gravimetric moisture content. Water activity readings, α_w = RH/100, (with RH being the relative humidity), were converted into matric potential values as $\Psi_m = (RT/M_w) \cdot \ln(RH/100)$ (Edlefsen and Anderson, 1943), where R is the universal gas constant ($8.314472 \text{ J} \cdot \text{K}^{-1} \cdot \text{mol}^{-1}$), T is the absolute temperature (K) and M_w is the molecular mass of water. The water potentials in the wetter range ($> -0.5 \text{ MPa}$) were measured using a WP4-T Dewpoint Potential Meter (DECAGON Devices, Pullman, WA, USA).

2.3 Geochemical analyses

Soil samples for isotopic and elemental analyses were oven dried (at 60°C) in the laboratory, sieved and homogenized using mortar and pestle. Each of the five replicates of samples collected from soils beneath tree canopies and open areas was analyzed for soil organic C, total nitrogen (N), $\delta^{13}\text{C}$ and $\delta^{15}\text{N}$. Total C and N content were measured using an Elemental Analyzer (EA, Carlo Erba, NA1500, Italy). Stable C/N isotopic analysis was performed using a Micromass Optima Isotope Ratio Mass Spectrometer

(IRMS) connected to the EA (GV/Micromass, Manchester, UK). Stable isotopic compositions are reported in the conventional form:

$$\delta^X E (\text{‰}) = [(X_E / Y_E)_{\text{sample}} / (X_E / Y_E)_{\text{standard}} - 1] \times 1000$$

where E is the element being measured, x is the heavier isotope and y is the lighter isotope. So that $(X_E / Y_E)_{\text{sample}}$ and $(X_E / Y_E)_{\text{standard}}$ are the isotopic ratios of the sample and standard, respectively. The stable isotopic composition of C and N will be denoted as $\delta^{13}\text{C}$ (‰) and $\delta^{15}\text{N}$ (‰), respectively. The standards for C and N stable isotopes are Pee Dee Belemnite (PDB) and atmospheric molecular N (N_2), respectively. Reproducibility of these measurements is typically better than 0.2‰. One-way ANOVA was used to test the significance of differences (0.05 significance level) found in each parameter between intercanopy and subcanopy soils at each site.

3. PHYSICAL PROPERTIES OF KALAHARI SANDS

3.1. Soil Texture

With the exception of the fine-textured soils found in pan and fluvial deposits, the Kalahari is dominated by sandy soils, mostly white, pink, and red in color (Leistner, 1967). The Kalahari sands are chiefly quartz, with small contributions of zircon, garnet, feldspar, ilmenite and tourmaline. Compared to other sand deposits in Africa (e.g., the Namib or the Sahara) the sand grains in the Kalahari are less well-rounded (Leistner, 1967) likely due to less weathering (Ringrose et al., 2006). The porosity of the Kalahari sands ranges between 0.43 to 0.49 for the four locations considered in this study (Table 2.2), whereas the bulk density is between 1.34 - 1.51 g/m^3 (Table 2.2). Both the

porosities and the bulk densities of the Kalahari sands have limited variation between the canopy and intercanopy (Table 2.2).

The soil texture is dominated by sand (>95%) at all sites (Table 2.2). Soils are acidic ($\text{pH} < 7.0$) along the entire transect. Soils at Ghanzi and Pandamatenga have a slightly higher pH than the other sites, possibly resulting from a proximity of near surface bedrock in these areas (Table 2.2). In the case of Ghanzi, the higher pH is probably due to the calcareous substrate, while the higher pH value in Pandamatenga is likely influenced by agriculture practices taking place in the commercial farms surrounding this site (e.g. fertilizer use, tillage). There are also only limited differences in soil pH between areas located under tree canopy and open canopy at all sites (Table 2.2). At the dry end of the Kalahari transect the carbonate rich layer is deeper under the canopy than in open canopy areas, while these differences are much smaller at the wet end (D'Odorico et al., 2007). In addition, the depth of the carbonate rich layer increases with the mean annual precipitation along the rainfall gradient, with a mean depth (between canopy and intercanopy sites) of 40 cm at Tshane, 65 cm at Pandamatenga and 72 cm at Mongu (D'Odorico et al., 2007). The variations in the depth of the carbonate rich layer between the soils under the canopy and open canopy areas are indicative of differences in long-term soil moisture dynamics, with deeper moisture percolation in the soils under tree canopies. This fact has implications for the nutrient distribution reported in Section 4.

Based on particle size distributions, the sands from Ghanzi are the finest among the four sites with mean particle size of 2.15ϕ under the canopies (0-192 cm) and 2.56ϕ for intercanopy samples (0-190 cm). No significant change in grain size is observed until the lower calcrete layer is reached, where the grain size increases to $1 \sim 1.8 \phi$. Sand

Table 2.2. Soil physical and hydraulic properties of Kalahari sands.

		Tshane	Ghanzi	Okwa	Pandamatenga	Mongu
Porosity	n	0.47 ^a , 0.45 ^b	0.49 ^a , 0.47 ^b		0.45 ^a , 0.43 ^b	0.44 ^a , 0.43 ^b
Sat. Hydr.		13.80 ^{aA}	11.03 ^{aA}		26.03 ^{aA}	39.85 ^{aA}
Conductivity K _s (m d ⁻¹)		8.00 ^{bB}	10.83 ^{bA}		31.20 ^{bB}	27.22 ^{bB}
Bulk						
Density	(g cm ⁻³)	1.41 ^a , 1.47 ^b	1.34 ^a , 1.42 ^b		1.46 ^a , 1.51 ^b	1.47 ^a , 1.50 ^b
Soil Texture ³		98.0-0.0-2.0 ¹	96-1-3 ²	95.9-2.4-1.6 ¹	96.8-2.1-1.1 ¹	97.5-1.9-0.6 ¹
pH		5.2 ¹ , 6.42	6.12 ^a , 6.16 ^b	5.6 ¹	6.62 ^a , 6.10 ^b	5.02 ^a , 5.11 ^b

1 Aranibar et al. 2004 Global Change Biology, 10:359-373

2 Ravi et al. 2006 Sedimentology, 53:597-609

3 Sand-Silt-Clay Ratio

a: under canopy, b: inter-canopy

Different capital letters in K_s indicate different means between under canopy and intercanopy at 0.05 significance level.

particle sizes from Tshane are the second finest with a mean particle size of 2.23 ϕ under the canopy and 2.11 ϕ for intercanopy (20-200 cm), and the particle size did not change with depth (20-500 cm) in both cases. Mean particle size in Pandamatenga is 1.84 ϕ under canopy (0-200 cm) and 1.79 ϕ for intercanopy (0-200 cm) with limited variation with depth in both cases. Mean particle size in Mongu is similar to Pandamatenga with particle size of 1.72 ϕ under the canopy (10 –300 cm) and 1.71 ϕ (10-300 cm) for intercanopy with limited variation with depth in both cases (Table 2.3). These results suggest that the soil profiles are relatively uniform and that at the wet end of the transect (Mongu and Pandamatenga) there are no significant differences in grain size between canopy and intercanopy soils, while the drier (Tshane and Ghanzi) sites have finer soils under the canopy. Moreover at the drier sites soils are slightly finer than at the wetter sites.

Table 2.3. Soil color and particle distribution with depth for under canopy and intercanopy soil samples for the four Kalahari-transect sites. Munsell color system has three components: hue (a specific color), value (lightness and darkness), and chroma (color intensity). Soil color is noted as: hue value/chroma and actual color.

Soil name	Mean (phi units)	Munsell Color
Mongu pit1-10cm ^a	1.70	5YR 6/4 Light reddish brown
Mongu pit1-50cm ^a	1.70	5YR 6/6 Reddish yellow
Mongu pit1-100cm ^a	1.75	5YR 6/6 Reddish yellow
Mongu pit1-150cm ^a	1.65	7.5YR 6/8 Reddish yellow
Mongu pit1-200cm ^a	1.72	5YR 6/6 Reddish yellow
Mongu pit1-300cm ^a	1.75	5YR 6/6 Reddish yellow
Mongu pit2-10cm ^b	1.62	5YR 6/2 Pinkish gray
Mongu pit2-50cm ^b	1.70	5YR 6/6 Reddish yellow
Mongu pit2-100cm ^b	1.75	5YR 6/6 Reddish yellow
Mongu pit2-150cm ^b	1.72	5YR 6/6 Reddish yellow
Mongu pit2-200cm ^b	1.73	7.5YR 7/6 Reddish yellow
Mongu pit2-300cm ^b	1.78	7.5YR 7/8 Reddish yellow
Mongu pit3-150cm ^b	1.77	5YR 6/6 Reddish yellow
Mongu pit3-200cm ^b	1.78	5YR 7/8 Reddish yellow
Mongu pit3-300cm ^b	1.80	5YR 7/8 Reddish yellow
Pandamatenga 0cm ^b	1.77	10YR 4/2 Dark grayish brown
Pandamatenga 50cm ^b	1.81	10YR 6/4 Light yellowish brown
Pandamatenga 100cm ^b	1.76	7.5YR 6/6 Reddish brown
Pandamatenga 150cm ^b	1.79	7.5YR 6/6 Reddish yellow
Pandamatenga 200cm ^b	1.81	10YR 6/6 Brownish yellow
Pandamatenga 0cm ^a	1.67	10YR 4/2 Dark grayish brown
Pandamatenga 50cm ^a	2.13	10YR 6/4 Light yellowish brown
Pandamatenga 100cm ^a	1.80	7.5YR 6/6 Reddish yellow
Pandamatenga 150cm ^a	1.75	10YR 6/8 Brownish yellow
Pandamatenga 200cm ^a	1.85	7.5YR 6/6 Reddish brown
Ghanzi 0cm ^a	2.50	5YR 4/6 Yellowish red
Ghanzi 50cm ^a	2.40	2.5YR 4/6 Red
Ghanzi 100cm ^a	2.45	2.5YR 4/6 Red
Ghanzi 150cm ^a	2.45	5YR 5/8 Yellowish red
Ghanzi 192cm ^a	0.97	10YR 6/4 Light yellowish red
(reaching calcrete layer)		
Ghanzi 0cm ^a	2.55	5YR 5/6 Yellowish red
Ghanzi 50cm ^a	2.52	5YR 5/6 Yellowish red
Ghanzi 100cm ^a	2.50	5YR 5/8 Yellowish red
Ghanzi 0cm ^b	2.50	5YR 4/4 Reddish brown
Ghanzi 50cm ^b	2.90	2.5YR 4/6 Red
Ghanzi 100cm ^b	2.37	2.5YR 4/6 Red
Ghanzi 150cm ^b	1.53	2.5YR 6/4 Light reddish brown

(reaching calcrete layer)		
Ghanzi 190cm ^b	1.83	2.5YR 6/4 Light reddish brown
(reaching calcrete layer)		
Tshane 20cm ^a	2.32	5YR 5/6 Yellowish red
Tshane 50cm ^a	2.20	5YR 5/6 Yellowish red
Tshane 100cm ^a	2.27	5YR 6/8 Yellowish red
Tshane 150cm ^a	2.30	5YR 6/6 Yellowish red
Tshane 200cm ^a	2.10	5YR 6/8 Yellowish red
Tshane 500cm ^a	2.18	5YR 6/8 Yellowish red
Tshane 20cm ^b	1.92	5YR 5/6 Yellowish red
Tshane 50cm ^b	2.18	5YR 5/6 Yellowish red
Tshane 100cm ^b	2.15	5YR 5/6 Yellowish red
Tshane 150cm ^b	2.02	5YR 5/8 Yellowish red
Tshane 200cm ^b	2.30	5YR 5/8 Yellowish red

a: under canopy, b: inter-canopy

For the surface soil (0-20 cm), there is no noticeable particle size difference between inter-canopy sands and those from under the canopy from Mongu. In Tshane, however, there is an obvious difference in particle size distribution between intercanopy and under canopy. In fact, the fine particle size fraction (i.e., with size <0.063 mm) was 1.44% and 0.34% in the soils located under and between the tree canopies, respectively (Table 2.4).

Table 2.4. Surface soil (0-20cm) particle distribution for under canopy and inter-canopy sands at the Mongu and Tshane locations.

	Depth	%Coarse sand (ϕ -1 to 1 or 2-0.5mm)	%Medium sand (ϕ 1-2 or 0.5-0.25mm)	%Fine sands (ϕ 2-4 or 0.25-0.063mm)	%Silt and Clay (ϕ >4 or < 0.063mm)
Mongu					
Under canopy	10cm	1.96	72.39	25.01	0.43
Inter-canopy	10cm	0.88	77.83	20.89	0.4
Tshane					
Under canopy	20cm	0.45	37.27	60.84	1.44
Inter-canopy	20cm	7.44	73.15	19.07	0.34

The portion of the sample finer than 0.063 mm was comprised of sub-rounded to sub-angular quartz particles, with evidence of a secondary Si coating for under canopy soils in Mongu (Fig. 2.2A). Coatings do not occur extensively around the grains although there is localized evidence of greater Si accumulation with subsequent coating disintegration in the form of pock-marking. There is no evidence of chemical etching on the grain surfaces with some of the surfaces being angular and depicting the original crystal structure. The under canopy sample from Mongu is chiefly quartz with less than 5% non-quartz. The non-quartz particles, which are mainly feldspars and micas, show more weathering effects (and are therefore more disintegrated) than the quartz. Fungal hyphae and organic remnants were also evident (Fig. 2.2A).

Similar patterns are evident in the intercanopy samples at Mongu. In the sample fraction finer than 0.063 mm, cleaner sub-rounded but mainly sub-angular quartz particles were evident with less evidence of a secondary Si coating (Fig. 2.2B). Again, the sample consists mainly of quartz particles with less than 5% non-quartz, comprising feldspars and micas which show more disintegrated weathering effects than the quartz. Fungal hyphae were also evident (Fig. 2.2B).

More equi-granular quartz grains were found under canopy in Tshane which also exhibited relatively abundant fungal hyphae. The sample consisted of mixed coated and angular (faces showing) fragments, but at this location the secondary silica-rich SiO_2 coating was more apparent, and much of the coating was pitted and disintegrated. The disintegration was flaking off the coating, adding fine particles which may be mixed with possible clay flakes and organic fragments (Fig. 2.2C).

The intercanopy sample in Tshane also consisted of equi-granular grains which are coated and weathered with evidence of coating disintegration. There was a higher proportion of quartz grains in the Tshane samples with non-quartz grains approximating 2%. There is more evidence of particle fracturing/fragmentation and coating induced angularity, i.e. when coating peels off, angular particles remain beneath, as the coating itself induces a form of weathering preferentially along the crystal faces as seen in Okavango delta samples. Organic fragments and fungal hyphae were also evident (Fig. 2.2D).

3.2 Soil hydraulic properties

The saturated hydraulic conductivity (K_s) was found to increase from south to north along the rainfall gradient (Table 2.2), presumably due to a higher soil organic matter existing at the more humid sites. At Tshane and Mongu (the two extreme ends of the transect), K_s was significantly higher under canopy than in open areas, while no difference existed at Ghanzi.

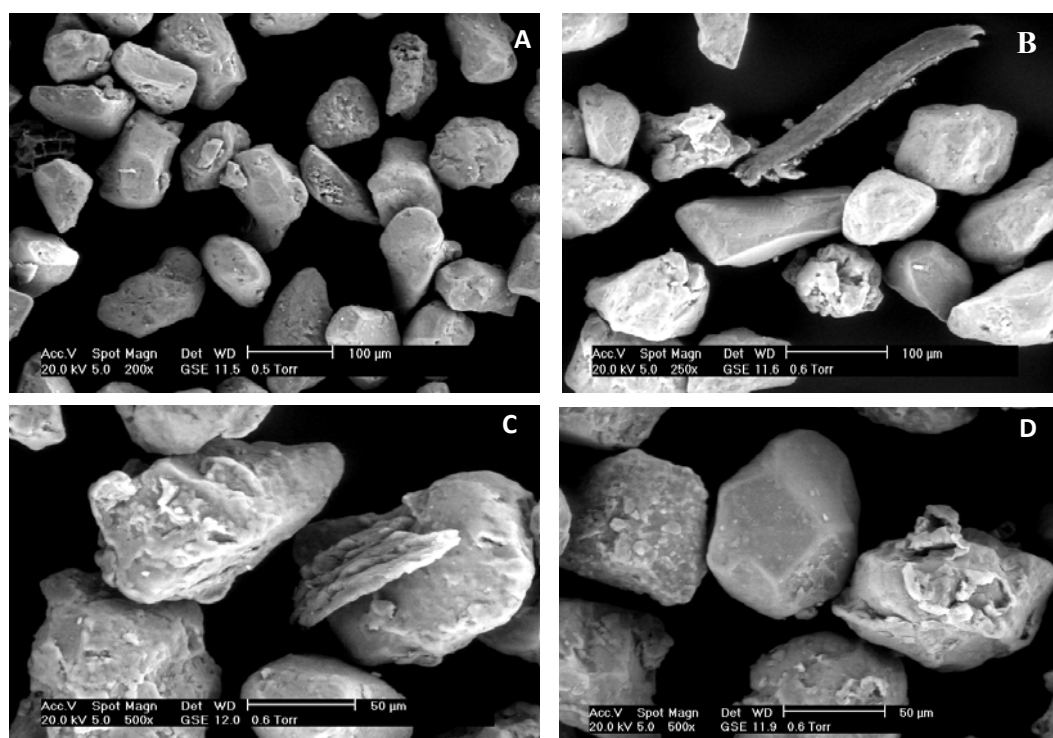


Figure 2.2. Scanning electron microscope analysis of soil particles under canopy (A), inter-canopy (B) in Mongu and under canopy (C), inter-canopy (D) in Tshane.

Moisture retention curves obtained for a range of soil water potentials vary between 0 and -7 MPa (Fig. 2.3). These curves were used to calculate the moisture content at the wilting point separately for areas located beneath the canopy and in the intercanopy (Table 2.5). The soil water potential at the wilting point, Ψ_w , for crops is typically assumed to be at -1.5 MPa; however, dryland vegetation is generally well-adapted to more arid conditions and can tolerate drier soil moistures. Thus, the values of Ψ_w for southern African vegetation have been observed to be significantly lower (Scholes and Walker, 1993). Values from the literature have been compiled for species observed at the different sites along the KT (Table 2.5). The moisture retention curves were used to calculate the corresponding relative soil water contents (fraction of pore space filled by water) at the wilting point. Because grasses have been observed to grow also beneath tree canopies, soil moisture values at the wilting point were calculated both for between canopy and under canopy soils. Moisture contents at the wilting point were found to be consistently higher under the canopy than in the interspace areas, suggesting the existence of slight differences in soil texture, i.e., the existence of higher clay fractions under the canopy (see Fig. 2.3), consistent with the differences in fine fractions found at the drier sites. Whether this difference implies higher likelihoods of water stress in vegetation growing under the canopy cannot be assessed on the basis of these data. In fact, differences in soil texture are also associated with different moisture contents which, in turn, could offset the effect of the higher wilting points on water stress conditions in vegetation (e.g., Noy-Meir, 1973; D'Odorico and Porporato, 2006).

4. BIOGEOCHEMICAL PROPERTIES OF KALAHARI SANDS

4.1 Vertical profiles of soil C, N and their isotopic composition

The vertical profile of soil organic carbon (SOC) exhibits higher concentrations in the top 10-20 cm at all sites along the KT for both the open areas and the areas under the canopy.

Table 2.5. Relative soil moisture at wilting point between inter-canopy and under canopy of the four locations along Kalahari Transect.

Species	Ψ_w (MPa)	Tshane (%)		Ghanzi (%)	
		Between Canopy	Under Canopy	Between Canopy	Under Canopy
Typical value for crops	-1.5	2.41	3.63	3.43	4.34
<i>Burkea africana</i> (Woody)	-3.1*				
<i>Ochna pulchra</i> (Woody)	-3.2*				
<i>Terminalia sericea</i> (Woody)	-1.9*		3.48		4.21
<i>Digitaria eriantha</i> (Grass)	-2.9*	2.26	3.23	3.22	3.98
<i>Eragrostis pallens</i> (Grass)	-3.9*	2.10	3.07	3.13	3.83
<i>Elionurus muticus</i> (Grass)	-2.9*	2.26	3.23	3.22	3.98

Species	Ψ_w (MPa)	Pandamatenga (%)		Mongu (%)	
		Between Canopy	Under Canopy	Between Canopy	Under Canopy
Typical value for crops	-1.5	3.41	4.28	1.10	1.35
<i>Burkea africana</i> (Woody)	-3.1*				0.69
<i>Ochna pulchra</i> (Woody)	-3.2*				0.66
<i>Terminalia sericea</i> (Woody)	-1.9*				
<i>Digitaria eriantha</i> (Grass)	-2.9*	2.94	3.88	0.25	0.76
<i>Eragrostis pallens</i> (Grass)	-3.9*	2.75	3.71	0.13	0.47
<i>Elionurus muticus</i> (Grass)	-2.9*	2.94	3.88		

* The values are from Scholes and Walker (1993).

The SOC is typically higher in the areas under canopy than in the intercanopy soil (Fig. 2.4). The soil total N content is also concentrated in the top 10 cm both in intercanopy and canopy areas with the total N content being higher under the canopy (Fig. 2.4).

Furthermore, the variation in C and N content in the soil column is higher under the canopy than in the open area for all four sites. At depth, the soil N content is higher at the drier sites (e.g. Tshane and Ghanzi) than at the wetter end of the KT (e.g. Mongu and

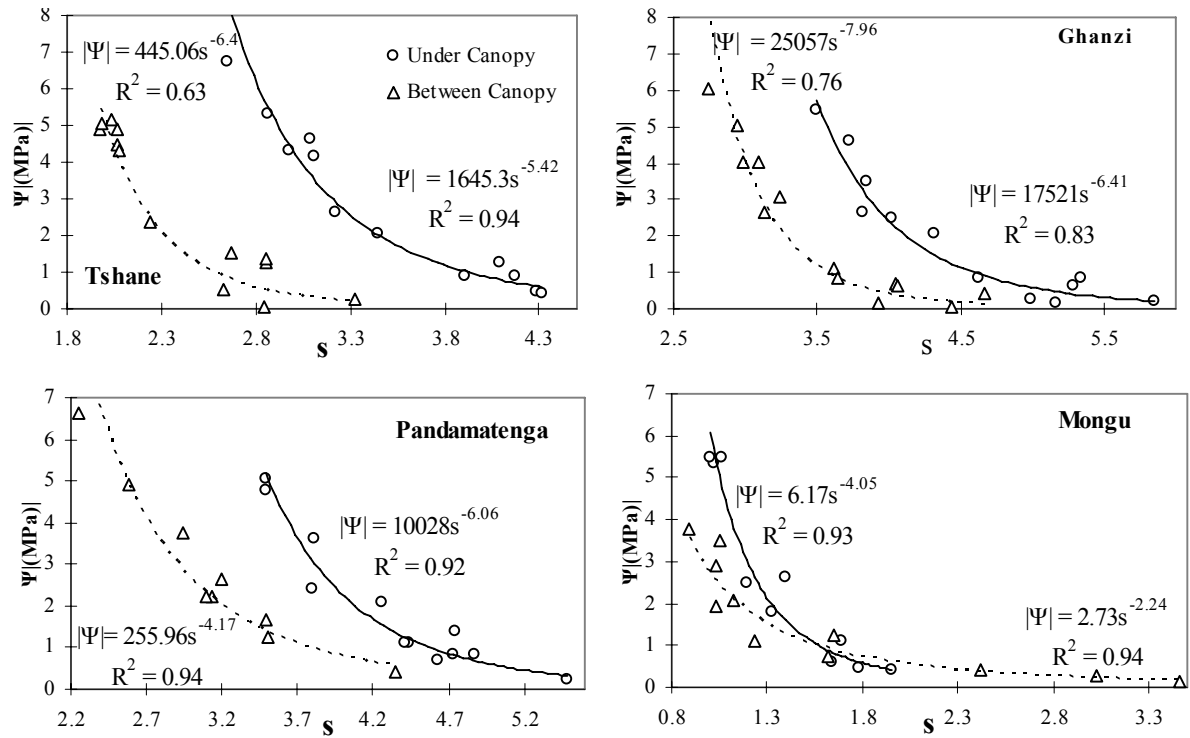


Figure 2.3. Water retention curves for both beneath canopy (solid line) and intercanopy (dashed line) at four sampling locations (-7 – 0 MPa).

Pandamatenga) both in intercanopy and canopy areas (Fig. 2.4), possibly suggesting that N is more limiting at the wetter sites of this transect (Scanlon and Albertson, 2003; Aranibar et al., 2004).

The $\delta^{13}\text{C}$ values increase with depth under canopy whereas there is no clear pattern of $\delta^{13}\text{C}$ in the soil profiles in intercanopy areas (Fig. 2.5). The $\delta^{13}\text{C}$ values in Pandamatenga exhibit large variations both in open areas and under the canopy, although in a different way, in that the $\delta^{13}\text{C}$ values were more variable in the top 40 cm under canopy but less

variable in open areas (Fig. 2.5). The anomalous and high variability in soil $\delta^{13}\text{C}$ throughout the soil column observed in Pandamatenga was likely influenced by the two major soil types existing in Pandamatenga, the vertisol and arenosols (Almendros et al., 2003; Pardo et al., 2003). The arenosols are light-textured soils like those found in most of the Kalahari region. The vertisols, however, are heavy, clayey, nutrient-rich soils used for dryland crop production in the Pandamatenga area (Pardo et al., 2003). Field sampling was carried out in the woodlands underlain by arenosols, however the proximity to the vertisols existing on the surrounding commercial farms inevitably influenced the soil chemical and physical properties at the woodland site in Pandamatenga.

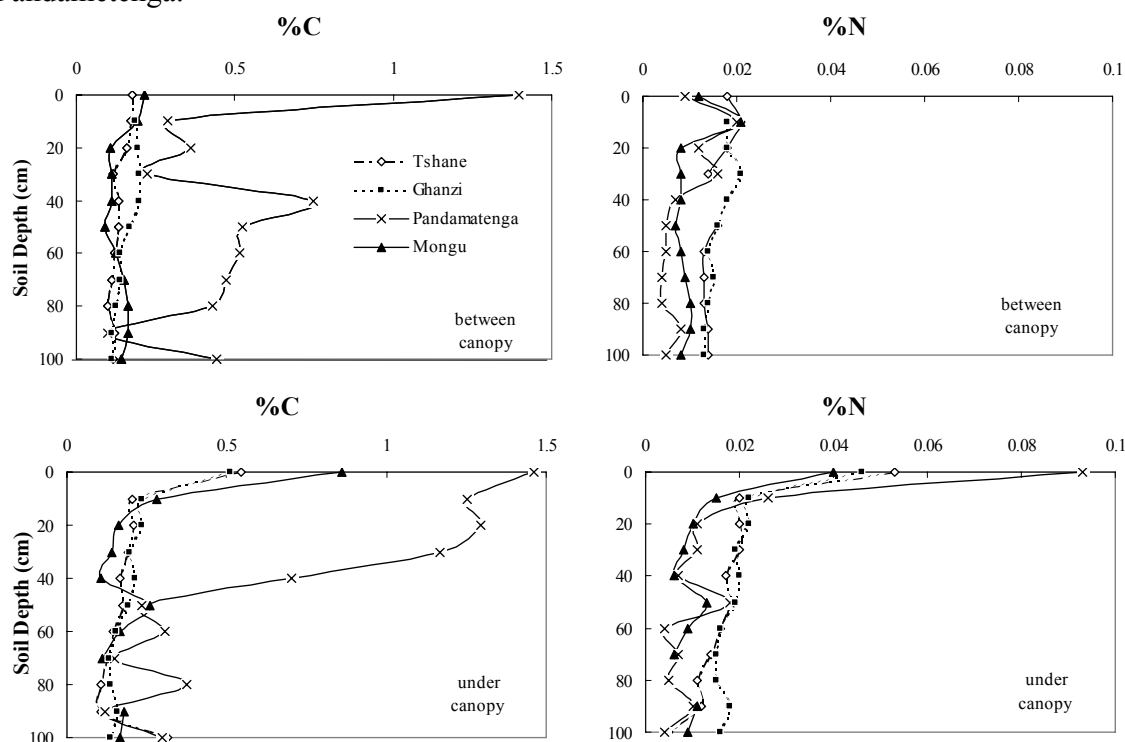


Figure 2.4. Depth profiles of carbon (left) and nitrogen (right) content of soils along Kalahari transect between and under canopies.

Depending on climate conditions, the vertical profile of soil $\delta^{15}\text{N}$ can either exhibit little variation like in montane elevation gradients, random distributions like in gravelly desert soil or, most commonly, a consistent (exponential) increase with depth like in grasslands (Amundson et al., 2003). Multiple factors contribute to the soil $\delta^{15}\text{N}$ variation along depth (Amundson et al., 2003) including N transport processes, depth-dependent plant N inputs as dead roots, and multiple N pools other than those from plant tissues (e.g., microbial biomass). Despite the presence of greater fluctuations in the vertical profile of soil $\delta^{15}\text{N}$, similar to those observed in gravelly desert soils (Brenner, 1999) (Fig. 2.5), the $\delta^{15}\text{N}$ in the Kalahari increases with depth through the “bulk” of the root zone (top 50 cm, see Section 5) to a maximum value and then decreases at greater depths; this pattern can be observed both in open areas and under canopy (Fig. 2.5). The variation of soil $\delta^{15}\text{N}$ content with depth is an important contributing factor to the plant

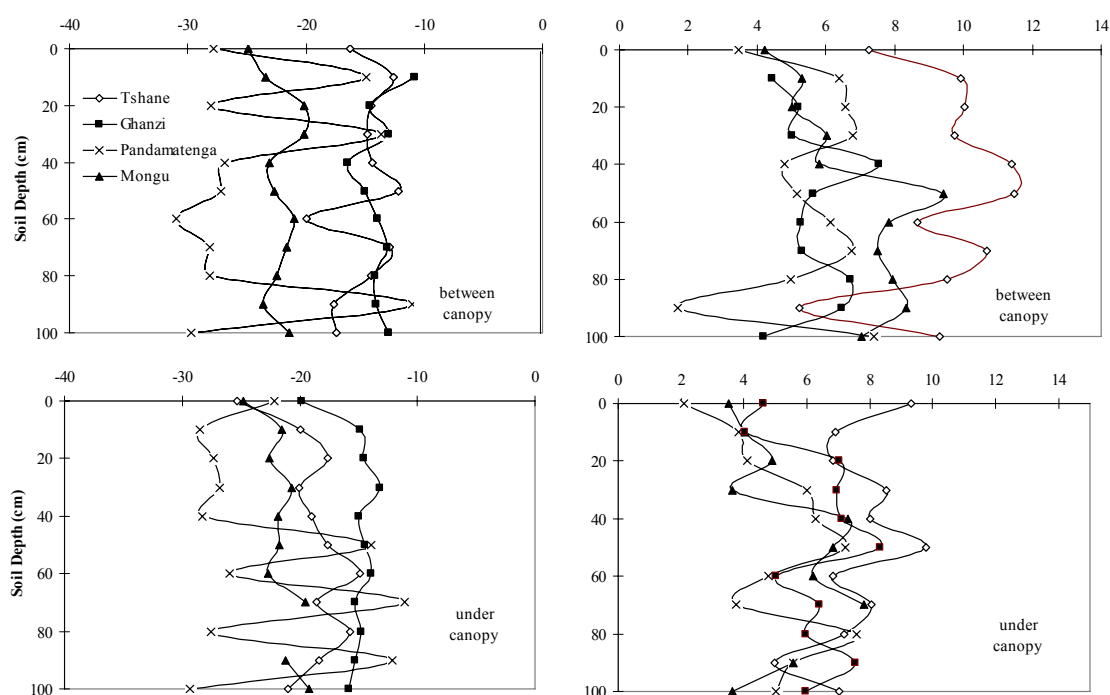


Figure 2.5. Depth profiles of soil $\delta^{13}\text{C}$ (left) and soil $\delta^{15}\text{N}$ (right) along Kalahari transect between and under canopies.

$\delta^{15}\text{N}$ signature (e.g. plants taking up N from deeper soil layers should have higher values of $\delta^{15}\text{N}$). The fact that grass roots dominate the surface soil (see Section 5), and the tendency of surface soils to have lower $\delta^{15}\text{N}$ values, explains the lower foliar $\delta^{15}\text{N}$ values found in grasses than tree tissues across southern Africa (Swap et al., 2004) as well as in semiarid and mesic sites of Australia (Cook, 2001). Although early hypotheses that trees and grasses utilize water from different layers (Walter, 1971) have been recently challenged both by field observations (Scholes and Walker, 1993; Hipondoka et al., 2003; Williams and Albertson, 2004) and theoretical models (Rodriguez-Iturbe et al., 1999), the fact that different plant functional types take N from different layers, at different times (e.g. grasses take up the recently mineralized N and trees take up the remaining N) or utilize different forms of N, could be one of the mechanisms contributing to tree-grass co-dominance in savannas.

4.2 Soil surface C, N and their isotopic composition changes along the transect

Both soil $\delta^{15}\text{N}$ and soil $\delta^{13}\text{C}$ content increase with elevated levels of aridity (Table 2.6), consistent with a number of other studies (Aranibar et al., 2004; Bird et al., 2004; Swap et al., 2004). The higher soil $\delta^{13}\text{C}$ with decreasing values of MAP was related to the changes in vegetation composition along the KT (i.e., C_4 vegetation has higher $\delta^{13}\text{C}$ values and higher proportions of C_4 plants exist at the dry end of the KT). The increase in soil $\delta^{15}\text{N}$ with decreasing values of MAP has been interpreted as the effect of higher N losses at the dry end of the transect owing to ammonia volatilization (Aranibar et al., 2004; Swap et al., 2004). In Pandamatenga the soil $\delta^{15}\text{N}$ is anomalously lower than the

values predicted by the empirical relation (between soil $\delta^{15}\text{N}$ and MAP) deduced by Swap et al. (2004) for the KT, presumably due to the existence of major commercial farms adjacent to the field sites (two 10000-hectare agricultural fields on both sides) and likely the use of inorganic fertilizers (application rates around 50-100 kg/hectare, personal communication from local farmers) in these cropland fields. Because the $\delta^{15}\text{N}$ in inorganic N fertilizer is approximately 0‰, the deposition of wind-blown farm soils at the research site likely decreases the soil $\delta^{15}\text{N}$.

The C and N content at the soil surface increases along the rainfall gradient reaching a maximum value at Ghanzi, while it decreases at the more humid sites. The C/N ratio of the soil organic matter from the top 5 cm of soil, however, consistently increases with the MAP (Table 2.6), suggesting the existence of greater N limitation at

Table 2.6. Soil surface (0-5cm) C, N and their isotopic composition changes (mean \pm stderr, n = 5) along the transect measured for dry season (August) 2004.

		%C	%N	C/N	$\delta^{13}\text{C}$	$\delta^{15}\text{N}$
Tshane	under canopy	0.35 ± 0.05^A	0.04 ± 0.00^A	9.90 ± 0.21^A	-18.5 ± 1.1^A	7.3 ± 0.6^A
	inter-canopy	0.18 ± 0.01^B	0.02 ± 0.00^B	9.11 ± 0.19^B	-12.8 ± 0.6^B	7.8 ± 0.9^A
Ghanzi	under canopy	0.61 ± 0.05^A	0.05 ± 0.01^A	11.35 ± 0.97^A	-16.5 ± 1.0^A	7.5 ± 1.9^A
	inter-canopy	0.42 ± 0.07^A	0.03 ± 0.00^A	12.09 ± 0.49^A	-13.4 ± 1.2^B	6.9 ± 0.3^A
Pandamatenga	under canopy	0.63 ± 0.09^A	0.04 ± 0.00^A	15.15 ± 0.40^A	-22.4 ± 0.5^A	0.6 ± 0.2^A
	inter-canopy	0.58 ± 0.12^A	0.04 ± 0.01^A	14.85 ± 0.35^A	-21.1 ± 0.6^A	1.2 ± 0.6^A
Mongu	under canopy	0.38 ± 0.07^A	0.02 ± 0.00^A	20.52 ± 1.40^A	-25.4 ± 2.6^A	1.7 ± 0.5^A
	inter-canopy	0.27 ± 0.01^A	0.01 ± 0.01^A	19.21 ± 0.55^A	-18.2 ± 0.9^B	2.9 ± 0.9^A

Different capital letters indicate different mean values between under canopy and intercanopy at 0.05 significance level for each measured parameter.

the wet end of this transect. The differences in SOC, soil total N, and C/N ratios between under canopy and open canopy soils are significant only at Tshane (Table 2.6). At all four sites soil $\delta^{15}\text{N}$ values are not significantly different between subcanopy soils and intercanopy areas, while differences in soil $\delta^{13}\text{C}$ values between subcanopy and

intercanopy areas are significant at all four sites except Pandamatenga (Table 2.6). These results suggest that the overall nutrient levels were similar beneath tree canopies and in intercanopy areas for these African savannas, except at the extreme dry end of the transect. Soil nitrate concentrations are relatively constant along the transect (around 1 - 2 $\mu\text{g g}^{-1}$), whereas ammonium concentrations are much higher at the wet end of the transect than at the drier sites (24 $\mu\text{g g}^{-1}$ vs. 11 $\mu\text{g g}^{-1}$) (Table 2.7). Aranibar et al. (2003) estimated gross N mineralization rates using $^{15}\text{N-NH}_4^+$ and $^{15}\text{N-NO}_3^-$ pool dilution techniques and found higher mineralization rates in soils under the canopy than in open areas. These rates were dramatically lower at Mongu. A similar pattern (Table 2.7) was found in the gross nitrification rates. Nitrification rates were much higher than mineralization rates at all locations except Mongu (Table 2.7). The higher mineralization rates and nitrification rates under the canopies indicate that conditions favorable to the formation of “fertility islands” (Schlesinger et al., 1990) also exist in these African savannas even when the overall N level and soil C/N are similar beneath tree canopies and in intercanopy areas. In particular, at research sites in Maun the NH_4^+ and NO_3^- contents were found (Feral et al., 2003) to be higher under the canopy (14.53 to 22.59 $\mu\text{g NH}_4^+ \text{ g}^{-1}$ and 4.50 to 13.11 $\mu\text{g NO}_3^- \text{ g}^{-1}$) than in inter-canopy areas (9.96 $\mu\text{g NH}_4^+ \text{ g}^{-1}$ and 2.29 $\mu\text{g NO}_3^- \text{ g}^{-1}$), consistent with differences detected in the mineralization and nitrification rates at the four sites considered in this review (Table 2.7). Nitrification rates were generally higher than mineralization rates, suggesting that ammonification is the limiting step in mineral N formation in these systems.

The isotopic analysis of ammonium and nitrate isolated from transect soils (Aranibar, 2003) revealed that the NH_4^+ is more enriched in ^{15}N than the NO_3^- , likely a

result of preferential use of ^{14}N during the oxidation of ammonium during nitrification. The magnitude of the difference between the $\delta^{15}\text{N}$ values of NH_4^+ and NO_3^- is greater at the drier end of transect. Such a change in the absolute difference could be an indication of the reaction proceeding closer to completion, or of increased volatilization of residual ammonia, or a contribution of an additional source of N.

4.3 Soil respiration before and after wetting

Before wetting, soil surface CO_2 fluxes at the four locations ranged between 0.23 and

Table 2.7. Soil ammonium and nitrate concentration and their isotopic compositions along the Kalahari transect.

	NH_4^{+1} (μgg^{-1})	NO_3^{-1} (μgg^{-1})	$\delta^{15}\text{NH}_4^+$ (‰) ²	$\delta^{15}\text{NO}_3^-$ (‰) ^{2,2}	Gross N mineralization rates (mg $\text{NH}_4\text{-N m}^{-2} \text{d}^{-1}$) ¹	Gross nitrification rates (mg $\text{NO}_3\text{-N m}^{-2} \text{d}^{-1}$) ¹
Tshane	11.15 ± 2.17	1.37 ± 0.26	12.3	5.2	50 ^a , 16 ^b	135 ^a , 35 ^b
Okwa	8.66 ± 3.34	1.64 ± 0.18	-0.3	-3.4	51 ^a , 20 ^b	105 ^a , 48 ^b
Maun	12.29 ± 1.36	1.91 ± 0.53	5.5	4.3	60 ^a , 25 ^b	100 ^a , 65 ^b
Mongu	24.00 ± 3.71	1.04 ± 0.41	5.8	1.4	38 ^a	10 ^a

1 Feral et al. 2003 Journal of Arid Environments, 54:327-343

2 Aranibar 2003 PhD thesis, 93-131

a: under canopy, b: inter-canopy

0.74 g (CO_2) $\text{m}^{-2} \text{hour}^{-1}$ along the transect. These fluxes increased with higher MAP and leveled off near Pandamatenga. Soil wetting significantly increased the soil surface CO_2 flux for all four locations. After wetting, the rate of soil respiration increased by a factor of 10 at Tshane, Ghanzi and Pandamatenga, while at Mongu, the wettest site along the transect, it increased 5-fold (Fig. 2.6).

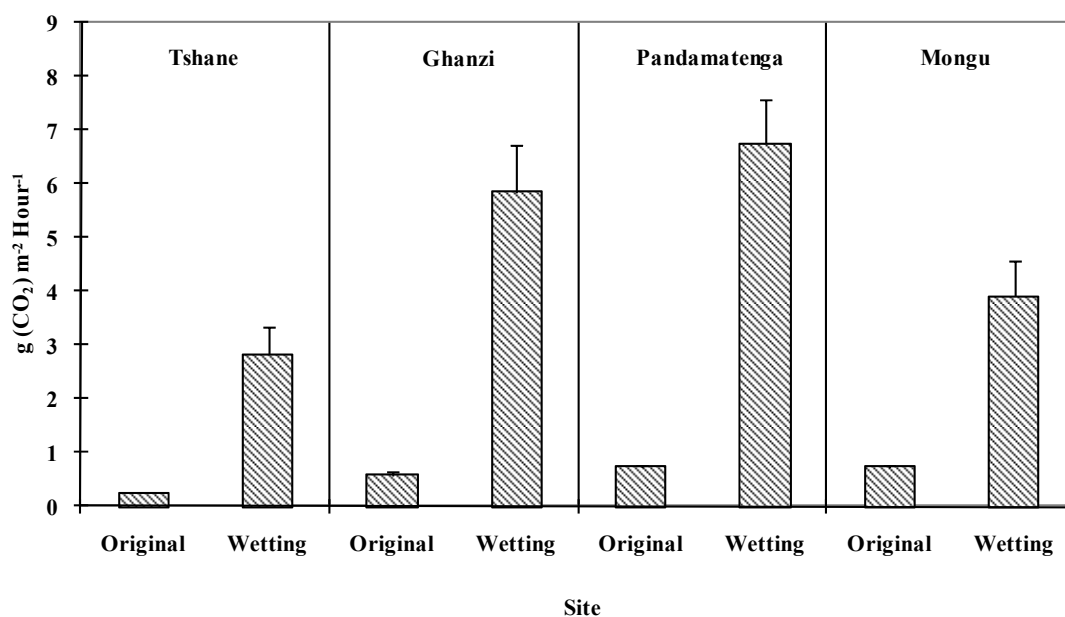


Figure 2.6. Soil surface CO₂ flux before and after the soil wetting in four locations along Kalahari transect.

5. ROOT DISTRIBUTION IN THE KALAHARI

Despite the existence of specific studies on root function in the Kalahari, including for example mycorrhizal nutrient uptake (Bohrer et al., 2001; Bohrer et al., 2003) and root inverse water transport phenomena (Schulze et al., 1998), a comprehensive study of root distributions for the different tree, shrub and grass species existing in the region is still unreported. In an early exploration of the southern Kalahari soils, Leistner (1967) noticed that, although the depth of root systems varies considerably depending on local conditions and plant species, the rooting depths generally range from 20 cm to more than 300 cm, with the highest root concentration being between 8 and 50 cm. Leistner (1967) also found a number of morphological and anatomical features such as sand coats, spongy cortex, and succulent roots, which seems to play an important role in plant adaptation to the semi-desert habitats of the southern Kalahari. Laterally, most shrubs and trees in the Kalahari possess root systems that extend horizontally beyond the footprint of

their canopies. For example, the horizontal roots of *Acacia erioloba* (formerly *A. giraffae*) and *Albizia anthelmintica* can be longer than 20 m, whereas those of *A. mellifera* can extend laterally for more than 10 m (Leistner, 1967). More recently, Hipondoka et al. (2003) explored the vertical root distribution of the two main life forms (i.e. trees and grasses) existing in the savannas at Tshane and Ghanzi. These authors used the profile count technique (Böhm, 1979) to determine the vertical root distribution and composition both at sites located beneath tree canopies and in open areas. Both plant functional types were found to develop most of their roots at the surface. Grass roots were found to be more abundant and dominant close to the surface (i.e., in the top 30-cm of the soil column) even in the soil pits located under the tree canopies. Moreover, the distribution of tree roots did not exhibit a clear dominance over grasses at deeper soil layers as suggested by previous studies (e.g., Walter, 1971; Knoop and Walker, 1984). The vertical profile of root distributions measured by Hipondoka et al. (2003) exhibits a well-defined decrease in grass root density with depth, whereas smaller variations can be noticed in the tree root profile, with a peak in tree root density at 20-50 cm depth (Fig. 2.7A, B). A similar root profile pattern (Fig. 2.7C) was found at the same site (Ghanzi) by Williams and Albertson (2004), though the actual values of root density differed by almost an order of magnitude, possibly owing to the different root sampling techniques used by those authors.

By measuring the isotopic composition of both root C and soil organic matter C at different depths, Hipondoka et al. (2003) determined the proportion of soil C contributed by each life form and found a dominance of grass root biomass at most depths, in agreement with their profiles of root density (Fig. 2.7A, B).

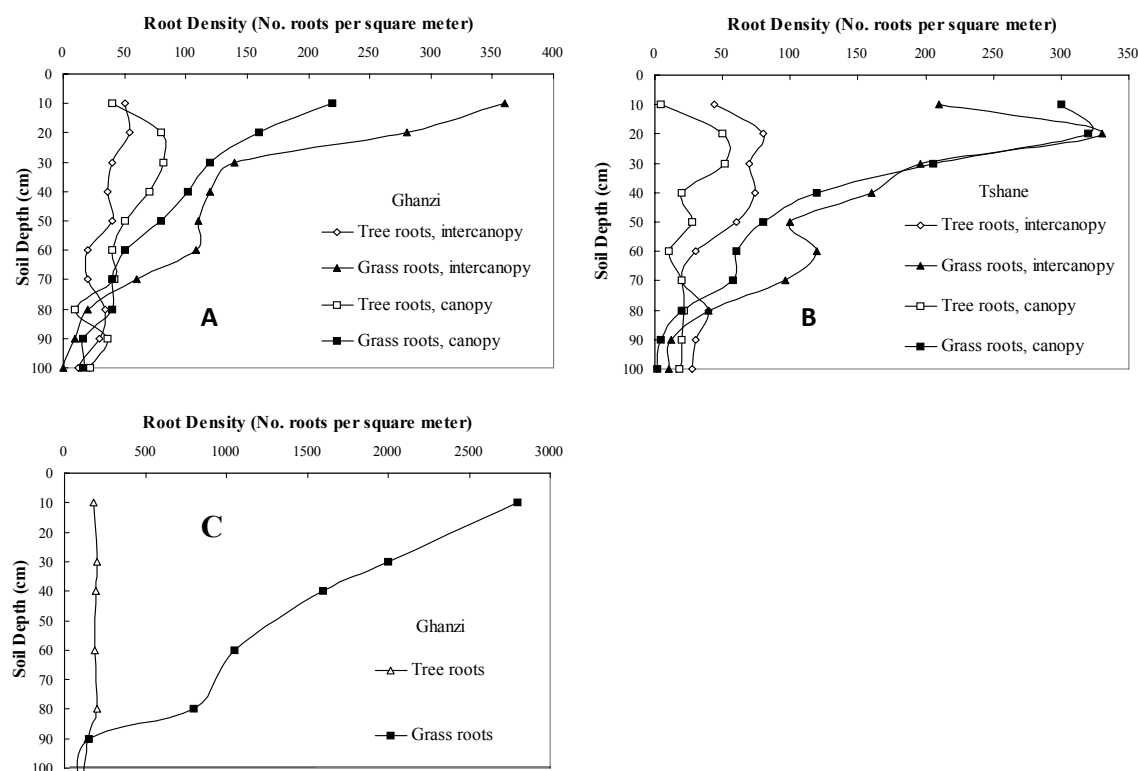


Figure 2.7. Root density profiles for tree and grass functional types in different locations. A and B are from Hipondoka et al. 2003 and C is from Williams and Albertson 2004.

6. SOIL CRUSTS IN KALAHARI SAND FORMATIONS

Biological soil crusts (a complex soil surface community dominated by cyanobacteria, microfungi, mosses, and lichens) are a recurrent feature of arid and semi-arid ecosystems (Belnap and Lange, 2003). Numerous studies have documented the importance of these crusts to the stabilization of the soil surface, i.e., the increase in the resistance to wind and water erosion (Campbell et al., 1989), the enhancement of seedling establishment (St. Clair et al., 1984), and soil fertilization through biological N fixation (Skarpe and Henriksson, 1986; Zaady et al., 1998). In addition, soil crust communities are very sensitive to small pulsed water events (desert precipitation are usually less than 3 mm per event), a common feature in arid and semi-arid environment. For larger rainfall events, crusts may reduce the rate of soil drying, giving vascular plants more time to respond to

increased water availability (Austin et al., 2004). However, the diverse functions of soil crusts in the Kalahari are still relatively understudied with only few reports available in the literature.

Aranibar et al. (2003) quantified the N-fixing activity of soil crusts in the Kalahari during the wet season using *in situ* acetylene reduction assays. The estimated annual rates of N fixation ranged from 8 to 44 g N ha⁻¹ year⁻¹ with higher N fixing activity at the dry end of the transect (Table 2.8). The N fixing activity of the soil crusts along the Kalahari transect were several orders of magnitude lower than those estimated by other authors for the Kalahari desert (Skarpe and Henriksson, 1986), and for other regions like the Negev desert (Zaady et al., 1998), or Tucson desert (MacGregor and Johnson, 1971). Aranibar et al. (2003) argued that this was due to the anomalously wet conditions experienced during the year of their study (2000), which may have temporarily increased the availability of soil mineral N, thereby leading to a decrease in N fixation rates.

The spatial distribution of cyanobacterial soil crusts has been recently investigated (Berkeley et al., 2005) in the context of bush encroachment studies in the Kalahari at sites with two different dominant plant species (*A. mellifera* and *Grewia flava*) and different

Table 2.8. Soil crusts N fixing activities along the Kalahari transect estimated by *in situ* acetylene reduction assays.

	g N fixed ha ⁻¹ year ⁻¹
Tshane	37
Okwa	44
Maun	14
Mongu (disturbed)	30
Mongu	8

Aranibar et al. 2003 Journal of Arid Environments, 54:345-358

disturbance regimes. They found the highest degree of crust cover under the canopies of *A. mellifera*, intermediate levels of crust cover under *G. flava* and the lowest cover in the bare soil interspaces. This pattern was clearer in the presence of disturbances. Those results showed an enhanced cyanobacterial crust cover under *A. mellifera* canopies, where the crust cover was found to be resistant to even higher levels of disturbance. Conversely, disturbances were observed to limit the development of soil crust under the canopies of *G. flava* and in the bare soil interspaces. Thus, this canopy-crust association suggests that the encroachment of *A. mellifera* is intrinsically more resilient because of the ability of the crust to stabilize the soil surface and increase both nutrient retention and the soil nutrient content.

7. SUMMARY

The data presented in this review show that the Kalahari soil is acidic, dominated by sand and nutrient poor. Soil nutrient dynamics in the Kalahari are significantly determined by the relatively strong rainfall gradient, whereas the soil physical properties remain overall the same along the transect. Differences in rainfall regime, vegetation composition and structure determine important changes in the soil organic matter, and vertical distribution of soil N content along the Kalahari Transect, as evidenced by the comparison of experimental results obtained at different sites, as well as at each site in canopy and inter-canopy areas.

Acknowledgements

The project was supported by NASA-IDS2 (NNG-04-GM71G). I greatly appreciate the team-work and field assistance from Lydia Ries, Natalie Mladenov, Kelly Caylor, Matt Therrell, Todd Scanlon, Ian McGlynn (University of Virginia), Greg Okin (UCLA), Billy

Mogojwa and Thoralf Meyer (University of Botswana), Barney Kgope (South African National Biodiversity Institute). I thank Dr. Howard Epstein from University of Virginia for lending the EGM-4 CO₂ analyzer. I thank Bill Gilhooly, Parameswar Sahu, and Sujith Ravi for their help with the laboratory instrumentation. The strength of this paper is improved by comments from two anonymous reviewers and the associate editor.

Chapter 3 Combined effects of soil moisture and nitrogen availability variations on grass productivity in African savannas

ABSTRACT

Savannas cover about 20% of the Earth's land area and 50% of Africa, across a wide range of climatic conditions. As an indispensable component of savanna, grasses play an important role in savanna ecosystems, and the dramatic grass expansion in Africa during the Miocene is closely linked to the origin of the modern savanna biome. A better understanding of grass productivity and its controlling factors in modern savanna ecosystems could therefore be a key to understanding the functioning of savannas (e.g., productivity and water use) and predict responses to future climatic changes (e.g., shifts in vegetation structure, changes in vegetation productivity). In this study, a stable isotope fertilization experiment was conducted to determine how factors limiting grass production in savanna ecosystems differ across regional climate gradients. The study was conducted on the geomorphically homogenous Kalahari Transect (KT), which traverses a dramatic gradient in mean annual rainfall and therefore offers an ideal setting to study nutrient and vegetation dynamics independent of confounding soil effects. The results of this study demonstrate that even at the wet end of the transect, water remains the principal factor limiting grass productivity. Although prior results have proposed a switch between water and nitrogen limitations where annual precipitation exceeds a certain critical value, these results suggest that grass productivity in the KT is determined by variations in rainfall rather than in nitrogen availability. Thus, although the traditional classifications of nutrient poor (broad-leaf savannas) and nutrient rich (fine-leaf savannas) savanna ecosystems may still be useful, this classification does not necessarily imply the

existence of nitrogen limitation in the nutrient poor area; it is more likely that the herbaceous species are already adapted to lower nitrogen availability.

Keywords: Savanna, Kalahari Transect, Fertilization Experiment, Stable Isotopes, Nitrogen, Water, Botswana, Zambia

Wang, L., P. D'Odorico, L. Ries, K. Caylor and S. Macko. Combined effect of soil moisture and nitrogen availability variations on grass productivity in African savannas: The case of the Kalahari Transect. *Global Change Biology* (in review).

1. INTRODUCTION

Savannas cover about 20% of the Earth's land area (Scholes and Walker, 1993) and can be found in large areas of Africa, Australia, North and South America, across a wide range of climatic conditions. As an important and distinct biome, savannas produce approximately 29% of global terrestrial net primary productivity (Grace et al., 2006). They are currently considered a carbon (C) neutral system (Veenendaal et al., 2004; Williams et al., 2007), although savannas have the potential to become either large sinks or sources of C, depending on changes in climate, disturbance regime, land management, and the time-scales under consideration (Williams et al., 2007). To understand the response of savannas to changes in these "external" drivers it is therefore essential to understand the factors controlling their productivity. Water availability, disturbance (e.g., fire, grazing) and nutrient availability are considered to be the three major factors determining the structure and function of savanna ecosystems (Walker et al., 1981; Sarmiento, 1984; Scholes and Walker, 1993; Scholes and Archer, 1997; Sankaran et al., 2004), but it remains unclear how the relative importance of water and nutrient limitations, especially that of nitrogen (N), varies with the mean climatic conditions (Sankaran et al., 2005).

Most attempts at regional syntheses of savanna structure and function are typically conducted at single sites or without experimental manipulation (Scholes and Walker, 1993; Toit et al., 2003; Sankaran et al., 2005; Scanlon et al., 2007). In addition, many studies have focused exclusively on the distribution and abundance of woody vegetation. However, the critical role that C₄ grass expansion played in governing the origin of the savanna biome during the Miocene (Beerling and Osborne, 2006) highlights

the importance of understanding large-scale controls on grass productivity when attempting to predict the responses of savannas to future climatic changes. By analyzing the results of over 50 fertilization experiments in arid and semi-arid grassland ecosystems across continents, Hooper and Johnson (1999) tested the hypothesis that N limitation increases with rising soil moisture in dryland ecosystems. It was concluded that water and N co-limit the aboveground net primary productivity (ANPP) along regional rainfall gradients. Building on this result and other evidences, Epstein et al. (2006) further proposed that N limitation does not vary along precipitation gradients and that other environmental factors (e.g., light) may constrain grass productivity in sub-humid grassland ecosystems. This is along the same line that there is a potential switch between “belowground constraints” and “aboveground constraints” when mean annual rainfall exceeds certain values (Burke et al., 1998). In the case of savanna ecosystems, there is experimental evidence (Ludwig et al., 2001) that N may limit grass productivity in a dry savanna during wet years.

In the present study, the Kalahari Transect (KT) in southern Africa is used as a representative ecosystem to investigate the interactions between the water and nutrient limitations on the productivity of grass vegetation in savannas. The KT is one of a set of IGBP (International Geosphere-Biosphere Programme) “megatransects” (Koch et al., 1995; Scholes et al., 2002) identified for global change studies. The KT traverses a dramatic aridity gradient on relatively homogenous soils (deep Kalahari sands), offering an ideal setting to study nutrient and vegetation dynamics without confounding soil effects (Wang et al., 2007a). Modeling results based on remote sensing data (Scanlon and Albertson, 2003) and leaf-level physiological data (Midgley et al., 2004) both

suggest the existence of two distinct regimes of vegetation productivity-rainfall relationships across the KT. In the northern, wetter, portion of the transect, a large fraction of the soil water content is lost in sandy soils, as leakage through the bottom of the root zone. Because water losses are associated with leaching outputs of N, it has been argued that the productivity of these mesic and sub-humid savannas may be limited by nutrient availability (D'Odorico et al., 2003). In contrast, productivity in the southern, drier portion of the transect is hypothesized to be limited by precipitation, which is sufficiently low to cause limited soil water availability (Scanlon and Albertson, 2003).

In this study, a stable isotope fertilization experiment was conducted at selected sites along a regional-scale transect to directly examine the existence of a switching point from water-limited to N-limited conditions that has been hypothesized to exist with increasing MAP along the Kalahari rainfall gradient.

2. MATERIALS AND METHODS

2.1 Study sites

The field experiment was conducted at four locations (Tshane, Ghanzi, Pandamatenga and Mongu) along the KT rainfall gradient (Fig. 3.1A). The detailed site description including soil physical and chemical characteristics can be found in Wang et al. (2007a). Here only the major site characteristics are summarized. The northernmost site was situated in Mongu, Zambia, with a MAP around 879 mm. Vegetation in Mongu is woodland savanna dominated by the tree species *Brachystegia spiciformis* Benth and the common grass species is *Eragrostis spp.* The other three sites were situated in Botswana at Tshane (southernmost site), Ghanzi and Pandamatenga (Fig. 3.1A). The MAP in these three areas ranges from 365 mm to 700 mm, respectively. The Tshane and

Ghanzi sites are open savannas dominated by *Acacia* species such as *Acacia luederizii* Engl. and *Acacia mellifera* Benth., and grass species, such as *Eragrostis lehmanniana* and *Schmidtia pappophoroides*. The Pandamatenga site is a woodland savanna dominated by tree species (e.g., *Kirkia Africana*) and grass species such as *Panicum maximum* and *Pogonarihria squarrosa*.

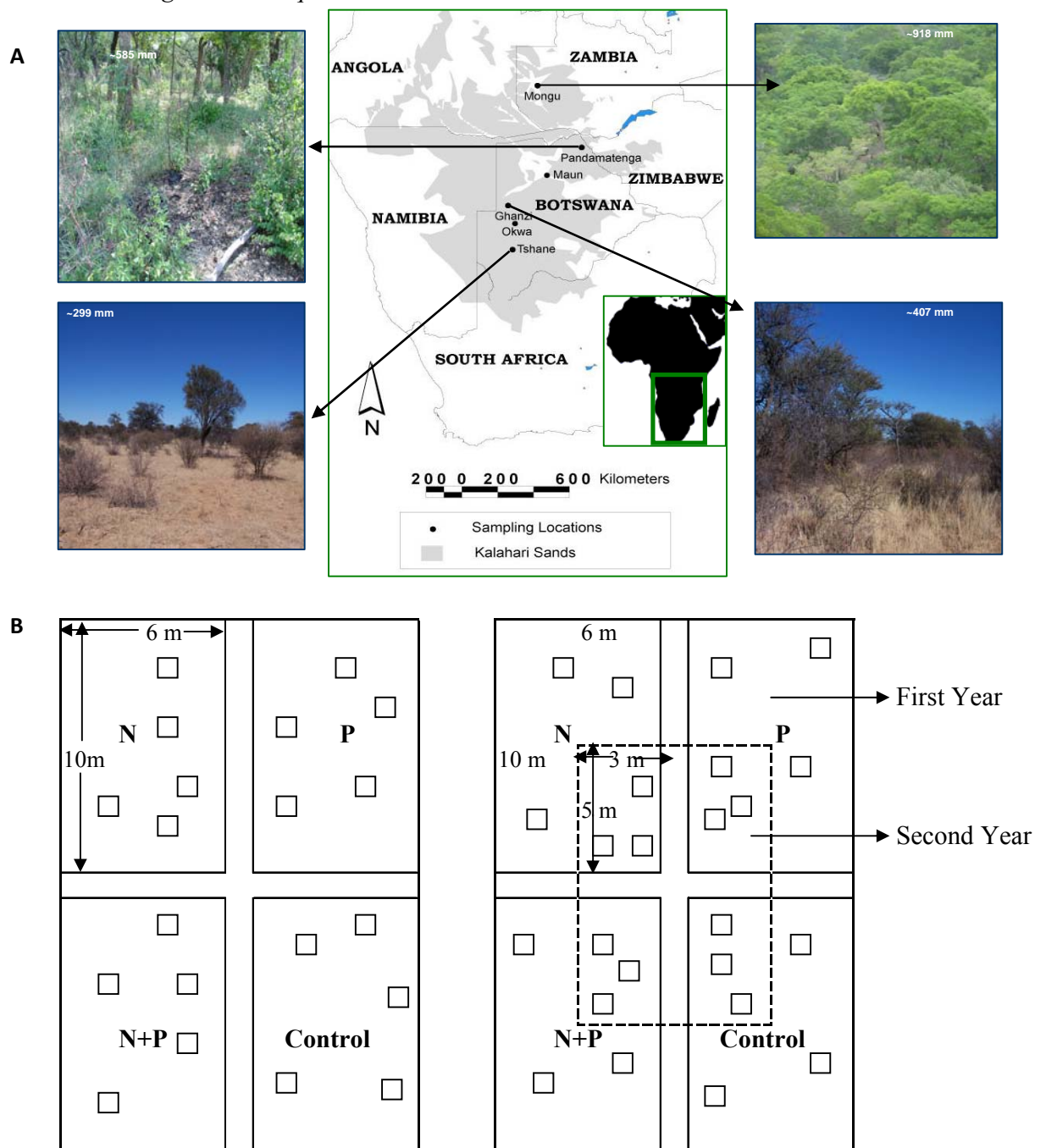


Figure 3.1. Study sites along the Kalahari Transect and the habitat characteristics. The values in each photo are the mean annual rainfall for each site (A). (B) The experimental layout and sampling scheme in 2005 (left) and 2006 (right).

2.2 Fertilization experimental setup

The experiment consisted of a randomized block design with four 21 m x 13 m plots at each of the four sites along the KT. Each plot was divided into four 10 m x 6 m subplots with 1 m buffer zone between each subplot (Fig. 3.1B). Owing to the logistical issues with the operation of field sites at these remote locations, it was not possible to set up fences around the plots and all the plots were open to potential grazing activity. Occasional presence of cows was observed in the Tshane area, while the other three sites were subject to wild grazers. In August 2004, four treatments (N addition, P addition, N+P addition and control) were randomly applied to the subplots using a backpack electric sprayer. For the N and N+P treatments, 783 kg/ha of $\text{Ca}(\text{NO}_3)_2$ (133 kg N/ha) was evenly applied to each subplot, and 292 kg/ha of $\text{Ca}(\text{H}_2\text{PO}_4)_2$ (33 kg P/ha) was applied to the P and N+P subplots, whereas the control subplots were supplied with water only. These application concentrations were chosen on the basis of data reported by Ludwig et al. (2001) for fertilization experiments in a Tanzanian dry savanna. For each treatment plot (60 m²), the fertilizers were dissolved into 10 L water. The fertilizer solution was applied to the soil surface and was observed to infiltrate into the soil with only a negligible interception by the sparse canopy of grass leaves. The N and N+P additions were enriched with ¹⁵N ($\text{Ca}^{15}\text{NO}_3)_2$) to an isotope signature of 10.3 ‰ (hereafter referred to as the “first year” treatment). In August 2005, the inner 3 x 5 m² portion of each subplot was re-fertilized using the same nutrient concentration, but

different isotopic enrichment, in that the N and N+P additions were enriched with ^{15}N ($\text{Ca}(^{15}\text{NO}_3)_2$) to a signature of 100 ‰ (hereafter referred to as “second year” treatment), which meant to increase the ability to discern N uptake patterns with a stronger label (Fig. 3.1B).

Soils and vegetation samples were collected from the sites for two wet seasons subsequent to the nutrient additions. In February-March, 2005, five random locations in each treatment subplot were selected using randomly-generated coordinates. Newly-formed (i.e., post-treatment) grass biomass was estimated by harvesting five $1 \times 1 \text{ m}^2$ plots from selected locations for each treatment at each site. Portions of each sample of grass biomass from each of the $1 \times 1 \text{ m}^2$ plots were reserved for nutrient and isotope analysis. In January-February 2006, grass biomass and subsamples for nutrient and isotope analysis were collected in a similar way as in the 2005 wet season, i.e. by harvesting three $1 \times 1 \text{ m}^2$ plot from each treatment (for both first year and second year treatment) at each site. In addition to vegetation samplings, three soil samples were taken at two different depths (0-5 cm and 30-35 cm) from each treatment (including the first year and second year fertilizer additions). The vegetation samples collected at Mongu in 2006 were lost in shipment and were unable to be evaluated for the grass biomass, nutrient content and isotope composition.

Soil respiration was measured in the fertilization plots in the 2005 and 2006 wet seasons using an EGM-4 CO_2 analyzer (PP Systems International, Inc. Amesbury, MA, USA) before the grass and soil sampling. To minimize the effect of differences (between sites) in soil water availability due to unexpected precipitation, one liter of water was poured into a soil collar (40 cm x 20 cm) and the soil respiration measurements were

accomplished following the complete infiltration of the added water (“wet” measurement). In the wet season of 2005, one measurement of soil respiration per treatment and per site was made in an open area, and another one under a tree canopy. Because no significant differences were detected between open-canopy and under-canopy soil respiration measurements made in 2005, these two microsites were not differentiated in 2006 with only three random locations being chosen for soil respiration measurements in each treatment area (including the first year and second year fertilizer additions).

Field rainfall data were not available for the 2005 and 2006 wet seasons at the KT sites considered in this study, due to instrument failure. Rainfall data (Figure 5B, inset) were obtained from satellite measurements from Tropical Rainfall Measuring Mission (TRMM) of NASA. For this study the 3B43 monthly data from precipitation radar were used (e.g., Huffman et al., 2007). Field soil moisture data (which, more closely reflect the conditions of plant available water) were continuously monitored at two-hour intervals using DECAGON ECH₂O probes from the 2004 wet season to the 2006 wet season. The ECH₂O probes are known for being sensitive to soil texture and bulk density (Czarnomski et al., 2005) and may not provide an accurate estimate of the soil water content. However, the relatively uniform soil texture/structure found across the whole transect (Wang et al. 2007a) allowed us to use the ECH₂O probe data in relative terms, i.e., to compare soil moisture levels among sites. The soil moisture data reported in this study were calculated as weighted averages across the soil profile (for each soil profile soil moisture was monitored at the depths of 0.10 m, 0.30 m, 0.50 m, and 1.00 m). A mean seasonal value is reported here for each of the two growing seasons (2005 and

2006). More details on the mean soil moisture data for wet season 2005 and 2006 used in this paper can be found in D'Odorico et al. (2007).

2.3 Chemical analyses

Plant and soil samples for isotope and elemental analysis were oven-dried (at 60°C) in the laboratory. Soil samples were sieved and homogenized by mortar and pestle, and plant samples were homogenized by grinding to powder. Total organic C and N contents were measured using an Elemental Analyzer (EA, Carlo Erba, NA1500, Italy). Stable N isotope analyses were performed using a Micromass Optima Isotope Ratio Mass Spectrometer (IRMS) connected to the EA (GV/Micromass, Manchester, UK). The N stable isotope compositions are reported in the conventional form (‰):

$$\delta^{15}\text{N} (\text{‰}) = [({}^{15}\text{N}/{}^{14}\text{N}_{\text{sample}} / {}^{15}\text{N}/{}^{14}\text{N}_{\text{standard}}) - 1] \times 1000$$

where $({}^{15}\text{N}/{}^{14}\text{N})_{\text{sample}}$ is the N isotope composition of a sample, and $({}^{15}\text{N}/{}^{14}\text{N})_{\text{standard}}$ is the N isotope composition of the standard material. The standard material for stable N isotopes is atmospheric molecular N (N_2). Reproducibility of these measurements is typically better than 0.2‰ (Wang et al., 2007c).

2.4 Statistical analyses

Two-way ANOVA for randomized block design with site and treatment as two main factors were used to test differences among various response variables such as soil $\delta^{15}\text{N}$, plant $\delta^{15}\text{N}$, plant %N and grass biomass (SAS v. 9.1 PROC MIX). To further explore the treatment effects at each particular site, subsequent one-way ANOVA within each site were then performed to test the differences between treatments for each

response variable; to this end, mean separations were achieved by Tukey *post hoc* test at $\alpha = 0.05$.

3. RESULTS

In the 2005 growing/wet season (February-March) the foliar $\delta^{15}\text{N}$ signatures were significantly higher in the N and N+P addition treatments than in the control and P addition plots at all sites except for Pandamatenga (Table 3.1, Fig. 3.2A). No significant differences in foliar $\delta^{15}\text{N}$ signatures were detected between the control and P addition, nor between the N and N+P addition plots (Table 3.1, Fig. 3.2A). In the 2006 wet season (February-March), differences in foliar $\delta^{15}\text{N}$ signatures among the four treatments exhibited a pattern similar to the one in the 2005 wet season except for Pandamatenga, where foliar $\delta^{15}\text{N}$ signatures in N, N+P and P addition treatments were significantly higher than in the control treatment (Table 3.1, Fig. 3.2B). Based on mixing ratio calculations of isotope signatures with soil organic matter and fertilizer as two end-members, the percentage of N uptake from the fertilizer (versus from original soil mineral N) in the wettest area (Mongu, 43%) was similar to the driest area (Tshane, 38%), and the highest N uptake percentage from the fertilizer was found at an intermediate precipitation regime (Ghanzi, 68%). This percentage showed a similar pattern in the 2006 wet season, although with much lower values, (8%, 14% and 2% in Tshane, Ghanzi and Pandamatenga, respectively).

For the surface soils (0-5 cm), there were significant differences in $\delta^{15}\text{N}$ signatures between the four locations (Table 3.1), however, in the 2006 wet season no significant differences in soil $\delta^{15}\text{N}$ were found among the four treatments (N, N+P, P and control) at any of the four locations, either for the second year (Fig. 3.3A) or the first year

Table 3.1. The two-way ANOVA results (F-values) on various response variables with site and treatment as two main effects.

	Site Effect (S)	Treatment Effect (T)	S*T
Foliar $\delta^{15}\text{N}$ (2005 Wet season)	155.90**	21.28**	4.82**
Foliar $\delta^{15}\text{N}$ (2006 Wet season First Year)	104.58**	3.55*	0.54
Foliar $\delta^{15}\text{N}$ (2006 Wet season Second Year)	159.20**	50.47**	10.94**
Foliar %N (2005 Wet season)	93.72**	1.86	1.79
Foliar %N (2006 Wet season First Year)	51.52**	1.31	1.04
Foliar %N (2006 Wet season Second Year)	42.45**	0.49	0.41
Soil $\delta^{15}\text{N}$ (2006 Wet season First Year)	66.51**	0.21	0.16
Soil $\delta^{15}\text{N}$ (2006 Wet season Second Year)	85.33**	2.45	4.12**
Vegetation biomass (2005 Wet season)	55.07**	1.21	0.30
Vegetation biomass (2006 Wet season First Year)	96.48**	0.05	0.27
Vegetation biomass (2006 Wet season Second Year)	55.51**	0.57	1.45
Foliar $\delta^{13}\text{C}$ (2005 Wet season)	12.43**	2.10	0.48
Foliar $\delta^{13}\text{C}$ (2006 Wet season First Year)	18.31**	0.95	0.46
Foliar $\delta^{13}\text{C}$ (2006 Wet season Second Year)	25.47**	2.15	1.14

* $p < 0.05$, ** $p < 0.0001$

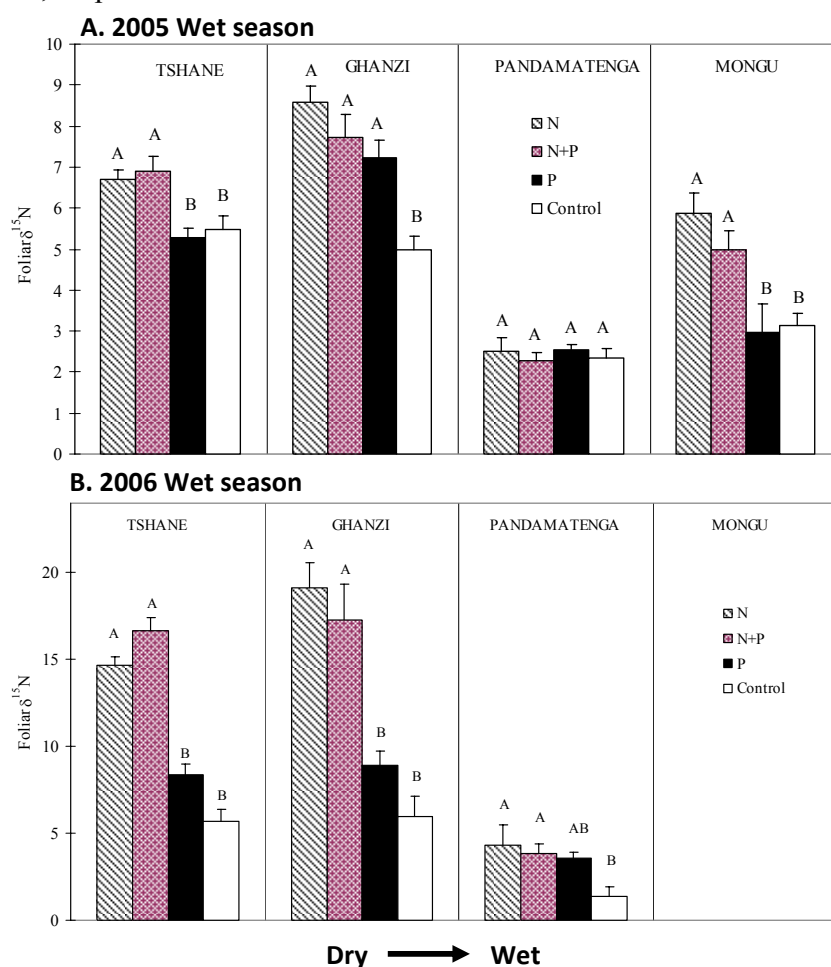


Figure 3.2. Foliar $\delta^{15}\text{N}$ signatures in each treatment at each site for the wet season 2005 (A) and 2006 (B). Different capital letters indicate different means for the four treatments at each location.

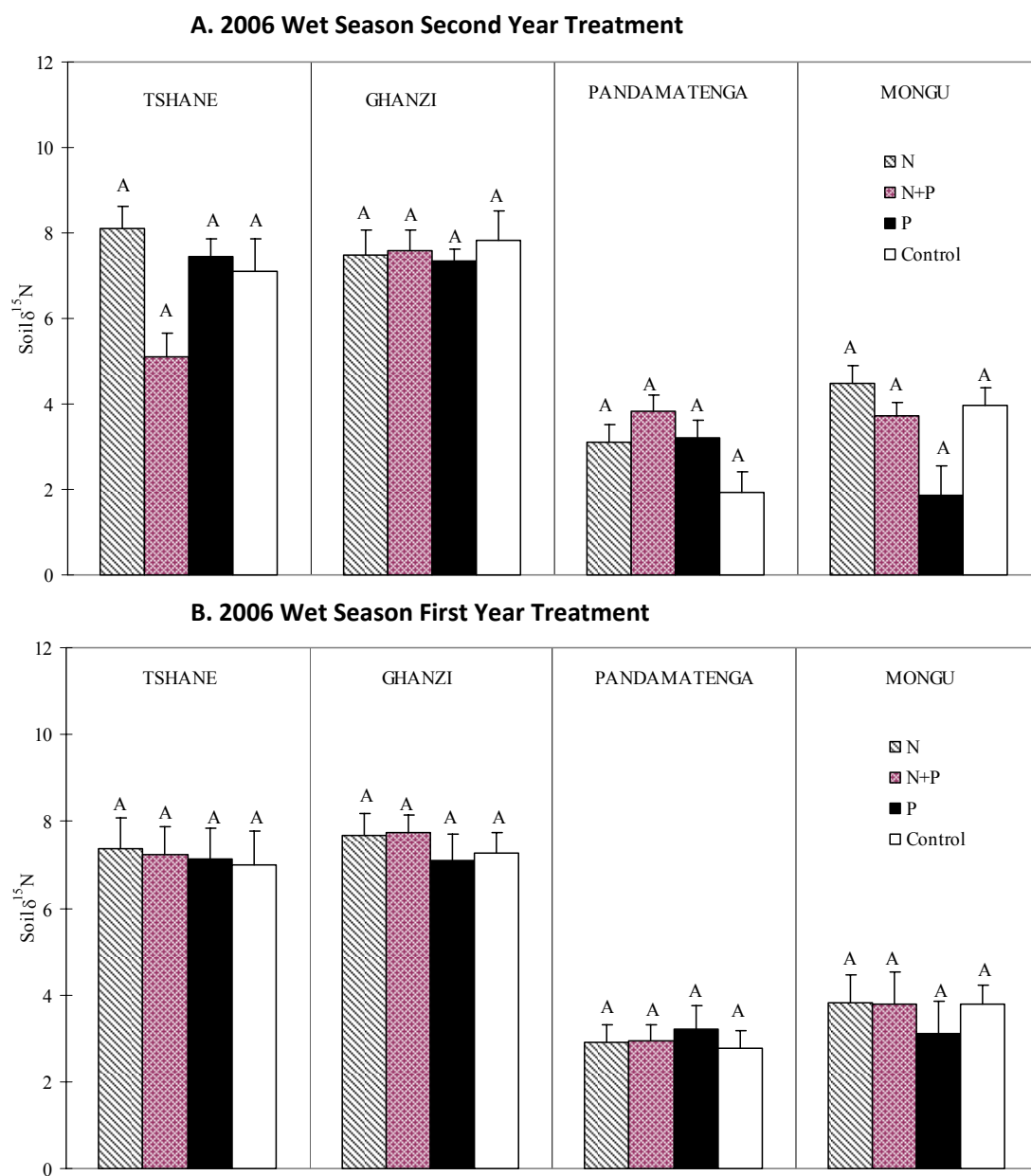
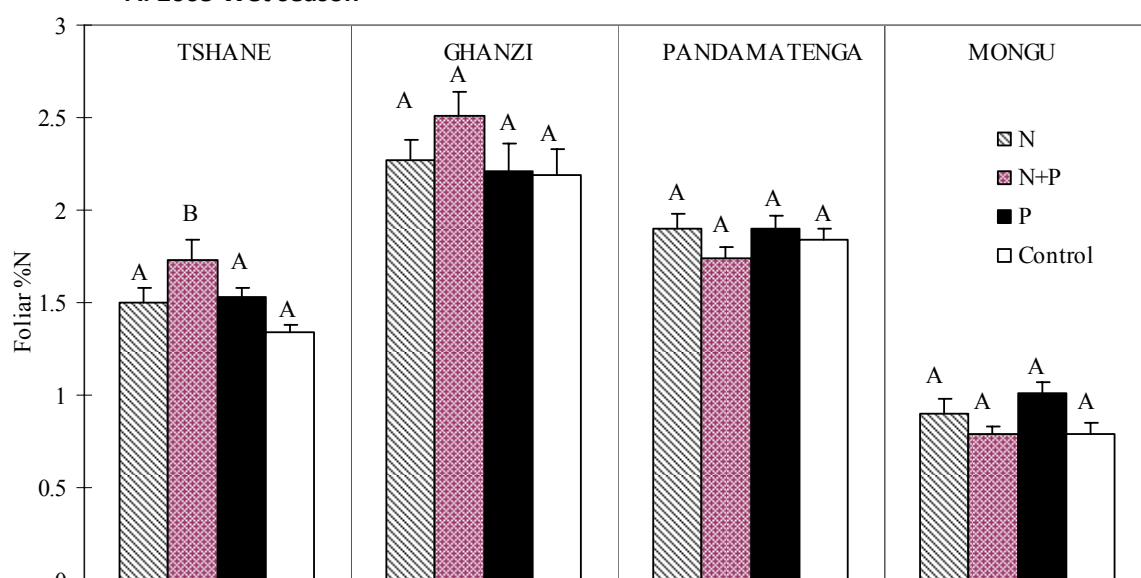


Figure 3.3. Soil $\delta^{15}\text{N}$ signatures (0-5 cm) in each treatment at each site for the first year treatment (A) and second year treatment (B) in 2006. Different capital letters indicate different means for the four treatments at each location.

treatments (Fig. 3.3B). There were similar patterns for soil in the deeper layer (30-35 cm) (data not shown).

There were significant differences in foliar %N among the four locations (Table 3.1), however, no significant differences were found among treatments in the wet seasons of 2005 or 2006 (Fig. 3.4). Both in 2005 and 2006 the foliar %N peaked at Ghanzi, a location with intermediate MAP between the two ends of the KT.

A. 2005 Wet season



B. 2006 Wet season

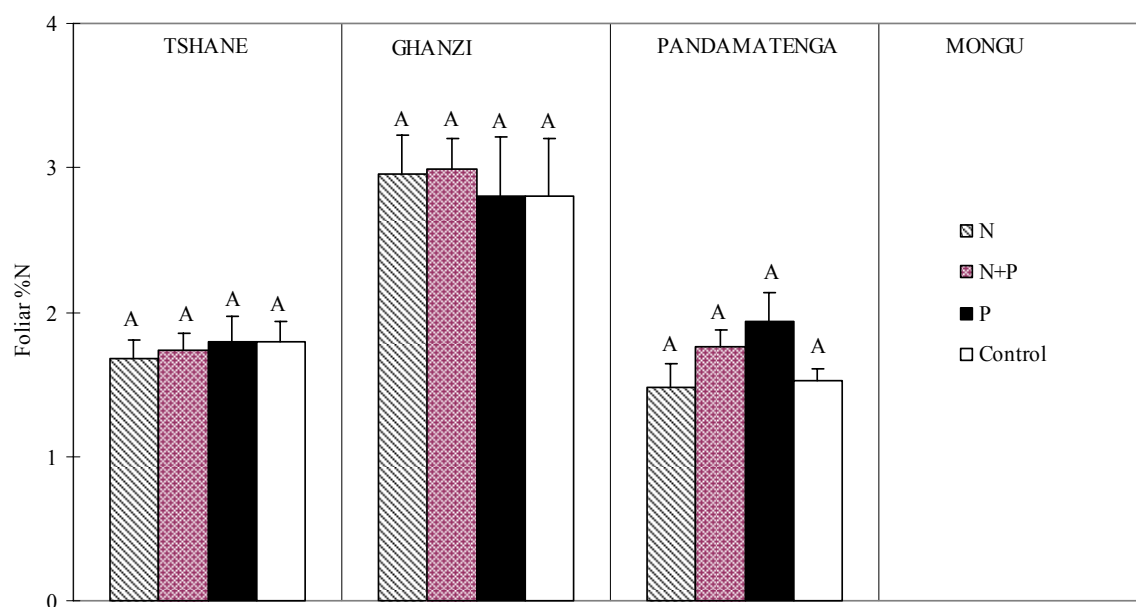


Figure 3.4. Foliar %N in each treatment at each site for the wet season 2005 (A) and 2006 (second year) (B). Different capital letters indicate different means for the four treatments in each location.

At all sites there was no significant increase in aboveground grass biomass for both one (Fig. 3.5A) and two (Fig. 3.5B) growing seasons after the nutrient additions. The grass biomass decreased from the dry to the wet end of the transect in 2005 and increased in 2006 (Table 3.1, Fig. 3.5). The soil moisture/rainfall pattern in 2005 was abnormal, in that soil moisture values in the dry end of the transect were higher than the wet end (Fig. 3.5A insert. Also see D’Odorico et al. (2007)) and rainfall values in the dry end of the transect were comparable to the wet end. The soil moisture/rainfall pattern in 2006 was “normal”, in that it was consistent with the long-term precipitation patterns (Shugart et al., 2004). The aboveground grass biomass did not respond to nutrient addition in both years (Fig. 3.5), while the patterns of grass biomass patterns along the KT matched the soil moisture trends in the corresponding year (Fig. 3.5). The changes in biomass were most significant for the wetter site (i.e., Pandamatenga), where soil moisture doubled from 2005 to 2006, while grass biomass increased more than seven fold (Fig. 3.5).

In general, there was no significant response of the soil respiration rates to fertilization (Fig. 3.6). In both years, soil respiration rates were greatest at the location (Pandamentaga) characterized by intermediate values of MAP (Fig. 3.6; 2005 year data not shown).

5. DISCUSSION

The foliar $\delta^{15}\text{N}$ signatures in the N and N+P additions were consistently and significantly higher than in the control and P-additions both in the 2005 and the 2006 wet seasons (Fig. 3.2), indicating that grasses along the KT took up and assimilated the applied N. However, the assimilated N did not induce a significant increase in foliar N content (Fig. 3.4), nor in aboveground biomass (Fig. 3.5), indicating that N may not be a limiting factor along the entire KT. Because the study sites covered a broad spectrum of

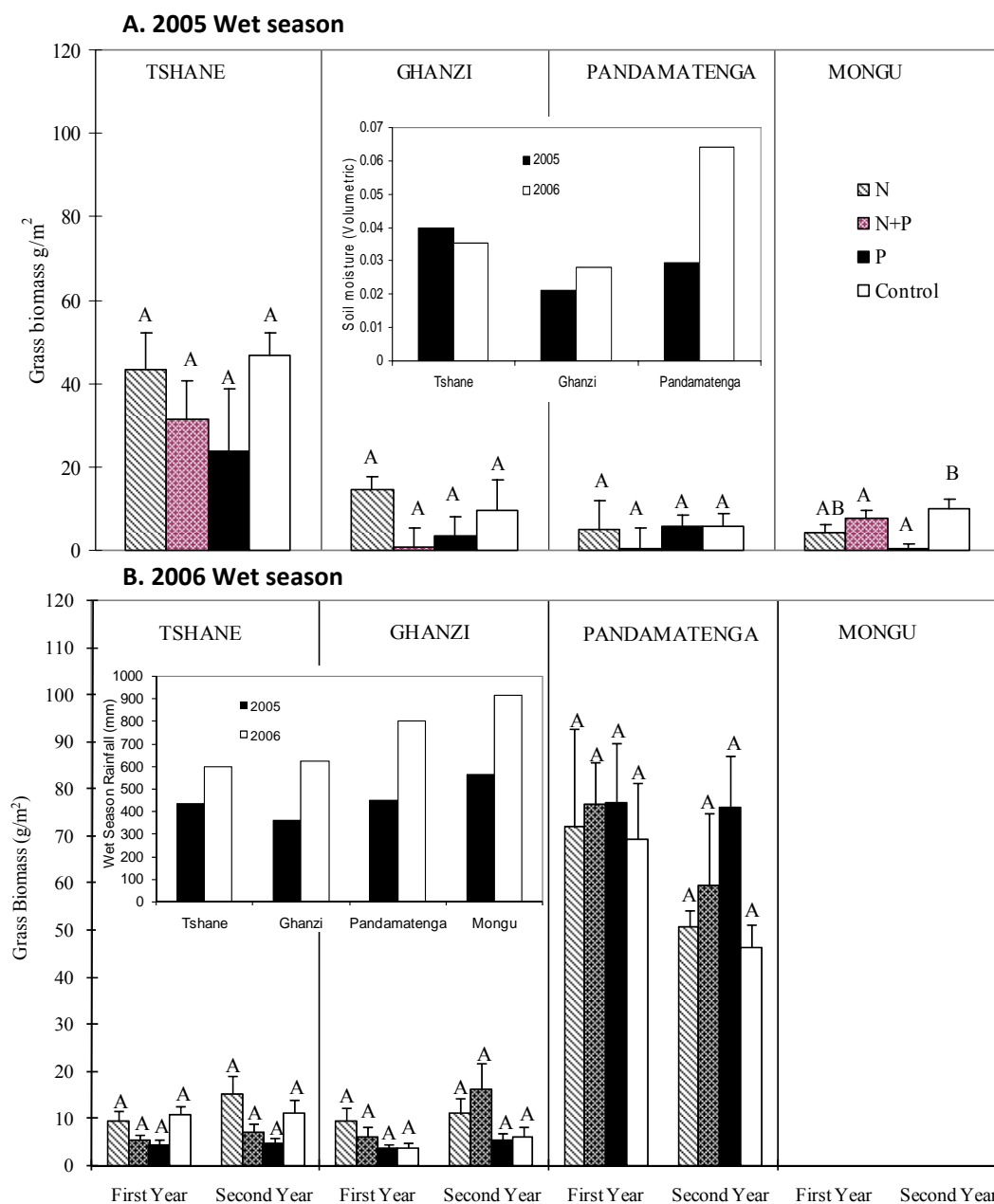


Figure 3.5. Plant biomass in each treatment from each location in the wet season 2005 (A) and 2006 (B). Different capital letters indicate different means for the four treatments in each location. The insert in A shows the average soil moisture for the 2005 and 2006 growing seasons (D'Odorico et al. 2007) and the insert in B shows the wet season (October-April) rainfall data from satellite measurements from NASA's Tropical Rainfall Measuring Mission for 2005 and 2006.

tropical savanna ecosystems, characterized by a variety of rainfall regimes, these results indicate that grass productivity in savannas along the whole KT may not be prone to N limitation (Fig. 3.5) regardless of the MAP. The lack of a response to N fertilization is contradictory to several grassland studies (e.g., Hooper and Johnson 1999) as well as to studies from other savanna ecosystems (e.g., Ludwig et al. 2001). This was presumably due to the nature of the sandy soil (Aranibar et al. 2004, Wang et al. 2007a) existing along the KT, which has limited water holding capacity compared with other regions. These results also differ from previous theoretical predications (Scanlon and Albertson, 2003; Toit et al., 2003; Midgley et al., 2004). The lack of differences in soil respiration rates between treatments (Fig. 3.6) further support the hypothesis that these savanna systems may not be N limited as previously suggested (Scanlon and Albertson, 2003; Aranibar et al., 2004).

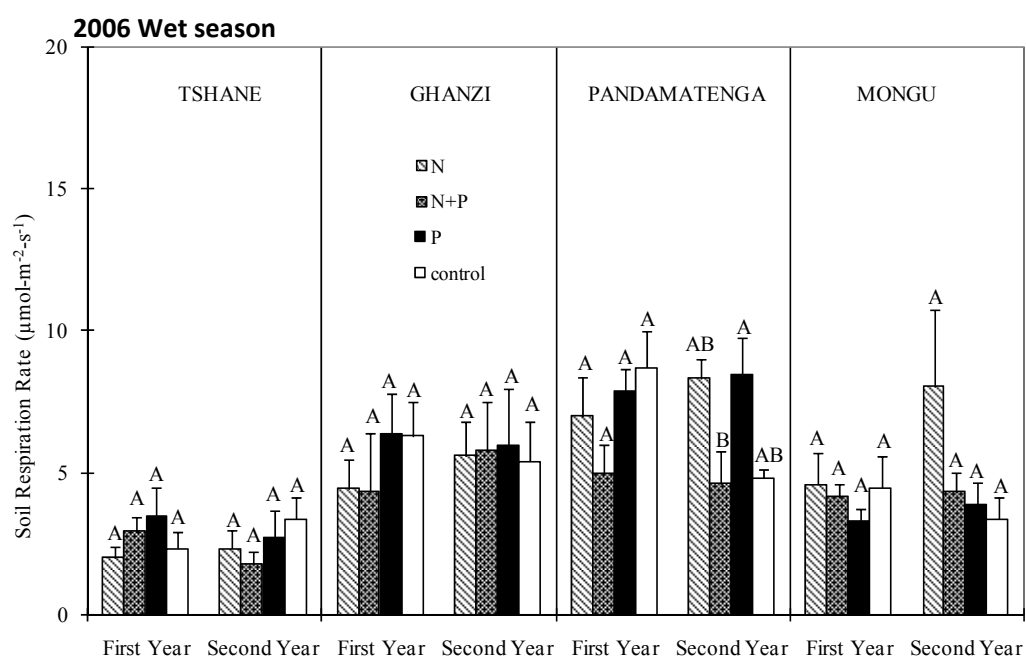


Figure 3.6. Soil respirations in each treatment from each location in the wet season 2006.

In both years, the percentage of assimilated N contributed by the fertilizer was highest at a site (Ghanzi) within the intermediate rainfall regime. This pattern matched the one observed for foliar %N (Fig. 3.4), suggesting that plants with higher N content tend to be more plastic in N uptake (e.g., more easily assimilating external sources of N). This observation supports that of Chapin et al. (1980; 1986) for wild plants that are restricted to infertile soils generally exhibiting lower maximum potential growth rates and responding less to nutrient addition than do related plants from more fertile soils. The patterns of N uptake found along the KT are therefore the result of intrinsic features of the plant communities at each site, and do not reflect different conditions of N limitation.

The decreasing trends in soil $\delta^{15}\text{N}$ signatures agree with previous findings (Aranibar et al., 2004; Wang et al., 2007a) from the same ecosystems, which possibly indicate at ecosystem scales a more open N cycle at the drier portion of the transect. The lack of differences in soil $\delta^{15}\text{N}$ signatures among the four treatments (Fig. 3.3) indicates that the fertilizer N represented only a minor part of the total soil N pool.

The fertilizer treatments applied at each site could have altered the structure and function of herbaceous vegetation in a number of ways that were not addressed in this study. For example, although the results appear to demonstrate a general lack of nutrient limitation in herbaceous vegetation across the sites, I am unable to determine if additional N availability altered either herbaceous allocation patterns (root/shoot ratios) or seed production/viability. In addition, our analyses focused on community-wide responses at each site, so if responses to N availability are strongly species-specific, I would not be

able to observe these effects. Grass biomass did not respond to nutrient addition at any site along the transect regardless of whether the growing season was “abnormal” (2005) or “normal” (2006) in terms of soil moisture/rainfall patterns along the KT. However, the opposite trends in grass biomass observed in 2005 and 2006 correspond to the different patterns of soil moisture, which occurred along the KT in the growing seasons of 2005 and 2006 (see inserts of Fig. 3.5). At the wetter site-Pandamatenga, where previous studies speculated about the existence of N-limitations (Scanlon and Albertson, 2003; Toit et al., 2003; Midgley et al., 2004), grass biomass increased more than seven times when soil moisture/rainfall increased between 2005 and 2006, while the levels of N uptake did not significantly change.

Grazing is inherent to the nature of savanna ecosystems. The present study design did not include any fencing system and assumed an equal consumption of grass biomass at the different treatments. This assumption was supported by the facts that: 1) the foliar N contents did not change after site fertilization. Thus, it is unlikely that fertilization resulted in changes in grass palatability and consequently preferential consumption of grass from the fertilized plots; 2) in the treatment blocks there were almost no animal traces such as dung or trampling marks.

On the basis of the results presented in this study, it is concluded that interannual rainfall variability appears to exert a dominant control on grass productivity in these savannas along the entire KT, even at the wet end of the transect. These findings may have profound implications for global change studies in this region. The KT covers 40-50% of the savanna ecosystems in Africa. The IPCC predictions (Solomon et al., 2007)(Intergovernmental Panel for Climate Change, 2007) indicate that a 5-10%

decrease in rainfall is expected to occur in the next 50 years. Since water is the principal limiting factor in these savanna ecosystems, the rainfall variations will induce profound differences in ecosystem composition/structure and function, including changes in soil carbon emissions, tree/grass ratios, and the reactivation of Kalahari dunes that are currently stabilized by savanna vegetation (e.g., Thomas et al., 2005).

6. CONCLUSIONS

In summary, this large spatial scale field manipulation experiment shows that N may not be a limiting factor in tropical savanna ecosystems. The results of this study demonstrate that even at the wet end of the transect, water remains the principal factor limiting grass productivity. Unlike other reports (Scanlon and Albertson, 2003; Midgley et al., 2004) that conjectured a switch between water and N limitations taking place as annual precipitation exceeded a critical value, these results suggest that grass productivity in the KT is determined by variations in rainfall rather than in N availability. Thus, although the traditional classifications of nutrient poor (broad-leaf savannas) and nutrient rich (fine-leaf savannas) savanna ecosystems may still be useful in the study of these locations and their dynamics (Scholes and Walker, 1993; Toit et al., 2003), this classification does not necessarily imply the existence of nitrogen limitation in the nitrogen poor area, in that the vegetation may already be adapted to nitrogen poor conditions.

Acknowledgements

The project was supported by NASA-IDS2 (NNG-04-GM71G). I greatly appreciate the teamwork and field assistance from Natalie Mladenov, Matt Therrell, Todd Scanlon, Ian McGlynn (University of Virginia), Greg Okin (UCLA), Billy Mogojwa and Thoralf

Meyer (University of Botswana), Barney Kgope (South African National Biodiversity Institute). I thank Dr. Howard Epstein from University of Virginia for loan of the EGM-4 CO₂ analyzer. The TRMM rainfall data were processed by Mr. Teferi Dejene. The clarity and strength of the paper was improved by two anonymous reviewers and subject editor Diane Pataki.

Chapter 4 Patterns and implications of plant-soil $\delta^{13}\text{C}$ and $\delta^{15}\text{N}$ values in African savanna ecosystems

ABSTRACT

Southern African savannas are mixed plant communities where C_3 trees co-exist with C_4 grasses. In this study, foliar $\delta^{15}\text{N}$ and $\delta^{13}\text{C}$ were used as indicators of nitrogen uptake and of water use efficiency, respectively. Its purpose was to investigate the effect of the rainfall regime on the use of nitrogen and water by herbaceous and woody plants in both dry and wet seasons along the Kalahari megatransect, where a distinct rainfall gradient exists on a homogeneous soil substrate. Foliar $\delta^{15}\text{N}$ increased as aridity rose for both C_3 and C_4 plants for both seasons, although the magnitude of the increase was different for these two plant functional types. Soil $\delta^{15}\text{N}$ also significantly increased with aridity. Foliar $\delta^{13}\text{C}$ signatures increased with aridity for C_3 plants in the wet season but not in the dry season, whereas in C_4 plants the relationship was more complex and non-linear. The consistently higher foliar $\delta^{15}\text{N}$ for C_3 plants suggests that C_4 plants may be a superior competitor for nitrogen. The different foliar $\delta^{13}\text{C}$ relationships with rainfall may indicate that the C_3 plants have an advantage over C_4 plants when competing for water resources. The differences in water and nitrogen use between C_3 and C_4 plants likely collectively contribute to the tree-grass coexistence in savannas.

Keywords: Stable Isotopes, Soil Nitrogen, Soil Carbon, Aridity, C_3 plants, C_4 plants, Africa, Savanna

Wang, L., P. D'Odorico, L. Ries and S. Macko. Patterns and implications of plant-soil $\delta^{13}\text{C}$ and $\delta^{15}\text{N}$ values in African savanna ecosystems. *Quaternary Research* (in review).

1.INTRODUCTION

Savannas cover approximately 20% of the Earth's land area including about 40% of Africa (Scholes and Walker, 1993). In Africa, savannas provide an ideal grazing/browsing habitat for both native herbivores such as the elephant, hippopotamus and buffalo as well as cattle brought in by humans. Humans depend heavily on savanna ecosystems both as rangelands for livestock grazing, and for fuel wood harvesting (Aranibar, 2003). The origin of the modern savanna biome in Africa is closely linked to the dramatic expansion of C₄ grasses in this continent during the Miocene (Beerling and Osborne, 2006). Natural and anthropogenic disturbances associated with climate fluctuations, fire regime, grazing and browsing pressure contributed to determine conditions favorable for the existence of mixed tree-grass communities (Sinclair, 1979; Scholes and Archer, 1997). The non-successional persistence of trees and grasses (mainly the C₃ and C₄ plants) on the savannas has intrigued scientists for decades (e.g., Sarmiento, 1984; Scholes and Archer, 1997; Sankaran et al., 2005, Wang et al. 2007a), however a few key aspects of savanna ecology remain poorly understood. For example, differences in the morphology and physiology of trees and grasses may explain their different access to nutrients and water, and their different efficiency in the use of these resources. It is still unclear how climate variables such as the mean annual precipitation (MAP) may affect the relative efficiency of grasses and trees in the use of water and in the uptake of soil nutrients such as nitrogen (N), and how changes in the rainfall regime may affect the coexistence of these two plant functional types.

The natural abundance of stable isotopes is routinely utilized as an indicator of ecosystem processes (Robinson, 2001). For example, foliar $\delta^{13}\text{C}$ is often used to

determine plant water use efficiency (Farquhar et al., 1989), whereas ^{15}N is an integrator of N cycling and reflects numerous processes occurring in soil, plants, and atmosphere (Högberg, 1997; Robinson, 2001). In fact, the $\delta^{15}\text{N}$ signatures of plant leaves and roots, and of soil organic matter result from a combination of a number of factors including access to different N sources and the effects of isotopic fractionation (Wang et al., 2007d). A few studies have investigated the relation between foliar $\delta^{13}\text{C}$ and $\delta^{15}\text{N}$ along gradients of rainfall, substrate age and disturbance pressure at different temporal and spatial scales (Austin and Vitousek, 1998; Brenner et al., 2001; Aranibar et al., 2004; Swap et al., 2004; Sah et al., 2006; Aranibar et al., 2007; Wang et al., 2007a). However, the presence of co-varying factors (e.g., plant species composition and seasonality, or soil properties) along some of these gradients has often prevented the interpretation of the ecosystem processes underlying the relation between foliar $\delta^{13}\text{C}$ and $\delta^{15}\text{N}$, and the apparent influence by the rainfall regime.

Situated in central part of southern Africa, the Kalahari is the ideal location to study these water and nitrogen controls in savannas. In fact, this region hosts a variety of savanna ecosystems - ranging from fine-leaved open savanna in the south to broad-leaved savanna woodlands in the north - along a dramatic rainfall gradient on relatively homogenous soils, i.e., the deep Kalahari sands (Wang et al., 2007a). Identified by the IGBP (International Geosphere-Biosphere Programme) as one of the “mega-transects” for global change studies (Koch et al., 1995), the Kalahari Transect (KT) provides the ideal setting to study nutrient and vegetation dynamics without confounding soil effects.

The present study examines patterns of foliar $\delta^{13}\text{C}$ and $\delta^{15}\text{N}$ along the KT both in the wet and in the dry season, for two distinct plant functional types typical of African

savannas, namely C₃ trees and C₄ grasses. Patterns of soil $\delta^{13}\text{C}$ and $\delta^{15}\text{N}$ from soil patches dominated by C₃ and C₄ plants are also investigated both in the dry and the wet season. Differences in foliar $\delta^{13}\text{C}$ and $\delta^{15}\text{N}$ between these two different plant functional types and seasons, and among different species within the same plant functional type are used to provide information on plant water and N use, thereby providing new insights on tree-grass interactions in savanna ecosystems. Moreover, the combined analysis of patterns of foliar and of soil $\delta^{13}\text{C}$ and $\delta^{15}\text{N}$ along the rainfall gradient, contributes to a better understanding of savanna carbon (C) and N dynamics at the ecosystem level.

2. MATERIALS AND METHODS

2.1 Study sites

The KT in southern Africa was used as a model ecosystem (due to its homogenous soils along a relatively strong rainfall gradient) to examine patterns of foliar and soil $\delta^{13}\text{C}$ and $\delta^{15}\text{N}$ under different climatic conditions. The most northern site was situated in Mongu, Zambia, with a MAP of 879 mm. The vegetation in Mongu is woodland savanna dominated by woody species such as *Brachystegia spiciformis* Benth. Three other sites from north to south were situated in Pandamatenga, Ghanzi and Tshane, Botswana (Fig. 4.1). The MAP in these three areas range from 700 mm to 365 mm, respectively. The vegetation in Tshane and Ghanzi is typical of an open savanna dominated by *Acacia* species such as *A. luederizii* Engl. and *A. mellifera* Benth. The vegetation cover in Pandamatenga is a woodland savanna dominated by tree species such as *Kirkia africana* and grass species such as *Schmidtia pappophoroides* and *Pogonarihria squarrosa*.

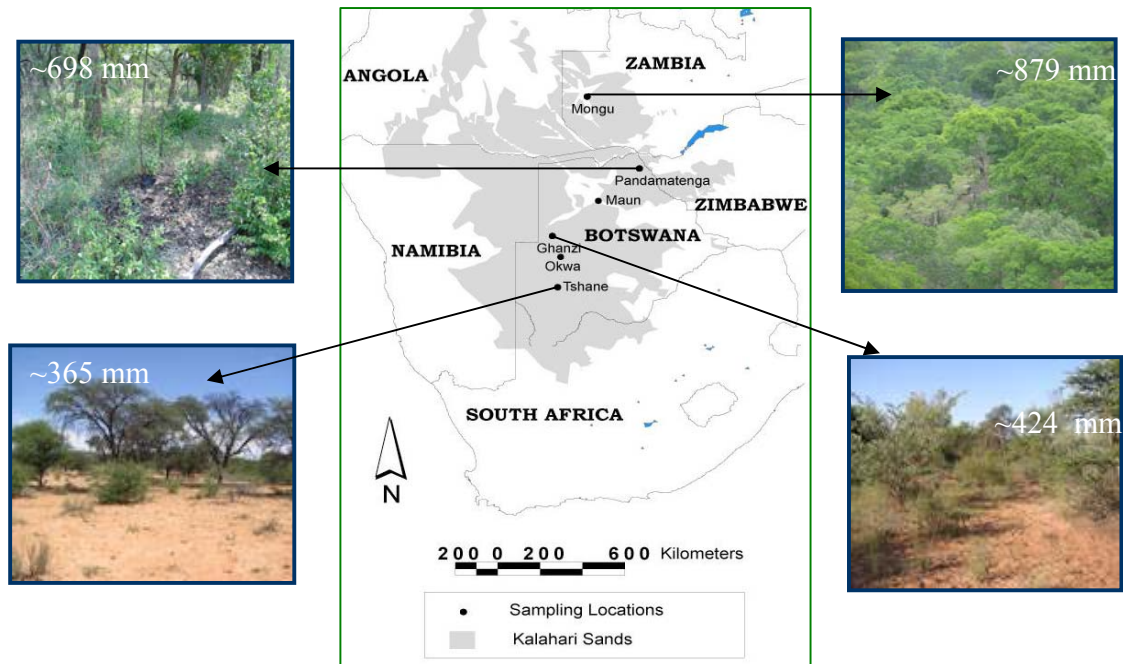


Figure 4.1. Sampling locations along the Kalahari Transect precipitation gradient in southern Africa. Numbers in each photo are the mean annual precipitation.

2.2 Field sampling and chemical analyses

The foliar samples of C_3 vegetation (mainly tree species) were collected during the 2004 dry season (August-September) and 2005 wet season (February-March). The foliar samples of C_4 vegetation (mainly grass species) were collected during the 2005 dry season (August-September) and the 2005 wet season (February-March). In the dry seasons of 2004 and 2005, 10-20 random samples for each plant functional type (i.e., C_3 vs. C_4) were collected at each of the four sites. In the 2005 wet season, a more systematic sampling scheme was employed: for the C_4 species, twenty $1 \times 1 \text{ m}^2$ plots were selected at each location and all the plants inside each plot were sampled and grouped by species; for C_3 species, foliar samples were collected from all the individuals inside four $6 \times 10 \text{ m}^2$ plots at each location and separated by species. For the C_3 species sampling, I concentrated on live leaves with similar heights above the ground. The genus and species

of the foliar samples were identified upon collection in the course of the 2005 wet season. The unidentified samples were reported in a specimen book and labeled incrementally (e.g., Unidentified (ID #8)). The soil samples were collected (in five replicates) from both beneath tree canopies and in open areas at each site in the dry season of 2004 and the wet season of 2005 using a stainless steel sand auger. The 2004 dry season soil data has been reported previously (Wang et al., 2007a).

Foliar and soil samples were dried at 60°C for 72 hours. After drying, they were ground and homogenized for isotope and elemental analysis. Stable C and N isotope analyses were performed using a Micromass Optima Isotope Ratio Mass Spectrometer (IRMS) connected to an elemental analyzer (EA) (GV/Micromass, Manchester, UK). Stable isotope compositions were reported in the conventional form:

$$\delta^xE \text{ (‰)} = [(^xE/ ^yE)_{\text{sample}} / (^xE/ ^yE)_{\text{standard}} - 1] \times 1000$$

where E is the element measured, x is the heavier isotope and y is the lighter isotope.

Thus, $(^xE/ ^yE)_{\text{sample}}$ and $(^xE/ ^yE)_{\text{standard}}$ are the isotopic ratios of the sample and standard, respectively. The stable isotopic composition of C and N will be denoted as $\delta^{13}\text{C}$ (‰) and $\delta^{15}\text{N}$ (‰), respectively. The standards for C and N stable isotopes are Pee Dee Belemnite (PDB) and atmospheric molecular N (N_2), respectively. Reproducibility of these measurements is typically better than 0.2‰. Foliar as well as soil %C and %N were measured using an elemental analyzer (EA).

2.3 Statistical analyses

Foliar and soil $\delta^{15}\text{N}$, $\delta^{13}\text{C}$, %C and %N data were normally distributed and were not transformed. To assess the relationships between foliar $\delta^{15}\text{N}$ and $\delta^{13}\text{C}$ with MAP along the rainfall gradient, the data were fitted with a linear or a polynomial function, depending on the data. Regressions with linear functions were used in the case of the relation between foliar $\delta^{15}\text{N}$ and MAP along the KT for both C_3 and C_4 vegetation, in both the dry and the wet seasons (SAS v. 9.1, PROC REG). Linear functions were also used for foliar $\delta^{13}\text{C}$ vs. MAP for C_3 vegetation, in the dry and wet seasons, as well. Polynomial functions were used in the cases of foliar $\delta^{13}\text{C}$ and MAP for C_4 vegetation in both seasons (SAS v. 9.1, PROC REG) owing to the non-monotonic relationship between $\delta^{13}\text{C}$ and MAP suggested by the data. To assess the within-site variations in foliar $\delta^{15}\text{N}$, $\delta^{13}\text{C}$, %C and %N, one-way ANOVA (SAS v. 9.1 PROC GLM) was used to compare the differences between species at each site. One-way ANOVA was also used to compare the within-site variations for soil $\delta^{15}\text{N}$ and $\delta^{13}\text{C}$ (SAS v. 9.1 PROC GLM). For all the statistical analyses, the significance levels were chosen as $\alpha = 0.05$.

3. RESULTS

The foliar $\delta^{15}\text{N}$ signatures increased with aridity for both C_3 and C_4 plants in both dry and wet seasons, but the magnitude of changes was different for the two plant functional types (Fig. 4.2). Within the same plant functional type, the foliar $\delta^{15}\text{N}$ signatures were not significantly different between the dry and wet seasons, as indicated by the slope (Fig. 4.2) of the regression lines (0.009 and 0.011 for C_3 plants in dry and wet seasons, respectively; 0.0069 for C_4 plants both in the dry and wet seasons). The

foliar $\delta^{15}\text{N}$ signatures of C_4 plants had consistently lower $\delta^{15}\text{N}$ signatures than C_3 plants at the dry end of the KT, whereas no significant differences existed at the sites with greater MAP (Fig. 4.2). These relationships were consistent for both dry and wet seasons (Fig. 4.2). Within each site, there were no significant differences in foliar $\delta^{15}\text{N}$ signatures among C_4 species at the drier end of the transect (i.e., at Tshane and Ghanzi) (Table 4.1). At the wetter end, the foliar $\delta^{15}\text{N}$ signatures changed significantly among the species of the same functional group, especially for the C_3 plants, with values ranging from 0.3 ‰ to 3.9 ‰ (Tables 4.1 and 4.2).

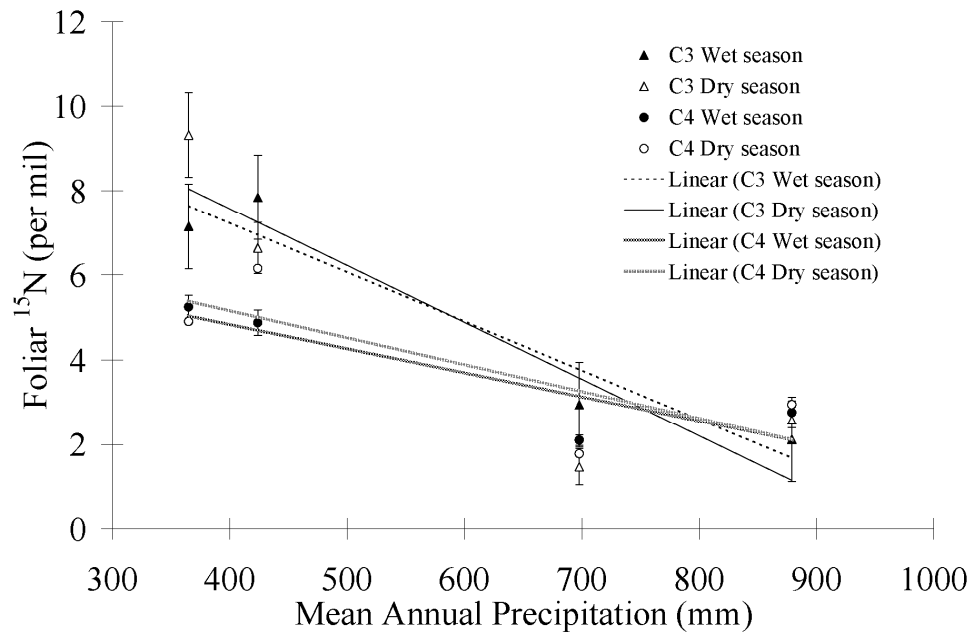


Figure 4.2. The relationships between foliar $\delta^{15}\text{N}$ signatures and mean annual precipitation for C_3 and C_4 vegetation during dry and wet seasons along the Kalahari Transect. The liner equations for C_3 and C_4 vegetation: C_3 in wet season: $y = -0.0094x + 10.23$, $R^2 = 0.78$, $p < 0.0001$; C_3 in dry season: $y = -0.0106x + 10.86$, $R^2 = 0.62$, $p = 0.0003$; C_4 in wet season: $y = -0.0069x + 7.60$, $R^2 = 0.49$, $p < 0.0001$; C_4 in dry season: $y = -0.0069x + 7.96$, $R^2 = 0.28$, $p = 0.008$.

The foliar $\delta^{13}\text{C}$ signatures of C_3 plants were lower than for C_4 plants regardless of the season (Fig. 4.3). The foliar $\delta^{13}\text{C}$ signatures increased as aridity increased for C_3

plants in the wet season but there were limited variations in foliar $\delta^{13}\text{C}$ signatures for C_3 plants in the dry season (Fig. 4.3A). The relationships between foliar $\delta^{13}\text{C}$ signatures and aridity in C_4 plants were more complex in both seasons (Fig. 4.3B). The foliar $\delta^{13}\text{C}$ signatures were higher in the wet season than the dry season for C_4 plants, with the opposite relation being found for the C_3 plants (Fig. 4.3). Within each site, there were no significant differences in foliar $\delta^{13}\text{C}$ signatures among species for C_4 plants both at the dry (Tshane and Ghanzi) and the wet end (Mongu) of the transect (Table 4.1). For C_3 plants, there were no significant differences in foliar $\delta^{13}\text{C}$ signatures among species in the three southern locations, while at Mongu, foliar $\delta^{13}\text{C}$ signatures exhibited a broader variability (Table 4.2), with values ranging from -29.6‰ to -26.9‰.

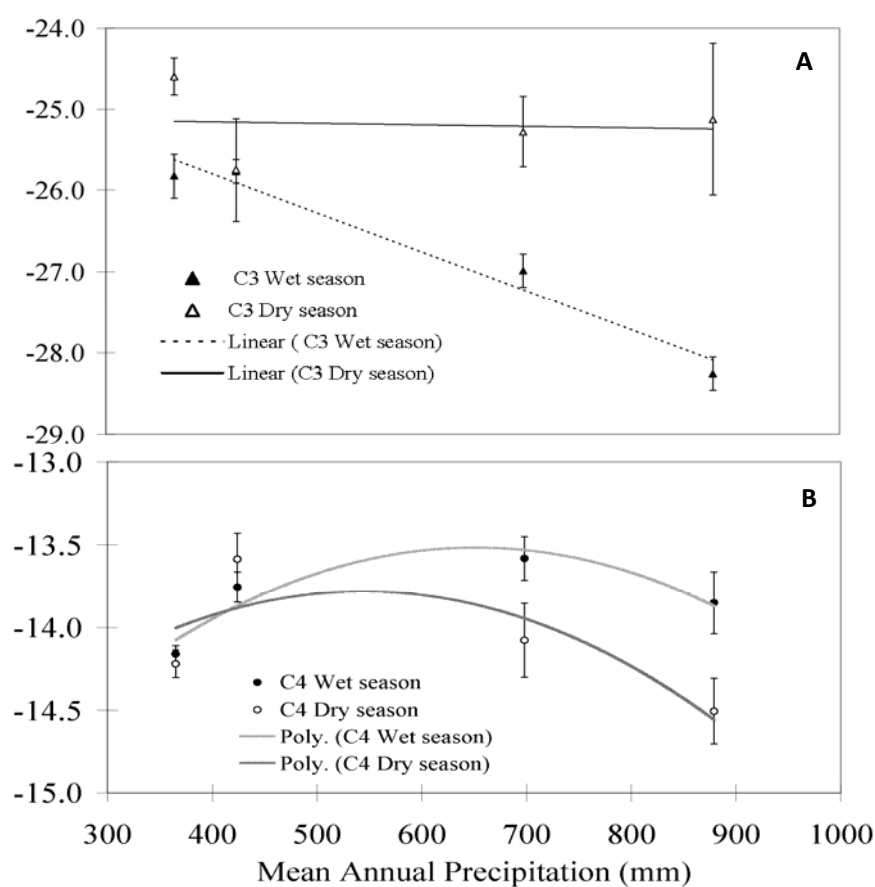


Figure 4.3. The relationships between foliar $\delta^{13}\text{C}$ signatures and mean annual precipitation for C_3 (A) and C_4 (B) vegetation during dry and wet seasons along the Kalahari Transect. The equations for C_3 and C_4 vegetation: C_3 in wet season: $y = -0.0042x - 24.37$, $R^2 = 0.96$, $p < 0.0001$; C_3 in dry season: $y = -0.0002x - 25.07$, $R^2 = 0.02$, $p > 0.05$; C_4 in wet season: $y = -0.000005x^2 + 0.0063x - 15.58$, $R^2 = 0.97$, $p < 0.0001$; C_4 in dry season: $y = -0.000004x^2 + 0.0042x - 14.93$, $R^2 = 0.61$, $p < 0.0001$.

Table 4.1. The %C, %N and isotope (^{13}C and ^{15}N) content (Mean \pm Standard error) for C_4 vegetation along the Kalahari Transect in wet season 2005.

	Sample size (n)	%C	%N	C/N	$\delta^{13}\text{C}$ (‰)	$\delta^{15}\text{N}$ (‰)
Tshane						
<i>Eragrostis lehmanniana</i>	13	43.8 \pm 0.3 ^a	1.3 \pm 0.1 ^a	35.3 \pm 2.9 ^a	-14.2 \pm 0.1 ^a	5.4 \pm 0.5 ^a
<i>Schmidtia pappophoroides</i>	17	41.5 \pm 0.5 ^b	1.3 \pm 0.1 ^a	32.1 \pm 1.4 ^a	-14.1 \pm 0.1 ^a	5.2 \pm 0.3 ^a
Ghanzi						
<i>Urochloa brachyura</i>	4	41.7 \pm 0.6 ^{ab}	2.8 \pm 0.1 ^a	14.8 \pm 0.8 ^a	-13.7 \pm 0.2 ^a	4.5 \pm 0.5 ^a
<i>Stipagrostis suniplumis</i>	5	45.4 \pm 0.6 ^a	1.4 \pm 0.1 ^b	33.3 \pm 2.3 ^b	-14.1 \pm 0.2 ^a	3.8 \pm 0.6 ^a
<i>Schmidtia pappophoroides</i>	13	37.4 \pm 1.3 ^b	2.2 \pm 0.2 ^a	18.2 \pm 1.2 ^a	-13.7 \pm 0.1 ^a	5.4 \pm 0.4 ^a
Pandamatenga						
<i>Panicum maximum</i>	7	43.6 \pm 0.3 ^a	2.5 \pm 0.1 ^a	17.9 \pm 1.0 ^a	-13.8 \pm 0.1 ^a	3.0 \pm 0.2 ^a
<i>Aristida stipitata</i>	6	43.8 \pm 0.6 ^a	1.6 \pm 0.1 ^b	28.1 \pm 1.6 ^b	-14.3 \pm 0.1 ^b	1.3 \pm 0.2 ^b
<i>Megaloprotachne albescens</i>	6	42.6 \pm 0.4 ^a	1.6 \pm 0.1 ^b	27.5 \pm 2.5 ^b	-12.5 \pm 0.1 ^c	1.7 \pm 0.1 ^{bc}
<i>Pogonarihria squarrosa</i>	3	40.5 \pm 1.2 ^a	1.8 \pm 0.1 ^b	22.8 \pm 1.6 ^{ab}	-14.4 \pm 0.1 ^b	2.2 \pm 0.4 ^{abcd}
<i>Tricholaena monachne</i>	6	43.5 \pm 0.4 ^a	1.9 \pm 0.1 ^b	22.7 \pm 0.8 ^{ab}	-14.3 \pm 0.1 ^b	1.9 \pm 0.2 ^{bc}
<i>Digitaria species</i>	6	41.1 \pm 1.5 ^a	1.6 \pm 0.1 ^b	26.3 \pm 1.2 ^b	-12.9 \pm 0.1 ^d	2.5 \pm 0.3 ^{acd}
<i>Heteropogon contortus</i>	1	42.1	1.7	24.7	-12.8	1.8
<i>Urochloa brachyura</i>	1	40.7	1.8	22.9	-12.3	1.9
Mongu						
Unidentified grass (ID #3)	9	40.9 \pm 2.9 ^a	0.7 \pm 0.1 ^a	62.4 \pm 5.1 ^a	-13.8 \pm 0.2 ^a	2.9 \pm 0.1 ^a
Unidentified grass (ID #6)	2	42.7 \pm 4.5 ^a	0.9 \pm 0.1 ^a	49.3 \pm 9.4 ^a	-13.1 \pm 0.5 ^a	2.6 \pm 1.5 ^a
Unidentified sedge	1	53.6	1.2	43.9	-14.5	0.7

Soil $\delta^{15}\text{N}$ signatures increased with aridity both in microsites dominated by C_3 and C_4 plants (Fig. 4.4A). The soil $\delta^{15}\text{N}$ signatures in samples collected in C_3 and C_4 microsites had about the same values in a given season at both the dry and wet extreme

end of the transect. At Ghanzi and Pandamatenga, the two intermediate rainfall regime locations, neither the plant functional type nor the season appear to affect the soil $\delta^{15}\text{N}$ (Fig. 4.4A). In the case of C_3 plants the soil $\delta^{15}\text{N}$ signatures explained 96% and 95% of the total variance in foliar $\delta^{15}\text{N}$ signatures in the wet and dry season, respectively, whereas for C_4 plants the soil $\delta^{15}\text{N}$ signatures explained 99% and 93% of the total variance in foliar $\delta^{15}\text{N}$ signatures in the wet and dry season, respectively.

In general, the soil $\delta^{13}\text{C}$ signatures increased with increasing aridity along the KT (Fig. 4.4B). At the wettest end of the transect (Mongu), the two plant functional types had similar soil $\delta^{13}\text{C}$ within the same season, with soil $\delta^{13}\text{C}$ signatures being higher in the dry season; at the dry end, such relationships still held though the trends were not as strong as those in the wet end of the transect (Fig. 4.4B).

4. DISCUSSION

The foliar $\delta^{15}\text{N}$ signatures for C_3 plants increased with increasing aridity (Fig. 4.2), being consistent with previous observations from a larger scale study in southern Africa (Swap et al., 2004). However, unlike Swap et al. (2004), in the current study linear relationships between foliar $\delta^{15}\text{N}$ signatures and MAP were also observed along the KT for C_4 plants both in the dry and wet seasons (Fig. 4.2). These differences may be due to the fact that, while the KT covers a relatively homogenous soil substrate, the study by Swap et al. (2004) covered a broader region (i.e., the whole southern Africa) with heterogeneous soil conditions and presumably different soil $\delta^{15}\text{N}$ signatures, thus confounding the rainfall effect on foliar $\delta^{15}\text{N}$. Along the KT, the foliar $\delta^{15}\text{N}$ signatures were not significantly different between dry and wet seasons both for C_3 and C_4 plants (Fig. 4.2), supporting the basic assumptions in Swap et al. (2004) that seasonality does not affect plant foliar $\delta^{15}\text{N}$.

Table 4.2. The % C, %N and isotope ($\delta^{13}\text{C}$ and $\delta^{15}\text{N}$) content (Mean \pm Standard error) for C_3 vegetation along Kalahari Transect in wet season 2005.

	Sample size (n)	%C	%N	C/N	$\delta^{13}\text{C}$ (‰)	$\delta^{15}\text{N}$ (‰)
Tshane						
<i>Grewia flava</i>	4	48.4 \pm 0.1 ^a	2.5 \pm 0.2 ^a	19.6 \pm 1.3 ^a	-26.6 \pm 0.5 ^a	7.5 \pm 1.0 ^a
<i>Rhigozum brevispinosum</i>	2	44.6 \pm 0.5 ^{bc}	2.0 \pm 0.4 ^a	23.1 \pm 4.1 ^a	-25.3 \pm 0.4 ^a	5.2 \pm 0.5 ^a
<i>Acacia leuderitzii</i>	2	50.4 \pm 1.0 ^{ad}	2.2 \pm 0.3 ^a	23.1 \pm 3.1 ^a	-24.8 \pm 0.3 ^a	7.2 \pm 0.5 ^a
<i>Boscia albitrunca</i>	3	44.8 \pm 0.9 ^c	3.9 \pm 0.7 ^a	12.4 \pm 2.7 ^a	-25.9 \pm 0.4 ^a	8.6 \pm 1.2 ^a
<i>Rhus aethiopica</i>	1	49.8	2.6	18.9	-27.2	5.2
<i>Acacia mellifera</i>	1	44.7	3.2	13.9	-25.8	7.2
Ghanzi						
<i>Acacia leuderitzii</i>	2	49.2 \pm 3.6 ^a	3.0 \pm 0.1 ^a	16.1 \pm 0.4 ^a	-25.3 \pm 0.1 ^a	6.6 \pm 0.1 ^a
<i>Acacia mellifera</i>	2	45.4 \pm 1.4 ^a	4.6 \pm 0.4 ^a	9.9 \pm 0.6 ^a	-25.7 \pm 0.4 ^a	7.5 \pm 0.9 ^a
<i>Grewia retinervis</i>	3	43.4 \pm 2.6 ^a	2.9 \pm 0.5 ^a	15.8 \pm 2.5 ^a	-26.0 \pm 0.2 ^a	7.7 \pm 0.3 ^a
<i>Grewia flava</i>	1	47.2	3.1	15.0	-26.6	11.4
Pandamatenga						
<i>Baikiaca plurijuga</i>	6	51.8 \pm 0.5 ^a	4.2 \pm 0.1 ^{ac}	12.4 \pm 0.3 ^{ac}	-26.0 \pm 0.6 ^a	3.1 \pm 0.3 ^{ac}
<i>Bauhimia macrantha</i>	3	50.0 \pm 0.2 ^{ac}	4.7 \pm 0.03 ^{bc}	10.6 \pm 0.1 ^{bcd}	-28.1 \pm 0.4 ^a	4.0 \pm 0.1 ^a
<i>Diplorhynchus condylocarpum</i>	4	50.0 \pm 0.6 ^{ac}	2.7 \pm 0.1 ^d	18.9 \pm 0.8 ^f	-26.0 \pm 0.4 ^a	2.8 \pm 0.1 ^{ac}
<i>Grewia monticola</i>	2	48.8 \pm 0.6 ^{bc}	5.4 \pm 0.2 ^b	9.0 \pm 0.1 ^d	-26.5 \pm 0.8 ^a	1.8 \pm 0.5 ^{cd}
Unidentified (ID #5)	2	48.9 \pm 0.6 ^{bc}	2.8 \pm 0.3 ^d	17.7 \pm 1.4 ^{ef}	-27.3 \pm 0.4 ^a	3.4 \pm 0.3 ^{ac}
<i>Baphia mossiensis</i>	5	50.8 \pm 0.4 ^{ac}	5.1 \pm 0.3 ^b	10.1 \pm 0.5 ^d	-27.7 \pm 0.3 ^a	1.6 \pm 0.3 ^{bd}
<i>Combretum hereroense</i>	1	49.1	3.5	14.1	-27.0	3.6
<i>Ricinodendron rautaninii</i>	1	48.5	4.5	10.8	-27.9	4.7
Unidentified (ID #6)	1	46.9	4.7	10.0	-27.8	1.6
<i>Burkea africana</i>	1	49.6	4.4	11.2	-27.1	3.8
<i>Croton gratissimus</i>	1	50.2	4.4	11.5	-26.7	5.9
Mongu						
<i>Rinorea ilicifolia</i>	3	51.6 \pm 1.0 ^a	2.0 \pm 0.2 ^{ab}	26.4 \pm 1.7 ^{ab}	-28.7 \pm 0.2 ^{ab}	3.9 \pm 0.4 ^a
<i>Bauhimia macrantha</i>	3	49.3 \pm 1.3 ^a	2.7 \pm 0.2 ^{ad}	18.6 \pm 1.5 ^a	-27.7 \pm 0.4 ^{ac}	3.2 \pm 0.1 ^a
<i>Guilbourita conjugata</i>	2	53.7 \pm 0.1 ^{ac}	2.8 \pm 0.2 ^{ae}	19.0 \pm 1.4 ^a	-27.1 \pm 0.1 ^{ac}	3.0 \pm 0.2 ^a
Unidentified (ID #13)	2	48.3 \pm 0.9 ^a	3.1 \pm 0.5 ^{cde}	16.1 \pm 4.0 ^a	-28.7 \pm 0.8 ^{abc}	0.3 \pm 0.7 ^b
<i>Copaifera baumiana</i>	4	56.3 \pm 0.4 ^{bc}	1.6 \pm 0.1 ^{bf}	35.7 \pm 2.6 ^b	-29.6 \pm 0.5 ^b	0.7 \pm 0.2 ^b
Unidentified (ID #30)	2	53.3 \pm 0.2 ^{ac}	2.0 \pm 0.0 ^{af}	26.5 \pm 0.0 ^{ab}	-27.9 \pm 0.0 ^{abc}	2.9 \pm 0.2 ^a
Unidentified (ID #23)	3	50.0 \pm 1.3 ^a	1.8 \pm 0.2 ^{bf}	28.3 \pm 3.0 ^{ab}	-26.9 \pm 0.2 ^c	2.6 \pm 0.4 ^a
Unidentified (ID #8)	1	57.4	1.7	34.0	-29.0	0.4
Unidentified shrub (ID #10)	1	50.0	2.5	19.9	-30.2	3.0
<i>Burkea africana</i>	1	51.8	1.5	34.4	-27.6	3.8
<i>Pseudolachnostylis maprouneifolia</i>	1	50.1	1.4	36.5	-27.4	0.8
<i>Ochna pulchra</i>	1	53.4	1.5	36.0	-28.0	2.7
<i>Quibourtia coleosperma</i>	1	50.9	2.8	18.5	-28.3	0.3
<i>Parinari curatellifolia</i>	1	52.7	3.4	15.5	-27.9	0.1
Unidentified (ID #24)	1	50.5	1.8	27.6	-28.0	3.2
Unidentified (ID #32-2)	1	50.2	1.8	28.5	-28.4	0.7

This finding is also consistent with the observations from a North American temperate forest (Garten, 1993; Handley and Scrimgeour, 1997). Regardless of the seasonality, the C_3 plants always had higher foliar $\delta^{15}N$ than the C_4 plants at the drier end of the KT able

4.2. The % C, %N and isotope ($\delta^{13}C$ and $\delta^{15}N$) content (Mean \pm Standard error)

for C_3 vegetation along Kalahari Transect in wet season 2005.

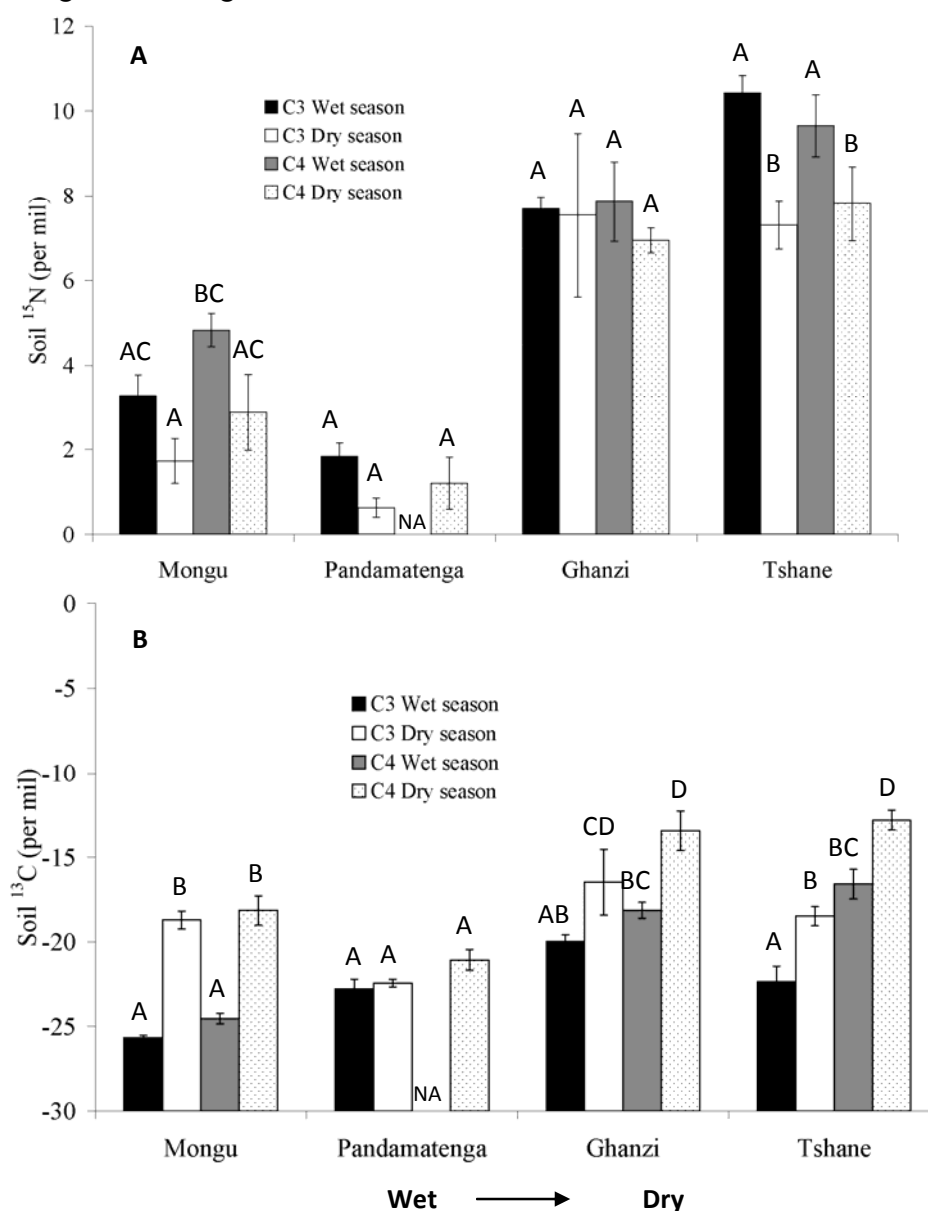


Figure 4.4. The soil $\delta^{15}N$ (A) and $\delta^{13}C$ (B) signatures for C_3 and C_4 vegetation at wet and dry seasons along the Kalahari Transect. Different letters at each location indicate

different means between four plant functional types and seasonality combinations within one site.

(Tshane and Ghanzi) (Fig. 4.2). Because the newly available N has lower $\delta^{15}\text{N}$ values and the levels of available N ($\text{NH}_4^+ + \text{NO}_3^-$) have been found (Feral et al., 2003) to be lower at the dry end of the KT, the lower foliar $\delta^{15}\text{N}$ observed in C_4 plants may indicate that C_4 plants are superior competitors for soil N and that they can readily acquire the available soil N (lower $\delta^{15}\text{N}$ values) in the wet seasons. Conversely, C_3 plants tend to take up the available N left unutilized by C_4 plants (with higher $\delta^{15}\text{N}$ values).

The high correlations between soil $\delta^{15}\text{N}$ and foliar $\delta^{15}\text{N}$ along the KT in both seasons indicate that soil $\delta^{15}\text{N}$ is the factor determining the patterns of foliar $\delta^{15}\text{N}$, consistent with similar findings from other ecosystems, including successional systems in temperate climates (Wang et al., 2007d). The higher soil water contents existing in the wet season limit the soil aeration, thereby inducing (anaerobic) conditions favorable for denitrification (Brady and Weil, 1999). Owing to the high solubility of nitrate and higher water availability during the wet season, there is an increase in nitrate leaching. These processes, preferentially remove ^{14}N , increasing the soil $\delta^{15}\text{N}$ signatures. In the current study, the soil $\delta^{15}\text{N}$ signatures were always higher in the wet season for both soils patches dominated by C_3 and C_4 plants (Fig. 4.4A), suggesting the possible occurrence of higher ecosystem-level N losses via denitrification and nitrate leaching during that period.

Based on their different physiological traits, the water use efficiency (WUE) is higher for C_4 than for C_3 plants; thus, C_4 plants tend to have higher $\delta^{13}\text{C}$ values (Farquhar et al., 1989). In the system studied in this paper, C_3 plants shows consistently lower foliar $\delta^{13}\text{C}$ in both seasons (Fig. 4.3). However, C_3 and C_4 plants exhibited different

relationships between foliar $\delta^{13}\text{C}$ and MAP, indicating the existence of a different water use strategy for these two plant functional types. In the case of C_3 plants there is a negative relationship between $\delta^{13}\text{C}$ and MAP in the wet season (Fig. 4.3A), while no such relationship is observed in the dry season (Fig. 4.3B), probably due to more limited photosynthetic activity. Thus, for annual time scales, the WUE of C_3 plants is determined by water availability in the wet season. In the dry season, however, the plants have more limited physiological activity with stomata being closed most of time, leading to higher $\delta^{13}\text{C}$ values. In the case of C_4 plants the non-linear relationships between foliar $\delta^{13}\text{C}$ and MAP are presumably due to the interaction of water stress and light stress as both of these two factors are known to affect foliar $\delta^{13}\text{C}$ (Buchmann et al., 1996). When moving from the open savanna in the south to the closer canopy woodland savannas at the northern end of the KT, light availability decreases, while water resources increase. Because these woodland savanna C_4 plants (mostly grasses) are often located in the understory, they are more likely affected by light limitations than C_3 trees. The balance between these two resources (i.e., light and water) may collectively contribute to the observed relationships between foliar $\delta^{13}\text{C}$ and MAP along the KT. At the dry end (Tshane and Ghanzi), the C_4 plants have higher WUE when MAP increases (Fig. 4.3B), whereas at the wet end, C_4 plants have higher WUE in the wet season (Fig. 4.3B). Both phenomena indicate that C_4 plants have a competitive disadvantage with respect to C_3 plants in relatively wet conditions, as the C_4 plants tend to increase their WUE when water is more available.

The soil $\delta^{13}\text{C}$ values generally reflected the relative contributions of C_3 and C_4 plants. It is not surprising that soil $\delta^{13}\text{C}$ values generally increase as aridity increases (Fig. 4.4B)

since higher aridity results in higher ground cover of C_4 plants with high foliar $\delta^{13}C$ values. The soil $\delta^{13}C$ values are generally higher in the dry seasons regardless of vegetation type, indicating higher contributions of C_4 plants to soil organic matter during the dry seasons in both humid and arid sites. These results also indicate that seasonality may play a role in determining the sources of soil organic matter C input. Based on the soil $\delta^{13}C$ values, at the most arid site (Tshane), C_4 plants always play a larger role in determining soil organic matter input; in the dry season the role of the C_4 plants becomes even stronger.

In summary, the differences in water and N use between C_3 and C_4 plants may collectively contribute to tree-grass coexistence in Southern African savanna ecosystems. Based on our observations and on known physiological and ecological processes, a conceptual model is proposed to facilitate interpretation of the observed patterns of isotopic signatures in plants and soils, and the interactions between these two plant functional types: in the wet season, there are higher ecosystem losses of N due to denitrification and nitrate leaching, which result in a higher soil $\delta^{15}N$ values both in soil patches dominated by C_3 and C_4 plants. Because the C_4 plants are superior competitors for soil N than C_3 plants -especially in environments with low levels of available soil N (e.g., the dry end of the KT) - the C_4 plants show lower foliar $\delta^{15}N$ values. The C_3 plants have lower WUE in general, but because of the rooting pattern or other factors, they compete well with the C_4 plants for water resources. The MAP determines WUE of C_3 plants in the wet season, not in the dry season, and MAP determines WUE of C_4 plants in both seasons.

Acknowledgement

The project was supported by NASA-IDS2 (NNG-04-GM71G). I greatly appreciate the species identification help from Kebonyethata Dintwe, Copper Sankhu and Lesedi Mutukwa in the middle of the Kalahari desert. I also appreciate the teamwork and field assistance from Kelly Caylor, Billy Mogojwa and Thoralf Meyer.

Chapter 5 Isotope composition and anion chemistry of soil profiles along the Kalahari Transect

ABSTRACT

Savannas cover about 20% of the Earth's land area across a wide range of climatic conditions. As an important and distinct biome, savannas produce approximately 29% of global terrestrial net primary productivity. In these ecosystems the distribution of belowground resources remains poorly investigated and the relationship to climatic conditions remains unclear. In the present study, vertical profiles of soil nutrients (chloride, nitrate, phosphate and sulfate) and nitrogen stable isotopes were analyzed at four sites along the Kalahari megatransect, where a distinct rainfall gradient exists on a homogeneous soil substrate. The results show clear differences in nutrients and $\delta^{15}\text{N}$ vertical distributions between wet and dry seasons. The results also show how the formation of "fertility islands" (i.e., the concentration of soil nutrients in the soils beneath tree canopies) is not necessarily coupled with belowground processes, in that the distribution of soil nutrients at the surface does not match belowground patterns. The results also indicate that phosphorus may be a limiting nutrient in these savanna ecosystems with seasonal dynamics in its cycling.

Keywords: ^{15}N , Belowground, Chloride, Kalahari, Nitrate, Phosphate, Sulfate

Wang, L., P. D'Odorico, G. Okin and S. Macko. Isotope composition and anion chemistry of soil profiles along the Kalahari Transect. *Journal of Arid Environments* (in review).

1. INTRODUCTION

Situated in southern Africa, the Kalahari sand sheet covers 2.5 million km² and is one of the largest continuous surface of sand in the world (Leistner, 1967). The Kalahari Transect (KT) within the Kalahari sand sheet was identified by the IGBP (International Geosphere-Biosphere Programme) as one of the “mega-transects” for global change studies (Koch et al., 1995). The KT traverses a dramatic aridity gradient (from ~ 200 mm to more than 1000 mm of mean annual precipitation (MAP), through the Republic of South Africa, Botswana, Namibia and Zambia), on relatively homogenous soils: the deep Kalahari sands (Fig. 5.1). Thus, with a remarkable rainfall gradient on a homogeneous soil substrate, the KT provides the ideal setting to study carbon, nutrient and vegetation dynamics without confounding soil effects.

Vegetation on the KT is dominated by different types of savannas ranging from the fine-leafed savannas (nutrient-rich) in the south to the broad-leafed savannas (nutrient-poor) in the north. Savannas exhibit a mixture of plant communities with different life forms (mainly trees and grasses) and life histories. The shared dominance between trees and graminoid life-forms across vast regions of the world such as the semi-arid tropics and sub-tropics is one of the most fascinating open issues in savanna ecology (Sarmiento, 1984; Scholes and Archer, 1997; Sankaran et al., 2005). Many theories have been put forth regarding the cause of this shared dominance, including mechanisms based on competition-facilitation and disturbance regime. Regardless of the processes underlying tree-grass co-dominance, the belowground distributions of resources (e.g., nutrients) and belowground processes likely play important roles in vegetation dynamics,

and the composition and structure of vegetation should exhibit the imprints of these distributions and belowground processes.

Vegetation distribution and surface soil biogeochemical properties along the KT have been documented by a number of studies (Ringrose et al., 1998; Scholes et al., 2002; Caylor et al., 2003; Privette et al., 2004; Scholes et al., 2004; Caylor et al., 2005; Wang et al., 2007a; Wang et al., in review). The plant-soil interactions along the KT have also been investigated (D'Odorico et al., 2007; Okin et al., in press). However, most of these studies have focused on the aboveground processes, and little is known about the belowground resource distributions and related processes. In fact, only limited data exist on soil profiles in southern Africa in general, as only few published datasets can be found in the literature (Hoffman et al., 1995; Hipondoka et al., 2003; Fritzsche et al., 2007). The vertical distribution of soil nutrients reflects nutrient inputs, outputs and cycling processes. Plants play an important role in determining the distribution of nutrients through soil profiles (Jobbágy and Jackson, 2001). Vegetation effects on nutrient profiles depend on the chemical nature of the nutrient and on whether or not it is limiting for plant productivity. For example: phosphorus (P) and nitrogen (N) may limit plant productivity and are expected to be depleted by root uptake. Sulfate and chloride are expected to accumulate below the root depth and have a different profile from N and P (Jobbágy and Jackson, 2001). This lack of information on belowground resources limits the current understanding of the dynamics of savanna ecosystems, particularly the tree-grass interactions and the response of savannas to further climate change. In this paper, soil profile data - including the concentration of major anions and the compositions of N isotopes, are reported from four sites, each with distinct rainfall regimes (e.g., MAP,

rainfall frequency, rainfall depth) (Caylor et al., 2006). A comparison based on samples collected both in a dry and in a wet season is also made. The objectives of this study are 1) to compare the belowground resource distributions among different sites along the KT; 2) to compare belowground resource variations for under canopy and between canopy areas; 3) to evaluate the seasonal differences in belowground resource distributions.

2. MATERIALS AND METHODS

2.1 Study sites

Four sites along the KT rainfall gradient (Fig. 5.1) were selected (from south to north: Tshane, Ghanzi, Pandamatenga and Mongu). The detailed site description including surface soil physical and chemical characteristics can be found in Wang et al. (2007a), and key parameters were reported in Table 5.1. The major site characteristics are summarized as follows. Three sites were situated in Botswana including Tshane (southernmost site), Ghanzi and Pandamatenga (Fig. 5.1). The MAP in these three areas ranges from 365 mm to 700 mm, respectively. The Tshane and Ghanzi sites are open savannas dominated by *Acacia* species such as *A. luederizii* Engl. and *A. mellifera* Benth., and grass species, such as *Eragrostis lehmanniana* and *Schmidtia pappophoroides*. The Pandamatenga site is a woodland savanna dominated by tree species (e.g., *Schinziophyton* spp.) and grass species such as *Panicum maximum* and *Pogonarihria squarrosa*. The northernmost site was situated in Mongu, Zambia, with a MAP ~880 mm. Vegetation at this site is woodland savanna dominated by the species *Brachystegia spiciformis* Benth.

2.2 Field sampling

In total, 16 soil pits were dug along the KT, eight in the dry season (August, 2004), and eight in the wet season (March 2005). The wet season 2005 was a dry year with

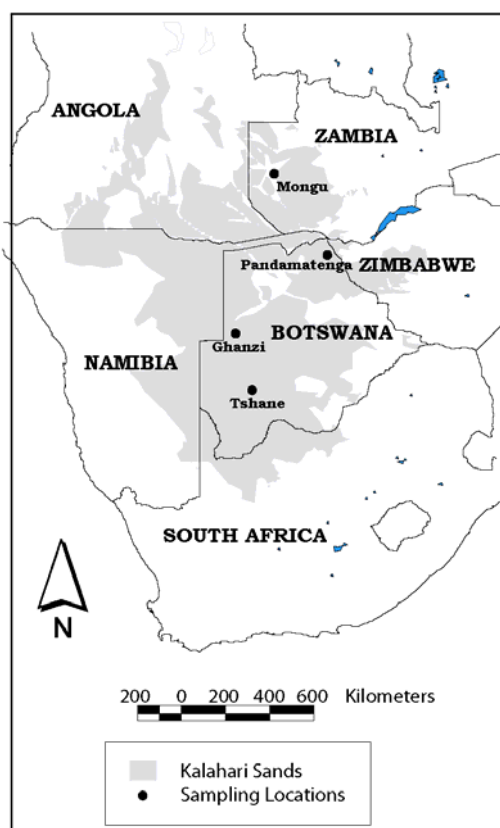


Figure 5.1. The Kalahari sands and sampling locations of the soil profiles. The Kalahari sand sheet distribution is adopted from Thomas and Shaw (1991).

precipitation lower than MAP except at Tshane (Table 5.1). There were occasional rainfall events at Tshane, Ghanzi and Mongu during the 2-3 days of pit digging in the 2005 wet season. At Tshane, there was a large storm the night (March 5, 2005) just before taking soil samples from the dug pits. Two pits were dug at each site, one under a tree canopy and the other in between two canopy areas (usually covered with grasses), for

a total of eight soil pits analyzed in each season. Both of the soil pits dug in Ghanzi in March 2005 could be classified as under canopy areas although one was further away from the vegetation thicket. The soil pits were dug to 1 meter depth in most cases, and soil samples were taken from soil pits along the soil profiles at 10 cm intervals. At Tshane, several samples were taken at depths up to 400 cm in the 2005 wet season, using a sand auger at the bottom of the soil pits.

Table 5.1. Location, site general characteristic and soil physical properties of the four sampling sites along the Kalahari Transect.

				2005 Wet Season Rainfall (mm)	Mean Rainfall Depth (mm)	Mean Rainfall Frequency (day ⁻¹)
	Location	Elevation (m)	MAP (mm/yr)			
Tshane	24.17°S 21.89°E	1115	365	436	10	0.150
Ghanzi	21.65°S 21.81°E	1125	424	362	10	0.175
Pandamatenga	18.66°S 25.50°E	1082	698	450	10	0.290
Mongu	15.44°S 23.25°E	1076	879	564	10	0.380

Woody Cover (%)	Porosity (n)	Bulk Density (g cm ⁻³)	Soil Texture ¹	pH
14	0.47 ^a , 0.45 ^b	1.41 ^a , 1.47 ^b	98.0-0.0-2.0	6.36 ^a , 6.10 ^b
20	0.49 ^a , 0.47 ^b	1.34 ^a , 1.42 ^b	96.0-1.0-3.0	6.12 ^a , 6.16 ^b
40	0.45 ^a , 0.43 ^b	1.46 ^a , 1.51 ^b	96.8-2.1-1.1	6.62 ^a , 6.10 ^b
65	0.44 ^a , 0.43 ^b	1.47 ^a , 1.50 ^b	97.5-1.9-0.6	5.02 ^a , 5.11 ^b

1. Sand-Silt-Clay Ratio

MAP: mean annual precipitation

a: under canopy, b: between canopy

The data are adopted from Wang et al. 2007a, Wang et al. in review and Caylor et al. 2006.

2.3 Chemical analyses

Soil samples were air dried in the field and stored in labeled, sealed plastic bags.

The anion concentrations of these soil samples were analyzed using a Dionex ICS-2000 ion chromatograph (Dionex, Sunnyvale, CA) with an Ion Pac AS 18 anion exchange

column. For these analyses, 6g subsamples were extracted with 30mL deionized water (conductivity lower than 1 μ S) in a 50mL centrifuge tube (Okin et al., in press). The mixture was agitated for 30 min and then was centrifuged for 9 min at 4150 rpm to produce a clear supernatant (Okin et al., in press). Nitrite (NO_2^-), nitrate (NO_3^-), phosphate (PO_4^{3-}), sulfate (SO_4^{2-}), and chloride (Cl^-) concentrations, expressed as $\mu\text{g/g}$ soil, were measured for each sample. Nitrite and nitrate were combined to provide a measure of total anionic inorganic N and reported as nitrate concentrations.

For N isotope analysis, the soil samples were further oven dried at 60°C for 72 hours in the laboratory. After drying, they were sieved and homogenized by mortar and pestle. Stable N isotope analyses were accomplished using a Micromass Optima Isotope Ratio Mass Spectrometer (IRMS) connected to an elemental analyzer (EA; GV/Micromass, Manchester, UK). The stable isotope compositions are reported in the conventional form:

$$\delta^{15}\text{N} (\text{‰}) = [({}^{15}\text{N}/{}^{14}\text{N})_{\text{sample}} / ({}^{15}\text{N}/{}^{14}\text{N})_{\text{standard}} - 1] \times 1000$$

where $({}^{15}\text{N}/{}^{14}\text{N})_{\text{sample}}$ is the ratio of the N isotopes in a sample, and $({}^{15}\text{N}/{}^{14}\text{N})_{\text{standard}}$ is the ratio of the N isotopes of the standard material, atmospheric molecular N_2 (AIR). Reproducibility of these measurements is approximately 0.2‰ (Wang et al., 2007d).

3. RESULTS AND DISCUSSION

3.1 Anion Distribution

Chloride does not generally constrain plant growth (Jobbágy and Jackson, 2001). The patterns of chloride in soils most likely results from physical mechanisms (Schlesinger et al., 1996). In arid soils, chloride is a relatively mobile element. Because

the amount of water that leaches salts decreases dramatically with depth owing to root water uptake, soil chloride levels usually increase with depth, being greatest at the maximum rooting depth (Jobbágy and Jackson, 2001). In the African savanna ecosystems considered in this study, surface chloride concentrations (0-20cm) are higher for the under canopy soils both in the wet and the dry season with higher differences between “under canopy” and “between canopy” soils occurring in the wet season (Fig. 5.2 and 5.3). In the wet season, except the under canopy soil of Tshane, chloride concentrations below the top 20 cm of soil tend to be constant for both under canopy and between canopy soil (Fig. 5.3). The maximum chloride concentrations could take place below 100 cm for all the sites in the wet season (Fig. 5.3). This depth corresponds to the rooting depth reported for the drier sites (the rooting depths in the drier sites are based on Hipondoka et al., 2003; Wang et al., 2007a). In the dry season, the chloride concentrations remain almost constant with depth in the between canopy soils for nearly all sites; at all sites, the chloride concentrations in the under canopy soils (Fig. 5.2) decrease with depth to reach minimum values at 40-60 cm and then increase until reaching the soil pit bottom (100 cm). The obvious differences in chloride distributions between wet and dry season are probably influenced by the differences in water availability between two periods. The more elevated chloride concentrations in the surface soils beneath woody vegetation are presumably caused by physical mechanisms such as canopy interception and stemflow (Okin et al., in press). The differences in vertical distribution between under canopy and between canopy soils, may also result from water movement from the relatively moist deep layers to the dry soil surface using

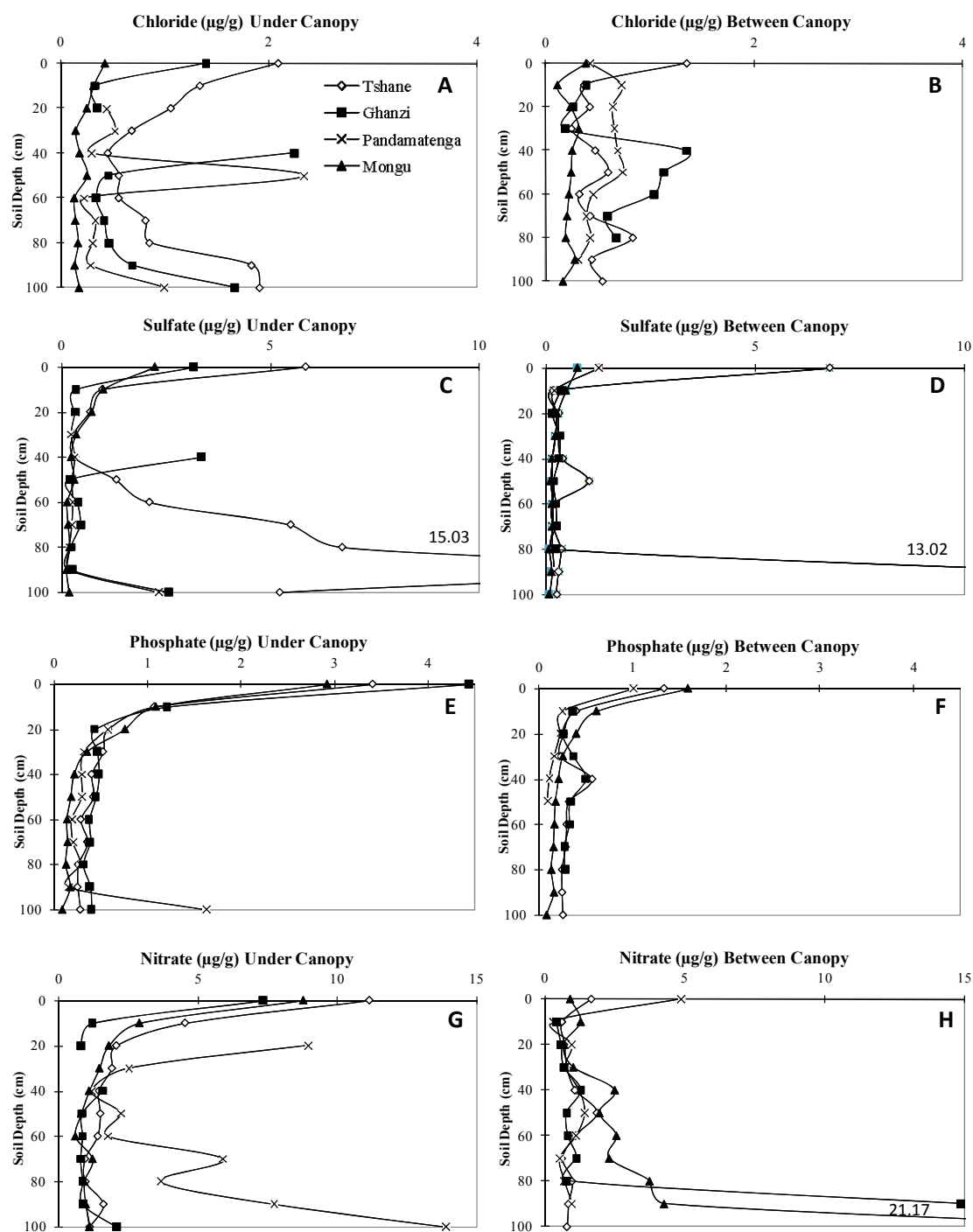


Figure 5.2. The anion concentrations along the soil profiles in the dry season 2004: chloride, under tree/shrub canopy (A); chloride, between canopy (B); sulfate, under tree/shrub canopy (C); sulfate, between canopy (D); phosphate, under tree/shrub canopy (E); phosphate, between canopy (F); nitrate, under tree/shrub canopy (G); and nitrate, between canopy (H).

plant root systems as a conduit (Caldwell et al., 1998), a process known as “hydraulic lift” (Richards and Caldwell, 1987), which is relatively common in arid environments.

Similar to chloride, sulfate is not a common limiting nutrients, and it is expected to accumulate below the root depth (Jobbágy and Jackson, 2001). With the exception of Tshane, sulfate tends to accumulate more in the surface soils (0-20 cm) under trees/shrubs than in the between canopy areas. This pattern is observed both in the wet and in the dry seasons. Moreover, sulfate concentrations are higher in the dry end of the transect (Tshane and Ghanzi, Fig. 5.2 and 5.3). The high sulfate concentrations at the dry sites is possibly due to 1) sulfate from salt pans located closer to the southern sites, and 2) the proximity to South Africa industrial sources, as evidenced by the higher sulfate concentrations in rainfall in these sites (Tshane = 5.01 ppm, Ghanzi = 3.95 ppm, Pandamatenga = 2.3 ppm, Kasane (~100 Km north of Pandamatenga) = 0.3 ppm based on rainfall events in the 2006 wet season). The sulfate distributions below the top 20 cm remain constant with depth in both seasons and at all sites except Tshane (Fig. 5.2 and 5.3). These patterns are different from the global pattern of sulfate distribution, which clearly shows sulfate concentrations increase with depth (Jobbágy and Jackson, 2001). The relatively high concentration of sulfate at depth that is observed at Tshane is quite different from all other sites (Fig. 5.2 and 5.3).

Phosphate is primarily mineral-derived and occurs in low concentrations in geological formations. The available inorganic phosphorus is limited in supply in the highly weathered soils of the tropics and therefore is often considered to be a limiting nutrient to ecosystem productivity in the tropics (Walker and Syers, 1976; Vitousek and Sanford, 1986). In the mineralogically mature Kalahari sands, which are comprised of

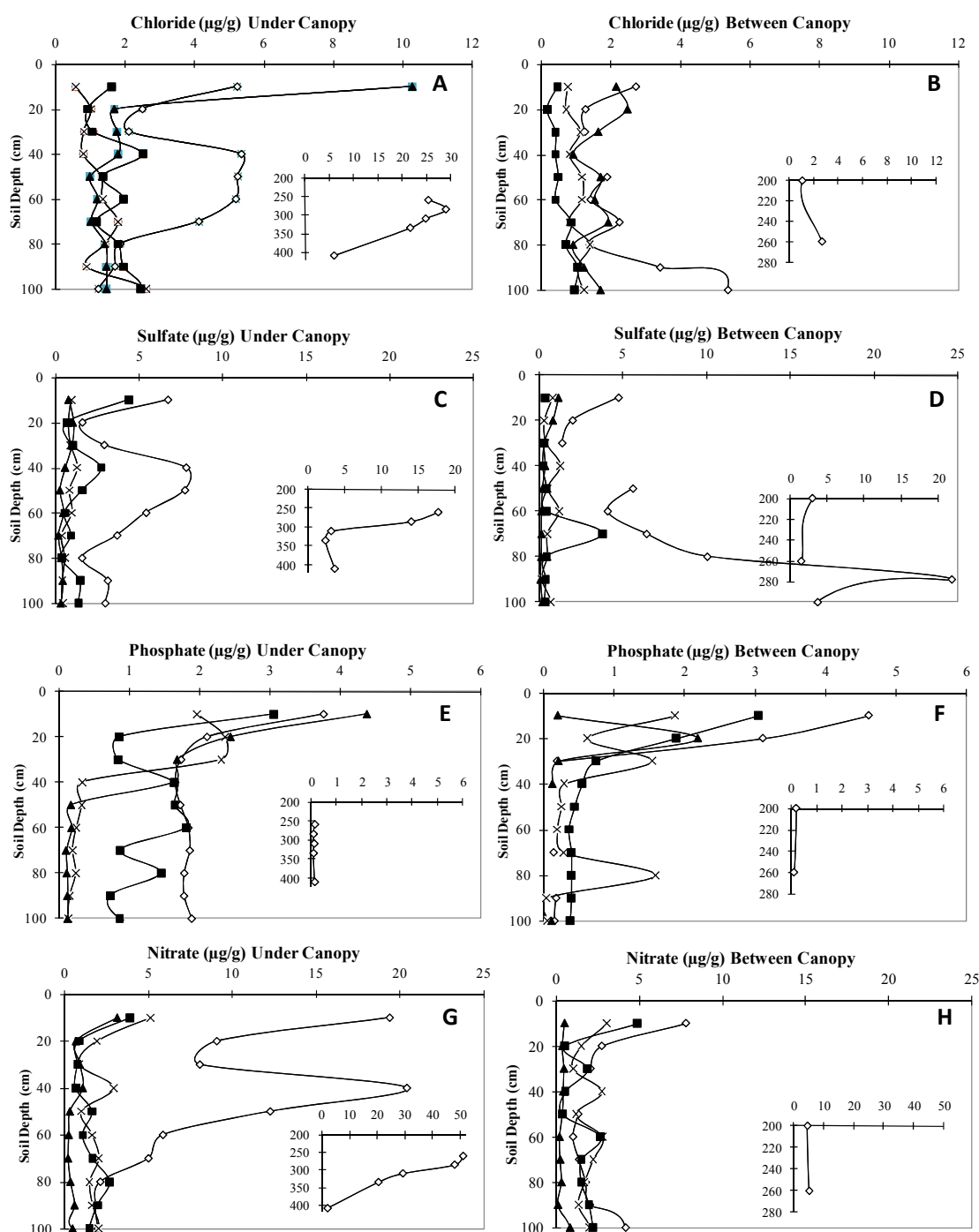


Figure 5.3. The anion concentrations along the soil profiles in the wet season 2005: chloride, under tree/shrub canopy (A); chloride, between canopy (B); sulfate, under tree/shrub canopy (C); sulfate, between canopy (D); phosphate, under tree/shrub canopy (E); phosphate, between canopy (F); nitrate, under tree/shrub canopy (G); and nitrate, between canopy (H).

nearly pure quartz (Wang et al., 2007a), P-bearing minerals are largely absent, suggesting that plants on the Kalahari sands may be P-limited. In the dry season, phosphate rich soils were found to accumulate under trees/shrubs (0-20 cm). Moreover, the phosphate levels are slightly higher at the dry end of the transect (Ghanzi and Tshane) for soils both under the canopy and in between canopy areas (Fig. 5.2). Unlike the surface soils, below the top 20 cm, the vertical distributions of phosphate are the same beneath and between canopies. During the wet season, however, the concentration of phosphate in the top 20 cm of soil is the same between and beneath canopies. The wet season subsurface (below 20 cm) concentrations of phosphate beneath canopies are higher at the drier sites (Tshane and Ghanzi) than at the two wetter sites (Pandamatenga and Mongu). During the wet season, the phosphate concentration below 40 cm beneath canopies is elevated compared to the dry season. In the wet season, the subsurface (below 20 cm) phosphate concentrations at Tshane and Ghanzi under canopy are also higher than in the soils from between canopy areas (Fig. 5.3). These differences do not exist in the two wetter sites (Pandamatenga and Mongu). If phosphate is one of the limiting nutrients in these savanna ecosystems, biological cycling has to play an important role in nutrient profile distributions. Unlike leaching, biological cycling generally moves nutrients upwards because some proportion of the nutrients absorbed by plants are transported aboveground and then recycled to the soil surface through litterfall, resupplying the nutrients to the soil surface (Trudgill, 1988). These results clearly show a strong concentration of phosphate near the surface, consistent with active P cycling in similar ecosystems (Jobbágy and Jackson, 2001). During the dry season this effect is strongest beneath tree canopies, but

an increase in near-surface phosphate is observed in all of our data. Decomposition of P-bearing litter and the related mineralization of P at the surface when water becomes available may explain the increase in phosphate between tree canopies during the wet season. The uptake of mineralized P by plants during the wet season may explain the relatively low concentration of phosphate near the surface during the dry season; all of the P is in plant tissue and litter, and there is not sufficient moisture to allow the microbial remineralization of P. This tight seasonal coupling of plant growth and phosphate in the surface soils argues strongly for P-limitation or low nutrient adaptation, at least among the grasses found between tree canopies. The P-limitation is also supported by the observed high foliar N/P ratios ($N/P \approx 20-30$) for C_3 plants at the drier Kalahari sites in a wet year (Aranibar, 2003).

Nitrogen is another potential factor that limits plant productivity in part of tropical savannas with higher water availability (Scanlon and Albertson, 2003) although recent studies show that in the KT nitrogen limitations are less important than water limitation (Wang et al., in review). With the exception of Tshane, soil surface (top 20 cm) nitrate concentration are much higher in the under canopy areas than the between canopy areas in the dry season but are similar in the wet season. Except Tshane, nitrate subsurface (>20 cm) profiles are not very different between the wet season and the dry season, nor under canopy or between canopies. Since nitrate is a mobile nutrient, the belowground nitrate distribution is expected to be influenced by aboveground distribution, especially for the sandy soil of the Kalahari. However, the nitrate subsurface profile distributions are different from the surface “fertility island” patterns found in the same region (Okin et

al., in press). The very high concentration of nitrate beneath trees during the wet season at Tshane probably results from N fixation by leguminous *Acacia* species at this site. This

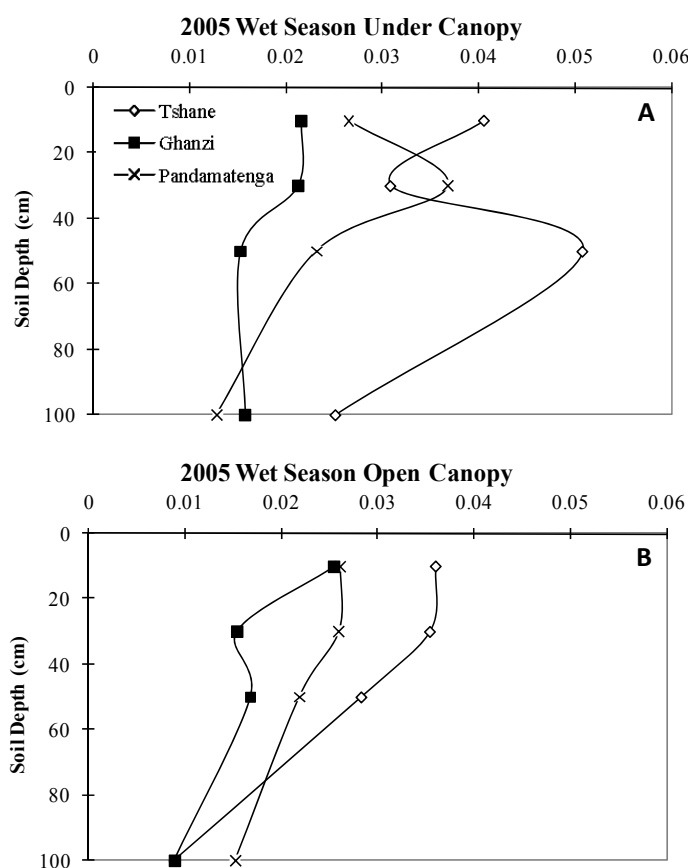


Figure 5.4. Soil moisture profiles from wet season 2005 (October-April) for under canopy (A) and between canopy (B) soils. The data are based on D’Odorico et al. (2007).

point is supported by the observation that soil $\delta^{15}\text{N}$ values are lower in the soil profiles under canopy compared to the between canopy soil (Fig. 5.5C, D), consistently with the fact that N fixation is expected to lower $\delta^{15}\text{N}$ values in these soils. Although *Acacia* species are also found at the Ghanzi site, the under canopy pit was actually located beneath *Terminalia* species, possibly explaining low nitrate concentration beneath the canopy at the Ghanzi site. During the dry season, the occasional increase in nitrate below

80 cm may result from leaching of nitrate, particularly at the wetter sites, Pandamatenga and Mongu.

The nitrate, chloride and sulfate profiles at Tshane exhibit much higher concentrations than the other three sites. The abnormal high values of soil moisture measured at Tshane in the 2005 wet season must have played an important role in determining these high concentrations of chloride, nitrate, and sulfate. In fact, these three anions are mobile and the pattern of their profiles matches the profile of average seasonal soil moisture (Fig. 5.4). The single storm event, on the other hand, is not expected to affect the distributions of these mobile nutrients to a great extent. For example, a relatively large storm occurred at Tshane the night before soil sampling; however, the wetting front reached only a depth of about 10 cm.

3.2 ^{15}N Distributions

Surface soil $\delta^{15}\text{N}$ can vary with aridity (Aranibar et al., 2004; Swap et al., 2004), rainfall (Austin and Vitousek, 1998), soil age (Brenner et al., 2001), successional age (Wang et al., 2007d) and soil crust density in arid environments (e.g., Aranibar et al., 2003; Berkeley et al., 2005) since cyanobacterial crusts are capable of fixing atmospheric N_2 . Soil $\delta^{15}\text{N}$ variations with depth are more complex and are affected by multiple factors, which include N transport processes, depth-dependent plant N inputs, and multiple N pools other than those from plant tissues (e.g., microbial biomass) (Amundson et al., 2003). Depending on climate conditions, the vertical profile of soil $\delta^{15}\text{N}$ can either exhibit random distributions like in gravelly desert soil, little variation as in montane environments or, most commonly, a consistent (exponential) increase with depth, commonly found in grasslands (Amundson et al., 2003). Despite the presence of

fluctuations in the vertical profile of dry season soil $\delta^{15}\text{N}$ (Fig. 5.5), similar to those observed in gravelly desert soils (Brenner et al., 2001), the $\delta^{15}\text{N}$ in the Kalahari increases with depth through the major portion of the root zone (top 50 cm based on Wang et al., 2007a) to a maximum value; at greater depths it exhibits larger fluctuations. This pattern is observed both in between canopy and under canopy areas for the dry season (Fig. 5.5). During the wet season, the $\delta^{15}\text{N}$ values generally show similar patterns. However, in the wet season $\delta^{15}\text{N}$ values are more enriched at all sites, and the depths with maximum $\delta^{15}\text{N}$ values are deeper (top 60 cm) when compared to those in the dry season (Fig. 5.5). The seasonal differences in $\delta^{15}\text{N}$ distributions are presumably caused by the higher levels of microbial activity (e.g., denitrification and mineralization) during the wet season, which results in ^{15}N enriched residual substrate (Robinson, 2001; Swap et al., 2004). At depths

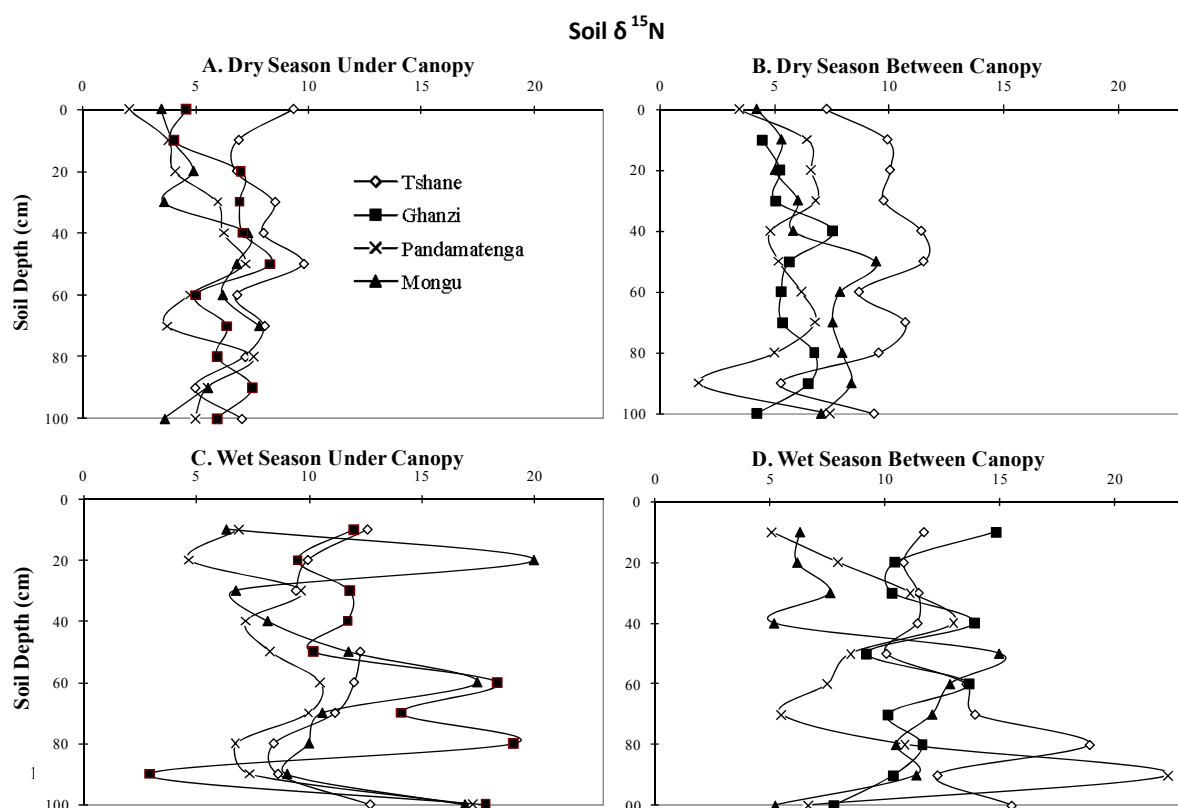


Figure 5.5. Soil $\delta^{15}\text{N}$ distributions for under tree/shrub canopy (A) and between canopy (B) soils in dry season 2004, and for under tree/shrub canopy (C) and between canopy (D) soils in wet season 2005.

greater than 10 cm, similar patterns in the distributions of $\delta^{15}\text{N}$ exist for under canopy and between canopy locations. This is presumably the result of the interactions of tree-grass roots at the subsurface (e.g., N uptake competition, N source differentiation and plant N input). These similarities were not observed in the surface soils, where soils are richer in nutrients under the tree canopies, a phenomenon known as the “fertility island”, as found in Wang et al. (2007a) and Okin et al. (in press) in the same region. In addition, a pattern of increasing $\delta^{15}\text{N}$ with increasing aridity can be observed along the KT rainfall gradient both in aboveground plant biomass (Aranibar et al., 2004; Swap et al., 2004) and in surface soils (Wang et al., 2007a). However, similar to nitrate distribution, the distributions of belowground $\delta^{15}\text{N}$ do not follow the aboveground trends, indicating different mechanisms governing N processes belowground.

4. SUMMARY

Nutrient and N isotope profiles analyzed at four sites along the KT rainfall gradient, provided valuable and timely information on the belowground distribution of resources in savannas of southern Africa. This information fills in an important knowledge gap in the study of soil biogeochemistry in this region and will enhance the understanding and prediction of aboveground vegetation structure, tree/grass ratios and nutrient dynamics. However, because the digging of soil pits was time and labor intensive, no replicates were available. This lack of replication places constraints on generalizations of these findings. The results do show clear differences in nutrients and

$\delta^{15}\text{N}$ vertical distributions between wet and dry seasons. The results also show that the aboveground nutrient “fertility islands” do not necessarily match the belowground patterns. Moreover, the results show the importance of soil moisture profiles in determining the patterns of mobile nutrients (e.g., chloride, sulfate and nitrate) distributions especially at the drier sites. Together with other evidence, the belowground P profiles also indicate that phosphorus may be a limiting nutrient in these savanna ecosystems and that there are seasonal dynamics in the cycling of P.

Acknowledgements

The project was supported by NASA-IDS2 (NNG-04-GM71G) and Moore Research Award to LW from Department of Environmental Sciences at University of Virginia. I greatly appreciate the team-work and field assistance from Natalie Mladenov, Todd Scanlon, Ian McGlynn (University of Virginia), Kelly Caylor (Princeton University), Billy Mogojwa, Dikitso Kolokose, O.G.S.O. Kgosidintsi and Thoralf Meyer (University of Botswana), Kebonyethata Dintwe (Department of Agriculture, Botswana). I thank Junran Li for his help with the laboratory instrumentation. The clarity and strength of the paper was improved by the comments of three anonymous reviewers to whom I am grateful.

Chapter 6 Preference and adaptation maintenance in plant nitrogen uptake

ABSTRACT

Nitrogen is a limiting nutrient in most terrestrial and aquatic ecosystems; its uptake and availability have long been subjects for ecological research. The determinant factors of nitrogen uptake preferences (ammonium vs. nitrate) and how they are modified in changing environments remains a mystery. In this study, two ^{15}N tracer experiments utilizing a unique doubly-labeled N source were employed. The experiments were conducted in both field and greenhouse settings, using native African grasses from a geomorphologically homogeneous region, namely, the Kalahari Transect. The results demonstrated that N uptake preferences are determined by the ammonium/nitrate ratios in the native habitats of the plants. Nitrogen uptake preference changed across different ecosystems, even for the same species. The preference changed from nitrate to no preference to a preference for ammonium, tracking the low to high ammonium/nitrate ratio in the local environment. More significantly, these experiments show that the plant progeny continue to exhibit the same clear N preference as the parent plants did in the field, even when removed from that environment and the source nitrogen is changed dramatically, indicating that plants maintain an “imprint” (at least for F1 generation) with respect to N uptake. Such constancy in adaptation may have important implications to predict the success of a plant community in its response to climate change, to seed bank use and to reforestation efforts.

Keywords: Ammonium, Enrichment, Kalahari Transect, Nitrate, Nitrogen

Wang, L. and S. Macko. Preference and adaptation maintenance in plant nitrogen uptake. *PNAS* (in review).

1. INTRODUCTION

Nitrogen (N) is the principal limiting nutrient for most terrestrial and aquatic ecosystems (Aber et al., 1989; Galloway et al., 2004; Howarth and Marino, 2006) with ammonium (NH_4^+) and nitrate (NO_3^-) the two major forms of available N for plants. Optimization of preference for available N presumably enhances the survivorship and fitness of plants. Even though differences in the rates of NH_4^+ and NO_3^- uptake have been documented by a number of physiological studies (Olsson and Falkengren-Grerup, 1995; Kronzucker et al., 1997; Wallander et al., 1997; Garnett and Smethurst, 1999), the ecological origins and significance of N uptake preference remains poorly understood. In particular, it is unclear what determines N uptake preferences (but see, Houlton et al., 2007) and how such preferences will be altered in a changing environment. The assimilation of ammonium is more energetically efficient when compared to nitrate, because ammonium can be directly incorporated into glutamate via an ammonium assimilation pathway. Nitrate, on the other hand, must first be modified via a reduction pathway before assimilation (Engels and Marschner, 1995). However, nitrate is usually more available for uptake in many ecosystems, owing to higher mobility (Brady and Weil, 1999). Either ammonium or nitrate can dominate the inorganic N pool of an ecosystem; for example, in most mature undisturbed forests, the soil inorganic N pools are dominated by ammonium (Kronzucker et al., 1997). In well-aerated agricultural soils or frequently disturbed sites, nitrate is the principal inorganic N source. Thus, an advantage for preference for either nitrate or ammonium uptake depends on the particular environment and situation.

In arid and semiarid ecosystems such as African savannas, nutrient availability varies spatially and temporally, and nutrients are considered to be a major limiting factor

for plant growth in addition to water availability (Scholes et al., 2002; Aranibar et al., 2004). The Kalahari Transect (KT) in southern Africa traverses a dramatic aridity gradient through Zambia, Botswana, Namibia, and the Republic of South Africa and is essentially composed of homogeneous soils, the deep Kalahari sands (Fig. 6.1) (Shugart et al., 2004; Wang et al., 2007a). The rainfall variability along the KT ranges from less than 200 mm mean annual precipitation (MAP) in southwest Botswana to over 1000 mm MAP in the north (i.e. western Zambia) (Shugart et al., 2004). Previous field observations along the KT showed that while nitrate levels remain fairly constant along the transect, ammonium is more abundant at the wetter end of the transect (Aranibar, 2003; Feral et al., 2003), leading to an ammonium/nitrate ratio gradient along the KT (Fig. 6.2). Therefore, the KT provides ideal conditions (homogenous soils, gradients in rainfall and ammonium/nitrate ratio) for studying, at subcontinent scales, the association between N uptake preferences, aridity and the abundances of different N forms, without confounding soil effects. Because the relative abundance of ammonium increases with respect to nitrate from the drier to wetter areas and assimilation of ammonium is more energetically efficient, species growing in the wetter areas could be expected to prefer ammonium.

A uniquely designed N uptake study was accomplished using ^{15}N , as a doubly-labeled source of N, in a greenhouse and in a field-based setting, to test the hypotheses that 1) N preferences are determined by ammonium/nitrate ratios in the native habitat of the plants, and that 2) plants may inscribe the adaptation for the N uptake preference in their progeny. All greenhouse and field plants were fertilized with ammonium nitrate;

some with $^{14}\text{NH}_4^{15}\text{NO}_3$, some with $^{15}\text{NH}_4^{14}\text{NO}_3$, to allow for monitoring of N uptake preference. A control (without fertilizer addition) was also employed for certain species (Fig. 6.3-6.5).

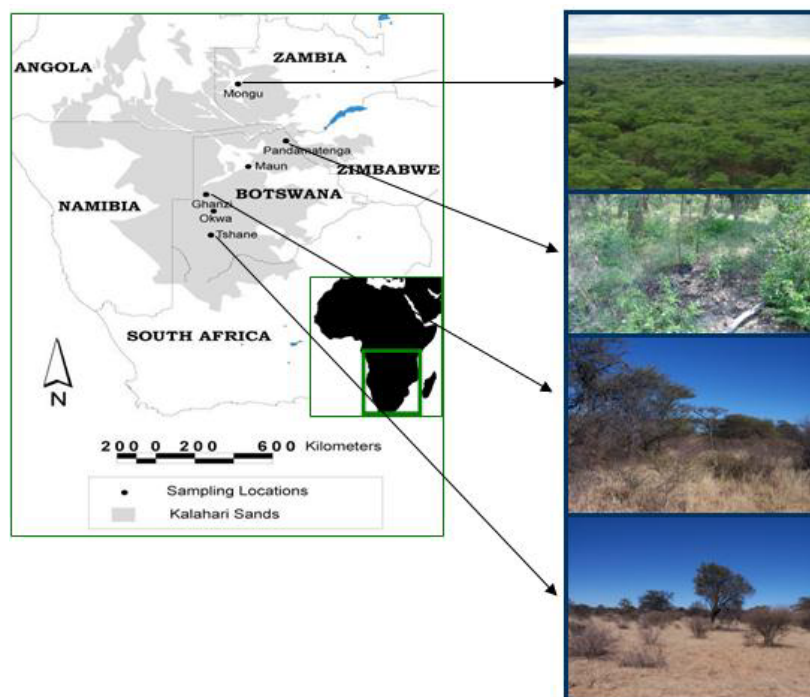


Figure 6.1. Geographic location and vegetation structure of each study site along the Kalahari Transect. The grey area in the map is the Kalahari sand sheet.

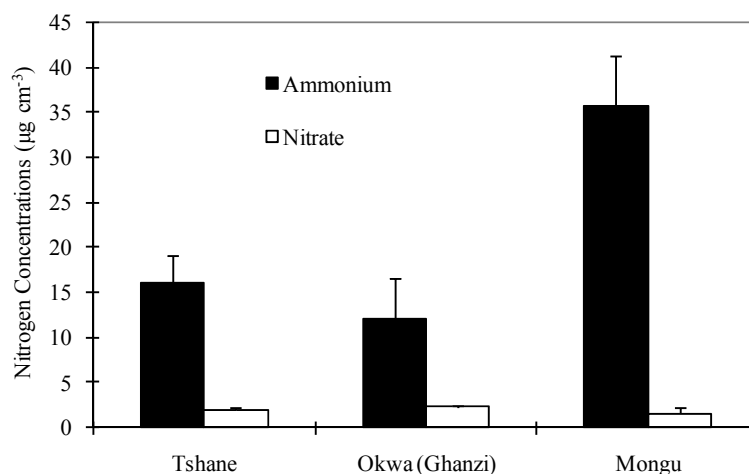


Figure 6.2. Ammonium and nitrate abundance ($\mu\text{g cm}^{-3}$) of each study site along the Kalahari Transect based on nutrient data (Feral et al. 2003) and soil bulk density data (Wang et al. 2007a).

2. MATERIALS AND METHODS

2.1 Greenhouse Experiment

For the greenhouse experiment, grass seeds were collected from their native habitat in August 2004, and two additional grass species seeds (*Schmidtia pappophoroides* from Pandamatenga and *Eragrostis spp.* from Mongu) were collected in March 2005. Six different grass species from four sites along the KT precipitation gradient (Fig. 6.1) were used in this study (Table 6.1). One species (*Eragrostis spp.*) was from Mongu (897 mm), the wettest area in this mega transect. Three species (*S. pappophoroides*, *Pogonarihria squarrosa* and *Leptocarydion vulpiastrum*) were from Pandamatenga (698 mm), the second wettest area in the transect. Two other species (*S. pappophoroides* and *E. lehmanniana*) were from Ghanzi (400 mm), Botswana, a relatively dry site with intermediate rainfall conditions. Two more species (*Enneapogon cenchroides* and *E. lehmanniana*) were from Tshane (365 mm), the driest site of this transect in southern Botswana (Table 6.1). The greenhouse experiment was conducted in Virginia between February and October 2005. The two additional grass species (*S. pappophoroides* from Pandamatenga and *Eragrostis spp.* from Mongu) were grown in a greenhouse between February and June 2006. The seeds were initially germinated in pans. Mature seedlings were then transferred into plastic pots (one individual per pot) containing commercial sand. Plants were equally well-watered during their germination and growth. During a two-week period of adjustment, a 300 ppm commercial soluble fertilizer (Peters N-P-K: 20-20-20) was applied to facilitate survival. After adjustment from transplanting, a ¹⁵N labeled fertilizer (NH₄NO₃, 50‰ in ¹⁵N) was applied to each individual plant to establish an N concentration of 15 µg/g dry soil. The total amount of N applied as fertilizer was

Table 6.1. Field characteristics of five study sites along the Kalahari Transect and species list for greenhouse and field experiment.

	Location	Elevation (m)	Mean Annual Rainfall, mm/yr	Greenhouse experiment	Field experiment
Tshane	24.17°S 21.89°E	1115	365	<i>Enneapogon cenchroides</i> <i>Eragrostis lehmanniana</i>	<i>Schmidtia pappophoroides</i> <i>Eragrostis lehmanniana</i>
Ghanzi	21.65°S 21.81°E	1125	400	<i>Schmidtia pappophoroides</i> <i>Eragrostis lehmanniana</i>	<i>Stipagrostis suniolumis</i> <i>Eragrostis lehmanniana</i>
Maun	19.92°S 23.59°E	929	460		<i>Schmidtia pappophoroides</i>
Pandamatenga	18.66°S 25.50°E	1082	698	<i>Schmidtia pappophoroides</i> <i>Leptocarydion vulpiastrum</i> <i>Pogonarihria squarrosa</i>	<i>Schmidtia pappophoroides</i> <i>Leptocarydion vulpiastrum</i> <i>Panicum maximum</i> <i>Digitaria spp.</i>
Mongu	15.44°S 23.25°E	1076	879	<i>Eragrostis spp.</i>	

comparable to the abundance of mineral N at the African field locations (Feral et al., 2003; Wang et al., 2007a). The ^{15}N labeled fertilizer was evenly sprayed over the pot surface twice in 48 hours. The two treatments ($\text{NH}_4^{15}\text{NO}_3$ and $^{15}\text{NH}_4\text{NO}_3$) received the same amount of total N fertilizer. In order to distinguish preference for uptake, the ^{15}N was labeled at a different molecular location in the N compounds ($^{15}\text{NH}_4^+$ vs. $^{15}\text{NO}_3^-$). Four individuals were used for each treatment/species combination (three individuals were used for species of *E. lehmanniana* from Tshane for $^{15}\text{NH}_4\text{NO}_3$, owing to lower seedling availability). Three other individual plants of each species were used as controls, and grown without fertilizer or labeled ^{15}N additions. To evaluate the effect of higher soil nitrogen content on N preference, a double amount of fertilizer (but the same ^{15}N signature) was applied to *P. squarrosa* and *L. vulpiastrum*. All grasses were harvested 24

hours after the second fertilizer application. The roots were carefully rinsed with tap water to remove excess N that was not assimilated. Leaves and roots from each individual were separated and stored in paper bags.

2.2 Field Experiment

In January and February 2006, a field ^{15}N labeling uptake experiment was carried out in four locations along the KT where the grass seeds were obtained. The species selected were essentially the same as those used in the greenhouse experiment (Table 6.1). The field N uptake experiment was conducted in exactly the same manner as the greenhouse experiment except utilizing a higher ^{15}N signature for both NH_4^+ and NO_3^- ($^{15}\text{NH}_4\text{NO}_3$ and $\text{NH}_4^{15}\text{NO}_3$ was labeled as 100‰ for N instead of 50‰). At Pandamatenga, control plants *S. pappophoroides*, *Panicum maximum* and *L. vulpiastrum* (without nutrient or water addition) were collected and analyzed for comparison.

2.3 Chemical analysis

All samples were then oven-dried at 60°C for 72 hours. After drying, foliar and root samples were ground to powder. Nitrogen isotope analysis was performed using a GV Micromass Optima Isotope Ratio Mass Spectrometer (IRMS) coupled to a Carlo Erba elemental analyzer (EA). The ^{15}N content of the plants are reported in the conventional notation:

$$\delta^{15}\text{N} (\text{‰}) = [(^{15}\text{N}/^{14}\text{N})_{\text{sample}} / (^{15}\text{N}/^{14}\text{N})_{\text{standard}} - 1] \times 1000$$

where $(^{15}\text{N}/^{14}\text{N})_{\text{sample}}$ is the N isotopic ratio of samples, and $(^{15}\text{N}/^{14}\text{N})_{\text{standard}}$ is the N isotopic ratio of the standard material. The standard for N stable isotopes is atmospheric molecular N. Reproducibility of these measurements is approximately 0.2‰.

2.4 Statistical analysis

The existence of N uptake preference was determined by the $\delta^{15}\text{N}$ difference between $^{15}\text{NH}_4^+$ and $^{15}\text{NO}_3^-$ treatments in either the roots or the leaves. A one-way ANOVA and Tukey *post hoc* test (at $\alpha = 0.05$ significance level) was used to evaluate the significance of the differences detected in the roots or leaves for all species from each site. The significant ^{15}N signature difference between $^{15}\text{NH}_4^+$ and $^{15}\text{NO}_3^-$ treatments either in root or leaves was used to indicate the N uptake preference. If the difference is a positive value, the plant prefers nitrate; if negative, the plant prefers ammonium. A value of 0 indicates no significant difference was detected. The larger difference value was used to indicate the maximum preference if the ^{15}N signature in both the root and foliar samples were significantly different between $^{15}\text{NH}_4^+$ and $^{15}\text{NO}_3^-$ treatments.

3. RESULTS AND DISCUSSION

For the greenhouse experiment, the individual species (*E. cenchroides* and *E. lehmanniana* from Tshane, and *S. pappophoroides* and *E. lehmanniana* from Ghanzi) from relatively dry areas (with a low ammonium/nitrate ratio) exhibited a clear preference for nitrate (Fig. 6.3A, B, E), whereas others (*S. pappophoroides*, *P. squarrosa* and *L. vulpiastrum* from Pandamatenga and *Eragrostis spp.* from Mongu) from the wetter areas (with a high ammonium/nitrate ratio) had a clear preference for ammonium (Fig. 6.3C, D, E). The preference for ammonium appearing only in root tissue is presumably due to the fact that unlike nitrate, which can be incorporated into organic compounds in both root and leaf tissue, ammonium is only synthesized into amino acids in the root tissues (Engels and Marschner, 1995).

The field experiment also showed that individuals (*S. pappophoroides* and *E. lehmanniana* from Tshane, and *S. suniplumis* from Ghanzi) from relatively dry areas (as well as a lower ammonium/nitrate ratio) exhibited a clear preference for nitrate (Fig. 6.4A, B, E), whereas individuals (*S. pappophoroides*, *P. maximum*, *L. vulpiastrum* and *Digitaria spp.* from Pandamatenga) from the wetter areas (with a high ammonium/nitrate ratio) had a preference for ammonium (Fig. 6.4D, E). Species (*S. pappophoroides*) from Maun (with an intermediate level in the rainfall) did not show a preference for either ammonium or nitrate (Fig. 6.4C, E).

The data from both the greenhouse and field N uptake experiments support the hypothesis that N preferences are influenced by ammonium/nitrate ratios in the native habitats of the plants, though the quantitative switching point for ammonium/nitrate ratio can not be assessed with the current dataset. More convincingly, the species (*S. pappophoroides*) that appeared in multiple environments (e.g. from low ammonium/nitrate ratios to high ammonium/nitrate ratios) changed N uptake preferences from nitrate to ammonium in the greenhouse experiment (Fig. 3E), and changed from nitrate to no preference and then to ammonium in the field experiment (Fig. 6.4E). These changes clearly tracked the ammonium/nitrate ratio in the environment in which they originally grew.

The hypothesis that the soil ammonium/nitrate ratio determines N uptake preference is further supported by laboratory and field observations from other geographic regions. For example, by using kinetic and compartment-analysis techniques with the radiotracer ^{13}N to compare the efficiency of N acquisition from ammonium and nitrate sources in seedlings of white spruce (*Picea glauca*) from western Canada, it was

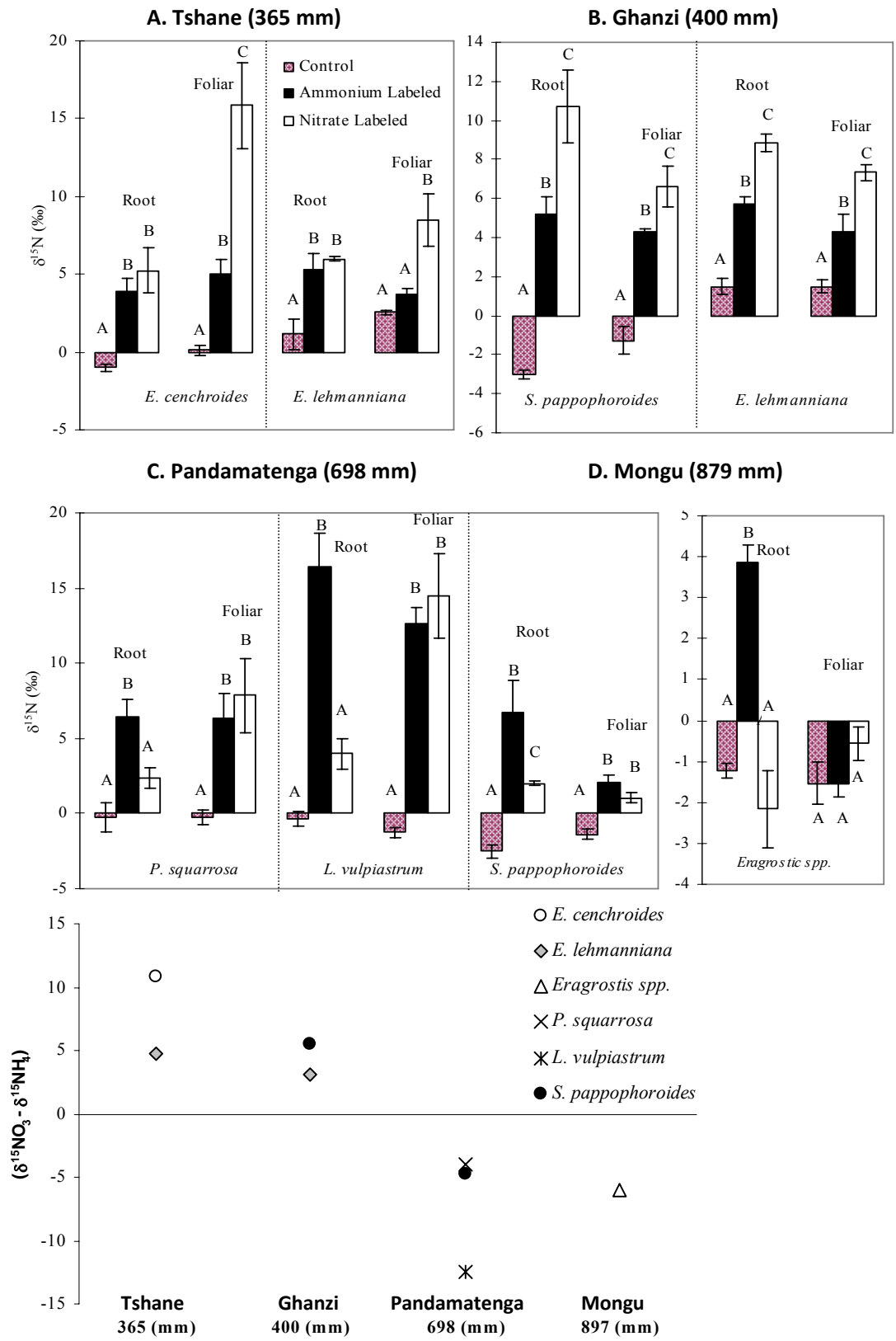


Figure 6.3. Greenhouse results for the $\delta^{15}\text{N}$ signature in plant roots and leaves for species from Tshane (A), Ghanzi (B), Pandamatenga (C) and Mongu (D) along the Kalahari Transect (KT). Dashed lines separate species at one site. The different capital letters indicate significantly different means between treatments (ammonium, nitrate and control) for either root or foliar samples for each species at each site using one-way ANOVA and Tukey *post hoc* test ($p < 0.05$). A significantly higher $\delta^{15}\text{N}$ signature in one of the labeled N forms (ammonium vs. nitrate) in any part of the plant sample (root, foliar or both) indicates the plant preference for that labeled N form. Panel E is the summary of changes in plant nitrogen uptake preference along the KT in greenhouse study. The x-axis identifies the different locations by mean annual precipitation (MAP). The y-axis is the $\delta^{15}\text{N}$ signature difference between $^{15}\text{NH}_4^+$ and $^{15}\text{NO}_3^-$ treatments for the species at each location. If the difference is a positive value, the plant prefers nitrate; if negative, the plant prefers ammonium. A value of 0 indicates no significant difference was detected. The larger difference was used to indicate the maximum preference if the ^{15}N signature in both the root and foliar samples were significantly different between $^{15}\text{NH}_4^+$ and $^{15}\text{NO}_3^-$ treatments.

found that the uptake of ammonium was 20 times higher than that of nitrate from an equimolar solution; cytoplasmic concentrations of ammonium were 10 times higher than that of nitrate (Kronzucker et al., 1997). Similarly, it was found that the ^{15}N uptake by Scotch pine (*Pinus sylvestris*) from Scandinavia from a labeled solution of ammonium was much higher (about tenfold) than from a ^{15}N -labeled solution of nitrate (Wallander et al., 1997). The chief form of inorganic N available for *P. glauca* and *P. sylvestris*, in their native habitats, was ammonium. On the other hand, trembling aspen (*Populus tremuloides* Michx.) and lodgepole pine (*Pinus contorta* Dougl. var. *latifolia*), two early successional species, were found to show a very high nitrate utilization rates at high external nitrate concentrations, and their common habitats are disturbed sites where available N is predominantly nitrate (Min et al., 1998). In a recent field study conducted in Hawaii on tropical forests, it was found that from drier sites to wetter sites the plants switched N source from nitrate to ammonium, and such a switch was in accordance with the ammonium/nitrate ratio changes (Houlton et al., 2007).

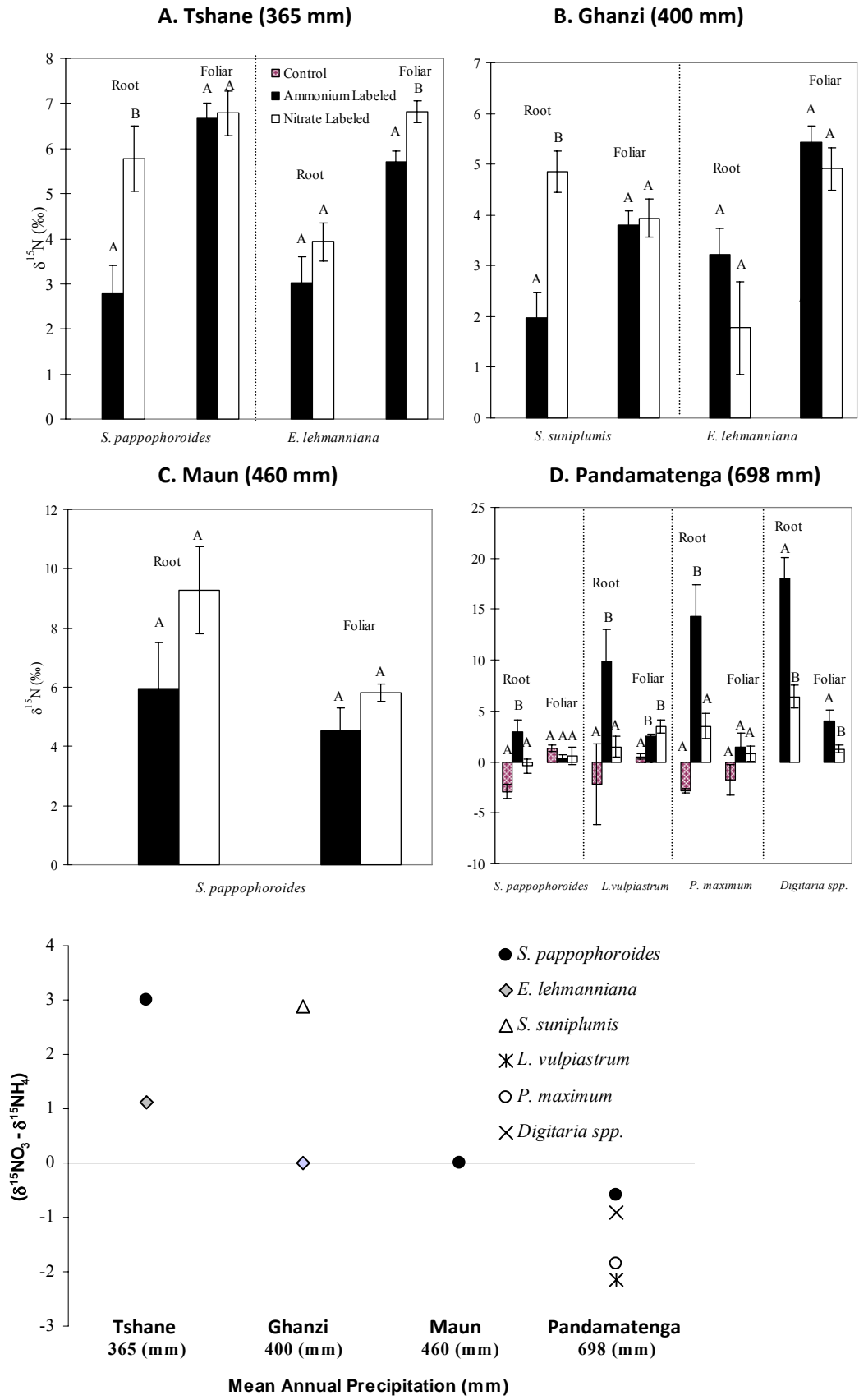


Figure 6.4. Field results for the $\delta^{15}\text{N}$ signature in plant roots and leaves for species from Tshane (A), Ghanzi (B), Maun (C) and Pandamatenga (D) along the Kalahari Transect (KT). Dashed lines separate species at one site. The different capital letters indicate significantly different means between treatments (ammonium, nitrate and control) for either root or foliar samples for each species at each site using one-way ANOVA and Tukey *post hoc* test ($p < 0.05$). A significantly higher $\delta^{15}\text{N}$ signature in one of the labeled N forms (ammonium vs. nitrate) in any part of the plant sample (root, foliar or both) indicates the plant preference for that labeled N form. Panel E is the summary of changes in plant nitrogen uptake preference along the KT in field study with the same layout as Figure 3E.

More significantly, these observations suggest that the plants may maintain the adaptation in N preference at least for the first generation. The field experiments demonstrated that plants along the KT showed N uptake preferences that track the ammonium/nitrate conditions. When seeds from each location (with different ammonium/nitrate ratio) were collected, germinated and grown in the greenhouse, and equal amounts of water and N were applied, they showed the same N preferences as the parent plants did in the field (Fig. 6.3E, 4E), indicating that plants appear to maintain the parental adaptation (at least for F1 generation) with respect to N uptake preference. This argument is further supported by the additional greenhouse observations that when higher concentrations of ammonium nitrate were applied to *P. squarrosa* and *L. vulpiastrum*, the uptake preferences for the form of N did not change (Fig. 6.5). Although the current findings do not distinguish genetic or maternal effects for the “imprint” of N uptake preference, such consistent results imply that, for example, during climate change scenarios, plant communities (at least for herbaceous plants) may keep their original physiological traits and pass them on to future generations. Longer-term studies of plant communities are clearly necessary to infer the physiological responses to climate change.

In summary, this study has illustrated a determinant factor for the preferential uptake of the different forms of inorganic N by plants. It suggests that “imprinting” of such preferences exists in seeds produced in the environment of the parent plants. From an ecological point of view, it has been shown that N uptake preferences are influenced by the relative abundances of the different forms of mineral N. From an evolutionary point of view, it supports the local adaptation concept (Endler, 1986; Chapin, 1988). But the results also show that plant seeds retain the adaptation towards the N uptake preference of their parent, even when the abundances of nitrate and ammonium change. Practically, the maintenance of plant N uptake preference across generations provides an

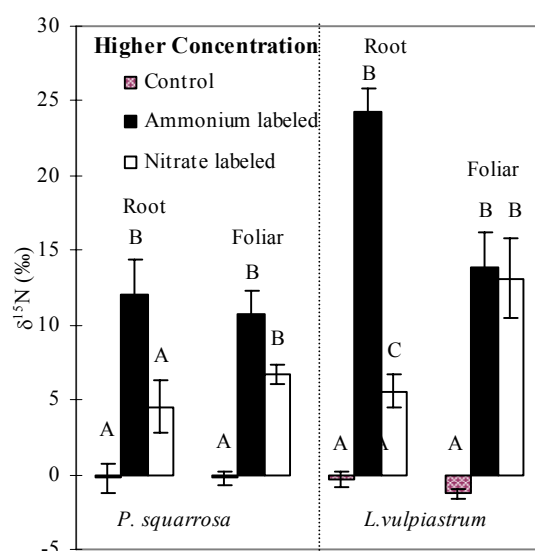


Figure 6.5. Greenhouse results for the $\delta^{15}\text{N}$ signatures in plant roots and leaves for species from Pandamatenga. A doubled mineral N concentration with the same $\delta^{15}\text{N}$ enrichment was used for these two species. Dashed lines separate the two species. The different capital letters indicate significant differences in the means among treatments (ammonium, nitrate and control) for either root or foliar samples for each species using one-way ANOVA and Tukey *post hoc* test ($p < 0.05$). A significantly higher $\delta^{15}\text{N}$ signature in one of the labeled N forms (ammonium vs. nitrate) in any part of the plant sample (root, foliar or both) indicates the plant (at the sample base, not the population base) preference for that labeled N form.

underlying mechanism explaining why, for example, a majority of the replanted conifer species in western Canada failed to survive (Kronzucker et al., 1997). Additionally, a recent study showed that plants under stress not only activate their own defenses, but also manage to pass on possible protective strategies to the descendants (Molinier et al., 2006). In accordance with this observation, a scenario describing the survival of plant communities to rapid climate change is suggested. With more rapid climate change, existing plants as well as the first generation progeny may retain their old physiological adaptation and face a greater mortality. A smaller percentage of the surviving individuals, however, will adjust to the change, passing the mechanism on to their offspring to facilitate the further survival of the species.

Acknowledgement

The project was funded by NASA-IDS2 (NNG-04-GM71G). I greatly appreciate the assistance in seedlings identification from Chris Feral and Kebonyethata Dintwe. Ms. Wendy Crannage provided tremendous help in the greenhouse maintenance. I also appreciate the teamwork and field assistance from Lydia Ries, Kelly Caylor and Todd Scanlon at University of Virginia, Billy Mogojwa, Thoralf Meyer at Harry Oppenheimer Okavango Research Center, University of Botswana. I thank Dr. Howard Epstein and Dr. Paolo D'Odorico for the thoughtful discussion at the beginning the experimental design. The clarity of this manuscript is significantly improved by comments from Dr. Manuel Lerda and the ecology discussion group in Department of Environmental Sciences of the University of Virginia.

Chapter 7 Carbon and nitrogen dynamics in southern African savannas: the effect of vegetation-induced patch-scale heterogeneities and large scale rainfall gradients

ABSTRACT

Savanna ecosystems are mixed plant communities in which trees and grasses co-exist thereby providing a heterogeneous landscape with a mosaic of tree-dominated and grass-dominated soil patches. Despite the important role that nutrient availability could play in these systems, detailed knowledge of differences in carbon and nitrogen cycling in soil patches covered by tree canopies or by grasses is still lacking. In this study, a process-based model was used to investigate the carbon and nitrogen dynamics in soil plots located in grass-dominated and tree/shrub-dominated soil patches along the Kalahari Transect (KT). The KT in southern Africa traverses a dramatic aridity gradient, across relatively homogenous soils, providing an ideal setting for global change studies. These results showed that there are distinct dynamics for soil moisture, decomposition and nitrogen mineralization between soil plots located under tree canopies and in open canopy areas. Such differences diminished when approaching the wetter end of this transect. This study shows that in savanna ecosystems, water availability determines the patterns and rates of nutrient cycling at the large scales, while at the local scale, vegetation patchiness plays an important role in nutrient cycling. Savannas are relatively stable ecosystems and resilient to certain climate changes (e.g., rainfall modification), but irreversible thresholds in climate conditions may exist.

Keywords: Carbon, Kalahari Transect, nitrogen, process-based model, savannas

Wang, L., P. D'Odorico, S. Manzoni, A. Porporato and S. Macko. Carbon and nitrogen dynamics in southern African savannas: the effect of vegetation-induced patch-scale heterogeneities and large scale rainfall gradients. *Climatic Change* (in press).

1. INTRODUCTION

Savanna ecosystems cover about 20% of the Earth's land surface, including about 40% of the African continent (Scholes and Walker, 1993). As an important and distinct biome, savannas contribute nearly 13% to global terrestrial net primary productivity, and, together with dry tropical forests, may explain approximately 15% of the annual global carbon sink (Veenendaal et al., 2004). Savannas exhibit an interesting mixture of plant communities with different life forms (mainly trees and grasses) and life histories. In the case of African savannas, trees and grasses differ in their physiological traits as the grasses exhibit the C_4 photosynthetic pathway, while the trees are C_3 woody species. The shared dominance between tree and graminoid life-forms across vast regions of the world such as the semi-arid tropics and sub-tropics is one of the most fascinating open issues in savanna ecology (e.g., Sarmiento, 1984; Scholes and Archer, 1997; Sankaran et al., 2005). Even though both equilibrium and non-equilibrium theories (Scholes and Archer, 1997) have been proposed to explain the co-dominance of trees and grasses in savanna ecosystems, it is still unclear what maintains the co-dominance of trees and grasses and how it may be disrupted by changes in climate and disturbance regime (Sankaran et al., 2004). Understanding tree-grass interactions and their feedbacks with water and nutrient availability is critical to predict the response of savanna ecosystems to global environmental change. To this end, the results from both field observations and process-based modeling was used to study the coupled soil moisture-carbon (C)-nitrogen (N) dynamics in tree- and grass-dominated soil patches. Recent soil moisture observations in soil profiles in the Kalahari reported important difference in soil moisture regimes in soil patches located under tree canopies and in "open" areas (D'Odorico et al., 2007; Wang et

al., 2007a): water infiltrates deeper in tree patches, and this difference decreases along a gradient of increasing mean annual precipitation (MAP). How such differences may affect the cycling/availability of soil nutrients with consequent effects on the dynamics of savanna ecosystems is still unclear. In this study, the south-north rainfall gradient (from ~ 200 mm in southern Botswana to more than 1000 mm of MAP in western Zambia) along the Kalahari Transect (KT) – was utilized to investigate how the effects of local vegetation heterogeneities on C and N cycling change with the rainfall regime.

The KT is one of a set of IGBP (International Geosphere-Biosphere Programme) “megatransects” identified for global change studies (e.g., Koch et al., 1995; Scholes et al., 2002). Owing to its relatively uniform, deep sandy soils (Wang et al., 2007a), the KT provides an ideal setting to investigate changes in ecosystem structure and function (including C or nutrient cycling) along a spatial precipitation gradient while minimizing the confounding effects of soil heterogeneity (Shugart et al., 2004). Thus, by contrasting soil moisture, soil C and N dynamics at selected tree and grass microsites along the KT, this study evaluates the potential long-term response of the system to changes in rainfall regime. In addition, the predicted precipitation changes of Kalahari region (~10% decrease by 2050 according to the IPCC (2007)) was applied to the process-based model enabling the short-term ecosystem responses to changes in rainfall regime to be evaluated.

2. MATERIALS AND METHODS

2.1 Field sites and data acquirement

Two sites (Tshane and Pandamatenga) along the KT were chosen to compare C and N dynamics under different climate conditions, with Tshane being at the dry end of the transect (~300 mm MAP) and Pandamatenga receiving about 700 mm MAP. Soil

Table 7.1. Soil, vegetation and rainfall parameters at Tshane and Pandamatenga along the Kalahari Transect.

			Tshane		Pandamatenga	
			Open	Under	Open	Under
<i>Soil Parameters</i>						
Porosity ¹	n		0.45	0.47	0.43	0.45
Field capacity ¹	s_{fc}		0.047	0.082	0.095	0.09
Hygroscopic point ²	s_h		0.015	0.015	0.02	0.021
Sat. hydraulic	K_s	m d ⁻¹	8.00	13.80	26.03	31.20
Soil depth ³	Z_r	m	0.30	0.55	0.60	0.65
<i>Rainfall Parameters</i>						
Average storm frequency ⁴	λ	d ⁻¹		0.10		0.32
Average storm depth ⁴	α	mm		9		10.5
Interception	Δ	mm	0.7	1.2	2	2.3
<i>Vegetation parameters</i>						
Max. Evapotranspiration ⁴	E_{max}	mm d ⁻¹	1.4	1.7	3.5	3.5
Evaporation	Vap	mm d ⁻¹	1.5	0.01	0.02	0.01
Added litter (avg. rate)	ADD	gC m ⁻² d ⁻¹	0.3	1.1	1.5	1.5
<i>Soil-vegetation parameters</i>						
Point of incipient stress ¹	s^*		0.04	0.078	0.085	0.085
Permanent wilting point ¹	s_w		0.022	0.036	0.035	0.037
<i>C/N ratios</i>						
Added Litter ⁶	$(C/N)_{add}$		50	15	60	29
Microbial biomass ⁵	$(C/N)_b$		9	9	9	9
Humus ¹	$(C/N)_h$		9.4	9.9	14.9	15.2

1. Wang et al. (2007a)
2. D'Odorico et al. (2003)
3. D'Odorico et al. (2007)
4. Porporato et al. (2003)
5. Stark and Hart (2003)
6. This study

physical properties such as porosity, field capacity, saturated hydraulic conductivity, as well as soil and litter C/N ratios were determined for these two sites from samples collected from the 2005 and 2006 wet seasons at both “tree” and “grass” microsites (Wang et al., 2007a). These values were used to parameterize the model (Table 7.1). The rates of evaporation and interception were estimated based on values from similar systems (Scholes and Walker, 1993); these values were also constrained by the observed soil moisture data. The other parameters used in the model were obtained from the literature (Table 7.1). The NO_3^- concentrations for open and under canopy soils in these two sites were analyzed using the samples collected from the 2005 wet season by Dionex ICS-2000 ion chromatograph (Dionex, Sunnyvale, CA) with an Ion Pac AS 18 anion exchange column. By analyzing these samples, 6g of sieved soil samples were extracted with 30mL deionized water (conductivity lower than $1\mu\text{S}$). Field soil moisture data were obtained from D’Odorico et al. (2007), in which soil moisture both beneath tree canopies and in open areas were continuously monitored at two-hour intervals using DECAGON ECH₂O probes from the 2004 wet season to the 2006 wet season. In addition to these direct (short-term) soil moisture measurements, the depth of the carbonate-rich soil horizon (D’Odorico et al, 2007) was used as an indicator of the long-term soil moisture regime and therefore of the active soil depth. These observed values in soil moisture and soil C and N pool sizes were reported in Table 7.2.

2.2 Model structure

A process-based coupled C and N model at the daily time scale was used, which was developed for water-limited systems by Porporato et al.(2003) . A prior application of this model to a South African savanna ecosystem can be found in D’Odorico et al. (2003).

Table 7.2. Observed soil moisture, nitrogen and carbon pool size and fluxes at Tshane and Pandamatenga along the Kalahari Transect.

	unit	Tshane		Pandamatenga	
		Open	Under	Open	Under
Average soil moisture ¹		0.06	0.07	0.14	0.15
N in nitrate pool ²	g N m ⁻³	5.64	19.11	3.02	3.21
N in ammonium pool ³	g N m ⁻³		7.6	-	-
Gross mineralization rate ^{4,5}	g N m ⁻³ d ⁻¹	0.04	0.08	-	-
C in humus pool ⁵	g C m ⁻³	2500	4950	8750	9200

1. D'Odorico et al. (2007)

2. This study

3. Feral et al. (2003)

4. Aranibar (2003)

5. Wang et al. (2007a)

Here only the main components of this modeling framework and some recent improvements are reported. To simulate the rainfall regime during the growing/rainy season, rainfall inputs are modeled at the daily time scale as a non-homogeneous Poisson process of storm arrival rate λ , and exponentially distributed depth event with mean α .

Soil moisture dynamics are thus modeled through a stochastic soil water balance following Laio et al. (2001):

$$nZ_r \frac{ds}{dt} = I(t,s) - ET(s) - L(s) \quad (1)$$

where s is the relative volumetric water content, n is the soil porosity, Z_r is active soil depth, $I(t,s)$ is the rate of rainfall infiltration, $ET(s)$ is rate of evapotranspiration, and $L(s)$

the rate of leakage through the bottom of the soil layer. The same soil depth, Z_r , was used both for water, C and N budgets. Eq. (1), thanks to the random infiltration $I(t,s)$, describes a stochastic soil water balance, which can be solved in terms of soil moisture probability density function (pdf), $p(s)$ (Laio et al., 2001; Fig. 7.2).

The C and N cycles are modeled using three soil organic matter pools (i.e., litter, humus and microbial biomass, indicated by subscripts l , h and b , respectively), and two pools describing mineral N (i.e., ammonium and nitrate, indicated by N^+ and N^- , respectively; see Fig. 7.1). Since the C/N ratios of humus and microbial biomass can be regarded as constant, the system is described by seven coupled ordinary differential equations, where the state variables are expressed in terms of g m^{-3} ,

$$\frac{dC_l}{dt} = ADD + BD - DEC_l \quad (2)$$

$$\frac{dC_h}{dt} = r_h DEC_l - DEC_h \quad (3)$$

$$\frac{dC_b}{dt} = (1 - r_h - r_r) DEC_l + (1 - r_r) DEC_h - BD \quad (4)$$

$$\frac{dN_l}{dt} = \frac{ADD}{(C/N)_{add}} + \frac{BD}{(C/N)_b} - \frac{DEC_l}{(C/N)_l} \quad (5)$$

$$\frac{dN^+}{dt} = MIN_{gross} - IMM_{gross}^+ - NIT - LE^+ - UP^+ \quad (6)$$

$$\frac{dN^-}{dt} = NIT - IMM_{gross}^- - LE^- - UP^- \quad (7)$$

The term ADD is the external organic matter input into the system, and here I assume that the only external C and N inputs to the system are through vegetation litter and that the rates are constant. The term BD is the rate at which C returns to the litter pool due to

microbial biomass death. DEC_l represents the litter decomposition rate and DEC_h is the humus decomposition rate. The decomposition fluxes drive both soil respiration and microbial growth and nonlinearly depend on soil moisture, microbial activity being inhibited both at low water potential and in conditions close to saturation (Brady and Weil, 1999). Nitrogen decomposition fluxes are equal to the C fluxes divided by the C/N ratio of the source pool. However, only a fraction of the decomposed N from litter and humus is directly assimilated by the microbes (Fig. 7.1), while the remaining is mineralized to ammonium according to the parallel mineralization scheme (Manzoni and Porporato, 2007). Details on the definition of the gross mineralization (MIN_{gross}) and immobilization fluxes (IMM_{gross}^+ , IMM_{gross}^-) are reported elsewhere (Porporato et al., 2003; Manzoni and Porporato, 2007). As shown in Eqs. (6) and (7), the dynamics of ammonium and nitrate (N^+ and N^-) were described by the balance of mineralization, immobilization, nitrification (NIT), leaching (LE^+ , LE^-) and root uptake (UP^+ , UP^-), which in turn strongly depend on soil moisture. Wet and dry deposition as well as N fixation are important only in the long-term balance and are neglected in this modeling framework. Denitrification, which may take place when soil moisture is high, is also neglected in this semiarid ecosystem (Porporato et al., 2003).

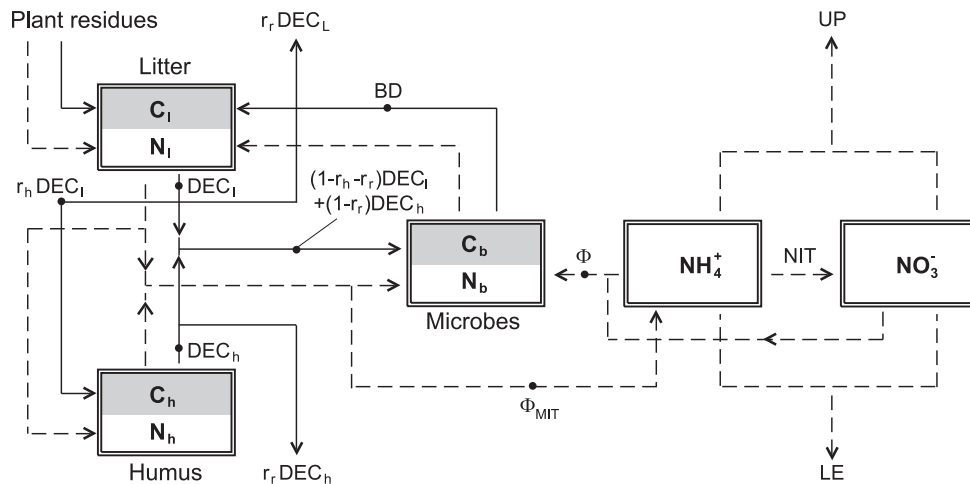


Figure 7.1. Schematic representation of compartments and fluxes of the coupled C-N model. White compartments and dashed lines represent N pools and fluxes; shaded compartments and continuous lines refer to the corresponding C pools and fluxes (Eqs. (2) – (7)). The combination of the fluxes Φ (defined to keep $(C / N)_b$ constant) and Φ_{MIT} (the fraction of decomposed N transferred to ammonium) define gross mineralization and immobilization, as described by Porporato et al. (2003) and Manzoni and Porporato (2007).

Owing to the dependence of C and N fluxes on soil moisture, the stochasticity of rainfall events is propagated through the soil system, giving rise to different-scale responses of C and N pools to soil moisture fluctuations (D’Odorico et al., 2003).

3. RESULTS

3.1 Tshane

There were significant differences in soil moisture dynamics between the under canopy and open canopy areas in Tshane, i.e., at the dry end of the transect (Fig. 7.2A). Soil moisture fluctuations were more intense in the open canopy than in the under canopy soils. The average soil moisture under canopy (0.07) was higher than that in the open areas (0.06). Soil moisture temporal variability – expressed in terms of its standard deviation, σ - was higher in the open areas ($\sigma=0.07$) than in the soils under the canopy ($\sigma=0.05$) (Table 7.3). These differences can be clearly seen in the shape of $p(s)$, with heavier tails and lower mode in the open canopy areas (Fig. 7.2A). The litter C pool was by an order of magnitude higher for the under canopy soils (1684 gC m^{-3}) than for the open canopy soils (109 gC m^{-3}) (Table 7.3). There was higher variability in litter carbon pool dynamics for soils under canopies than in the open areas (118 vs. 30 gC m^{-3} ; Table 7.3, Fig. 7.3A). The humus pool for the under canopy soils (5017 gC m^{-3}) was over twice the size of the humus pool in open canopy soils (1982 gC m^{-3}), whereas the microbial C

pool for the under canopy soils (114 gC m^{-3}) was only one quarter of that in open areas

(467

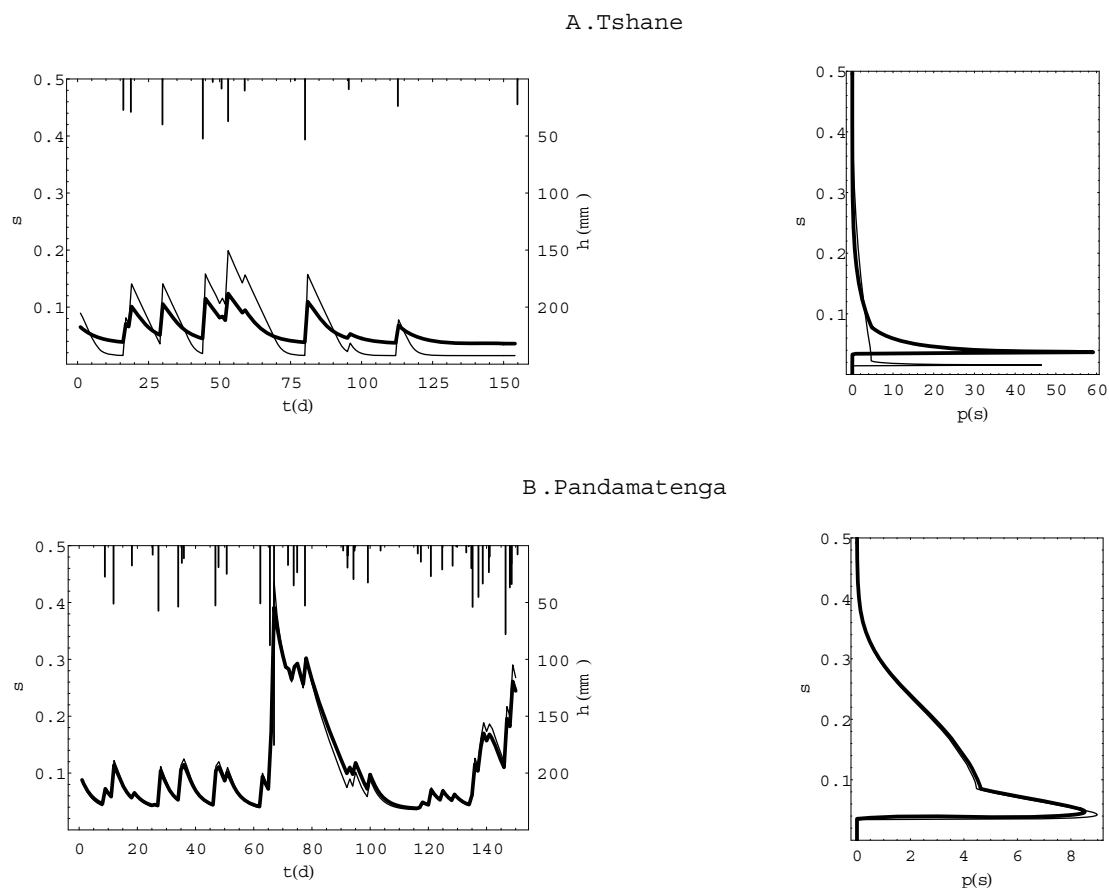


Figure 7.2. Soil moisture dynamics (s) and rainfall depth time series (h) in the under canopy (thick lines) and in the open canopy areas (light lines) in Tshane (A) and Pandamatenga (B). Right panels show the theoretical steady state soil moisture pdfs for the different locations and microsites (pdfs are computed following Laio et al., 2001).

gC m^{-3} ; Table 7.3). The litter C/N ratios varied only slightly in both under canopy and open canopy areas, with values around 25 and 13, respectively (Table 7.3). The ammonium and nitrate level were much higher for under canopy soils (3.9 and 18.1 g N m^{-3} respectively) than that in the open areas (0.03 and 4.1 g N m^{-3} respectively) (Table 7.3, Fig. 7.4A, B). There was a substantial difference in the N cycling between the under

canopy and open canopy areas (Table 7.3): in the soils under the canopy gross N mineralization rates were on average equal to $0.13 \text{ g N m}^{-3} \text{ d}^{-1}$ and no immobilization

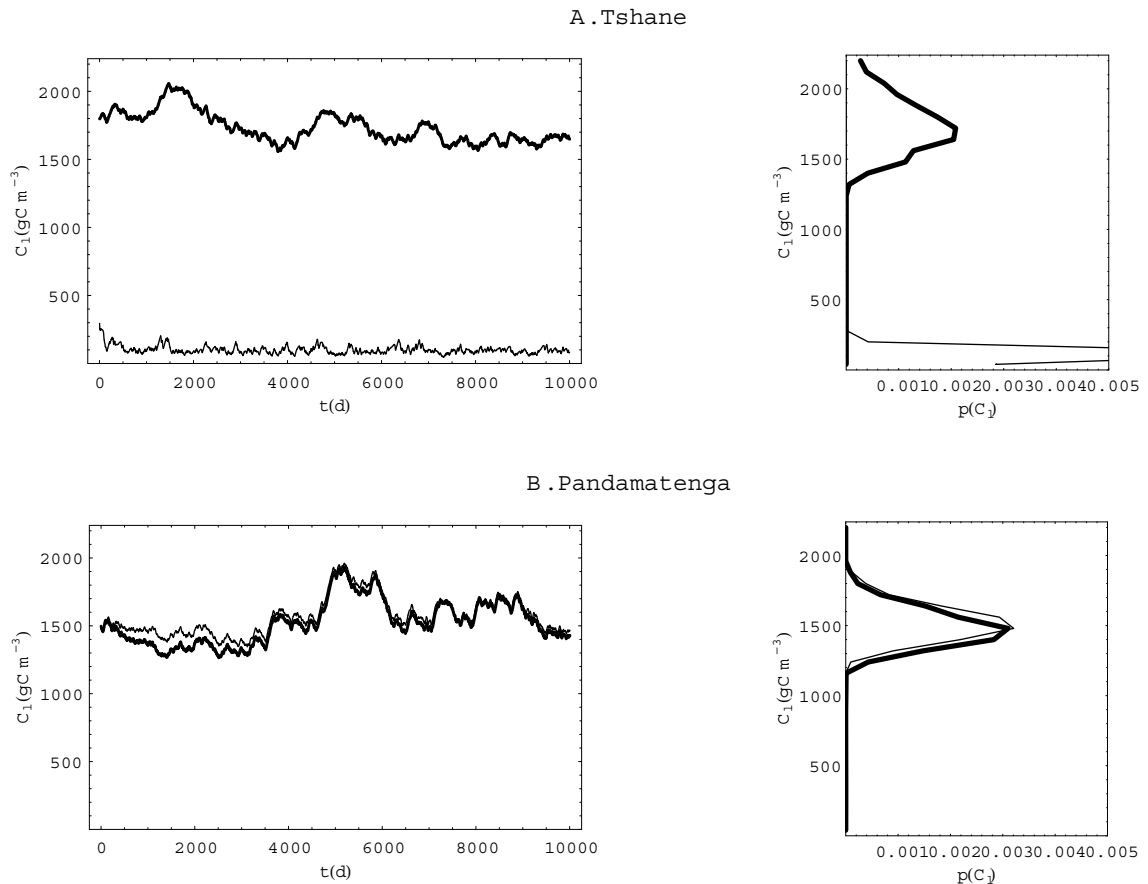


Figure 7.3. Soil litter C dynamics (left panels) and pdfs (right panels) in the under canopy (thick lines) and in the open canopy soils (thin lines) in Tshane (A) and Pandamatenga (B). Note that, at a certain site, the same stochastic rainfall realization has been used for both open canopy and under canopy areas.

occurred; in the open areas, the rates of gross N mineralization were only about $0.02 \text{ g N m}^{-3} \text{ d}^{-1}$ with mineralized N sporadically being immobilized ($0.0001 \text{ g N m}^{-3} \text{ d}^{-1}$) (Table 7.3).

Nitrate leaching was negligible for under canopy soils ($0.0002 \text{ g N m}^{-3} \text{ d}^{-1}$) and it was $0.001 \text{ g N m}^{-3} \text{ d}^{-1}$ for open canopy soils (Table 7.3).

3.2 Pandamatenga

In Pandamatenga, the wetter site, there were no significant differences in the soil moisture dynamics between microsites located under canopy and in open areas (Figure 2B). The average soil moisture at both microsites was 0.15 (Table 7.3), and the soil moisture pdfs did not significantly differ (Fig. 7.2B). The litter, humus and microbial C pool sizes were all similar for the soils under canopy and in the open areas (Table 7.3; Fig. 7.3B). The litter C/N ratios showed relatively small variability in both microsites, although with higher values for the open canopy areas (Table 7.3). Both the ammonium and nitrate level were similar for the under canopy (13.8 and 3.9 g N m⁻³ respectively) and the open canopy (12.8 and 3.6 g N m⁻³ respectively) areas (Table 7.3). Gross N mineralization rates under the canopy (0.08 g N m⁻³d⁻¹) were twice as much the rates of the open canopy soils (0.04 g N m⁻³d⁻¹) (Table 7.3). There was no immobilization for the under canopy soils (Table 7.3) but there were sporadic immobilization (0.0005 g N m⁻³d⁻¹) episodes for the open canopy soils (Table 7.3). Nitrate leaching was 0.003 g N m⁻³d⁻¹ and 0.004 g N m⁻³d⁻¹ for the under canopy and the open canopy soils (Table 7.3, Fig. 7.5).

3.3 Difference between Tshane and Pandamatenga

Soil moisture values were lower at Tshane than at Pandamatenga both at the open area and the under the canopy microsites (Table 7.3, Fig. 7.2). The litter, humus and microbial C pool were also, in most cases, lower at Tshane than that at Pandamatenga (Table 7.3, Fig. 7.3). At Tshane there were significant differences between under and open canopies in soil moisture, litter C/N ratios, litter carbon dynamics and nitrate leaching, while these differences diminished at Pandamatenga. Net N mineralization was

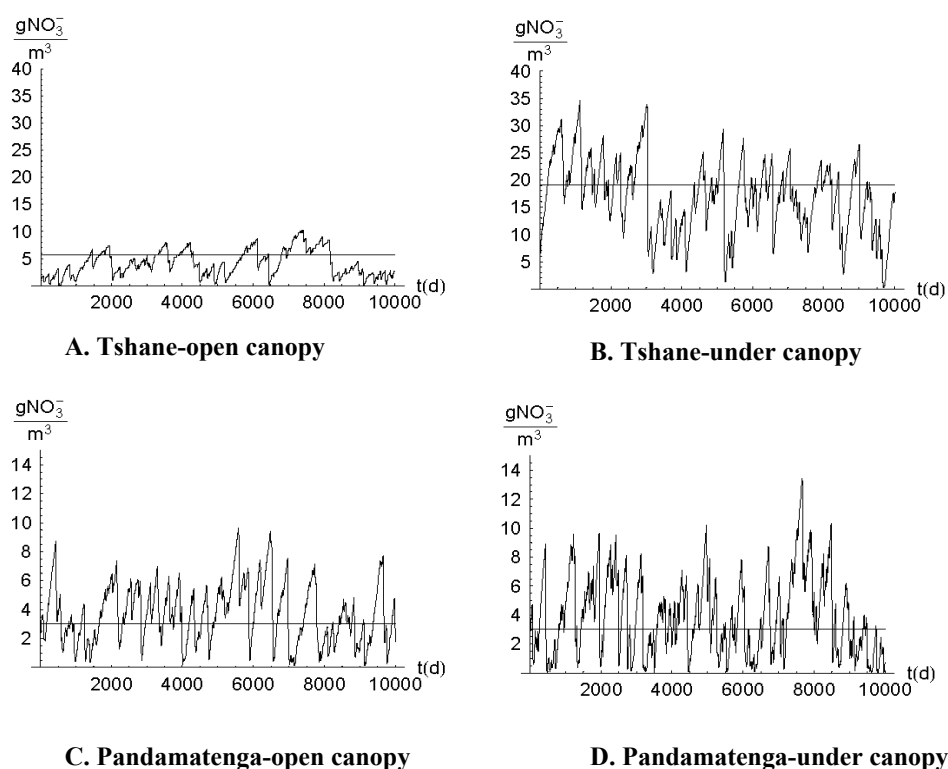


Figure 7.4. Soil nitrate pool dynamics in the under canopy soils and in the open canopy areas in Tshane and Pandamatenga. The solid line represents the mean of the observed values.

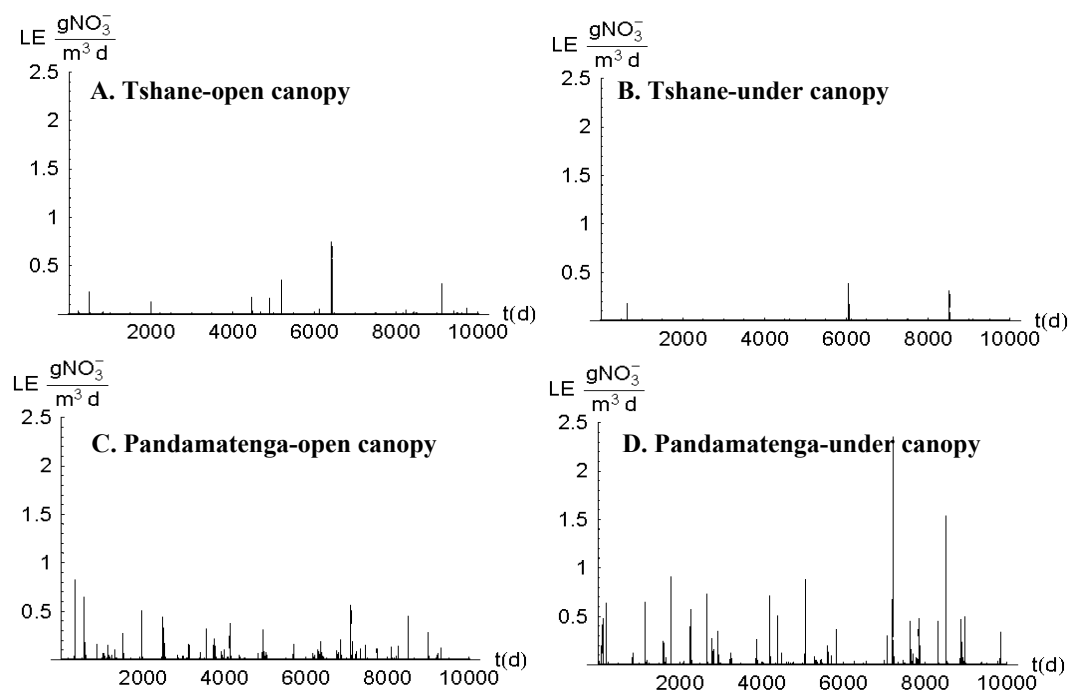


Figure 7.5. Soil nitrate leaching dynamics in the under canopy soils and in the open canopy areas in Tshane and Pandamatenga.

higher under the canopy both at Tshane and Pandamatenga, but the differences were much higher at Tshane (Table 7.3). The nitrate levels at Tshane were significantly higher than that at Pandamatenga and such difference was larger for the under canopy soils (Fig. 7.4). The total nitrate leaching was much higher at Pandamatenga than that in Tshane, especially for open canopy soils (Table 7.3, Fig. 7.5).

3.4 Effect of predicted rainfall changes at Tshane and Pandamatenga

The effect of the predicted changes in precipitation (Solomon et al., 2007, IPCC 2007) on the N and C dynamics was also investigated. A predicted decrease in rainfall (~10% in amount according to IPCC 2007) induced a lower soil moisture both at the dry end (except for the open canopy soils in Tshane) and at the wet end of the transect, with more obvious effects at the wetter site (Table 7.3). There were no significant changes in the soil C and N pool sizes (Table 7.3), nor did the N fluxes (e.g., N mineralization, N immobilization) undergo strong changes either at Tshane or at Pandamatenga. However, the ammonium and nitrate concentrations increased at Tshane (only in the soils under the canopy) and at Pandamatenga, (Table 7.3). At either site the mean rates of nitrate leaching did not change considerably, while there were substantial increases in the standard deviation of nitrate leaching rates in the under canopy soils at Tshane and in the open canopy soils at Pandamatenga (Table 7.3).

4. DISCUSSION

The model outputs for soil moisture and the C and N pools agree well with the data available for the two sites (Tables 2 and 3). The model results generally show that there are higher soil C and N stocks and higher soil moisture at the wetter end of the transect

Table 7.3. Model output of the current and predicted changes in soil moisture, nitrogen and carbon pool size and fluxes (mean \pm standard deviation) at Tshane and Pandamatenga along the Kalahari Transect.

Units		Tshane			
		Open canopy		Under canopy	
Climate scenario		Current	Future	Current	Future
Soil moisture		0.06 \pm 0.07	0.06 \pm 0.07	0.07 \pm 0.05	0.06 \pm 0.03
Litter carbon	g C m ⁻³	109 \pm 30	101 \pm 32	1684 \pm 118	1807 \pm 159
Humus carbon	g C m ⁻³	1982 \pm 52	1881 \pm 114	5017 \pm 43	5133 \pm 77
Biomass carbon	g C m ⁻³	467 \pm 21	480 \pm 31	114 \pm 13	109 \pm 17
Soil litter pool C/N		25 \pm 0.4	24 \pm 0.6	13 \pm 0.2	13 \pm 0.1
Soil NH ₄ ⁺	g N m ⁻³	0.03 \pm 0.01	0.03 \pm 0.01	3.9 \pm 0.5	4.3 \pm 0.5
Soil NO ₃ ⁻	g N m ⁻³	4.1 \pm 2.4	2.9 \pm 1.6	18.1 \pm 7.1	23.5 \pm 8.0
Gross N Mineralization	g N m ⁻³ d ⁻¹	0.02 \pm 0.02	0.02 \pm 0.02	0.13 \pm 0.05	0.13 \pm 0.05
Gross N	g N m ⁻³ d ⁻¹	0.0001 \pm 0.001	0.0001 \pm 0.001	0 \pm 0	0 \pm 0
Net N mineralization	g N m ⁻³ d ⁻¹	0.02 \pm 0.02	0.02 \pm 0.02	0.13 \pm 0.05	0.13 \pm 0.05
NO ₃ ⁻ leaching	g N m ⁻³	0.001 \pm 0.01	0.002 \pm 0.02	0.0002 \pm 0.004	0.0008 \pm 0.03

Units		Pandamatenga			
		Open canopy		Under canopy	
Climate scenario		Current	Future	Current	Future
Soil moisture		0.15 \pm 0.11	0.13 \pm 0.10	0.15 \pm 0.10	0.13 \pm 0.09
Litter carbon	g C m ⁻³	1603 \pm 131	1552 \pm 151	1566 \pm 99	1514 \pm 99
Humus carbon	g C m ⁻³	9171 \pm 213	9026 \pm 196	9394 \pm 94	9288 \pm 55
Biomass carbon	g C m ⁻³	399 \pm 29	402 \pm 28	402 \pm 24	407 \pm 21
Soil litter pool C/N ratio		25 \pm 0.7	25 \pm 0.6	19 \pm 0.3	19 \pm 0.3
Soil NH ₄ ⁺	g N m ⁻³	12.8 \pm 1.2	13.7 \pm 1.2	13.8 \pm 1.6	14.4 \pm 1.4
Soil NO ₃ ⁻	g N m ⁻³	3.6 \pm 2.3	5.1 \pm 2.7	3.9 \pm 2.6	4.9 \pm 2.8
Gross N Mineralization	g N m ⁻³ d ⁻¹	0.04 \pm 0.02	0.04 \pm 0.02	0.08 \pm 0.03	0.08 \pm 0.03
Gross N immobilization	g N m ⁻³ d ⁻¹	0.0005 \pm 0.001	0.001 \pm 0.001	0 \pm 0	0 \pm 0
Net N mineralization	g N m ⁻³ d ⁻¹	0.04 \pm 0.02	0.04 \pm 0.02	0.08 \pm 0.03	0.08 \pm 0.03
NO ₃ ⁻ leaching	g N m ⁻³	0.004 \pm 0.03	0.004 \pm 0.05	0.003 \pm 0.02	0.004 \pm 0.03

(Pandamatenga) than that at the dry end (Tshane), where ecosystem productivity and litter inputs to the soil are lower, also in agreement with field observations (Feral et al., 2003; Veenendaal et al., 2004).

Soil moisture is consistently higher for the under canopy soils at the dry end of the transect, while only minimal differences exist at the wet end. Soil C stocks in under canopy soils are higher than those in the open canopy soils at both the dry and the wet end of the transect (Table 7.3). However, the differences are much larger at the dry end, presumably due to the larger differences in litter input rates between the open and under canopy areas at the more arid site. In arid and semiarid landscapes the spatial distribution of nutrients tends to be fairly heterogeneous, especially when shrub encroachment and land degradation occur (Schlesinger et al., 1996). In these conditions, nutrient-rich and highly-permeable soils tend to develop under tress/shrub canopies leading to the formation of the so-called “islands of fertility” (Schlesinger et al., 1990). Along the KT, the existence of well-defined islands of fertility are observed at the drier end of the transect (Tshane), although at both sites, the under-canopy soils show higher permeability and porosity (Table 7.1). In Tshane, the rates of N mineralization and the levels of ammonium and nitrate are higher for the under canopy than in the open canopy soils (Table 7.3), while higher N immobilization is predicted by the model in open areas where the litter C/N ratio and hence microbial N demand are higher (Chapin et al., 2002; Manzoni and Porporato, 2007). In Pandamatenga, despite the different rates of N mineralization and immobilization, the ammonium and nitrate levels are similar in the under canopy and the open canopy soils, indicating that there are either higher rates of plant N uptake (e.g., ammonium) or higher rates of leaching (e.g., nitrate) in the soils

under canopy. In general, changes in soil moisture availability along the KT rainfall gradient affect nutrient cycling: the levels of soil ammonium increase, while nitrate levels decrease (more leaching at the wet end) with increasing values of MAP along the KT (Table 7.3, Feral et al., 2003). However, the rates of N mineralization are not consistently higher at the dry or at the wet end (Table 7.3), due to the combined effect of local vegetation heterogeneities and the large scale rainfall gradient. These results indicate that at the larger scales, water availability (e.g., soil moisture) determines the patterns and rates of nutrient cycling, while at the local scale, vegetation patchiness play an important role in nutrient cycling.

The long term simulations (Fig. 7.3, 7.4 and 7.5) clearly illustrate how not only inter-site variability shapes the C and N dynamics, but also, within a single location, significant variability of C and N pools and fluxes occurs. The simplified model used for these simulations (Eqs. (2)-(7)) does not account explicitly for vegetation changes over time, thus allowing us to highlight the complex intrinsic dynamics of the soil system in response to soil moisture fluctuations and internal nonlinearities (D'Odorico et al., 2003). The external stochastic forcing, in fact, results in fluctuations of soil variables at different time scales, ranging from high-frequency oscillations of inorganic N, mineralization and leaching (Fig. 7.4 and 7.5), to lower-frequency variability of litter (Fig. 7.3) and other pools with slow turnover time.

The predicted changes in rainfall regime would cause a decrease in soil moisture both at the dry and at the wet end of the transect, though with no significant effects on the size of the soil C and N pools and fluxes (Table 7.3). Changes in the rates of nitrate leaching do not exhibit a consistent pattern along the Kalahari Transect (Table 7.3). The

slight increase in soil ammonium and nitrate concentrations at both sites is presumably due to the decrease in plant uptake induced by the lower soil moisture and is in agreement with patterns observed in other semiarid savanna ecosystems (Augustine and McNaughton, 2004). The relative stability of the soil C and N pool and of their fluxes under changing rainfall regimes indicates that these savanna ecosystems might be resilient to relative small climate shifts. However, this prediction is based on a rather conservative climate change scenario, as it only accounts for changes in the rainfall regime changes without including changes in other climate variables (e.g., potential evapotranspiration and temperature).

In summary, this study shows that in savanna ecosystems, water availability determines the patterns and rates of nutrient cycling at regional scale, while at the local scale, vegetation patchiness play an important role in determining the rates of nutrient cycling. Savannas seem relatively stable and resilient ecosystems with respect to expected changes in rainfall regime for the next 10-50 years. Notably, the Kalahari Transect itself can be interpreted as a chronosequence where the drier sites may provide useful information on the long-term ecosystem responses to a decrease in mean annual rainfall. The existence along the Kalahari of savannas with different vegetation composition and structure, and with different soil moisture, C and N dynamics, indicates that large and prolonged shifts in precipitation may lead to important changes in ecosystem functioning.

Acknowledgements

The project was supported by NASA-IDS2 (NNG-04-GM71G). I greatly appreciate the team-work and field assistance from Lydia Ries, Natalie Mladenov, Matt Therrell, Todd Scanlon, Ian McGlynn, Thoralf Meyer (University of Virginia), Kelly Caylor (Indiana University), Greg Okin (UCLA), Billy Mogojwa (University of Botswana). I thank Junran Li and Ryan Emmanuel for their help with the laboratory and computing instrumentation.

Chapter 8 Carbon and nitrogen parasitism by xylem-tapping mistletoe along the Kalahari Transect: a stable isotope study

ABSTRACT

The present study explores the xylem-tapping parasitism by mistletoe on native tree species along the Kalahari Transect (KT) using the stable isotopes of carbon and nitrogen. Mistletoe-host pairs were collected at three geographical locations (each with a different mean annual precipitation) along the KT in wet season 2005 and 2006. Foliar total carbon, total nitrogen and their stable isotopes compositions ($\delta^{13}\text{C}$ and $\delta^{15}\text{N}$) were measured. Heterotropy (H) was calculated using foliar $\delta^{13}\text{C}$ values of mistletoes and their hosts as an indicator of proportion of carbon in the mistletoes derived from host photosynthate. Based on the mistletoe H value and relationship between the mistletoe foliar $\delta^{15}\text{N}$ and their host foliar $\delta^{15}\text{N}$, the results showed that mistletoes along the Kalahari derived both nitrogen and carbon from their hosts. Mistletoes may regulate water use in relation to N supply. The proportion of carbon in the mistletoes derived from host photosynthate was between 35% to 78%, and the degree of heterotropy is species-specific with only limited annual variation. The study emphasizes the importance of incorporating parasitic associations when studying carbon, water and nutrient cycling along the Kalahari in future studies.

Keywords: Stable isotopes, Mistletoe, Kalahari Transect, Nitrogen-15, Carbon-13,

Parasitism

Wang, L., B. Kgope, P. D'Odorico and S. Macko. Carbon and nitrogen parasitism by a xylem-tapping mistletoe (*Tapinanthus oleifolius*) along the Kalahari Transect: a stable isotope study. *African Journal of Ecology* (in press).

1. INTRODUCTION

Xylem-tapping mistletoes are obligate parasites that rely completely on their hosts for water (Ehleringer et al., 1985), and subsequent reports added nitrogen and carbon as other key benefits of mistletoes from the parasitic relationship with the hosts (Schulze et al., 1991; Marshall et al., 1994; Bannister and Strong, 2001). Parasitism by mistletoe inevitably affects water, nitrogen and carbon assimilation of the host plants at individual scales. Additionally, parasitic plants may also affect carbon, nitrogen and water cycling at larger scales, especially in arid and semi-arid environments (like the Kalahari), where both water and nutrient act as limiting factors on ecosystem dynamics (Aranibar, 2003), in that both nutrients and soil moisture interactively control vegetation dynamics. The Kalahari, situated in central southern Africa, represents an ancient biome, which has evolved to its present state over several million of years (Skinner and McCarthy, 1998). Embedded within the Kalahari biome is the Kalahari Transect (KT), an IGBP (International Geosphere-Biosphere Programme) “Mega transect” dominated by different types of savanna vegetations. Savannas throughout the KT exhibit an intriguing combination of plants, including a variety of different grasses and trees. These savannas provide ideal grazing habitat for both native herbivores such as elephant, hippopotamus and buffalo, as well as livestock such as cattle (Aranibar, 2003). Humans also depend heavily on savanna ecosystems for fuel wood and rangeland. The KT is an area with a strong gradient in rainfall, with mean annual precipitation (MAP) from 200 mm in the south to more than 1000 mm in the north (Scholes et al., 2002). This mega-transect (the KT) provides an excellent basis (similar soil substrate and huge rainfall gradient) for

studies on nutrient and carbon cycling at the subcontinental scales as well as for testing global carbon and vegetation models (Shugart et al., 2004; Wang et al., 2007a).

Thus far, research along the KT has been confined to soil-plant-atmosphere relationships while overlooking the parasitic relationships along this transect (Shugart et al., 2004), prompting the current study. To date, no studies have documented the carbon and nitrogen stable isotope compositions (i.e., $\delta^{13}\text{C}$ and $\delta^{15}\text{N}$) of mistletoes along the KT and the degree of xylem-tapping mistletoe parasitism (e.g., the percentage of carbon and nitrogen in the mistletoes directly come from their hosts) on native vegetation is still unclear. Schulze et al. (1991) reported $\delta^{13}\text{C}$ and $\delta^{15}\text{N}$ of mistletoe along an aridity gradient in the Namib Desert. However, recent studies have shown a difference in nitrogen uptake strategies for the same species in the Namib Desert and the KT (Aranibar et al., 2004) thus the $\delta^{15}\text{N}$ values of mistletoe in the Namib Desert may not apply to the KT vegetation. For example, Schulze et al. (1991) considered *Acacia mellifera* Benth. to be nitrogen-fixing plants in the Namib Desert, while Aranibar et al. (2004) found no indication of nitrogen fixing capability for the same species along the KT. Historical records document that losses in productivity caused by mistletoe parasitism can be up to 20% in *Acacia nilotica* (L.) Delile forests in Sudan (Gibson, 1967). Similarly, in the drier portion of the KT, I found that parasitism by mistletoe is a common phenomenon and I observed mistletoes on leafless but living branches of *A. mellifera*, with unaffected host branches bearing leaves. A preliminary analysis on the mistletoe associations in different geographic locations along the KT was conducted to explore the utilization of carbon and nitrogen by parasitic mistletoes on different host species. Field sampling was carried out during wet seasons of 2005 and 2006 in three geographic locations (Tshane,

Ghanzi and Maun) along KT (Fig. 8.1), each with different MAP. In addition to total carbon, total nitrogen and their stable isotope composition analyses, heterotropy (H), the proportion of carbon in the mistletoes derived from host photosynthate was also calculated.

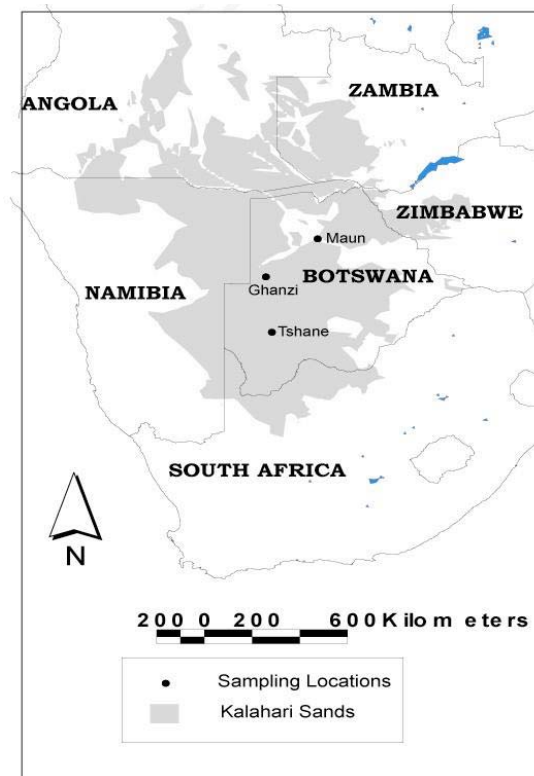


Figure 8.1. Sampling locations for mistletoe-host pairs along the Kalahari transect.

2. MATERIAL AND METHODS

2.1 Study sites and field sampling

The field sampling periods were in March, 2005 and February, 2006. The specific geographic locations of the three sampling sites were: Tshane (24.17°S, 21.89°E), Ghanzi (21.65°S, 21.81°E) and Maun (19.93°S, 23.59°E) (Fig. 8.1). In order to avoid species-

specific effects as much as possible, only one mistletoe species, *Tapinanthus oleifolius* (Wendl.) Danser was used along the whole transect. *T. oleifolius* grows on a large range of plant species including nitrogen-fixing Mimosaceae, as well as non-N fixing trees (Schulze et al., 1991). One host species was used at each location except at Tshane (Table 8.1), where two host species, *A. mellifera* (Fig. 8.2A) and *Acacia leuderitzii* Engl. (Fig. 8.2B), were obtained in both 2005 and 2006. Three to four pairs of mistletoes and their host plants were selected at each location. Ten to fifteen fully expanded leaves from each pair were collected and combined for subsequent analyses (Table 8.1).



Figure 8.2. *Tapinanthus oleifolius* (Wendl.) Danser grows on *Acacia mellifera* Benth. (A) and *Acacia leuderitzii* Engl. (B) in Tshane.

2.2 Chemical analyses

Leaf samples were dried at 60°C for 72 hours. After drying, the leaves were ground to fine powder and homogenized for isotopic and elemental analysis. Total carbon and nitrogen content were measured using an Elemental Analyzer (Carlo Erba, NA1500, Italy). The $\delta^{13}\text{C}$ and $\delta^{15}\text{N}$ compositions (‰) were determined using a Micromass Optima

Isotope Ratio Mass Spectrometer (IRMS) coupled to the elemental analyzer (EA) (GV/Micromass, Manchester, UK). Stable isotopic compositions are reported in the conventional form: $\delta^X E (\text{‰}) = [(X E / Y E)_{\text{sample}} / (X E / Y E)_{\text{std}} - 1] \times 1000$

where E is the element being measured, x is the atomic weight of the heavier isotope and y is the atomic weight of the lighter isotope and $(X E / Y E)$ is the isotopic ratio of sample, or of the standard material. Stable carbon isotope ratios are reported as $\delta^{13}\text{C}$ (‰), and stable nitrogen isotopic ratio as $\delta^{15}\text{N}$ (‰). The standards for carbon and nitrogen stable isotopes are Pee Dee Belemnite (PDB) and atmosphere molecular nitrogen, respectively. Reproducibility for these measurements is typically better than 0.2‰ (Wang et al., 2007d).

2.3 Calculation and Statistical analyses

Heterotropy (H) of the mistletoe may be estimated from $\delta^{13}\text{C}$ of host (δ_h) and mistletoe (δ_m) using the formula of Marshall and Ehleringer (1990), where:

$$H = (\delta_{\text{mg}} - \delta_m) / (\delta_{\text{mg}} - \delta_h)$$

and δ_{mg} is the theoretical $\delta^{13}\text{C}$ value of the mistletoe that is predicted from the relationship proposed by Farquhar et al. (1982):

$$\delta_p = \delta_a - a - (b - a) (c_i / c_a)$$

This relates the $\delta^{13}\text{C}$ of the plant tissue (δ_p) to that of the air (δ_a), the partitioning of $\delta^{13}\text{C}$ into a diffusive component (a) and a carboxylation component (b) and the ratio of the long-term average of intercellular CO_2 concentration to that in the air (c_i / c_a). Here, δ_{mg} is estimated as -31‰ following Schulze et al. (1991) for the Namib Desert plants.

The paired *t*-test was used to compare the foliar $\delta^{15}\text{N}$, $\delta^{13}\text{C}$, %C, %N and C/N between mistletoes and their host plants at each geographical location, sampling time and species combination. For *A. leuderitzii* and *A. mellifera*, because two year samplings were conducted in Tshane, foliar $\delta^{15}\text{N}$, $\delta^{13}\text{C}$, %C, %N and C/N in both host and mistletoes was also compared between two years using ANOVA (model I) to test the annual variations. For *A. mellifera*, because two geographical locations (Tshane vs. Ghanzi) were used, ANOVA was used to compare site differences in foliar $\delta^{15}\text{N}$, $\delta^{13}\text{C}$, %C, %N and C/N in host and mistletoes for same species (only 2005 data were used for Tshane to avoid the confounding effect from yearly variation). Correlation analysis was used to explore the relationship between foliar $\delta^{15}\text{N}$, $\delta^{13}\text{C}$ and %N between mistletoes and their host plants. All statistical analyses were accomplished using SAS (SAS v. 9.1, SAS Institute Inc, Cary, NC). For all the statistical tests, the significance levels were chosen as $\alpha = 0.05$.

3. RESULTS

The $\delta^{13}\text{C}$ in the mistletoes were significant lower ($P < 0.05$) than their host plants on all occasions, with the differences being between 1 and 4‰, depending on host species and geographical location (Table 8.1). There was no significant difference in $\delta^{15}\text{N}$ between mistletoes and their host plants (Table 8.1). In Tshane, the %C and %N in *A. leuderitzii* were higher than the mistletoes both in 2005 and 2006, though no significant difference was detected in C/N (Table 8.1). There was no difference in %C, %N and C/N between *A. mellifera* and the associated mistletoe in 2005. In 2006, there is no difference in %C between *A. mellifera* and mistletoes but there was higher nitrogen content in *A. mellifera*,

resulting in a lower C/N in *A. mellifera* (Table 8.1). In Ghanzi, carbon and nitrogen content and C/N relationship in *A. mellifera* and mistletoes were essentially the same as in Tshane of 2006. In Maun, there was no difference in %N between *Colophospermum mopane* (J.Kirk ex Benth.) J.Léonard and mistletoes but there was higher carbon content in *C. mopane*, resulting a higher C/N (Table 8.1).

There were no large temporal differences in foliar nutrients and isotope compositions for the hosts and the mistletoes. In Tshane, for *A. leuderitzii*, both hosts and mistletoes showed no difference in foliar $\delta^{15}\text{N}$, $\delta^{13}\text{C}$, %C, %N and C/N between two sampling times (Table 8.1). For *A. mellifera*, both hosts and mistletoes also showed no difference in foliar $\delta^{15}\text{N}$, $\delta^{13}\text{C}$, %C, %N and C/N between two sampling times but N% was different for mistletoes (Table 8.1).

There were site differences in foliar nutrient and isotope composition either for the hosts or for the mistletoes. For *A. mellifera*, foliar %C, %N and C/N were not different between two geographical locations (Tshane vs. Ghanzi), but $\delta^{15}\text{N}$ and $\delta^{13}\text{C}$ were different ($P < 0.05$, Table 8.1). For mistletoes on *A. mellifera*, foliar $\delta^{15}\text{N}$, %C, %N and C/N were significantly different ($P < 0.05$) between two locations (Table 8.1) but $\delta^{13}\text{C}$ was not different.

The heterotropy (H) of mistletoes was different depending on host species and it was similar for the same host species at different geographical locations and in different sampling times. In Tshane, the H values of *A. leuderitzii* were 37.9 and 34.5 in 2005 and 2006, respectively; the H values of *A. mellifera* were 71.2 and 61.4 in 2005 and 2006 (Table 8.1) and the H values of *A. mellifera* and *C. mopane* were 77.5 and 49.0 in Ghanzi and Maun, respectively (Table 8.1).

Table 8.1. The foliar $\delta^{15}\text{N}$, $\delta^{13}\text{C}$, %C, %N and C/N of mistletoe samples (*Tapinanthus oleifolius*) and their host plant at different sampling times and locations, and the heterotropy (*H*) of mistletoes. For each specific index (e.g., %C), different numbers indicate different means between the mistletoes and its host (paired *t*-test, $\alpha = 0.05$); different lower-case letters indicate different means for the same species (*Acacia leuderitzii* and *Acacia mellifera*) at two sampling times in Tshane (ANOVA, $\alpha = 0.05$); different upper-case letters indicate different means for *Acacia mellifera* at different locations (ANOVA, $\alpha = 0.05$).

				%C		%N		C/N	
Location	Mean Annual Precipitation	Sampling Time	Species	Host	Mistletoe	Host	Mistletoe	Host	Mistletoe
Tshane	365 mm	Mar-05	<i>Acacia leuderitzii</i> (Ale)	52.54 ^{1a}	43.82 ^{2a}	2.21 ^{1a}	1.79 ^{2a}	24.05 ^{1a}	24.79 ^{1a}
			<i>Acacia mellifera</i> (Ame)	46.61 ^{1aA}	43.92 ^{1aA}	4.01 ^{1aA}	3.93 ^{1aA}	11.68 ^{1aA}	11.29 ^{1aA}
		Feb-06	<i>Acacia leuderitzii</i>	51.35 ^{1a}	45.66 ^{2a}	2.82 ^{1a}	2.22 ^{2a}	18.29 ^{1a}	20.69 ^{1a}
			<i>Acacia mellifera</i>	44.67 ^{1a}	45.17 ^{1a}	4.09 ^{1a}	2.77 ^{2b}	10.93 ^{1a}	16.81 ^{2a}
Ghanzi	424 mm	Mar-05	<i>Acacia mellifera</i>	46.28 ^{1A}	46.37 ^{1B}	3.56 ^{1A}	1.31 ^{2B}	12.99 ^{1A}	36.60 ^{2B}
<i>Colophospermum mopane</i>									
Maun	460 mm	Mar-05		51.45 ¹	40.86 ²	2.65 ¹	4.28 ¹	19.70 ¹	9.98 ²
				$\delta^{13}\text{C}$ (‰)		H	$\delta^{15}\text{N}$ (‰)	$\delta^{15}\text{N}$ (‰)	Number of Pairs
Location	Mean Annual Precipitation	Sampling Time	Species	Host	Mistletoe		Host	Mistletoe	
Tshane	365 mm	Mar-05	<i>Acacia leuderitzii</i> (Ale)	-24.4 ^{1a}	-28.5 ^{2a}	37.9	6.6 ^{1a}	5.6 ^{1a}	4
			<i>Acacia mellifera</i> (Ame)	-25.0 ^{1aA}	-26.7 ^{2aA}	71.2	9.3 ^{1aA}	9.7 ^{1aA}	3
		Feb-06	<i>Acacia leuderitzii</i>	-24.9 ^{1a}	-28.9 ^{2a}	34.5	6.7 ^{1a}	6.3 ^{1a}	3
			<i>Acacia mellifera</i>	-25.0 ^{1a}	-27.3 ^{2a}	61.4	7.9 ^{1a}	9.2 ^{1a}	3
Ghanzi	424 mm	Mar-05	<i>Acacia mellifera</i>	-26.1 ^{1B}	-27.2 ^{2A}	77.5	6.2 ^{1B}	6.9 ^{1B}	3
<i>Colophospermum mopane</i>									
Maun	460 mm	Mar-05		-25.9 ¹	-28.5 ²	49.0	8.0 ¹	7.8 ¹	3

There was a significant positive correlation between host and mistletoe leaf nitrogen isotope values, $\delta^{15}\text{N}$ ($r = 0.64$, $p = 0.02$) (Fig. 8.3) but the relationship was not

significant for leaf N ($r = 0.13$, $p = 0.68$) (Fig. 8.4). The $\delta^{13}\text{C}$ of mistletoes were positively correlated to host nitrogen contents ($r = 0.66$, $p = 0.01$), but $\delta^{13}\text{C}$ in host tissue was not correlated with its nitrogen content ($r = -0.14$, $p = 0.64$) (Fig. 8.5).

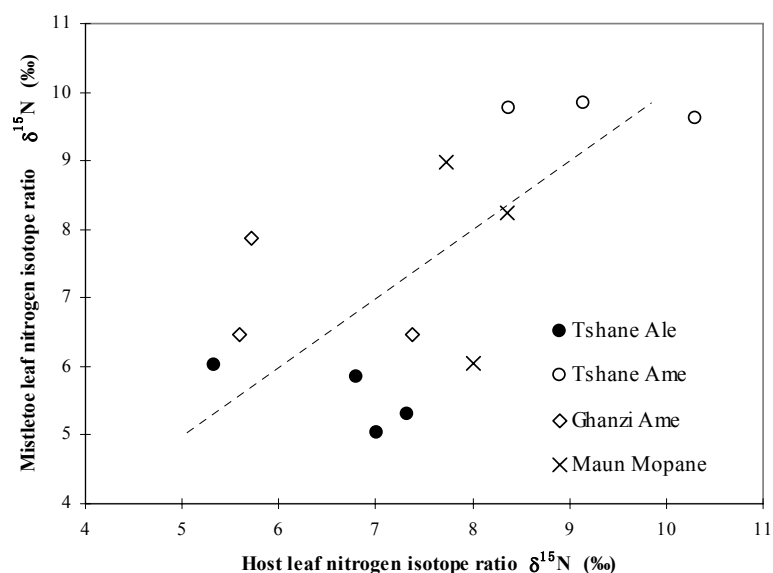


Figure 8.3. The correlation between foliar $\delta^{15}\text{N}$ of mistletoes and their host plants. Each point represents a mistletoe-host pair ($r = 0.64$, $p = 0.02$).

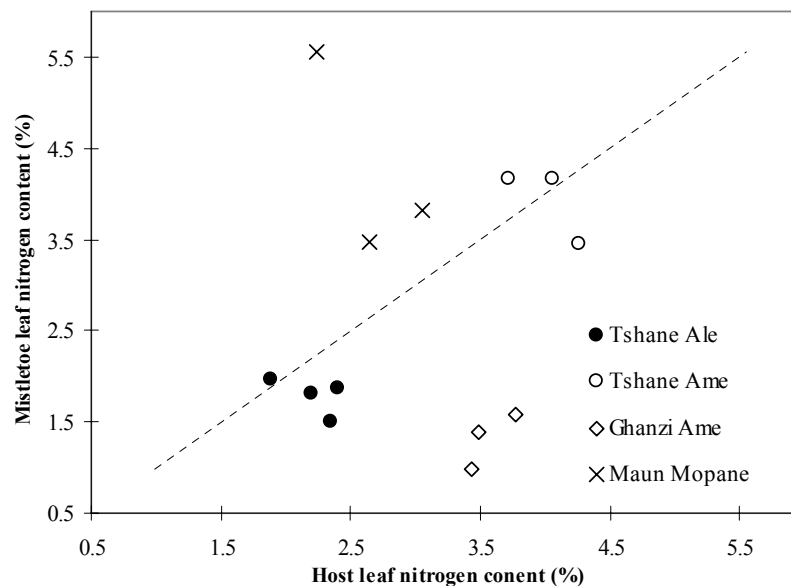


Figure 8.4. The correlation between foliar %N of mistletoes and their host plants. Each point represents a mistletoe-host pair ($r = 0.13$, $p = 0.68$).

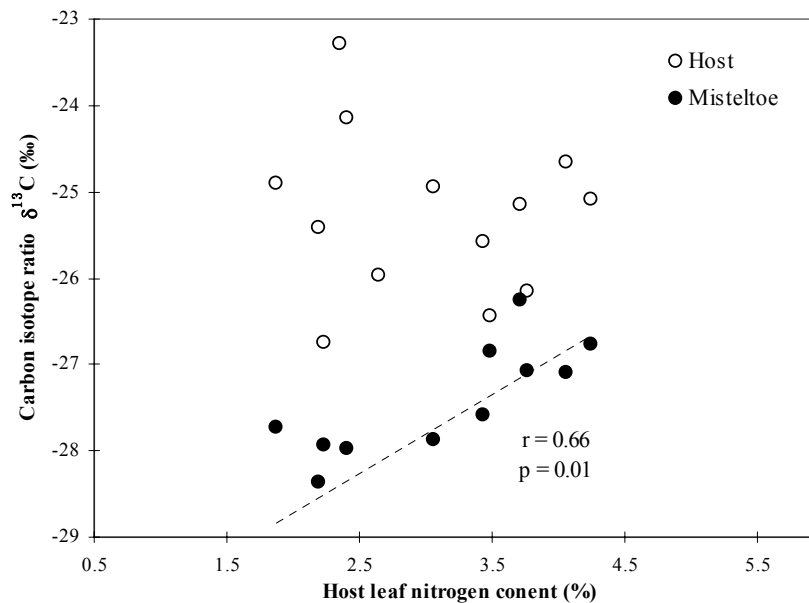


Figure 8.5. The correlation between $\delta^{13}\text{C}$ and host %N for either mistletoes or host plants. Each point represents either an individual mistletoe or an individual host ($r = 0.66$, $p = 0.01$ for mistletoes and $r = -0.14$, $p = 0.64$ for hosts).

4. DISCUSSION

The significant correlation between host and mistletoe in the leaf $\delta^{15}\text{N}$, the similar C/N ratios between host and mistletoe, and the similarity between host and mistletoe leaf $\delta^{15}\text{N}$ confirmed that mistletoes acquire nitrogen from their hosts. The correlation and similarity between host and mistletoe in the leaf $\delta^{15}\text{N}$ also suggests that in the process of acquiring nitrogen from their host, there is no nitrogen isotope discrimination. This observation is in agreement with previous findings for the mistletoe *T. oleifolius* growing on *Acacia spp.* in the Namib Desert (Schulze et al., 1991). The foliar nitrogen content of mistletoes is as much as 56% greater than in the host plants, although sometime it is found that the foliar nitrogen content of mistletoes is lower than their hosts (Lamont, 1983). In the KT, however, the foliar nitrogen content of the hosts was equal to or higher

than those in mistletoes across all geographic regions and species. This may indicate that, in addition to water, available nitrogen along the KT is an additional factor in limiting productivity, and influences the host plants to protect their N content more than in other environments. This strengthens the earlier contention that at leaf level, along the Kalahari Transect, there appears to be a strong trade-off between nitrogen use efficiency and water use efficiency (Midgley et al., 2004).

Foliar $\delta^{13}\text{C}$ in mistletoes was significantly lower than their host plants in all locations, supporting the $\delta^{13}\text{C}$ relationship observed between mistletoes and their hosts in Africa, North America and Australia (Schulze et al., 1991; Marshall et al., 1994; Bannister and Strong, 2001). Lower $\delta^{13}\text{C}$ in mistletoes have been traditionally interpreted as an indication of lower water-use-efficiency, mainly due to the mistletoes transpiring large volumes of water while conducting photosynthesis at diminished rates to facilitate assimilation of the low concentration N dissolved in host xylem waters (Ehleringer et al., 1985; Schulze et al., 1991). Other fertilization experiments and model simulations showed, however, the lower $\delta^{13}\text{C}$ in mistletoes are a consequence of an imbalance in C and N assimilation (Marshall et al., 1994). The fact that the $\delta^{13}\text{C}$ of mistletoes were positively correlated with host nitrogen content, but $\delta^{13}\text{C}$ in host tissue was not related its nitrogen content in this study partially supports the previous hypothesis that mistletoes regulate water use in relation to N supply, at least along the KT. A small seasonal variation in the foliar $\delta^{13}\text{C}$ in both host and mistletoes, is similar to that seen in host-mistletoes pairs analyzed in New Zealand (Bannister and Strong, 2001). The host species *Acacia mellifera* selected both at Tshane and Ghanzi exhibited different foliar $\delta^{13}\text{C}$ and $\delta^{15}\text{N}$ content at the two locations, in agreement with previous findings along the Kalahari

(Aranibar et al., 2004; Swap et al., 2004). Moreover, there is an apparent inverse relationship between foliar $\delta^{13}\text{C}$ and $\delta^{15}\text{N}$ and MAP for the host plants. This phenomenon was interpreted as an increase in water-use-efficiency by the host plants and an increase in N loss from the system when aridity increases (Swap et al., 2004). At the same time, the $\delta^{15}\text{N}$ values in mistletoes were different but $\delta^{13}\text{C}$ compositions were the same between two locations, which may result from small differences in the degree of carbon parasitism by the mistletoes.

An estimate of the proportion of carbon in the mistletoes derived from host photosynthate using H was between 34.5 and 77.5, depending on the species and locations. The H values along the KT are within the range found in the Namib Desert (Schulze et al., 1991). The H values were different between the host species but show little annual variation.

This study shows that mistletoes along the Kalahari derive both nitrogen and carbon from their hosts. Mistletoes may regulate water use in relation to N supply. The proportion of carbon in the mistletoes derived from host photosynthate can be up to 77%, and the degree of heterotrophy is species-specific with little annual variation. The sample size in this study is small and the lack of significance in some tests may be due to the limitation of the sample size. The goal of current study is to stimulate interests for more rigorous studies emphasizing the importance of incorporating mistletoes associations in budgets of carbon, water and nutrient cycling along the Kalahari.

Acknowledgements

The project was supported by NASA-IDS2 (NNG-04-GM71G). I greatly appreciate the team-work and field assistance from Lydia Ries, Natalie Mladenov, Kelly Caylor, Greg

Okin, Matt Therrell, Todd Scanlon, Ian McGlynn at University of Virginia, Billy Mogojwa, Thoralf Meyer at Harry Oppenheimer Okavango Research Center, University of Botswana. I thank Bill Gilhooly for the help working with the isotope ratio mass spectrometer. The clarity and strength of this paper is improved by comments from two anonymous reviewers.

Chapter 9 Spatial heterogeneity and sources of soil carbon in southern African savannas

ABSTRACT

Knowledge of the southern Africa soil carbon pool, its heterogeneity, sources (from trees or grasses), and potential response to climate is extremely limited. In this study the Kalahari Transect (KT) was used as a representative savanna ecosystem to quantitatively evaluate the spatial heterogeneity of the soil carbon pool and its contributing sources. The KT encompasses a dramatic aridity gradient on relatively homogenous soils. Two sites were chosen along the KT, representing dry and wet conditions. In February-March 2005, soil samples were collected at each site along a 300-m transect. Stable carbon isotope ($\delta^{13}\text{C}$) and organic carbon content (%C) of the soils were utilized in the assessment in conjunction with geostatistical analysis of the spatial patterns of soil $\delta^{13}\text{C}$ and %C. At the dry savanna site, well-defined patterns in both $\delta^{13}\text{C}$ and %C were observed that were related to the distribution of woody vegetation. At the wet savanna site, the spatial patterns of $\delta^{13}\text{C}$ and %C were somewhat less pronounced, but still were impacted by the distribution of woody vegetation. The relative contributions from C_3 and C_4 vegetation to the soil carbon pool at the wet site were independent of tree locations, but dependent on woody plant locations at the dry site. At the dry site, ~40% of the soil carbon was derived from C_3 vegetation, whereas at the wet site ~90% of the soil carbon originated from C_3 vegetation. These results represent a vital step in the understanding the impact of regional climate change on carbon

sequestration in southern Africa by providing quantitative information on soil carbon spatial distributions and sources under different climatic conditions.

Keywords: C₃ plants, C₄ plants, Geostatistics, Kalahari, Savannas, Soil $\delta^{13}\text{C}$, Soil organic carbon, Stable isotope

Wang, L., G. Okin, K. Caylor and S. Macko. Spatial heterogeneity and sources of soil carbon in southern African savannas. *Plant and Soil* (in review).

1. INTRODUCTION

Soil organic matter (SOM) is one of the largest and most dynamic reservoirs of carbon (C) in the global C cycle. The amount of C stored in SOM is about twice that stored in the biosphere and atmosphere combined (Schlesinger, 1997; Williams et al., 2007). Africa is the second largest continent on Earth (20% of the Earth's land area), but knowledge of the soil C pool in Africa is extremely limited (Schlesinger, 1997; Williams et al., 2007). The shared dominance of trees and grasses in savannas, the dominant physiognomy in southern Africa, adds more complexity in soil C pool partitioning and dynamics than is found in landscapes dominated by a single physiognomy. Previous works on regional C stock estimate have been treating trees and grasses as one vegetation pool without differentiating their contributions (Williams et al., 2007), which may limit our understanding of the African C cycling since tree-grass composition is dynamic both spatially and temporally. By using stable C isotopes and soil organic carbon content in conjunction with geostatistical analysis, this study aims to investigate the spatial variability of the soil C pool, partition the contributions of soil C from trees and grasses, and assess the variations in soil C spatial variability and sources under different climatic conditions.

The research was conducted at sites along the Kalahari Transect (KT), one of a set of IGBP (International Geosphere-Biosphere Programme) "megatransects" (Koch et al., 1995; Scholes et al., 2002) identified for global change studies. The soil substrate along the entire Transect is relatively homogenous, being covered by the Kalahari sands. The physical and hydraulic parameters such as soil texture (>96% of sand) and bulk density (around 1.4-1.5 g cm⁻³ along the whole Transect) do not have significant variations along

the KT (Wang et al., 2007a). The KT thus provides an ideal setting to investigate changes in ecosystem dynamics, vegetation composition and structure, and C or nutrient cycles along a gradient of precipitation while minimizing confounding effects of soil heterogeneity.

As the two main plant functional types, the trees and grasses in African savannas differ in their photosynthetic pathways. Trees in this region utilize the C₃ photosynthetic pathway whereas grasses typically utilize the C₄ pathway (Caylor et al., 2005). The relative distribution of C₃ and C₄ vegetation along the KT has been extensively investigated in field (Ringrose et al., 1998; Scholes et al., 2002; Caylor, 2003; Privette et al., 2004; Scholes et al., 2004) and modeling studies (Jeltsch et al., 1998; Jeltsch et al., 1999a; Caylor et al., 2004; Privette et al., 2004). However, the relative contributions of each vegetation type to the soil C pool and its variability under different climatic conditions are not well-understood. Because of the distinct $\delta^{13}\text{C}$ signatures for C₃ and C₄ plants (Farquhar et al., 1989), mixing models using $\delta^{13}\text{C}$ (C₃ vs. C₄) of plants and soil provide a unique tool to partition the soil C sources between C₃ and C₄ vegetation types. Carbon isotopes have been used to partition source carbon in many ecosystems (Balesdent et al., 1987; McPherson et al., 1993; Bond et al., 1994; Mariotti and Peterschmitt, 1994; Biggs et al., 2002). Although the SOM may undergo changes both spatially and temporally, the C isotope variations are not large enough to mask the difference between C₃ and C₄ plants (~14‰). The average C isotopic values in the SOM and vegetation have been previously reported at sites along the KT (Bird et al., 2004; Swap et al., 2004; Wang et al., 2007a), though the spatial patterns at sites within this regional rainfall gradient, to our knowledge, have not been studied. In the present study,

the spatial patterns in $\delta^{13}\text{C}$ and %C were explored at two sites along the KT that represent different climatic conditions (dry and wet). The contributions of soil C from trees and grasses were partitioned to assess the variations in such contributions between the two climatic conditions. Three hypotheses were tested: 1) there are spatial patterns for soil $\delta^{13}\text{C}$ and %C at both ends of the KT (dry vs. wet); 2) the spatial pattern is better defined at the dry end of the Transect; and 3) the contribution to soil C from C_3 and C_4 vegetations differs between wet and dry ends of the KT.

2. MATERIALS AND METHODS

2.1 Field sites and field samplings

Two sites along the KT in Botswana with different climate conditions were chosen to compare the soil $\delta^{13}\text{C}$ and %C spatial patterns (Fig. 9.1). The present-day Kalahari climate ranges from arid to subhumid with relatively strong seasonal and interannual variations in precipitation. The rainfall variability ranges from less than 200 mm in southwest Botswana to over 1000 mm in the north (i.e., western Zambia) (Shugart et al., 2004; Wang et al., 2007a). The two sites represent locations near the extremes for mean annual precipitation (MAP). Tshane is at the dry end of the Transect (~365 mm MAP) and Mongu is at the wet end of the Transect (~900 mm MAP). The vegetation in Mongu is woodland savanna dominated by tree species such as *Brachystegia spiciformis* Benth and the common grass species are *Eragrostis spp.* The vegetation in Tshane is open savanna dominated by *Acacia* species such as *A. luederizii* Engl. and *A. mellifera* Benth, the dominant grass species are *Eragrostis lehmanniana* and *Schmidtia pappophoroides*. A 300-m transect oriented N-S was set up at each site. Surface soil samples (5-cm depth) were randomly collected along the 300 m transect: 271 samples were collected and

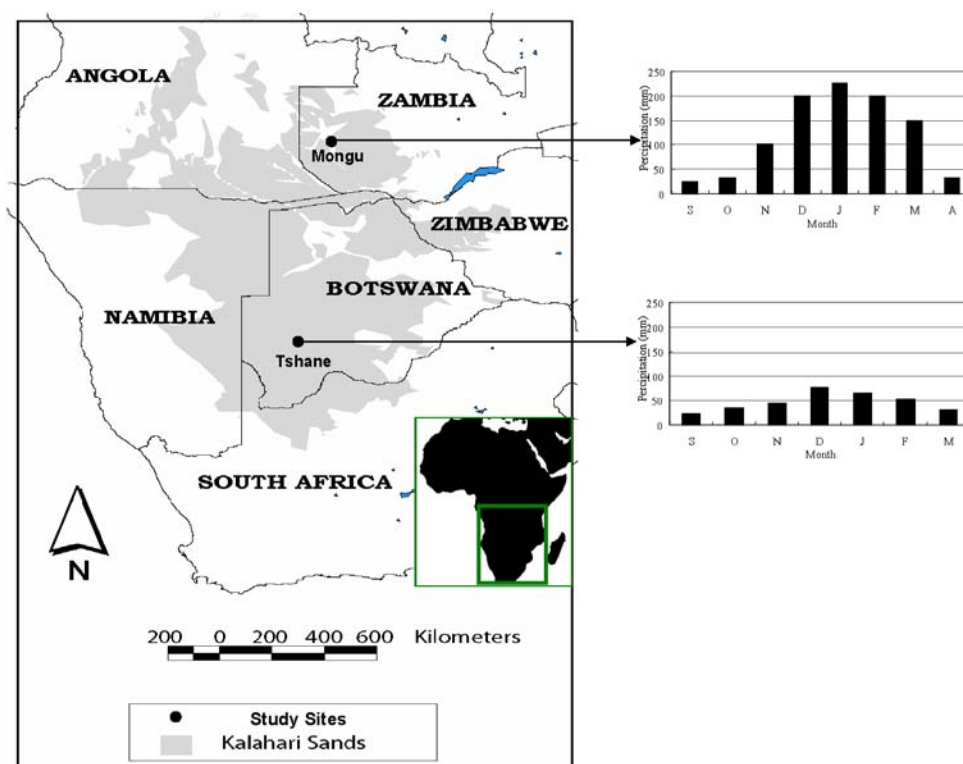


Figure 9.1. Sampling locations and rainfall characteristics along the Kalahari Transect. The column charts are the mean annual monthly precipitation data (1961-1990) of the two sampling locations from Shugart et al. (2004).

analyzed from the Mongu (wet) site and 296 samples were collected and analyzed from the Tshane (dry) site. The sampling locations were selected by the generation of random numbers prior to fieldwork. Irregular spacing of samples along the transect allowed us to have a large number of pairs that are closely spaced when calculating the variogram, while also allowing the transect to cover a relatively large distance. With the use of a transect, however, the sampling technique was not capable of identifying anisotropy in the distribution of soil nutrients of vegetation (Okin et al. in press). Presence/absence of trees and shrubs (C_3 vegetation) at each sampling point was recorded. If C_3 vegetation is present, the soil is classified as under canopy soil, otherwise it is a between canopy soil.

2.2 Laboratory analysis

Soil samples collected for elemental and isotope analyses were oven dried at 60°C in the laboratory, sieved to remove plant debris and homogenized using mortar and pestle. The presence of carbonates was tested by treating the soils with dilute hydrochloric acid (1 M) and no effervescence was observed. The %C was measured using an Elemental Analyzer (EA, Carlo Erba, NA1500, Italy) on the untreated soil samples. The stable C isotope analyses were performed using an Optima Isotope Ratio Mass Spectrometer (IRMS) connected to the EA (GV/Micromass, Manchester, UK). Stable isotope compositions are reported in the conventional form:

$$\delta^{13}\text{C} (\text{‰}) = [({}^{13}\text{C}/{}^{12}\text{C})_{\text{sample}} / ({}^{13}\text{C}/{}^{12}\text{C})_{\text{standard}} - 1] \times 1000 \quad (1)$$

where $({}^{13}\text{C}/{}^{12}\text{C})_{\text{sample}}$ and $({}^{13}\text{C}/{}^{12}\text{C})_{\text{standard}}$ are the isotopic ratios of the sample and standard, respectively. The standard for C stable isotopes is PDB. Reproducibility of these measurements is typically better than 0.2‰ (Wang et al., 2007a).

2.3 Geostatistical analysis

Both conventional statistics and geostatistics were used to analyze the spatial features of the measured variables. Conventional statistics were used to indicate the degree of overall variation. Geostatistics were used to examine whether or not that variability is spatially structured.

Data normality for all data sets was tested (SAS 9.1, SAS Inc., Cary, NC, USA) before conventional statistical and geostatistical analyses. Data were log transformed when necessary to meet the normality requirement. Conventional statistics (i.e., mean, standard deviation and coefficient of variation (CV)) were calculated to indicate the overall variability for each analyzed item.

Geostatistical analysis was used to infer the spatial variation of soil $\delta^{13}\text{C}$ and %C at each site. Before semivariogram computation, the data were tested for 1st or 2nd order trends (Davis, 2002) using GS⁺ software (Version 7.0, Gamma design software, Plainwell, MI, USA) and no trends were found.

A semivariogram (SV hereafter) is a plot of a series of semivariance values (γ) against the corresponding lag distances (h). The semivariance γ at each h is defined as:

$$\gamma(h) = \frac{1}{2N(h)} \sum_{i=1}^{N(h)} [z(i) - z(i+h)]^2 \quad (2)$$

where $N(h)$ is the number of sample pairs separated by the lag distance h . The $Z(i)$ is a measured value at location i and $Z(i+h)$ is a measured value at location $i+h$. There are several commonly used SV models. The model selection is based on two criteria: high R-square and fitted model shape. A spherical model was chosen to facilitate the comparison of parameters between variables and because this model has been shown in many cases to be adequate for soil data (Schlesinger et al., 1996; Su et al., 2006; Wang et al., 2007b). Three SV parameters were derived and used in the analysis: nugget (C_0), range (A_0) and the ratio of structure variance (C) and sill variance ($C + C_0$) ($C/(C+C_0)$, thereafter). Nugget reflects either the variability at scales finer than data resolution or variability due to measurement or locational error. Range indicates the distance of spatial autocorrelation between data pairs. The value $C/(C+C_0)$ is the proportion of the total variance that is spatially structured. A high $C/(C+C_0)$ indicates that variability in the dataset is strongly structured (Brooker, 1991; Li and Reynolds, 1995; Wang et al., 2007b). The SVs were constructed using the jackknife method presented by (Shafer and Varljen, 1990) and discussed by (Huisman et al., 2003) in a code written in the Interactive Data

Language (IDL). All SVs were fit to the spherical model using a non-linear least squares fit employing the Levenberg-Marquardt algorithm, which combines the steepest descent and inverse-Hessian function fitting methods (Press et al., 1992). The uncertainties (95% confidence limits) were determined using the variance-covariance method of (Pardo-Iguzquiza and Dowd, 2001).

Because the sill of the semivariograms of $\delta^{13}\text{C}$ and %C at Tshane demonstrated periodicity, a hole effect model (3) was also used to better fit these data following (Ma and Jones, 2001):

$$\gamma(h) = V[1 - \exp(-3h/A_0)\cos(bh)] \quad h \geq 0 \quad (3)$$

where V is the sill of the semivariogram plot, h is lag distance, A_0 is the effective range, $b = 2\pi/\lambda$ is the angular frequency, and λ is the wavelength of the periodicity.

2.4 Soil C source partitioning

The main purpose of partitioning SOM according to the relative contribution from C_3 and C_4 plants is to assess the relative contribution of soil C from the two main plant functional types (trees vs. grasses) in a savanna ecosystem and the climatic dependence of such contributions. The soil C partitioning was calculated at each sampling point across the entire 300 m transect to reflect the overall variability in soil C partitioning at each site. The partition data were also combined with the tree/shrub presence data to assess how much of the C under canopy is from grass, how much from between canopy area is from trees and how they vary across the two sites. At each sampling location, the $\delta^{13}\text{C}$ of C_3 and C_4 plants were used as two end-members in the two-source mixing ratio equation (4) to calculate the relative contributions of trees and grasses to soil C,

$$\delta^{13}\text{C}_{\text{SOM}} = \delta^{13}\text{C}_{\text{C}_3} \times f_{\text{C}_3} + \delta^{13}\text{C}_{\text{C}_4} \times f_{\text{C}_4} \quad (4)$$

where $\delta^{13}\text{C}_{\text{SOM}}$ is the $\delta^{13}\text{C}$ value of SOM, $\delta^{13}\text{C}_{\text{C}_3}$ and $\delta^{13}\text{C}_{\text{C}_4}$ are the $\delta^{13}\text{C}$ end-member values of C_3 and C_4 vegetation and f_{C_3} and f_{C_4} , which must sum to one, are relative contributions of trees and grasses to soil C. The end-member values of C_3 and C_4 vegetation were locally determined averages of root and foliar $\delta^{13}\text{C}$ of C_3 and C_4 plants at each site. The foliar $\delta^{13}\text{C}$ of C_3 and C_4 plants at each location were obtained during the 2005 wet season field campaign. The averages of 2-10 species (with 1-17 individuals for each species based on availability) for each plant functional type at each site were used to calculate foliar $\delta^{13}\text{C}$ of C_3 and C_4 plants. Five random individuals of both the C_3 and C_4 plants at each site were collected for the root $\delta^{13}\text{C}$ measurements (0-10 cm). The resulting $\delta^{13}\text{C}$ values of C_3 and C_4 end-members in Tshane were -25.4‰ and -13.6‰ respectively and the $\delta^{13}\text{C}$ values of C_3 and C_4 end-member in Mongu were -26.6‰ and -13.4‰ respectively.

3. RESULTS AND DISCUSSION

Soil $\delta^{13}\text{C}$ is higher at the Tshane (dry) site with mean value of -17.2 ‰, whereas the value at the Mongu (wet) site is -24.9 ‰ (Table 9.1). In contrast, the soil %C is higher at Mongu with mean value of 0.79%, compared to 0.24% at Tshane (Table 9.1). These results are in agreement with previous findings in this region (Hipondoka et al., 2003; Bird et al., 2004; Wang et al., 2007a). The coefficient of variation (CV) of soil $\delta^{13}\text{C}$ is much higher at Tshane (20.4%) compared to Mongu (3.9%) (Table 9.1). The CVs of soil %C are comparable at the two sites, with CV values of 55.5% and 60.4% at Tshane and Mongu respectively (Table 9.1).

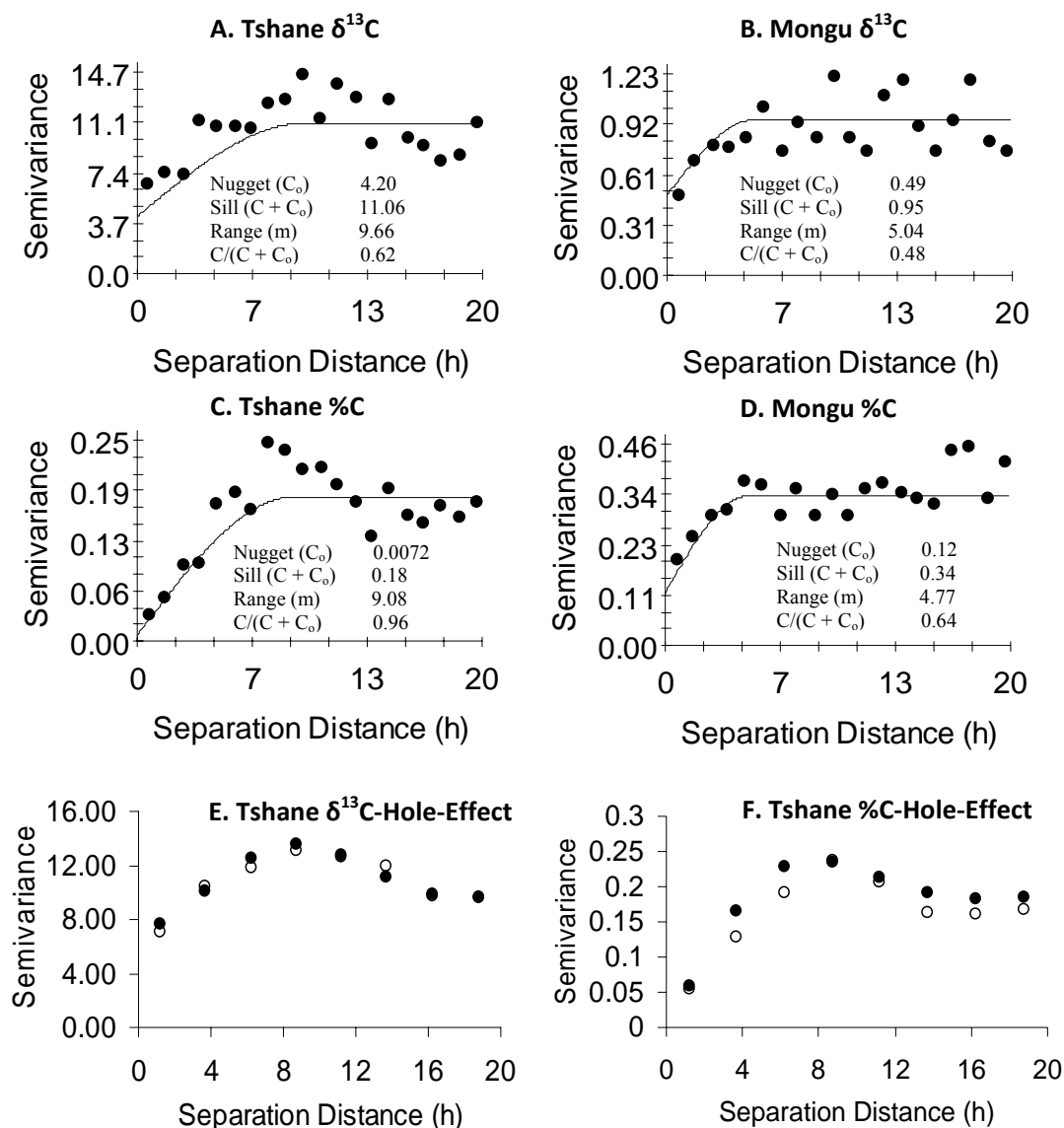


Figure 9.2. Semivariograms of $\delta^{13}\text{C}$ at Tshane (A), Mongu (B), and semivariograms of %C at Tshane (C) and Mongu (D) along the Kalahari Transect using spherical models, and semivariograms of $\delta^{13}\text{C}$ (E) and %C (F) at Tshane using hole-effect model. For (E) and (F), the open circles are actual data points and the filled circles are the modeled data points, and the $R^2 = 0.932$ and 0.928 for (E) and (F) respectively. Under the curve is the summary of semivariogram spherical model parameters. Proportion structural variation ($C/(C + C_0)$) is used as an index of the magnitude of spatial dependence.

There appear to be spatial patterns for both soil $\delta^{13}\text{C}$ and %C at both Tshane and Mongu but the range of autocorrelation is much larger at Tshane than at Mongu (Table 9.2; Fig. 9.2). At Tshane, the range of autocorrelation of soil $\delta^{13}\text{C}$ and %C is 9.66 m and 9.08 m, respectively (Fig. 9.2A, 9.2C). The excellent fit provided by the hole-effect model ($R^2 = 0.932$ and 0.928 for $\delta^{13}\text{C}$ and %C respectively) to the Tshane SVs underscores the strong spatial structuring of $\delta^{13}\text{C}$ and %C at this site (Fig. 9.2E, 9.2F). At Mongu, the range of autocorrelation of $\delta^{13}\text{C}$ and %C is 5.04 m and 4.77 m, respectively (Table 9.2; Fig. 9.2). The $C/(C+C_o)$ values for soil $\delta^{13}\text{C}$ are comparable between the two sites (Table 9.2; Fig. 9.2A and 9.2B) but the $C/(C+C_o)$ values for soil %C are much higher at Tshane (0.96) compared to Mongu (0.64) (Table 9.2; Fig. 9.2C, 9.2D). These results generally support the expectation that spatial patterns of soil $\delta^{13}\text{C}$ and %C would exist at both ends of the rainfall gradient and the spatial patterns would be stronger at the dry end, as denoted by higher values of $C/(C_o+C)$ at Tshane. The SVs of $\delta^{13}\text{C}$ and %C at Tshane showed a clear periodic pattern (Fig. 9.2A, 9.2C), which were successfully modeled using hole effect equation (equation (3)) with a wavelength (λ) of 18 m for both $\delta^{13}\text{C}$ and %C (Fig. 9.2E, 9.2F). The hole-effect behavior in Tshane also suggests a higher soil C heterogeneity at the dry end of the KT since hole-effect model generally represents the existence of multiple hierarchies in spatial patterns (Ma and Jones, 2001).

The spatial distributions of soil C are strongly influenced by tree distributions at both ends of the Transect as indicated by the fact that the range of autocorrelation of soil $\delta^{13}\text{C}$ and %C at both Tshane and Mongu are close to the mean woody-plant spacing distance at the corresponding locations ($\sim 6\text{-}10$ m at Tshane and $\sim 2\text{-}5$ m at Mongu, (Caylor, 2003; Okin et al., in press). The canopy effects on soil $\delta^{13}\text{C}$ and %C

distributions have also been found in other ecosystems such as bush encroached grassland in southwest US (Biggs et al. 2002).

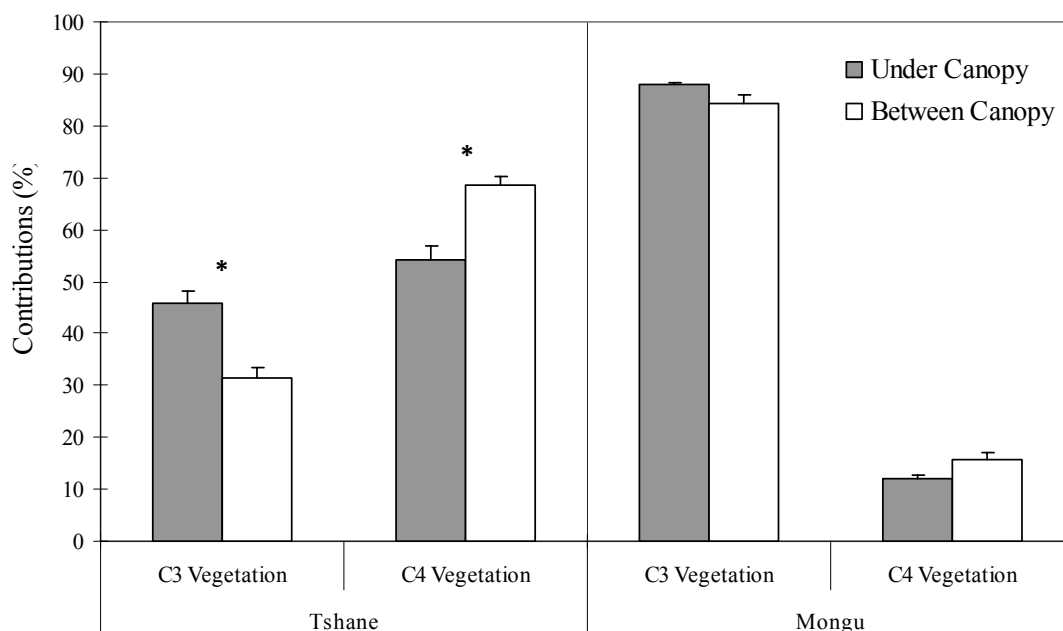


Figure 9.3. The relative contributions to soil C from C₃ and C₄ vegetation for both under canopy (grey bar) and between canopy (white bar) areas at Tshane and Mongu. The contribution differences between under and between canopy areas for each vegetation type at one particular location (e.g., C₃ vegetation contributions to soil C at under and between canopy areas at Tshane) were tested using Kuiper two-sample nonparametric test (due to the spatial correlations between the data points) and the significant differences at 0.05 significance level were indicated by asterisk.

Table 9.1. Summary of statistical parameters of soil $\delta^{13}\text{C}$ and %C at Tshane (dry) and Mongu (wet).

Location		Mean	SD	CV (%)	Min	Max
Tshane	$\delta^{13}\text{C}$ (‰)	-17.2	3.5	-20.4	-25.1	-8.0
	%C	0.24	0.13	55.5	0.75	0.10
Mongu	$\delta^{13}\text{C}$ (‰)	-24.9	1.0	-3.9	-27.1	-21.7
	%C	0.79	0.48	60.4	3.28	0.14

SD: Standard deviation.

CV: Coefficient of variation.

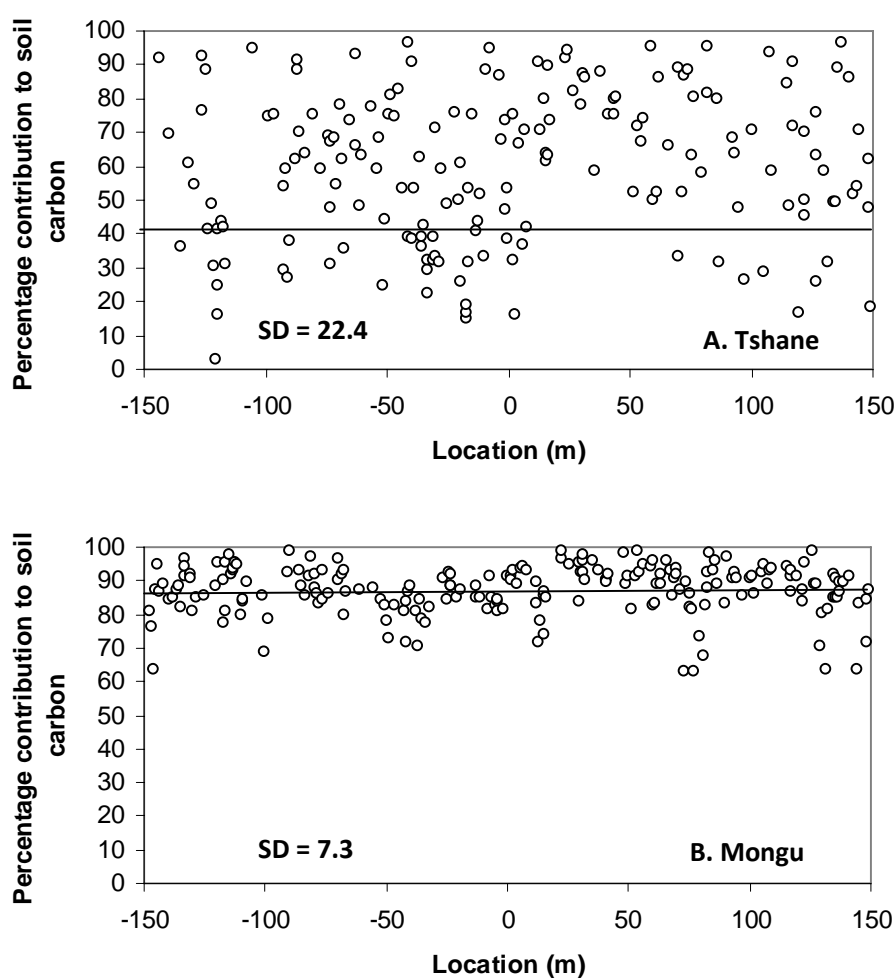


Figure 9.4. The percentage of tree contributions to soil carbon at Tshane (A) and Mongu (B) along the entire 300 m transect using $\delta^{13}\text{C}$ mixing ratio calculations. The solid lines are the means of the contribution at each site. SD stands for standard deviation.

Table 9.2. Range (m) and proportion of structured variance ($C/(C_0 + C)$) for spherical models of variograms from both sites. "M" denote the mean jackknife estimate. "L" and "U" denote the lower and upper bounds of the 95% confidence estimates, respectively.

Location	Analyte	Range (m)			$C/(C_0 + C)$		
		M	L	U	M	L	U
Tshane	%C	9.08	8.96	9.20	0.96	0.92	1.00
	$\delta^{13}\text{C}$	9.66	9.42	9.90	0.62	0.58	0.66
Mongu	%C	4.77	4.59	4.95	0.64	0.59	0.68
	$\delta^{13}\text{C}$	5.04	4.59	5.49	0.48	0.44	0.52

There are significant differences in soil C partitions for under canopy and between canopy areas for both C₃ and C₄ vegetations in Tshane, but there are no differences in such partitions between “under canopy” and “between canopy” areas for both vegetation types in Mongu (Fig. 9.3). The results indicate that relative contributions from C₃ and C₄ vegetation to the soil C pool at the wet site is independent of tree locations, but dependent on woody plant locations at the dry site. The relative contribution of C₃ woody vegetation and C₄ grasses differs at the two sites. At the dry site, the grasses contributed the majority to soil C with ~40% of the soil C is derived from woody C₃ vegetation. At the wet site, Mongu, the trees contributed the majority to soil C with ~90% of the soil C being derived from C₃ vegetation (Fig. 9.4). The variability in such contributions is much higher at the drier site, Tshane, than at Mongu (Fig. 9.4), providing further evidence that soil C heterogeneity is higher at the dry end of the KT. Due to the limited belowground information such as root density and root distribution, the SOM C source from vegetation in this study is calculated by averaging foliar and surface root (0-10 cm) $\delta^{13}\text{C}$ values as one end-member. Further studies of the weighted average of root $\delta^{13}\text{C}$ will be able to provide more accurate information on belowground C partition from C₃ and C₄ plants. In addition, considering root and foliar litter as separate end-members will better differentiate the SOM C source partition from aboveground and belowground litter input.

4. SUMMARY AND CONCLUSIONS

The purpose of this study was to test three hypotheses: 1) there are spatial patterns for soil organic C at the wet and dry ends of the KT; 2) the spatial patterns are stronger at the dry end of the Transect and 3) the contributions to soil C from C₃ and C₄ vegetations differ between wet and dry ends of the KT. Geostatistical analyses of $\delta^{13}\text{C}$ and %C and

isotope partitioning of soil C source in surface soils support all three of these hypotheses. In particular, the results suggest that the distribution of woody vegetation is a major determinant of the size and spatial structure of the soil C pool as well as the spatial structure of C isotopic composition. The results also suggest that the contribution of C₄ vegetation to the C pool of surface soils is greater in drier savannas compared to wet savannas, a consequence of the greater grass productivity at the drier sites. Although there are grasses in at the wet end of the KT, they do not appear to contribute significantly to the surface C pool.

These results indicate that in structurally complex savanna ecosystems, accurate estimates of C storage must take into account both patterns of soil C (i.e., soil C distributions) as well as the processes that contribute to the soil C pool (i.e., soil C sources). I further find that there is a close relationship between the patterns of soil organic C and the process that give rise to these patterns. Specifically, a heterogeneous woody structure is largely responsible for the heterogeneity in both the source and amount of organic C in the surface soils. This relationship suggests that high-resolution remote sensing techniques that can identify and characterize the spatial distribution of woody vegetation (Scanlon and Albertson, 2003; McGlynn and Okin, 2006) may be able to contribute substantively to the estimation of C stocks in savannas. For instance, covariance between soil organic C concentrations and isotopic compositions documented here may be able to be used in a co-kriging approach to estimate C reservoir and isotopic compositions on a regional scale.

Field and modeling results, such as the co-kriging exercise described above, are vital for understanding the role of savannas in the terrestrial C budget. Recent analyses

by (Thomas et al., 2005) suggest that climate change may result in substantial drying in southern Africa, potentially resulting in the remobilization of sand dunes throughout the Kalahari. The realignment of vegetation associated with this regional drying suggests that there may be significant changes in soil C stocks in southern African savannas. In particular, the loss of woody vegetation associated with regional drying suggests, on the basis of this analysis, more heterogeneous and smaller soil C pools in the future. Winnowing associated with sand dune remobilization would also certainly result in the overall loss of soil C to the atmosphere. Thus, an important consequence of global climate change may be the reduction of the size of the soil C pool in southern African savannas, with excess C released to the atmosphere through soil respiration of organic C from remobilized sands. Understanding the size, patterns, and sources of soil organic C in savanna soils is a vital first step in determining the potential impact regional climate change on global C cycling.

Acknowledgements

The project was supported by NASA-IDS2 (NNG-04-GM71G). I greatly appreciate the team-work and field assistance from Paolo D'Odorico, Natalie Mladenov, Matt Therrell (University of Virginia), and Billy Mogoju, Dikitso Kolokose, O.G.S.O. Kgosidintsi and Thoralf Meyer (University of Botswana) as well as Kebonyethata Dintwe (Department of Agriculture, Botswana).

Chapter 10 Predicting leaf and canopy ^{15}N compositions from reflectance spectra

ABSTRACT

I explored whether ^{15}N concentration could be predicted from reflectance spectra of fresh leaves, and, if so, whether the spectral features were related to the ^{15}N concentration on a canopy scale. Leaf scale reflectance (R) measurements were conducted in Ghanzi, Botswana using a spectrophotometer in March 2005 and canopy scale leaf R was measured in a series of successional fields in Northern Virginia, USA using the same instrument in September 2005. Results showed that there was a strong correlation between foliar ^{15}N concentration and spectral data in both visible and near-infrared wavelength regions. Stepwise regressions showed that the first-difference of the $\log 1/R$ [$(\log 1/R)'$] could explain 76 to 92% of the variation in foliar $\delta^{15}\text{N}$, providing the most reliable correlations with foliar ^{15}N at bands near 600 and 700 nm. The present study indicates the possibility of estimating fresh leaf ^{15}N abundance from high-resolution reflectance at leaf and canopy levels.

Keywords: Blandy Experimental Farm, Remote Sensing, Reflectance Spectra, Stable Isotope, ^{15}N

Wang, L., G. S. Okin, J. Wang, H. Epstein and S. A. Macko. 2007. Predicting leaf and canopy ^{15}N compositions from reflectance spectra. *Geophysical Research Letters*, 34, L02401, doi:10.1029/2006GL028506.

1. INTRODUCTION

In terrestrial ecosystems, the ratio of the rare, but naturally occurring, ^{15}N isotope to the highly abundant ^{14}N isotope is an index of many processes occurring in soils, plants, and the atmosphere (Robinson, 2001). Methods for analyzing ^{15}N contents therefore are powerful tools that can be used to elucidate biogeochemical relationships. Traditionally, the concentration of foliar ^{15}N is measured in the laboratory using Isotope Ratio Mass Spectrometer (IRMS) with reproducibility better than 0.2‰. The purpose of this report is to comment on the feasibility of using high-resolution spectral data to estimate relative ^{15}N abundances in leaves.

Analyses of foliar nitrogen concentration with reflectance spectrometry can be as accurate as traditional wet-chemistry procedures and in fact, in many laboratories, near-infrared spectrometry has replaced wet chemistry as the standard analytical procedure for plant biochemicals for dried and ground leaves (Yoder and Pettigrew-Crosby, 1995). Furthermore, Yoder and Pettigrew-Crosby (1995) showed that nitrogen concentrations could be predicted from reflectance spectra of fresh leaves in the laboratory and possibly at canopy scales. Martin and Aber (1997) further demonstrated that foliar nitrogen concentrations could be estimated using satellite data. Because there is a close relationship between foliar ^{15}N concentrations and foliar N contents in many ecosystems (e.g., Hobbie et al., 2000), there is a potential relationship between foliar ^{15}N and spectral reflectance. Here, I report on the relationship between foliar ^{15}N concentration and spectral reflectance (350-2500 nm) at both leaf and canopy scales for fresh leaves.

2. MATERIALS AND METHODS

2.1 Study sites and field measurements

Leaf-level spectral reflectance was measured in Ghanzi, Botswana in March 2005 (21.65°S, 21.81°E). The vegetation in Ghanzi is open savanna dominated by *Acacia* species such as *Acacia luederizii* Engl. and *Acacia mellifera*. The mean annual precipitation is 370 mm and mean annual temperature is around 21°C (Shugart et al., 2004). Individual leaves from eight individual plants including both trees and grasses were chosen and 10-15 measurements were made for each individual. Leaf reflectance was measured with an ASD FieldSpec Pro FR portable spectroradiometer using a leaf contact probe with a halogen light source (ASD, Inc., Boulder, CO). This instrument has a spectral range of 350-2500 nm with 1 nm sampling intervals and a 10 Hz sampling rate. A one-second integration time was used for each measurement. Reflectance was calculated as the ratio of the reflected radiance of the leaf (minus dark-target radiance) to the reflected radiance of a Spectralon panel (Spectralon, Inc.) (minus dark-target radiance). Leaves were clipped from plants after spectral measurement, and placed in labeled paper bags to dry.

Canopy-level reflectance was measured at the Blandy Experimental Farm (BEF) in four successional fields (two early stages and two middle stages). The BEF study site is located in Clarke County, Virginia (39°09'N, 78°06'W). The BEF is a 283.5-ha experimental field with distinct successional ages, which is owned and operated by the Department of Environmental Sciences at the University of Virginia. The BEF can be described as an agro-ecosystem consisting of agricultural fields, successional fields,

deciduous woodlands and ephemeral wetlands. The average annual temperature (1971-2000) is 15°C and the mean annual precipitation is 100 cm (data obtained from the Martinsburg weather station, 40 km from BEF). This research utilized two sets of successional fields at the BEF, approximately 2 km apart. Four distinct successional fields have been maintained over the two sites: a 5-year-old field (early stage1), a 3-year-old field (early stage2), a 19-year-old field (middle stage1), and an 18-year-old field (middle stage2). The 5-year-old field and 19-year-old field are adjacent to each other, and the 3-year-old field and 18-year-old field are located at another site (Bowers, 1993; Riedel and Epstein, 2005; Emanuel et al., 2006). The 3-year-old field and 5-year-old field are relatively homogeneous and dominated by *Solidago spp.*; there are other dicots such as *Asclepias syriaca* and *Carduus spp.*, and some shrub seedlings in the understory such as *Rhamnus cathartica* and *Celastrus orbiculatus*. The 18-year-old field is dominated by *Celastrus orbiculatus*, *Rhamnus cathartica*, *Maclura pomifera*, *Solidago spp.* and *Daucus carota*. The 19-year-old field is a mixture of woody species such as *Rhamnus cathartica*, *Celastrus orbiculatus* and *Ailanthus altissima*, and herbaceous dicots such as *Solidago spp.*, *Daucus carota*, *Asclepias syriaca*, *Carduus spp.*

Canopy-level reflectance was measured with the ASD FieldSpec Pro FR spectroradiometer with a 20° field of view. The sun was used as the light source and a Spectralon panel was used to convert reflected radiance to reflectance. Around 20 nadir-viewing reflectance measurements were taken within five randomly located 1 x 1 m locations at each of the four sites. Different successional ages were used because there are distinct foliar ¹⁵N signatures among successional ages (Fig. 10.1A). After the spectral

measurement, foliage was sampled from each 1 x 1 m² location, separated by species, and stored in paper bags to dry.

2.2 Isotope and elemental analyses

Leaf-level foliar $\delta^{15}\text{N}$ was estimated by averaging $\delta^{15}\text{N}$ for all leaves collected from individual plants. Canopy-level foliar $\delta^{15}\text{N}$ was estimated by averaging foliar $\delta^{15}\text{N}$ of all species (in general, the foliar $\delta^{15}\text{N}$ was similar across species for the same successional stage) for each sample location. Prior to isotope and elemental analysis, foliar samples were dried at 60°C for 72 hours. After drying, they were ground and homogenized for isotope and elemental analysis. Stable nitrogen isotope analysis was performed using a Micromass Optima Isotope Ratio Mass Spectrometer (IRMS) coupled to an elemental analyzer (EA) (GV/Micromass, Manchester, UK). Nitrogen stable isotope compositions are reported in the conventional form (‰):

$$\delta^{15}\text{N} (\text{‰}) = [({}^{15}\text{N}/{}^{14}\text{N})_{\text{sample}} / ({}^{15}\text{N}/{}^{14}\text{N})_{\text{std}} - 1] \times 1000$$

where $({}^{15}\text{N}/{}^{14}\text{N})_{\text{sample}}$ is the nitrogen isotope composition of a sample, and $({}^{15}\text{N}/{}^{14}\text{N})_{\text{std}}$ is the nitrogen isotope composition of the standard material. The standard material for stable nitrogen isotopes is atmospheric molecular nitrogen (AIR). Reproducibility of these measurements is approximately 0.2‰.

2.3 Data analysis

No pre-processing was applied to leaf-level reflectance spectra. To minimize the effect of variable shading in the canopy-level spectra, raw reflectance spectra were scaled so that the reflectance from wavelength 350 nm to 1780 nm spanned the interval [0,1]. Excessive noise due to low solar irradiance in the short-wave infrared (the region > 1780

nm) prohibited the scaling and subsequent analysis. Leaf and scaled canopy reflectance spectra were smoothed with running averages, plus and minus four nanometers ($R_{\lambda(\text{smooth})} = \text{average}(R_{\lambda-4 \text{ nm}}, R_{\lambda-3 \text{ nm}}, R_{\lambda-2 \text{ nm}}, R_{\lambda-1 \text{ nm}}, R_{\lambda}, R_{\lambda+1 \text{ nm}}, R_{\lambda+2 \text{ nm}}, R_{\lambda+3 \text{ nm}}, R_{\lambda+4 \text{ nm}})$) following Yoder and Pettigrew-Crosby (1995). First-difference spectra of $\log 1/R$ ($(\log 1/R)'$) was calculated from the difference between the values at each λ , plus and minus four bands, divided by the range of wavelength ($R' = (R_{\lambda+4} - R_{\lambda-4}) / 8$) (Yoder and Pettigrew-Crosby, 1995).

Foliar $\delta^{15}\text{N}$ values between different successional stages were compared using one-way ANOVA (SAS v. 9.1 PROC GLM), and a Tukey *post hoc* test was used to separate the means. The Pearson correlation coefficients were calculated between foliar $\delta^{15}\text{N}$ and R , between foliar $\delta^{15}\text{N}$ and $(\log 1/R)'$ at all wavelengths using SAS (v. 9.1), and correlograms were created based on Pearson correlation coefficients to easily visualize the results.

The method of Sokal and Rohlf (1995) was used to determine the significance of correlations for each band for R and $(\log 1/R)'$. Stepwise regressions (SAS v. 9.1) were performed to find the best predictors (e.g. the best wavelengths) of foliar $\delta^{15}\text{N}$ at both leaf and canopy levels. Wavelength selection was based on the correlograms, and only the wavelengths associated with significant peaks ($p < 0.05$) were selected in stepwise regressions.

3. RESULTS AND DISCUSSION

Foliar $\delta^{15}\text{N}$ range in Virginia was between -1.5 to 3.4 (Fig. 10.1A). In both sets of successional series, foliar $\delta^{15}\text{N}$ at the canopy level was significantly higher in the early successional field than that in the middle successional field (Fig. 10.1A) although the

difference between middle stage 1 and early stage 2 was not significant. Foliar $\delta^{15}\text{N}$ range in Ghanzi was between 4.2 to 8.8 (Fig. 10.1B).

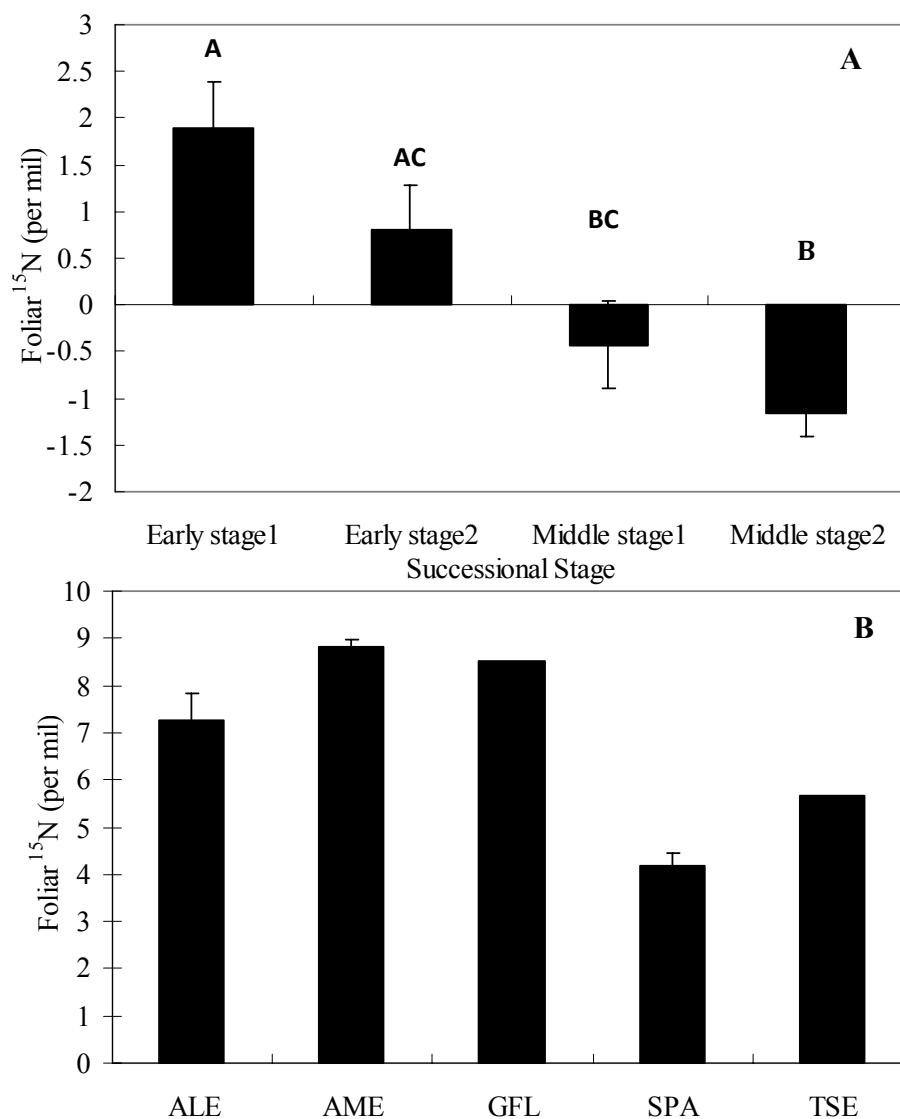


Figure 10.1 (A) Canopy level foliar $\delta^{15}\text{N}$ in four successional fields at the Blandy Experimental Farm, Virginia (Different capital letters indicate different mean values of foliar $\delta^{15}\text{N}$). (B) Species sampling list and leaf level foliar $\delta^{15}\text{N}$ in Ghanzi, Botswana. ALE (*Acacia leuderitzii*), AME (*Acacia mellifera*), GFL (*Grewia flava*), SPA (*Schmidtia pappophoroides*), TSE (*Terminalia sericea*).

Correlograms provide a clear picture of the relationships between spectral reflectance and foliar $\delta^{15}\text{N}$. Horizontal bars in the correlograms of Fig. 10.2 and Fig.

10.3 are the boundary of correlation coefficients beyond which the results are significant (dash line for $p < 0.05$ and solid line for $p < 0.01$). The regions marked with an asterisk

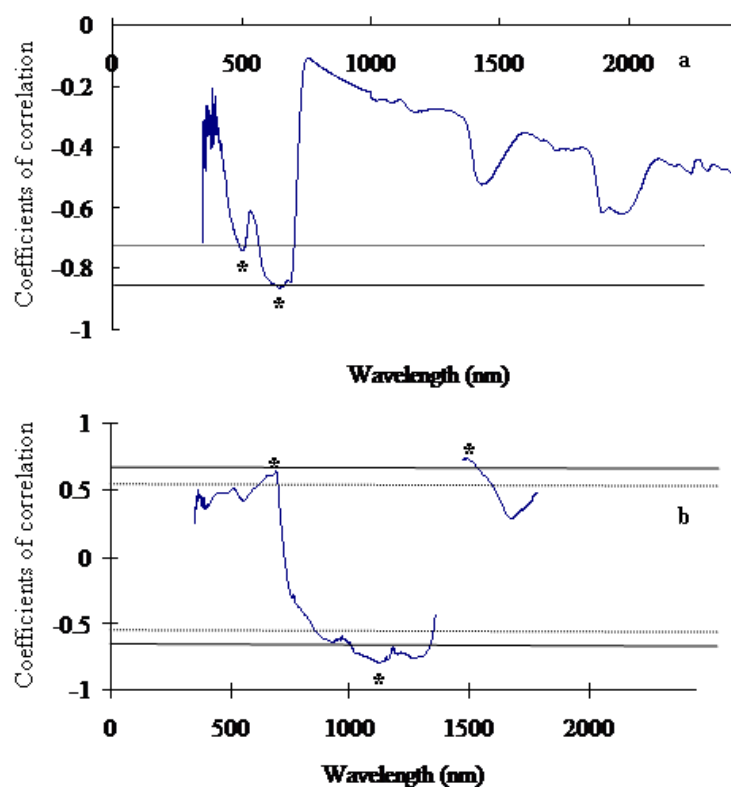


Figure 10.2 (A) Coefficients of correlation between foliar $\delta^{15}\text{N}$ and leaf-level reflectance (R) (dash horizontal bars indicate the area of significance, $p < 0.05$; solid horizontal bars indicate the area of significance, $p < 0.01$, the regions marked with an asterisk indicate regions that may be useful for predicting foliar $\delta^{15}\text{N}$, the ranges of wavelength for asterisk regions from left to right are $\lambda = 483\text{--}517$ and $\lambda = 617\text{--}703$ nm). (B) Coefficients of correlation between foliar $\delta^{15}\text{N}$ and canopy-level reflectance (R) (dash horizontal bars indicate the area of significance, $p < 0.05$; solid horizontal bars indicate the area of significance, $p < 0.01$, the regions marked with an asterisk indicate regions that may be useful for predicting foliar $\delta^{15}\text{N}$, the ranges of wavelength for asterisk regions from left to right are $\lambda = 670\text{--}694$, $\lambda = 1098\text{--}1319$ and $\lambda = 1480\text{--}1522$ nm).

indicate regions that may be useful for predicting foliar $\delta^{15}\text{N}$. These regions were chosen based on three criteria: 1) correlation coefficients are statistically significant ($p < 0.05$), 2) the region is wide enough to be used in normal field and laboratory conditions (>15 nm)

and 3) the regions do not fall in wavelength ranges where atmospheric water vapor or other factors might interfere with field or remote sensing-based spectroscopy. For instance, water vapor absorptions at ~940 nm, ~1140 nm, 1360-1470 nm and 1800-2000

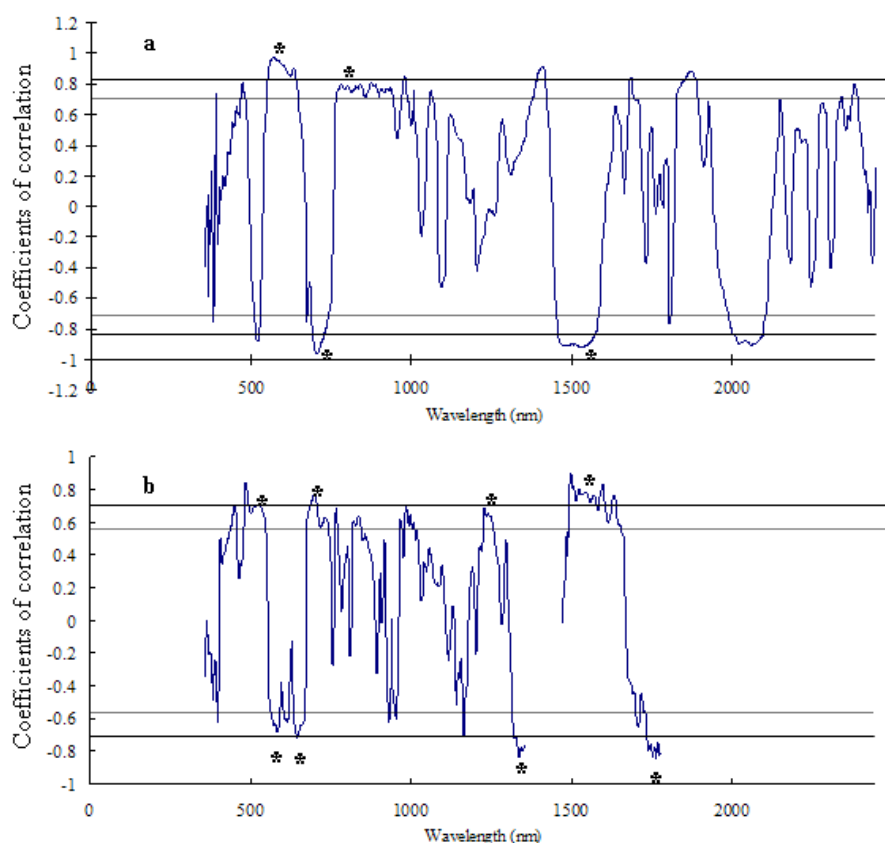


Figure 10.3 (A) Coefficients of correlation between foliar $\delta^{15}\text{N}$ and leaf-level first difference of $\log 1/R$ ($\log 1/R$)' (dash horizontal bars indicate the area of significance, $p < 0.05$; solid horizontal bars indicate the area of significance, $p < 0.01$, the regions marked with an asterisk indicate regions that may be useful for predicting foliar $\delta^{15}\text{N}$, the ranges of wavelength for asterisk regions from left to right are $\lambda = 587-637$, $690-745$, $798-940$ and $1504-1573$ nm). (B) Coefficients of correlation between foliar $\delta^{15}\text{N}$ and canopy-level first difference of $\log 1/R$ ($\log 1/R$)' (dash horizontal bars indicate the area of significance, $p < 0.05$; solid horizontal bars indicate the area of significance, $p < 0.01$, the regions marked with an asterisk indicate regions that may be useful for predicting foliar $\delta^{15}\text{N}$, the ranges of wavelength for asterisk regions from left to right are $\lambda = 517-535$, $580-590$, $639-661$, $693-708$, $1249-1254$, $1345-1358$, $1509-1604$ and $1760-1778$ nm).

nm preclude the use of these regions in practical applications. Significant noise >1780 nm due to weak solar irradiance in this region also eliminates these regions from practical use for the spectroscopic estimation of ^{15}N .

At the leaf scale, two broad regions were observed in which the correlation between R and foliar $\delta^{15}\text{N}$ were significant ($\lambda = 481 - 523$ and $564 - 703$ nm, $|r| = 0.71$ to 0.86) (Fig. 10.2A). At the canopy scale, the strong relationship between R and foliar $\delta^{15}\text{N}$ appears at several ranges including both visible and near-infrared (VNIR) regions ($|r| = 0.60 - 0.80$) (Fig. 10.2B). Although VNIR wavelength regions exhibit very high correlations, the use of R to estimate foliar ^{15}N may not be practical for remote sensing applications. This is due to the fact that variable lighting conditions can cause significant changes in the overall reflected brightness. The use of R to estimate ^{15}N should be limited to cases where lighting conditions and geometry can be controlled (e.g., a leaf-contact probe or laboratory conditions) or R empirically showing the advantages.

With the first-difference transformation $[(\log 1/R)']$, there are several narrow regions in the VNIR that appear to be useful for the estimation of ^{15}N (Leaf level: Fig. 10.3A; Canopy-level: Fig. 10.3B). First-difference spectra highlight regions where the spectral reflectance changes due to variations in absorption or scattering in the foliage. The $(\log 1/R)'$ spectra therefore tend to highlight the edges of absorption features, such as those due to chlorophyll. At both the leaf and canopy levels, significant correlations between foliar $\delta^{15}\text{N}$ and $(\log 1/R)'$ at ~ 600 nm and ~ 700 nm were found. These wavelengths occur at the edge of chlorophyll absorptions and most likely arise from variable widths of chlorophyll absorption bands in samples with different ^{15}N abundances. Because first-difference spectra are less sensitive to lighting conditions, I consider $(\log$

1/R)' to be more practical for remote sensing-based determination of ^{15}N than R. In this way, our finding concerning ^{15}N abundance follows those of Martin and Aber (1997) for N concentration. Based on (log 1/R)' stepwise regressions results, at leaf scale, the best predictors for foliar $\delta^{15}\text{N}$ are $\lambda = 603$ nm and $\lambda = 704$ nm; at the canopy scale, the best predictor for foliar $\delta^{15}\text{N}$ is $\lambda = 702$ nm (Table 10.1).

Table 10.1. Regressions predicting foliar $\delta^{15}\text{N}$ at both leaf level and canopy level.

		λ (nm)	Partial R^2	Cumulative R^2	p
Leaf Level	R	619	0.46		0.06
		695	0.36	0.82	0.02
	Log (1/R)'	603	0.46		0.07
		704	0.46	0.92	0.004
Canopy Level	R	1135	0.63	0.63	0.004
	Log (1/R)'	702	0.67		0.0006
		639	0.09	0.76	0.08

Note: See text for an explanation of the choice of bands. At the leaf level, regressions for R, were performed with $\lambda = 483\text{-}517$ nm, $617\text{-}703$ nm; regressions for Log (1/R)', were performed with $\lambda = 587\text{-}637$ nm, $690\text{-}745$ nm, $798\text{-}846$ nm, $904\text{-}940$ nm and $1504\text{-}1573$ nm. At the canopy level, regressions for R, were performed with $\lambda = 670\text{-}694$ nm, $1098\text{-}1136$ nm, $1261\text{-}1319$ nm and $1480\text{-}1522$ nm; regressions for Log (1/R)', were performed with $\lambda = 517\text{-}535$ nm, $639\text{-}661$ nm, $693\text{-}708$ nm, $932\text{-}934$ nm and $1249\text{-}1254$ nm.

4. CONCLUSIONS

Both visible and NIR wavelengths have been used to estimate foliar nitrogen (Yoder and Pettigrew-Crosby, 1995; Martin and Aber, 1997; Read et al., 2002). Because of the close relationship between foliar N concentration and foliar ^{15}N abundance, it is not surprising that there are strong correlations between foliar ^{15}N concentration and spectral data in the VNIR at the leaf scale and canopy scales. The R exhibits correlograms with wider regions of significance than those of (log 1/R)'. However, the

first-difference (derivative) spectra are probably better predictors than the simple reflectance spectra. Environmental factors such as brightness and shading can influence total reflectance, whereas the shape of the reflectance curve, as characterized by the first-difference curve is more conservative (that is, is less impacted by environmental or analytical conditions). This is why traditionally first-difference spectra have been used to resolve fine-scale spectra from background noise (Wessman et al., 1988; Yoder and Pettigrew-Crosby, 1995; Martin and Aber, 1997). In the current study, $(\log 1/R)'$ shows stronger correlations with foliar $\delta^{15}\text{N}$ than R , and the correlated bands occur over narrower wavelength regions. In stepwise regressions, $(\log 1/R)'$ predictors generated higher R^2 values ($R^2 = 0.76$ and 0.92 respectively) than R predictors at both leaf scale and canopy scale (Table 10.1). Based on $(\log 1/R)'$ stepwise regressions results, at leaf scale, the best predictors for foliar $\delta^{15}\text{N}$ are within visible ranges ($\lambda = 603$ nm and $\lambda = 704$ nm); at the canopy scale, the best predictor for foliar $\delta^{15}\text{N}$ is $\lambda = 702$ nm.

Although there are factors such as waxy cuticles (Vanderbilt et al., 1985) and trichome density (Levizou et al., 2005) that may constrain the application of remote sensing on foliar chemical analysis, as found in this study, there is a strong relationship between foliar $\delta^{15}\text{N}$ and leaf reflectance at both leaf scale and canopy scale. Spectral analysis of foliar $\delta^{15}\text{N}$, by its non-destructive and continuous nature, is a promising tool to detect terrestrial foliar $\delta^{15}\text{N}$ spatial patterns and dynamics using airborne or satellite-borne sensors through ground validation processes.

Acknowledgements

The project was supported by NASA-IDS2 (NNG-04-GM71G). I also greatly appreciate the Blandy Experimental Farm of University of Virginia to provide site, facility and partial funding toward this research.

Chapter 11 Summary

This dissertation combined multiple tools (e.g., stable isotope and chemical analysis, greenhouse work, field fertilization experiment and modeling) to understand the soil biogeochemistry variations and subsequent plant responses across a large rainfall gradient along the Kalahari Transect in southern Africa. The following are the major results and implications from this dissertation,

1. The Kalahari soils are acidic, dominated by sand, and are nutrient poor. Nutrient contents, soil texture and soil hydraulic properties differ between soil patches located under the canopy and in the intercanopy. Roots are concentrated in the top 80 cm of the soil, with grass roots being more abundant and dominant close to the surface. Moreover, the distribution of tree roots does not exhibit a clear dominance over grasses at deeper soil layers.
2. The large spatial scale field manipulation experiment shows that N may not be a limiting factor in tropical savanna ecosystems. The fertilization experiment demonstrates that even at the wet end of the transect, water remains the principal factor limiting grass productivity. Unlike other reports (Scanlon and Albertson, 2003; Midgley et al., 2004) that conjectured a switch between water and N limitations taking place as annual precipitation exceeded a critical value, these results suggest that grass productivity in the KT is determined by variations in rainfall rather than in N availability. Thus, although the traditional classifications of nutrient poor (broad-leaf savannas) and nutrient rich (fine-leaf savannas) savanna ecosystems may still be useful in the study of these locations and their dynamics (Scholes and Walker, 1993; Toit et al., 2003), this classification does

not necessarily imply the existence of nitrogen limitation in the nitrogen poor area, in that the vegetation may already be adapted to nitrogen poor conditions.

3. The natural abundance of foliar $\delta^{15}\text{N}$ and $\delta^{13}\text{C}$ reveals different water and N use for C_3 and C_4 plants. The consistently higher foliar $\delta^{15}\text{N}$ for C_3 plants suggests that C_4 plants may be a superior competitor for N. The different foliar $\delta^{13}\text{C}$ relationships with rainfall may indicate that the C_3 plants have an advantage over C_4 plants when competing for water resources. The differences in water and nitrogen use between C_3 and C_4 plants likely collectively contribute to the tree-grass coexistence in savannas.

4. The soils along the KT rainfall gradient show clear differences in belowground nutrients and $\delta^{15}\text{N}$ vertical distributions between wet and dry seasons. The results also show how the formation of “fertility islands” (i.e., the concentration of soil nutrients in the soils beneath tree canopies) is not necessarily coupled with belowground processes in that the distribution of soil nutrients at the surface does not match belowground patterns. The results also indicate that phosphorus may be a limiting nutrient in these savanna ecosystems with seasonal dynamics in its cycling.

5. The double ^{15}N labeling experiments demonstrate that N uptake preferences are determined by the ammonium/nitrate ratios in the native habitats of the plants. Nitrogen uptake preference changed across different ecosystems, even for the same species. The preference changed from nitrate to no preference to a preference for ammonium, tracking the low to high ammonium/nitrate ratio in the local environment. More significantly, these experiments show that the plant progeny continue to exhibit the same clear N preference as the parent plants did in the field. This preference remains even in plants growing away from their native environment and the source nitrogen is changed

dramatically, indicating that plants maintain an “imprint” (at least for F1 generation) with respect to N uptake. Such constancy in adaptation may have important implications to predict the success of a plant community in its response to climate change, to seed bank use and to reforestation efforts. With more rapid climate change, existing plants as well as the first generation progeny may retain their old physiological adaptation and face a greater mortality. A smaller percentage of the surviving individuals, however, will adjust to the change, passing the mechanism on to their offspring to facilitate the further survival of the species.

6. The modeling framework shows that there are distinct dynamics for soil moisture, decomposition and nitrogen mineralization between soil plots located under tree canopies and in open canopy areas. Such differences diminished when approaching the wetter end of this transect. It shows that in savanna ecosystems, water availability determines the patterns and rates of nutrient cycling at large scale, while at the local scale, vegetation patchiness plays an important role in nutrient cycling. Savannas are relatively stable ecosystems and resilient to certain climate changes (e.g., rainfall modification) but irreversible thresholds in climate conditions may exist.

7. With foliar $\delta^{15}\text{N}$ and $\delta^{13}\text{C}$ measurements of both host and mistletoe and the subsequent calculation, the results show that mistletoes along the Kalahari derive both nitrogen and carbon from their hosts. Mistletoes may regulate water use in relation to N supply. The proportion of carbon in the mistletoes derived from host photosynthate was between 35% to 78%, and the degree of heterotrophy is species-specific with only limited annual variation. The study emphasizes the importance of incorporating parasitic associations when studying carbon, water and nutrient cycling along the Kalahari in future studies.

8. At the dry savanna site, well-defined patterns in both soil $\delta^{13}\text{C}$ and %C are observed that are related to the distribution of woody vegetation. At the wet savanna site, the spatial patterns of $\delta^{13}\text{C}$ and %C are somewhat less pronounced, but still are impacted by the distribution of woody vegetation. The relative contributions from C_3 and C_4 vegetation to the soil carbon pool at the wet site are independent of tree locations, but dependent on woody plant locations at the dry site. At the dry site, ~40% of the soil carbon is derived from C_3 vegetation, whereas at the wet site ~90% of the soil carbon originated from C_3 vegetation.
9. To date, the combination of isotopic and remote sensing techniques is still in the exploratory stage. Experimental results show that there is a strong correlation between foliar ^{15}N abundances and spectral reflectance in certain visible and near-infrared wavelengths. Stepwise regression shows that the first-difference of the $\log 1/R$ [$(\log 1/R)'$] could explain 76 to 92% of the variation in foliar ^{15}N , providing the most reliable correlations with foliar ^{15}N at bands near 600 and 700 nm. Although limitations still exist, because of the non-destructive and continuous nature, remote sensing is a promising tool to expand measurements of terrestrial $\delta^{15}\text{N}$ spatial patterns and dynamics.

References

- Aber, J., Nadelhoffer, K., Steudler, P., Melillo, J., 1989. Nitrogen saturation in northern forest ecosystems. *BioScience* 39, 378-386.
- Almendros, G., Kgathi, D., Sekwhela, M., Zancada, M.C., Tinoco, P., Pardo, M.T., 2003. Biogeochemical assessment of resilient humus formations from virgin and cultivated northern Botswana soils. *Journal of Agricultural and Food Chemistry* 51, 4321-4330.
- Amundson, R., Austin, A.T., Schuur, E.A.G., Yoo, K., Matzek, V., Kendall, C., Uebersax, A., Brenner, D., Baisden, W.T., 2003. Global patterns of the isotopic composition of soil and plant nitrogen. *Global Biogeochemical Cycles* 17(1), 1031, doi:10.1029/2002GB001903.
- Aranibar, J.N., 2003. Nitrogen cycling in southern African soils and plants along rainfall and land-use gradients: a stable isotope study. PhD thesis, University of Virginia, p 270.
- Aranibar, J.N., Anderson, I.C., Epstein, H.E., Feral, C.J.W., Swap, R.J., Ramontsho, J., Macko, S.A., 2007. Nitrogen isotope composition of soils, C3 and C4 plants along land use gradients in southern Africa. *Journal of Arid Environments*, doi:10.1016/j.jaridenv.2007.06.007.
- Aranibar, J.N., Anderson, I.C., Ringrose, S., Macko, S.A., 2003. Importance of nitrogen fixation in soil crusts of southern African arid ecosystems: acetylene reduction and stable isotope studies. *Journal of Arid Environments* 54, 345-358.
- Aranibar, J.N., Otter, L., Macko, S.A., Feral, C.J.W., Epstein, H.E., Dowty, P.R., Eckardt, F., Shugart, H.H., Swap, R.J., 2004. Nitrogen cycling in the soil-plant system along a precipitation gradient in the Kalahari sands. *Global Change Biology* 10(3), 359-373.
- Assessment, M.E., 2005. Ecosystems and human well-being: desertification synthesis. World Resources Institute, Washington, DC.
- Augustine, D., McNaughton, S., 2004. Temporal asynchrony in soil nutrient dynamics and plant production in a semiarid ecosystem. *Ecosystems* 7, 829-840.
- Austin, A.T., Vitousek, P.M., 1998. Nutrient dynamics on a precipitation gradient in Hawaii. *Oecologia* 119, 519-529.
- Austin, A.T., Yahdjian, L., Stark, J.M., Belnap, J., Porporato, A., Norton, U., Ravetta, D.A., Schaeffer, S.M., 2004. Water pulses and biogeochemical cycles in arid and semiarid ecosystems. *Oecologia* 141(2), 221-235.
- Baillieul, T.A., 1975. A reconnaissance survey of the cover sands in the Republic of Botswana. *Journal of Sedimentary Petrology* 45, 494-503.
- Balesdent, J., Mariotti, A., Guillet, B., 1987. Natural ^{13}C abundances as a tracer for studies of soil organic matter dynamics. *Soil Biol. Biochem.* 19, 25-30.
- Bannister, P., Strong, G.L., 2001. Carbon and nitrogen isotope ratios, nitrogen content and heterotrophy in New Zealand mistletoes. *Oecologia* 126, 10-20.
- Beerling, D.J., Osborne, C.P., 2006. The origin of the savanna biome. *Global Change Biology* 12(11), 2023-2031.
- Belnap, J., Lange, O.L., 2003. Biological soil crusts: structure, function, and management. Springer-Verlag, Berlin.

- Berkeley, A., Thomas, A.D., Dougill, A.J., 2005. Cyanobacterial soil crusts and woody shrub canopies in Kalahari rangelands. *African Journal of Ecology* 43, 137-145.
- Biggs, T.H., Quade, J., Webb, R.H., 2002. $\delta^{13}\text{C}$ values of soil organic matter in semiarid grassland with mesquite (*Prosopis*) encroachment in southeastern Arizona. *Geoderma* 110, 109-130.
- Bird, M.I., Veenendaal, E.M., Lloyd, J.J., 2004. Soil carbon inventories and d^{13}C along a moisture gradient in Botswana. *Global Change Biology* 10(3), 342-349.
- Böhm, W., 1979. Methods of studying root systems. Springer-Verlag, New York.
- Bohrer, G., Kagan-Zur, V., Roth-Bejerano, N., Ward, D., 2001. Effects of environmental variables on vesicular-arbuscular mycorrhizal abundance in wild populations of *Vangueria infausta*. *Journal of Vegetation Science* 12(2), 279-288.
- Bohrer, G., Kagan-Zur, V., Roth-Bejerano, N., Ward, D., Beck, G., Bonifacio, E., 2003. Effects of different Kalahari-desert VA mycorrhizal communities on mineral acquisition and depletion from the soil by host plants. *Journal of Arid Environments* 55(2), 193-208.
- Bond, W.J., Stock, W.D., Hoffman, M.T., 1994. Has the Karoo spread? A test for desertification using carbon isotopes from soils. *S. Afr. J. Sci.* 90, 391– 397.
- Bowers, M.A., 1993. Influence of herbivorous mammals on an old-field plant community years 1-4 after disturbance. *Oikos* 67, 129-141.
- Brady, N.C., Weil, R.R., 1999. The nature and properties of soil. Prentice Hall, Upper Saddle River.
- Brenner, D.L., Amundson, R., Baisden, W.T., Kendall, C., Harden, J., 2001. Soil N and N-15 variation with time in a California annual grassland ecosystem. *Geochimica et Cosmochimica Acta* 65(22), 4171-4186.
- Brooker, P.I., 1991. A geostatistical primer. World Scientific Publishing Co. Pte. Ltd, Singapore.
- Buchmann, N., Brooks, J.R., Rapp, K.D., Ehleringer, J.R., 1996. Carbon isotope composition of C4 grasses is influenced by light and water supply. *Plant Cell and Environment* 19(4), 392-402.
- Burke, I.C., Lauenroth, W.K., Vinton, M.A., Hook, P.B., Kelly, R.H., Epstein, H.E., Aguiar, M.R., Robles, M.D., Aguilera, M.O., Murphy, K.L., Gill, R.A., 1998. Plant-soil interactions in temperate grasslands *Biogeochemistry* 42, 121-143.
- Caldwell, M.M., Dawson, T.E., Richards, J.H., 1998. Hydraulic lift: consequences of water efflux from the roots of plants. *Oecologia* 113, 151-161.
- Campbell, S.E., Seeler, J., Goulic, S., 1989. Desert crust formation and soil stabilization. *Arid Soil Research and Rehabilitation* 3, 217–228.
- Caylor, K.K., 2003. The structure and function of Kalahari transect vegetation. PhD dissertation.
- Caylor, K.K., D'Odorico, P., Rodriguez-Iturbe, I., 2006. On the ecohydrology of structurally heterogeneous semiarid landscapes. *Water Resources Research* 42, W07424, doi:10.1029/2005WR004683.
- Caylor, K.K., Dowty, P.R., Shugart, H.H., Ringrose, S., 2004. Relationship between small-scale structural variability and simulated vegetation productivity across a regional moisture gradient in southern Africa. *Global Change Biology* 10(3), 374-382.

- Caylor, K.K., Shugart, H.H., Dowty, P.R., Smith, T.M., 2003. Tree spacing along the Kalahari transect in southern Africa. *Journal of Arid Environments* 54, 281-296.
- Caylor, K.K., Shugart, H.H., Rodriguez-Iturbe, I., 2005. Tree canopy effects on simulated water stress in southern African savannas. *Ecosystems* 8(1), 17-32.
- Chapin, F., Matson, P., Mooney, H., 2002. *Principles of terrestrial ecosystem ecology*. Springer-Verlag, New York.
- Chapin, F.S., 1980. The mineral nutrition of wild plants. *Annual Review of Ecology and Systematics* 11, 233-260.
- Chapin, F.S., 1988. Ecological aspects of plant mineral nutrition.
- Chapin, F.S., Vitousek, P.M., Cleve, K.V., 1986. The nature of nutrient limitation in plant communities. *The American Naturalist* 12(1), 48-58.
- Charney, J., 1975. Dynamics of deserts and drought in the Sahel. *Quart. J. Roy. Meteor. Soc.* 101, 193-202.
- Cook, G.D., 2001. Effects of frequent fires and grazing on stable nitrogen isotope ratios of vegetation in northern Australia. *Austral Ecology* 26, 630-636.
- Cooke, H.J., 1980. Landform evolution in the context of climatic changes and neotectonics in the middle Kalahari of north-central Botswana. *Transactions Institute of British Geographers* 5, 80-99.
- Cooke, H.J., Verstappen, H.T., 1984. The landforms of the western Makgadikgadi basin in northern Botswana, with consideration of the chronology of the evolution of Lake Palaeo-Makgadikgadi. *Zeitschrift für Geomorphologie* 1, 1-19.
- Czarnomski, N., Moore, G., Pypker, T., Licata, J., Bond, B., 2005. Precision and accuracy of three alternative instruments for measuring soil water content in two forest soils of the Pacific Northwest. *Can. J. For. Res.* 35, 1867-1876.
- D'Odorico, P., Caylor, K., Okin, G.S., Scanlon, T.M., 2007. On soil moisture-vegetation feedbacks and their possible effects on the dynamics of dryland ecosystems. *Journal of Geophysical Research* 112, G04010, doi:10.1029/2006JG000379.
- D'Odorico, P., Laio, F., Porporato, A., Rodriguez-Iturbe, I., 2003. Hydrologic control on soil carbon and nitrogen cycles, II A case study. *Advances in Water Resources* 26, 59-70.
- D'Odorico, P., Porporato, A., 2006. Soil moisture dynamics in water-limited ecosystems. In: P. D'Odorico, A. Porporato (Eds.), *Dryland Ecohydrology* (Ed. by P. D'Odorico, A. Porporato), pp. 31-46. Springer.
- Davis, J.C., 2002. *Statistics and data analysis in geology*. John Wiley & Sons, New York.
- Dougill, A.J., Heathwaite, A.L., Thomas, D.S.G., 1998. Soil water movement and nutrient cycling in semi-arid rangeland: vegetation change and system resilience. *Hydrological Processes* 12, 443-459.
- Ehleringer, J.R., Schulze, E.D., Ziegler, H., Lange, O.L., Farquhar, G.D., Cowan, I.R., 1985. Xylem-tapping mistletoes: water or nutrient parasites? . *Science* 227, 1479-1481.
- Emanuel, R.E., Albertson, J.D., Epstein, H.E., Williams, C.A., 2006. Carbon dioxide exchange and early old-field succession. *Journal of Geophysical Research* 111, G01011.
- Endler, J., 1986. *Natural selection in the wild*. Princeton University Press, Princeton, NJ.

- Engels, C., Marschner, H., 1995. Plant uptake and utilization of nitrogen. In: P. Bacon (Ed.), *Nitrogen Fertilization in the Environment* (Ed. by P. Bacon), pp. 41-81. Woodlots & Wetlands Pty. Ltd, Sydney.
- Epstein, H.E., Pareuelo, J.M., Piñeiro, G., Burke, I.C., Lauenroth, W.K., 2006. Interactions of water and nitrogen on primary productivity across spatial and temporal scales in grasslands and shrubland ecosystems. In: P. D'Odorico, A. Porporato (Eds.), *Dryland Ecohydrology* (Ed. by P. D'Odorico, A. Porporato). Springer, Dordrecht.
- Farquhar, G., Ehleringer, J., Hubick, K., 1989. Carbon isotope discrimination and photosynthesis. *Ann. Rev. Plant Physiol. Mol. Biol.* 40, 503-537.
- Farquhar, G.D., O'Leary, M.H., Berry, J.A., 1982. On the relationship between carbon isotope discrimination and the intercellular carbon dioxide concentration in leaves. *Australian Journal of Plant Physiology* 9, 121-137.
- Feral, C.J.W., Epstein, H.E., Otter, L., Aranibar, J.N., Shugart, H.H., Macko, S.A., Ramontsho, J., 2003. Carbon and nitrogen in the soil-plant system along rainfall and land-use gradients in southern Africa. *Journal of Arid Environments* 54, 327-343.
- Folk, R.L., Ward, W.C., 1957. Brazos River bar: a study in the significance of grain size parameters. *Journal of Sedimentary Petrology* 27, 3-26.
- Fritzsche, F., Zech, W., Guggenberger, G., 2007. Soils of the main Ethiopian rift valley escarpment: A transect study. *Catena* 70(2), 209-219.
- Galloway, J.N., Dentener, F.J., Capone, D.G., Boyer, E.W., Howarth, R.W., Seitzinger, S.P., Asner, G.P., Cleveland, C.C., Green, P.A., Holland, E.A., Karl, D.M., Michaels, A.F., Porter, J.H., Townsend, A.R., Vorosmarty, C., 2004. Nitrogen Cycles: Past, Present, and Future. *Biogeochemistry* 70(2), 153-226.
- Garnett, T., Smethurst, P., 1999. Ammonium and nitrate uptake by *Eucalyptus nitens*: effects of pH and temperature. *Plant and Soil* 214, 133-140.
- Garten, C.T., 1993. Variation in foliar ^{15}N abundance and the availability of soil nitrogen on walker branch watershed. *Ecology* 74(7), 2098-2113.
- Gibson, I.A.S., 1967. The influence of disease factors on forest production in Africa, Report for Asia for 14th IUFRO Congress. IUFRO, Munich, Bavaria, Germany.
- Grace, J., José, J.S., Meir, P., Miranda, H.S., Montes, R.A., 2006. Productivity and carbon fluxes of tropical savannas. *Journal of Biogeography* 33, 387-400, doi:10.1111/j.1365-2699.2005.01448.x.
- Grove, A.T., 1969. Landforms and climate change in the Kalahari and in Ngamiland. *Geographical Journal* 135, 191-212.
- Haddon, I.G., 2000. Kalahari group sediments. In: T.C. Partridge, R.R. Maud (Eds.), *The Cenozoic of southern Africa* (Ed. by T.C. Partridge, R.R. Maud), pp. 73-87. Oxford Monographs on Geology and Geophysics.
- Handley, L.L., Scrimgeour, C.M., 1997. Terrestrial plant ecology and ^{15}N natural abundance: the present limits to interpretation for uncultivated systems with original data from a Scottish old field. In: M. Begon, A.H. Fitter (Eds.), *Advances in Ecological Research* 27 (Ed. by M. Begon, A.H. Fitter), pp. 133-212. Academic Press, San Diego.

- Hipondoka, M.H.T., Aranibar, J.N., Chirara, C., Lihavha, M., Macko, S.A., 2003. Vertical distribution of grass and tree roots in arid ecosystems of Southern Africa: niche differentiation or competition? *Journal of Arid Environments* 54, 319-325.
- Hobbie, E.A., Macko, S.A., Williams, M., 2000. Correlations between foliar $\delta^{15}\text{N}$ and nitrogen concentrations may indicate plant-mycorrhizal interactions. *Oecologia* 122, 273-283.
- Hoffman, M.T., Bond, W.J., Stock, W.D., 1995. Desertification of the eastern Karoo, south Africa: Conflicting paleoecological, historical, and soil isotopic evidence. *Environmental Monitoring and Assessment* 37(1-3), 159-177.
- Högberg, P., 1997. ^{15}N natural abundance in soil-plant systems. *New Phytologist* 137(2), 179-203.
- Hooper, D.U., Johnson, L., 1999. Nitrogen limitation in dryland ecosystems: responses to geographical and temporal variation in precipitation. *Biogeochemistry* 46, 247-293.
- Houlton, B.Z., Sigman, D.M., Schuur, E.A.G., Hedin, L.O., 2007. A climate-driven switch in plant nitrogen acquisition within tropical forest communities. *PNAS* 104(21), 8902-8906.
- Howarth, R.W., Marino, R., 2006. Nitrogen as the limiting nutrient for eutrophication in coastal marine ecosystems: Evolving views over 3 decades. *Limnol. Oceanogr.* 51, 364-376.
- Hudak, A.T., Wessman, C.A., Seastedt, T.R., 2003. Woody overstorey effects on soil carbon and nitrogen pools in South African savanna. *Austral Ecology* 28(2), 173-181.
- Huffman, G., Adler, R., Bolvin, D., Gu, G., Nelkin, E., Bowman, K., Hong, Y., Stocker, E., Wolff, D., 2007. The TRMM multi-satellite precipitation analysis: quasi-global, multi-year, combined-sensor precipitation estimates at fine scale. *J. Hydrometeor.* 8, 38-55.
- Huisman, J.A., Snepvangers, J.J.J.C., Bouten, W., Heuvelink, G.B.M., 2003. Monitoring temporal development of spatial soil water content variation: comparison of ground penetrating radar and time domain reflectometry. *Vadose Zone Journal* 2, 519-529.
- Huntsman-Mapila, P., Kampunzu, A.B., Vink, B., Ringrose, S., 2005. Cryptic indicators of provenance from the geochemistry of the Okavango Delta sediments, Botswana. *Sedimentary Geology* 174, 123-148.
- Huntsman-Mapila, P., Kampunzu, A.B., Vink, B., Ringrose, S., 2006. Geochemical record of water quality in the sediments of Lake Ngami, NW Botswana: implications for Quaternary lake levels and climate change. *Quaternary International* 148, 51-64.
- Jeltsch, F., Milton, S.J., Dean, W.R.J., Rooyen, N.V., Moloney, K.A., 1998. Modelling the impact of small-scale heterogeneities on tree-grass coexistence in semi-arid savannas. *Journal of Ecology* 86, 780-793.
- Jeltsch, F., Moloney, K., Milton, S.J., 1999a. Detecting process from snapshot pattern: lessons from tree spacing in the southern Kalahari. *Oikos* 85, 451-466.
- Jeltsch, F., Moloney, K., Milton, S.J., 1999b. Detecting process from snapshot pattern: lessons from tree spacing in the southern Kalahari. *Oikos* 85(3), 451-466.

- Jobbágy, E.G., Jackson, R.B., 2001. The distribution of soil nutrients with depth: Global patterns and the imprint of plants *Biogeochemistry* 53, 51-77.
- Joshua, W.D., 1981. Physical properties of the soils of Botswana. Soil Mapping and Advisory Services, FAO/UNDP/Government of Botswana, Gaborone.
- Knoop, W.T., Walker, B.H., 1984. Interactions of woody and herbaceous vegetation in two savanna communities at Nyesvley. *Journal of Ecology* 73, 235-253.
- Koch, G.W., Scholes, R.J., Steffen, W.L., Vitousek, P.M., Walker, B.H., 1995. The IGBP terrestrial transects: Science plan, Report No. 36. International Geosphere-Biosphere Programme, Stockholm.
- Kronzucker, H., Siddiqi, M., Glass, A., 1997. Conifer root discrimination against soil nitrate and the ecology of forest succession. *Nature* 385, 59-61.
- Laio, F., Porporato, A., Ridolfi, L., Rodriguez-Iturbe, I., 2001. Plants in water-controlled ecosystems. Active role in hydrological processes and response to water stress. II Probabilistic soil moisture dynamics. *Advances in Water Resources* 24(7), 707-723.
- Lamont, B., 1983. Mineral nutrition of mistletoes. In: M. Calder, P. Bernhardt (Eds.), *The biology of mistletoes* (Ed. by M. Calder, P. Bernhardt). Academic Press, North Ryde, New South Wales, Australia.
- Lancaster, N., 1986. Grain size characteristics of linear dunes in the southwestern Kalahari. *Journal Sedimentary Petrology* 56, 395-400.
- Lancaster, N., 2000. Aeolian deposits. In: T.C. Partridge, R.R. Maud (Eds.), *The Cenozoic of southern Africa* (Ed. by T.C. Partridge, R.R. Maud), pp. 73-87. Oxford University Press, New York.
- Leistner, O.A., 1967. The plant ecology of the southern Kalahari. *Botanical Survey Memoir* No. 38.
- Levizou, E., Drilias, P., Psaras, G.K., Maneras, Y., 2005. Nondestructive assessment of leaf chemistry and physiology through spectral reflectance measurements may be misleading when changes in trichome density co-occur. *New Phytologist* 165, 463-472.
- Li, H.R., Reynolds, J.F., 1995. On the quantification of spatial heterogeneity. *Oikos* 73, 280-284.
- Ludwig, F., de Kroon, H., Prins, H.H.T., Berendse, F., 2001. Effects of nutrients and shade on tree-grass interactions in an east African savanna. *Journal of Vegetation Science* 12, 579-588.
- Ma, Y.Z., Jones, T.A., 2001. Teacher's aide Modeling hole-effect variograms of lithology-indicator variables. *Mathematical Geology* 33(5), 631-648.
- MacGregor, A.N., Johnson, D.E., 1971. Capacity of desert algal crusts to fix atmospheric nitrogen. *Soil Science Society of America Proceedings* 35, 843-844.
- Manzoni, S., Porporato, A., 2007. A theoretical analysis of nonlinearities and feedbacks in soil carbon and nitrogen cycles. *Soil Biology and Biochemistry* 39, 1542-1556.
- Mariotti, A., Peterschmitt, E., 1994. Forest savanna ecotone dynamics in India as revealed by carbon isotope ratios of soil organic matter. *Oecologia* 97, 475-480.
- Marshall, J.D., Dawson, T.E., Ehleringer, J.R., 1994. Integrated nitrogen, carbon, and water relations of a xylem-tapping mistletoe following nitrogen fertilization of the host. *Oecologia* 100, 430-438.

- Marshall, J.D., Ehleringer, J.R., 1990. Are xylem-tapping mistletoes partially heterotrophic? *Oecologia* 84, 224-248.
- Martin, M.E., Aber, J.D., 1997. High spectral resolution remote sensing of forest canopy lign, nitrogen and ecosystem process. *Ecological Applications* 7(2), 431-443.
- McFarlane, M.J., Eckardt, F.D., 2004. The 'transparent' linear dunes of northwest Ngamiland, Botswana. *Botswana Notes and Records* 36, 136-139.
- McGlynn, I.O., Okin, G.S., 2006. Characterization of shrub distribution using high spatial resolution remote sensing: ecosystem implication for a former Chihuahuan Desert grassland. *Remote Sensing of Environment* 101(4), 554-566.
- McPherson, G.R., Boutton, T.W., Midwood, A.J., 1993. Stable carbon isotope analysis of soil organic matter illustrates vegetation change at the grassland/woodland boundary in southeastern Arizona, USA. *Oecologia* 93, 95-101.
- Midgley, G.F., Aranibar, J.N., Mantlana, K.B., Macko, S.A., 2004. Photosynthetic and gas exchange characteristics of dominant woody plants on a moisture gradient in an African savanna. *Global Change Biology* 10(3), 309-317.
- Min, X., Siddiqi, M., Guy, R., Glass, A., Kronzucker, H., 1998. Induction of nitrate uptake and nitrate reductase activity in trembling aspen and lodgepolepine. *Plant Cell Environ* 21, 1039-1046.
- Molinier, J., Ries, G., Zipfel, C., Hoh, B., 2006. Transgeneration memory of stress in plants. *Nature* 442, 1046-1049.
- Noy-Meir, I., 1973. Desert ecosystems: environment and producers. *Ann. Rev. Ecol. Systemat.* 4, 25-51.
- Okin, G.S., Mladenov, N., Wang, L., Cassel, D., Caylor, K.K., Ringrose, S., Macko, S., in press. Spatial patterns of soil nutrients in two southern African savannas. *Journal of Geophysical Research-Biogeosciences*.
- Olsson, M., Falkengren-Grerup, U., 1995. Potential nitrification as an indicator of preferential uptake of ammonium or nitrate by plants in an Oak woodland understorey. *Annals of Botany* 85, 299-305.
- Pardo-Iguzquiza, E., Dowd, P., 2001. Variance-covariance matrix of the experimental variogram: Assessing variogram uncertainty. *Mathematical Geology* 33(4), 397-419.
- Pardo, M.T., Ristori, G., P., D.A.L., Almendros, G., 2003. An assessment of soil fertility and agronomic constraints in southern African savannas: a case study of the Pandamatenga area, Botswana. *South African Geographical Journal* 85(1), 35-41.
- Porporato, A., D'Odorico, P., Laio, F., Rodriguez-Iturbe, I., 2003. Soil moisture controls on the nitrogen cycle I: Modeling scheme. *Adv. Water Res.* 26, 45-58.
- Press, W.H., Teukolsky, S.A., Vetterling, W.T., Flannery, B.P., 1992. Numerical recipes in C: the art of scientific computing. Cambridge University Press, Cambridge.
- Privette, J.L., Tian, Y., Roberts, G., Scholes, R.J., Wang, Y., Caylor, K.K., Frost, P., Mukelabai, M., 2004. Vegetation structure characteristics and relationships of Kalahari woodlands and savannas. *Global Change Biology* 10, 281-291.
- Ravi, S., Zobeck, T.M., Over, T.M., Okin, G.S., D'Odorico, P., 2006. On the effect of moisture bonding forces in air-dry soils on threshold friction velocity of wind erosion. *Sedimentology* 53(3), 597-609.

- Read, J.J., Tarpley, L., McKinion, J.M., Reddy, K.R., 2002. Narrow-waveband reflectance ratios for remote estimation of nitrogen status in cotton. *Journal of Environmental Quality* 31, 1442-1452.
- Reynolds, J., Smith, D.S., Lambin, E., Turner, B., Mortimore, M., Batterbury, S., Downing, T., Dowlatabadi, H., Fernández, R., Herrick, J., Huber-Sannwald, E., Leemans, R., Lynam, T., Maestre, F., Ayarza, M., Walker, B., 2007. Global desertification: building a science for dryland development. *Science* 316, 847-851.
- Richards, J., Caldwell, M., 1987. Hydraulic lift: substantial nocturnal water transport between soil layers by *Artemisia tridentata* roots. *Oecologia* 73, 486-489.
- Riedel, S.M., Epstein, H.E., 2005. Edge effects on vegetation and soils in a Virginia old-field. *Plant and Soil* 270, 13-22.
- Ringrose, S., Huntsman-Mapila, P., Kampunzu, A.B., Matheson, W., Downey, W.S., Vink, B., 2002. Geomorphological evidence for MOZ palaeo-wetlands in northern Botswana; implications for wetland change, Presentation to monitoring of tropical and sub-tropical wetlands conference. HOORC and the University of Florida, Center for Wetlands Maun.
- Ringrose, S., Jellema, A., Huntsman-Mapila, P., Baker, L., Brubaker, K., 2006. Use of remotely sensed data in the analysis of soil-vegetation changes along a drying gradient peripheral to the Okavango Delta, Botswana. *International Journal of Remote Sensing* 26(19), 4293-4320.
- Ringrose, S., Matheson, W., Vanderpost, C., 1998. Analysis of soil organic carbon and vegetation cover trends along the Botswana Kalahari Transect. *Journal of Arid Environments* 38, 379-396.
- Robinson, D., 2001. $\delta^{15}\text{N}$ as an integrator of the nitrogen cycle. *Trends in Ecology and Evolution* 16, 153-162.
- Rodriguez-Iturbe, I., D'Odorico, P., Porporato, A., Ridolfi, L., 1999. Tree-grass coexistence in savannas: the role of spatial dynamics and climate fluctuations. *Geophys. Res. Lett.* 26(2), 247-250.
- Sah, S.P., Rita, H., Ilvesniemi, H., 2006. ^{15}N natural abundance of foliage and soil across boreal forests of Finland. *Biogeochemistry* 80(3), 307-318.
- Sankaran, M., Hanan, N.P., Scholes, R.J., Ratnam, J., Augustine, D.J., Cade, B.S., Gignoux, J., Higgins, S.I., Roux, X.L., Ludwig, F., Ardo, J., Banyikwa, F., Bronn, A., Bucini, G., Caylor, K.K., Coughenour, M.B., Diouf, A., Ekaya, W., Feral, C.J., February, E.C., Frost, P.G.H., Hiernaux, P., Hrabar, H., Metzger, K.L., Prins, H.H.T., Ringrose, S., Sea, W., Tews, J., Worden, J., Zambatis, N., 2005. Determinants of woody cover in African savannas. *Nature* 438, 846-849.
- Sankaran, M., Ratnam, J., Hanan, N.P., 2004. Tree-grass coexistence in savannas revisited – insights from an examination of assumptions and mechanisms invoked in existing models. *Ecology Letters* 7, 480-490.
- Sarmiento, G., 1984. *The ecology of Neotropical savannas*. Harvard University Press, Cambridge, MA.
- Scanlon, T.M., Albertson, J.D., 2003. Inferred controls on tree/grass composition in a savanna ecosystem: Combining 16-Year NDVI data with a dynamic soil moisture model. *Water Resource Research* 39(8), 1224, doi:10.1029/2002WR001881.

- Scanlon, T.M., Caylor, K.K., Levin, S.A., Rodriguez-Iturbe, I., 2007. Positive feedbacks promote power-law clustering of Kalahari vegetation. *Nature* 449, 209-212.
- Schlesinger, W.H., 1997. *Biogeochemistry: an analysis of global change*. Academic Press, New York.
- Schlesinger, W.H., Raikes, J.A., Hartley, A.E., Cross, A.F., 1996. On the spatial pattern of soil nutrients in desert ecosystems. *Ecology* 77(2), 364-374.
- Schlesinger, W.H., Reynolds, J.F., Cunningham, G.L., Huenneke, L.F., Jarrell, W.M., Virginia, R.A., Whitford, W.G., 1990. Biological feedbacks in global desertification. *Science* 247, 1043-1048.
- Scholes, R.J., Archer, S.R., 1997. Tree-grass interactions in savannas. *Annual Review of Ecology and Systematics* 28, 517-544.
- Scholes, R.J., Dowty, P.R., Caylor, K., Parsons, D.A.B., Frost, P.G.H., Shugart, H.H., 2002. Trends in savanna structure and composition along an aridity gradient in the Kalahari. *Journal of Vegetation Science* 13, 419-428.
- Scholes, R.J., Frost, P.G.H., TIAN, Y., 2004. Canopy structure in savannas along a moisture gradient on Kalahari sands. *Global Change Biology* 10(3), 292-302.
- Scholes, R.J., Walker, B.H., 1993. *An African savanna*. Cambridge University Press.
- Schulze, E.-D., Caldwell, M.M., Canadell, J., Mooney, H.A., Jackson, R.B., Parson, D., Scholes, R., Sala, O.E., Trimborn, P., 1998. Downward flux of water through roots (i.e. inverse hydraulic lift) in dry Kalahari sands. *Oecologia* 115(4), 460-462.
- Schulze, E.-D., Lange, O.L., Ziegler, H., Gebauer, G., 1991. Carbon and nitrogen isotope ratios of mistletoes growing on nitrogen and non-nitrogen-fixing hosts and on CAM plants in the Namib desert confirm partial heterotrophy. *Oecologia* 88, 451-462.
- Shafer, J.M., Varljen, M.D., 1990. Approximation of confidence-limits on sample semivariograms from single realizations of spatially correlated random-fields. *Water Resources Research* 26(8), 1787-1802.
- Shugart, H.H., Macko, S.A., P.Lesolle, Szuba, T.A., Mukelabai, M.M., Dowty, P., Swap, R.J., 2004. The SAFARI 2000-Kalahari transect wet season campaign of year 2000. *Global Change Biology* 10, 273-280.
- Sinclair, A., 1979. Dynamics of the Serengeti ecosystem. In: A. Sinclair, M. Norton-Griffiths (Eds.), *Serengeti: Dynamics of an ecosystem* (Ed. by A. Sinclair, M. Norton-Griffiths), pp. 1-30. Univ. Chicago Press, Chicago.
- Skarpe, C., Bergstrom, R., 1986. Nutrient content and digestibility of forage plants in relation to plant phenology and rainfall in the Kalahari. *Journal of Arid Environments* 11, 147-164.
- Skarpe, C., Henriksson, E., 1986. Nitrogen fixation by cyanobacterial crusts and by associative-symbiotic bacteria in Western Kalahari, Botswana. *Arid Soil Research and Rehabilitation* 1, 55-59.
- Skinner, J.D., McCarthy, T.S., 1998. The Kalahari Colloquium. *Trans. Roy. Soc. S. Afr.* 53, 1-85.
- Sokal, R.R., Rohlf, F.J., 1995. *Biometry: the principles and practice of statistics in biological research*. W. H. Freeman and Company, New York.
- Solomon, S., Qin, D., Manning, M., Chen, Z., Marquis, M., Averyt, K., Tignor, M., Miller, H., 2007. IPCC, 2007: *Climate Change 2007: The Physical Science Basis*.

- Contribution of Working Group I to the Fourth Assessment Report of the Intergovernmental Panel on Climate Change. Cambridge University Press, Cambridge and New York.
- St. Clair, L.L., Webb, B.L., Johansen, J.R., Nebeker, G.T., 1984. Cryptogamic soil crusts: enhancement of seedling establishment in disturbed and undisturbed areas. *Reclamation and Revegetation Research* 3, 129–136.
- Stark, J.M., Hart, S.C., 2003. Nitrogen storage (communication arising): UV-B radiation and soil microbial communities. *Nature* 423, 137–138, doi:10.1038/423137a.
- Stokes, S., Thomas, D.S.G., Washington, R., 1997. Multiple episodes of aridity in southern Africa since the last interglacial period. *Nature* 388, 154–158.
- Su, Y., Li, Y., Zhao, H., 2006. Soil properties and their spatial pattern in a degraded sandy grassland under post-grazing restoration, Inner Mongolia, northern China. *Biogeochemistry* 79(3), 297–314.
- Swap, R.J., Aranibar, J.N., Dowty, P.R., Gilhooly, W.P., Macko, S.A., 2004. Natural abundance of ^{13}C and ^{15}N in C_3 and C_4 vegetation of southern Africa: patterns and implications. *Global Change Biology* 10(3), 350–358.
- Thomas, D.S., Shaw, P.A., 1991. *The Kalahari environment*. Cambridge University Press, Cambridge.
- Thomas, D.S.G., Brook, G., Shaw, P., Bateman, M., Haberyan, K., Appleton, C., Nash, D., McLaren, S., Davies, F., 2003. Late Pleistocene wetting and drying in the NW Kalahari, an integrated study from the Tsodilo Hills, Botswana. *Quaternary International* 104, 53–67.
- Thomas, D.S.G., Knight, M., Wiggs, G.F.S., 2005. Remobilization of southern African desert dune systems by twenty-first century global warming. *Nature* 435, 1218–1221.
- Thomas, D.S.G., Shaw, P.A., 1993. The evolution and characteristics of the Kalahari, southern Africa. *Journal of Arid Environments* 25, 97–108.
- Thomas, D.S.G., Shaw, P.A., 2002. Late Quaternary environmental change in central southern Africa: new data, synthesis, issues and prospects. *Quaternary Science Reviews* 21, 783–797.
- Thomas, G.W., 1996. Soil pH and soil acidity. In: J.M. Bigham (Ed.), *Methods of Soil Analysis Part3-Chemical Methods* (Ed. by J.M. Bigham), pp. 475–490. American Society of Agronomy Inc. and Soil Science Society of America Inc., Madison.
- Toit, J.T.D., Rogers, K.H., Biggs, H.C., 2003. *The Kruger experiment-ecology and management of savanna heterogeneity*. Island Press, Washington, DC.
- Trudgill, S., 1988. *Soil and vegetation systems*. Oxford University Press, New York, USA.
- Tucker, M.E., 2001. *Sedimentary Petrology*. Blackwell Science, Oxford.
- Vanderbilt, V.C., Grant, L., Biehl, L.L., Robinson, B.F., 1985. Specular, diffuse, and polarized light scattered by two wheat canopies. *Appl. Opt.* 24, 2408–2418.
- Veenendaal, E.M., Kolle, O., Lloyd, J., 2004. Seasonal variation in energy fluxes and carbon dioxide exchange for a broad-leaved semi-arid savanna (Mopane woodland) in Southern Africa. *Global Change Biology* 10(3), 318–328.
- Vitousek, P.M., Sanford, J., R.L., 1986. Nutrient cycling in moist tropical forest. *Annual Review of Ecology and Systematics* 17, 137–167.

- Walker, B.H., Ludwig, D., Holling, C.S., Peterman, R.N., 1981. Stability of semi-arid savanna grazing systems. *Journal of Ecology* 69, 473-498.
- Walker, T.W., Syers, J.K., 1976. The fate of phosphorus during pedogenesis. *Geoderma* 15, 1-19.
- Wallander, H., Arnebrant, K., Ostrand, F., Karen, O., 1997. Uptake of ^{15}N -labelled alanine, ammonium and nitrate in *Pinus sylvestris* L. ectomycorrhiza growing in forest soil treated with nitrogen, sulphur or lime. *Plant and Soil* 195, 329-338.
- Walter, H., 1971. Ecology of tropical and subtropical vegetation. Oliver and Boyd, Edinburg.
- Wang, G., Eltahir, E., 1999. Biosphere-atmosphere interactions over West Africa. 2. multiple climate equilibria. *Quart. J. Roy. Meteor. Soc.* 126, 1261-1280.
- Wang, L., D'Odorico, P., Ringrose, S., Coetzee, S., Macko, S., 2007a. Biogeochemistry of Kalahari sands. *Journal of Arid Environments* 71(3), 259-279
doi:10.1016/j.jaridenv.2007.03.016.
- Wang, L., D'Odorico, P., Ries, L., Caylor, K., Macko, S., in review. Combined effects of soil moisture and nitrogen availability variations on grass productivity in African savannas. *Global Change Biology*.
- Wang, L., Mou, P.P., Huang, J., Wang, J., 2007b. Spatial variation of nitrogen availability in a subtropical evergreen broadleaved forest of southwestern China. *Plant and Soil* 295, 137-150.
- Wang, L., Okin, G.S., Wang, J., Epstein, H., Macko, S.A., 2007c. Predicting leaf and canopy ^{15}N compositions from reflectance spectra. *Geophysical Research Letters* 34, L02401, doi:10.1029/2006GL028506.
- Wang, L., Shaner, P.-J.L., Macko, S., 2007d. Foliar $\delta^{15}\text{N}$ patterns along successional gradients at plant community and species levels. *Geophysical Research Letters* 34, L16403, doi:10.1029/2007GL030722.
- Wessman, C.A., Aber, J.D., Peterson, D.L., Melillo, J.M., 1988. Foliar analysis using near infrared reflectance spectroscopy. *Canadian Journal of Forest Research* 18, 6-11.
- Williams, C.A., Albertson, J.D., 2004. Soil moisture controls on canopy-scale water and carbon fluxes in an African savanna. *Water Resources Research* 40, W09302.
- Williams, C.A., Hanan, N.P., Neff, J.C., Scholes, R.J., Berry, J.A., Denning, A.S., Baker, D.F., 2007. Africa and the global carbon cycle. *Carbon Balance and Management* 2, 3 doi:10.1186/1750-0680-2-3.
- Xue, Y., Shukla, J., 1993. The influence of land surface properties on Sahel climate. Part I: desertification. *Journal of Climate* 6, 2232-2245.
- Xue, Y., Shukla, J., 1996. The influence of land surface properties on Sahel climate. Part II: afforestation. *Journal of Climate* 9, 3260-3275.
- Yoder, B., Pettigrew-Crosby, R., 1995. Predicting nitrogen and chlorophyll content and concentrations from reflectance spectra (400–2500 nm) at leaf and canopy scales. *Remote Sensing of Environment* 53, 199–211.
- Zaady, E., Groffman, P., Shachak, M., 1998. Nitrogen fixation in macro- and microphytic patches in the Negev desert. *Soil Biology and Biochemistry* 30, 449–454.
- Zeng, N., Neelin, J., Lau, K., Tucker, C., 1999. Enhancement of interdecadal climate variability in the Sahel by vegetation interaction. *Science* 286, 1537-1540.